Author:
Slattery, David Anthony

Title:
Characterisation of a novel antidepressant : Org 34167

Characterisation of a novel antidepressant;

Org 34167

by

David Anthony Slattery

A dissertation submitted to the University of Bristol in accordance with the requirements of the degree of Doctor of Philosophy in the Faculty of Science

June 2003

Psychopharmacology Unit,

University of Bristol

Word count: 64,713

Abstract

The drug Org 34167 is a novel antidepressant, which is currently undergoing clinical trials. The mechanism of action is unknown but *in vitro* testing revealed that the compound only displayed high affinity at the channel responsible for the generation of the hyperpolarisation-activated current (I_h).

A possible way to address the mechanism of action is utilising antisense technology in rats to specifically and reversibly inhibit protein expression. Recently, four members of a gene family have been identified, which are believed to represent the molecular identity of I_h and termed Hyperpolarisation-activated, cyclic-nucleotide gated (HCN1 - 4). HCN2 was targeted with seven different phosphorothioate antisense sequences, one to a region encompassing the initiation-codon, and six designed to areas of the transcript predicted to be devoid of secondary structure. None of these sequences, when i.c.v. infused for 3- or 7-days, resulted in significant alteration of HCN2 mRNA expression. Similar findings were demonstrated following infusion of an end-modified oligonucleotide; employed to reduce toxicity. A HCN2 antibody was not validated at the time of study and [^{3}H]-Org 34167 was demonstrated to be unsuitable for autoradiography thus preventing quantification of protein. Therefore, no successful antisense action was demonstrated following infusion of any sequence.

Induction of immediate early genes (IEG) is commonly believed to reflect neuronal activity. The novel antidepressant, mirtazapine, was demonstrated to induce *c-fos* and Egr-1 mRNA in a number of regions common to known antidepressants; anterior insular cortex, septum and central amygdala. This provided proof of the concept that IEG expression can be used to classify psychoactive compounds. Org 34167 was also shown to induce IEG expression in these brain regions but also displayed a robust cortical induction, which is akin to psychostimulant compounds, and regions high in HCN1 and 2 expression. This agrees with behavioural tests, which demonstrated that Org 34167 was active in depression models and also induced tremors, headweaving and intracranial self-administration.

Chronic antidepressant administration is required for clinical benefit due to adaptive changes. HCN1 – 3 mRNA expression was significantly altered following Org 34167 (0.5 mg/kg, 28d), fluoxetine (5 mg/kg, 21d) or mirtazapine (2 mg/kg, 21d) administration. This provides further insight into Org 34167's mechanism of action and also a link between clinically used antidepressants and the channel.

The observations made in this thesis contribute to the characterisation of the novel antidepressant Org 34167, and also provide a link between I_h (HCN) channels and depression, which was not previously apparent.

This thesis is dedicated to my parents

ACKNOWLEDGEMENTS

Firstly, I would like to thank my supervisors, Professor David Nutt, Dr Alan Hudson, Dr John Morrow and Dr David Hill, for their support and encouragement throughout my PhD and enabling me to have the opportunity to work both in academia and industry.

I would especially like to thank Dr Brian Henry for putting up with an unexpected visitor to his lab at Organon for almost 2 yrs and then reading my thesis. His help and enthusiasm was greatly appreciated.

I am also very grateful to Dr Emma Robinson for her help throughout my PhD and agreeing to read through my thesis at the end.

I am very grateful for the valuable assistance of Prof Neil Marrion and Dr Adrian Mason for reading my HCN channel section with its large level of electrophysiological terminology!

Thanks also to Dr Barbara Sumner for her help discussing my *c-fos* work, teaching me AChe staining and reading my *c-fos* chapter.

I would also like to thank everyone in the lab for making my time spent at Organon a happy and productive one; especially Lorcan, Leonie, Fiona and Mark Anderson for his help with molecular biology.

The same goes for everyone in the Psychopharmacology Unit, for making my time in Bristol enjoyable.

To Mr Dave for letting me sleep on his floor for a fortnight when I had nowhere to stay when I came back to Bristol to do some antisense infusions.

I would also like to thank Zsuzsi for making me to take breaks from writing-up and helping me take my mind off the final weeks before the viva in Budapest.

And finally to my family, for their help and support throughout my studies, and enabling me to have the opportunity to do a PhD.

AUTHOR'S DECLARATION

I declare that the work in this thesis was carried out in accordance with the Regulations of the University of Bristol. The work is original except where indicated by special reference in the text and no part of the thesis has been submitted for any other degree. Any views expressed in the thesis are those of the author and in no way represent those of the University of Bristol. The thesis has not been presented to any other University for examination either in the United Kingdom or overseas.

Signed..... Date.25/09/03....

David Anthony Slattery

Statement endorsed by:

Signed.....

Professor D.J. Nutt

Signed.....

Dr A.L. Hudson

Contents

List of Figures

List of Tables

Chapter 1 General introduction

1.1 Org 34167 – a novel antidepressant

1.1.1 Preclinical and clinical observations

Org 34167 is a novel antidepressant compound, which is about to enter into Phase II clinical trials. It has been shown to be very potent in a number of animal models of depression (Table 1.1). Despite this, *in vitro* testing revealed that the compound displayed very low affinity for over fifty G-protein coupled receptors (Ruigt, Personal communication). It also lacks affinity and efficacy at numerous traditional depression targets; such as monoamine receptors, transporters and monoamine oxidase; although weak affinity was shown for α_{2B}- and α_{2C}-adrenoceptors (pK_i; negative logarithm of the equilibrium dissociation constant, 5.4 & 5.7, respectively; Ruigt *et al.*, Personal communication). Org 34167 only displayed high affinity for was the channel responsible for the hyperpolarisation-activated current (I_h channels); the compound was shown by electrophysiological recordings from CA1 pyramidal cells to negatively modulate this current with a pIC_{50}; negative logarithm of molar concentration of agonist which produces 50 % of the maximum response, 8.0 (Ruigt *et al.*, Personal communication). Additionally, weak affinity was been shown for Type 1 and Type 2 binding sites on the sodium channel (pK_i 5 – 7; Ruigt *et al.*, Personal communication).

Table 1.1 Effect of Org 34167 in various animal models

BEHAVIOURAL MODEL	ACTIVE DOSE OF ORG 34167
Rat sleeping stage test	0.3 mg/kg s.c; 10 mg/kg p.o.
Rat 'intracranial self-stimulation test'	MED 0.5 mg/kg i.p.
Mouse marble burying test	ID_{50} 0.4 mg/kg s.c.; 10.7 mg/kg p.o.
DRL72 (rat)	MED 0.75 mg/kg i.p.; > 10 mg/kg p.o.
Porsolt test (mouse)	MED 0.32 – 1 mg/kg s.c.; > 10 mg/kg p.o.
ACSO antidepressant profile	Thr 0.32 mg/kg i.p.
Rat penile erection antagonism	ID_{50} 0.3 mg/kg s.c
Rat lower lip retraction antagonism	ID_{50} 0.4 mg/kg s.c
Induction of forepaw treading	ED_{50} 0.46 mg/kg s.c

Abb: ACSO, Automated sleep analysis system, DRL72, Differential Rates of Low reinforcement 72, ED_{50}, effective dose at which 50 % change in baseline activity is observed, ID_{50}, Dose causing 50 % inhibition of maximum response, i.p., intraperitoneal, MED, minimum effective dose, sc subcutaneous, Thr, Threshold.

[^{3}H]-Org 34167 was found to label a single, membrane-associated, binding site in rat CNS membrane preparations (K_d = 25 nM; Makkink, Personal communication). However, comparision of the estimated I_h channel density (8 – 40 fmol/mg protein), and the density of Org 34167 binding sites (1000 – 6000 fmol/mg protein) indicates a clear discrepancy, which would seem to suggest it binds to more than one site (Ruigt *et al.*, Personal communication). Rat autoradiography experiments reveal that [^{3}H]-Org 34167 has a widespread distribution with high levels of binding in the substantia nigra, amygdala, globus pallidus, stria terminalis, geniculate nuclei, ventral tegmental area and the central grey of the cerebellum (Makkink, Personal communication).

In July 2001, Org 34167 completed Phase 1 clinical trials and was found to be well tolerated at low doses (< 2.5 mg) with a range of moderate adverse effects being reported by the patients at this and higher doses (15 and 40 mg; see Table 1.2). In healthy male volunteers, a significant prolongation of REM sleep latency was observed at 2.5 mg/kg, but not the higher doses (vanBerkel, Personal communication). This suggests that the drug may have antidepressant activity in humans and concurs with the potent effect in animal models of depression (vanBerkel, Personal communication).

Table 1.2 Adverse effects of Org 34167 reported from Phase 1 clinical trials

ADVERSE EFFECTS OF ORG 34167 REPORTED IN CLINICAL TRIALS	
Dizziness	Daytime somnolence and fatigue
Impaired concentration	Headache
Nausea and vomiting	Palpitation
Sleeping problems	Agitation
Vertigo	Visual disturbances

1.2 Hyperpolarization-activated, cyclic-nucleotide-gated channels

1.2.1 Introduction

The description of a current, which activates upon hyperpolarization, to cause an inwards current that depolarises the cell, originated from studies using sino-atrial (SA) cells (Brown *et al.*, 1979a; Brown *et al.*, 1979b). It was shown to partially mediate the increase in cell firing evoked by adrenaline and termed I_f, for 'funny' current (Brown *et al.*, 1979a; Brown *et al.*, 1979b). Within a few years, similar currents were reported in Purkinje fibres (DiFrancesco, 1981a; DiFrancesco, 1981b), photoreceptors (Attwell *et al.*, 1980; Bader *et al.*, 1984; Barnes *et al.*, 1989), ventricular muscle (Yu *et al.*, 1993), peripheral (Mayer *et al.*, 1983) and central neurones (Halliwell *et al.*, 1982). The additional terms I_h (for Hyperpolarization-activated current) in the CNS (Bader *et al.*, 1984; Mayer *et al.*, 1983) or I_q (for 'queer' current) and pacemaker channel (DiFrancesco *et al.*, 1991; Gauss *et al.*, 2000) were coined to describe them.

Despite increasing knowledge regarding the properties of the current, it was not until the late 1990's before the cloned channel subunits, believed to be responsible for the generation of the current was identified. Three groups, almost simultaneously, published findings; two of which were based on the hypothesis that the channel would be related to voltage-gated potassium (K^+) and cyclic-nucleotide gated (CNG) channels, while the other serendipitously isolated the channel (Gauss *et al.*, 1998; Ludwig *et al.*, 1998; Santoro *et al.*, 1997). When the cDNAs identified by these groups are heterologously expressed in cell systems, the resultant channels properties are very similar to those of native I_h channels (as will be discussed in the following sections). However, despite the strong likelihood of these cloned channels, subsequently termed

Hyperpolarisation-activated, cyclic nucleotide-gated (HCN) channels, representing the molecular identity of the family of channels responsible for native I_h, this has yet to be fully confirmed. Therefore, throughout the remainder of this thesis, I_h or pacemaker channel will refer to native channels, and the term HCN to work performed on cloned channels.

1.2.2. Molecular identification of HCN channels

The first member of the gene family was identified using a yeast two-hybrid system, and the Src-homology 3 (SH3) domain of a neural specific form (N-Src) as bait. The authors isolated a novel murine cDNA, encoding a 132-kDa glycoprotein, which they termed brain cyclic nucleotide gated 1 (BCNG-1; Santoro *et al.*, 1997). In the initial report the authors were unable to functionally express the cDNA but determined that it likely encoded for an ion channel based on sequence homology to voltage-gated K^+ channels, CNG channels and plant inward rectifing K^+ channels (Santoro *et al.*, 1997). When successful heterologous expression was achieved, it demonstrated that the cDNA did indeed encode for a functional channel with properties akin to that of I_h in the brain (Santoro *et al.*, 1998). Reverse-transcription polymerase chain reaction experiments performed on murine BCNG-1 identified an additional two homologous murine gene fragments (subsequently termed murine BCNG-2 and murine BCNG-3; Santoro *et al.*, 1998). Furthermore, a Basic Local Alignment Search Tool (BLAST) search in mouse and human Expressed Sequence Tag (EST) database homology search using the protein sequence of murine BCNG-1 revealed a further mouse gene (murine BCNG-4) and two human genes (hBCNG-1 and -2) that shared homology with murine BCNG-1 sequence (Santoro *et al.*, 1998). Each of the mouse genes was shown to display a different distribution pattern using Northern blot analysis, with members found in the brain, heart, liver, kidney, skeletal muscle and lung (Santoro *et al.*, 1998). Murine BCNG-1

was found to be mainly located in the brain, murine BCNG-2 in both brain and heart tissue, murine BCNG-3 in brain, heart, lung and skeletal muscle, and murine BCNG-4 mainly in liver, but also in brain, lung and kidney (Santoro *et al.*, 1998).

An EST BLAST database using the conserved cyclic nucleotide binding domain (CNBD) of CNG channels performed by Ludwig *et al.*, (1998), identified a sequence fragment of a new class of channel. The authors termed this Hyperpolarisation-activated channel (HAC)-1. Full-length cloning of this murine fragment identified a further two related sequences, HAC2 and HAC3, which shared an overall homology of 60 %. The amino acid sequence of the newly identified family was shown to share significant homology with cyclic-nucleotide-gated (CNG) channel α-subunits (28%) and ether-à-gogo K^+ channels (27%); with a pore region similar to K^+ channels and a cyclic-nucleotide-binding domain (Ludwig *et al.*, 1998).

Another group designed primers based on the CNG channels to clone cDNA from a sea urchin *Strongylocentrotus purpuratus* (Sp) testis library. Functional expression of this cDNA demonstrated that it encoded a weakly K^+ selective, hyperpolarisation-activated channel, which the authors termed SPIH (Gauss *et al.*, 1998). After these initial findings further clones were identified in rat, rabbit and human, and were named based around the initial three group's classification (see Table 1.3 for list of known HCN channel isoforms). Due to the confusing nomenclature Hyperpolarisation-Activated, Cyclic Nucleotide-Gated (HCN) channel was proposed to be an appropriate name based on two of the main properties of the channel (Clapham, 1998). Cloning of these channels enabled the testing of Org 34167, which had demonstrated affinity for I_h channels, in cell lines expressing these new identified channels. As expected, Org 34167 displayed high affinity for HCN channels (Ruigt *et al.*, Personal communication)

and provides a further link suggestive that these channels represent the molecular identity of I_h.

1.2.3 Functional properties of I_h and HCN channels

Native and recombinant channels display a 3:1 – 4:1 ratio for K^+ : sodium (Na^+) ions, which sets the reversal potential for the channels at -35 mV (Gauss *et al.*, 1998; Ho *et al.*, 1994; Ludwig *et al.*, 1998; McCormick *et al.*, 1990b; Pape, 1996; Santoro *et al.*, 1998; Wollmuth *et al.*, 1992). Therefore, there is an inward current, mainly carried by Na^+ ions, at the hyperpolarised potentials (< -50 mV) at which the channel is open. These properties cause pacemaker channels to generate a rebound depolarisation following an action potential or inhibitory postsynaptic potential (IPSP), which increases the membrane potential thereby contributing to rhythmic activity of cells and contributes to the resting membrane potential (Pape, 1996).

Table 1.3 Details of known HCN channel gene members (with both original and updated nomenclature).

NEW NOMENCLATURE	ORIGINAL NAME	SPECIES	REFERENCES
HCN1	mBCNG-1 / HAC2	Mouse	1, 2
	hBCNG-1	Human	4
	HCN1	Rat	AF247453
	HCN1	Rabbit	7
HCN2	mBCNG-2 / HAC1	Mouse	2, 4
	hBCNG2 / hHCN2	Human	4, 5, 6
	HCN2	Rat	7, AF247451
	HCN2	Rabbit	7
HCN3	mBCNG-4 / HAC3	Mouse	2, 4
	HCN3	Rat	AF247452
	HCN3	Rabbit	7
HCN4	mBCNG-3	Mouse	4
	hHCN4	Human	5, 8
	HCN4	Rat	AF247450
	HCN4	Rabbit	7, 9
SpHCN	SPIH	Sea urchin	3
HvHCN	HvCNG	Silkmoth	AJ012664
DmHCN	DMIH	Fruitfly	AF124300

Adapted from Kaupp *et al.*, (2001). References: 1. (Santoro *et al.*, 1997); 2. (Ludwig *et al.*, 1998); 3. (Gauss *et al.*, 1998); 4. (Santoro *et al.*, 1998); 5. (Ludwig *et al.*, 1999); 6. (Vaccari *et al.*, 1999); 7. (Shi *et al.*, 1999); 8. (Seifert *et al.*, 1999); 9. (Ishii *et al.*, 1999). AF24750-AF24753, AJ012664 and AF124300 refer to National Centre for Biotechnology Information accession numbers (NCBI).

Pacemaker channels have been well studied in the heart where there are four main channels, which are believed to contribute to the action potential (L- and T-type calcium (Ca^{2+}) channels, a K^+ channel and pacemaker channels). I_h generates an inward current during the falling phase of the action potential, which causes a resultant increase in membrane potential thereby facilitating the firing of another action potential. Addition of β-adrenoceptor agonists (Brown *et al.*, 1979a), or cAMP (DiFrancesco *et al.*, 1991), shifts the half-maximal activation ($V_{1/2}$) of I_h to more positive membrane potentials, causing a resultant increase in heart rate. This is one of the reasons why sympathetic stimulation by adrenaline increases the heart rate and conversely why parasympathetic

innervation by acetylcholine (ACh) slows the heart rate (Brown *et al.*, 1979a; Brown *et al.*, 1979b; see Figure 1.1).

Figure 1.1 Effect of I_h on heart rate under normal conditions and the addition of β-adrenoceptor agonists.

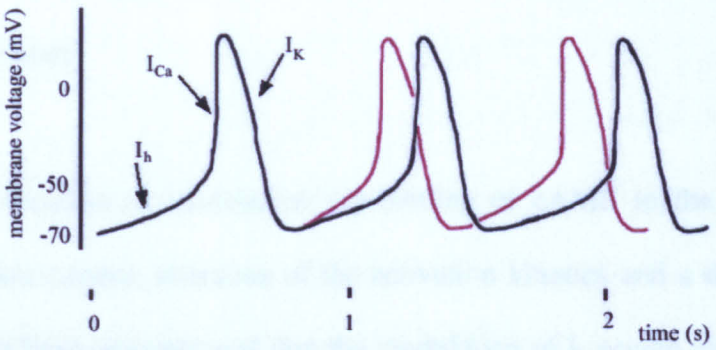

Adapted from Biel *et al.*, (1999). I_h current shows the slow depolarisation caused by activation of this current. I_{Ca} refers to both T- and L-type Ca^{2+} channels, which are the main channels responsible for the depolarising phase of the action potential. I_K is the K^+ currents that underlie the repolarisation phase. The black trace shows action potentials under normal conditions and the red trace demonstrates the acceleration of their rate following addition of β-adrenoceptor agonists.

Many different $V_{1/2}$ values, which provide information as to the operational voltage range of the channels, have been reported for recombinant HCN channels. Initial studies placed the values at < -105 mV (Ludwig *et al.*, 1998; Ludwig *et al.*, 1999; Santoro *et al.*, 1998) and there was debate regarding the functional significance of the channel. However, Seifert *et al.*, (1999) demonstrated that $V_{1/2}$ critically depended on the length of the hyperpolarising pulse and that the actual values lie between -70 to -80 mV, which is similar to the $V_{1/2}$ of native pacemaker channels (Bader *et al.*, 1984; Mayer *et al.*, 1983; McCormick *et al.*, 1990a; Pape, 1996). Following this, Santoro *et al.*, (2000) re-evaluated HCN1 and HCN2 properties and found similar values in the physiological range (see Table 1.4 for list of $V_{1/2}$ values of native and HCN channels).

Additionally, each of the HCN channel isoforms display distinct tau (τ)-activation properties (see Table 1.4 for values). Throughout the brain, native I_h activation properties have been demonstrated to vary significantly, which may be due to the presence of different isoforms (see Table 1.4). These different activation properties may have important physiological implications, such as the contribution to thalamic spindle wave activity (McCormick *et al.*, 1997), in addition to the role already mentioned in the heart.

The channel is sensitive to modulation *via* binding of cAMP to the CNBD, which results in increased current, alteration of the activation kinetics and a shift in $V_{1/2}$ (see Table 1.4). It has been demonstrated that the modulation of I_h occurs *via* direct binding of cAMP to the channel, independently of protein phosphorylation (DiFrancesco *et al.*, 1991; Gauss *et al.*, 1998; Ludwig *et al.*, 1998). There is also a degree of voltage modulation by protein kinase A (PKA) dependent phosphorylation (Vargas *et al.*, 2002; Yu *et al.*, 1993). Additionally, a number of HCN isoforms contain PKA-consensus phosphorylation sites, which indicate why cAMP modulation is more apparent than PKA-modulation (Santoro *et al.*, 1998).

Table 1.4 Functional properties of native and recombinant HCN channels

ISOFORM	$V_{1/2}$ (MV)	$V_{1/2}$ MODULATION BY CAMP (MV)	P_{NA}/P_K	τ-ACTIVATION
HCN1	-71.6[k]	+ 2[a]	0.25[a]	100 -300 ms (at -130 to -100mv)[a,g]
HCN2	-78.3[k]	+ 12 – 14[b,c]	0.24[b,c]	200 – 500 ms (at -140 to -100mV)[b,c]
HCN3	n.d	n.d.	n.d	n.d
HCN4	-75.2[f]	+11 – 23[c,d,f]		400 ms (at -140mV) to 23s (at -110mV)[c]
SpHCN	-26[e]	-24[e]	0.23[e]	n.d
I_h	-74 to -85[h,l,m]	+ 2 - 13	0.2 – 0.4[i,j,m]	300ms to 8.3s[h, l, m]

References: a) Santoro *et al.*, (1998) b) Ludwig *et al.*, (1998) c) Ludwig *et al.*, (1999) d) Ishii *et al.*, (1999) e) Gauss *et al.*, (1998) f) Seifert *et al.*, (1999) g) Santoro *et al.*, 2000) h) McCormick *et al.*, 1990b) i) Wollmuth *et al.*, (1992) j) Kaupp *et al.*, (2001) k) Santoro *et al.*, (1999) l) Luthi *et al.*, (1998) m) Pape, (1996).

Recombinant HCN channels have high affinity for cAMP; HCN2 has been demonstrated to have a $K_{1/2}$ of 0.5 μM, and that of SpHCN is 0.7 μM, but cGMP has 10-fold less affinity at HCN2 channels and 1000-fold at SpHCN (Gauss *et al.*, 1998; Ludwig *et al.*, 1998). Truncation mutants of HCN1 and HCN2 channels lacking a CNBD have been used to further investigate the role cAMP exerts on the channel (Wainger *et al.*, 2001). These studies suggest that the CNBD inhibits gating of HCN channels by blocking the pore and that binding of cAMP, or deletion of this domain removes this inhibition (Wainger *et al.*, 2001; Wang *et al.*, 2001). Deletion of the HCN1 channel CNBD does not produce as dramatic an alteration in the channel properties as the corresponding HCN2 mutant, which is suggestive that the differences in cAMP modulation between HCN1 and HCN2 may be due to differences in the inhibitory CNBD (Wainger *et al.*, 2001).

Extracellular caesium (Cs^+) ions block I_h currents in hippocampal slices, at millimolar concentrations (Halliwell *et al.*, 1982), while it is relatively insensitive to barium (Ba^+) ions (Ludwig *et al.*, 1998; Pape, 1996; Santoro *et al.*, 1998). Similar findings have been demonstrated for recombinant HCN channels (Ludwig *et al.*, 1998; Santoro *et al.*, 1998). Aside from these cations, there are only a few compounds that display affinity for the HCN channel. One such compound is the bradycardiac agent, ZD 7288, which is an antagonist at micromolar concentrations (BoSmith *et al.*, 1993; Gasparini *et al.*, 1997; Ghamari-Langroudi *et al.*, 2000; Harris *et al.*, 1995; Khakh *et al.*, 1998). Studies performed on recombinant mHCN1 channels demonstrate that ZD 7288 reversibly blocks the current in a concentration-dependent fashion. This block took ~ 4 s when applied to inside-out patches but a few minutes when applied to the extracellular surface (Shin *et al.*, 2001). Moreover, this block was highly voltage-dependent, at more depolarised potentials where the channel is not fully open, ZD 7288 produced an effective block, which was diminished at more hyperpolarised potentials (BoSmith *et al.*, 1993; Shin *et al.*, 2001). Ivabradine has also recently been shown to be an open-channel blocker, similar to ZD 7288 in rabbit SA-node cells (Bucchi *et al.*, 2002). Zatebradine, a bradycardic agent with a similar structure to verapamil (L-type Ca^{2+} channel blocker), has been demonstrated to be a use-dependent blocker of I_h channels but also to inhibit voltage-gated outwards K^+ currents (I_K) and L-type Ca^{2+} channels (Goethals *et al.*, 1993; Satoh *et al.*, 2002).

The common physical properties of native and recombinant HCN channels are summarised in Table 1.5. Auxiliary proteins, formation of heteromeric channels and/or β-subunits may be able to explain the subtle differences between native and recombinant channels. However, the available evidence is highly suggestive of HCN

channels representing the molecular identity of pacemaker channels. Although, until dominant-negative mutants are available there remains a question mark over this.

Table 1.5 Common physical properties of native and recombinant HCN channels

PHYSICAL PROPERTIES OF NATIVE AND RECOMBINANT HCN CHANNELS
Slow activation (although kinetics vary between both brain regions and cloned isoforms) and do not inactivate
Conduction of both K^+ and Na^+ ions, with a ratio of 3:1 – 4:1.
Direct enhancement of channel current and shift in $V_{1/2}$ by binding of cAMP
Extracellular Cs^+ blocks the current
Removal of external K^+ blocks the inward current (Frace *et al.*, 1992; Wollmuth *et al.*, 1992)
External Cl^- ions modulate the channel (Frace *et al.*, 1992; Santoro *et al.*, 1998; Zong *et al.*, 2001)

1.2.4 Structural properties of HCN channels

There is a good deal now known about the structural features of HCN channels due to homology screening and mutagenesis studies performed on the different channel isoforms. Hydropathicity plots of the initial sequences were predictive of a channel with six transmembrane segments, with intracellular hydrophilic N- and C- termini and a putative CNBD in the C-termini (Gauss *et al.*, 1998; Santoro *et al.*, 1997; Santoro *et al.*, 1998).

Figure 1.2 Structural representation of an HCN channel isoform

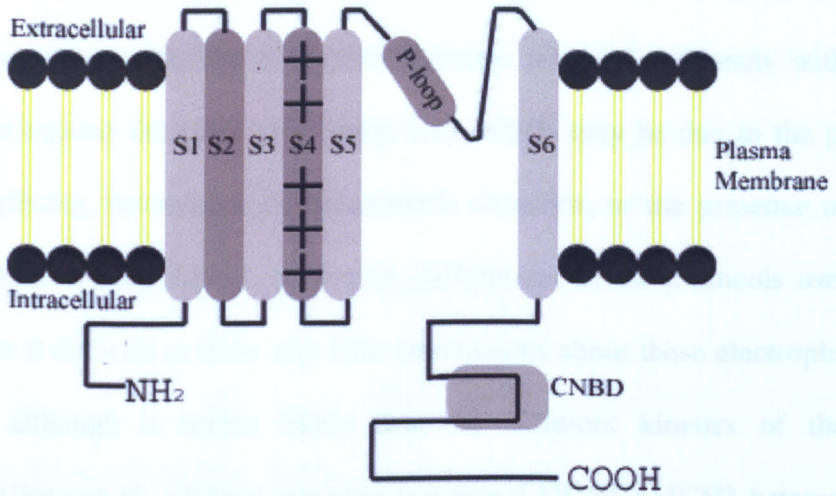

Adapted from Kaupp *et al.*, (2001).

The four different HCN isoforms display an overall sequence homology of ~ 60 %, although this is increased to 80 – 90 % around the core region (the S1 transmembrane segment to the CNBD). Primary structure analysis of the core region reveals that HCN channels are most closely related to voltage-gated K^+ channels, including Shaker (14 % homology), ether-à-gogo (27 %), HERG (22 %), and CNG channel α-subunits (28 %; Ludwig *et al.*, 1998). It has been postulated that the fusion of an ancestral K^+ channel and CNG occurred before the evolutionary separation of plants and animals (Warmke *et al.*, 1994) and that the newly identified HCN channel represents the closest link known to this ancestral channel (Santoro *et al.*, 1997).

HCN channels are predicted to comprise of four subunits due to the resemblance to both Shaker and CNG channels (Santoro *et al.*, 1998). It is unclear whether, homomeric or heteromeric channels, are formed, or a combination of both. Recombinant studies have demonstrated that homomeric channels are functional (Ishii *et al.*, 1999; Ludwig *et al.*, 1998; Ludwig *et al.*, 1999; Santoro *et al.*, 1998; Vaccari *et al.*, 1999). The expression profile of the different subunits does little to resolve this question, as it reveals areas

that are predominantly one isoform but other regions where the four subunits are equally distributed (Moosmang *et al.*, (1999); see Section 1.2.5 for full details of HCN channel expression). Studies on native channels reveal I_h channels with differing properties throughout the CNS (see Table 1.4), which may be due to the presence of alternative splicing, homomeric or heteromeric channels, or the presence of auxiliary subunits (Santoro *et al.*, 1999). However, differences in the protocols used between groups render it difficult to draw any firm conclusions about these electrophysiological differences, although it seems likely that the different kinetics of the subunits contribute. Ulens *et al.*, (2001a) reported functional HCN1 / HCN2 heteromers based upon co-expression studies of HCN1 and HCN2 channels in oocytes. The heteromers displayed properties lying between the fast kinetics and low cAMP modulation of HCN1, and slow gating HCN2 isoform; similar to native I_h in CA1 pyramidal neurones (Ulens *et al.*, 2001a). Additionally, chimeric cDNA constructs of HCN1 and HCN2, covalently linked at the C-terminus of HCN1 and N-terminus of HCN2 subunits (concatenated), gave rise to a functional channel with properties similar to that in co-expressing cells (Ulens *et al.*, 2001a).

In another mutagenesis study, using Chinese hamster ovary cells, HCN2 channels lacking an amino terminus did not locate to the cell surface, as determined using immunofluorescence, and unsurprisingly therefore, did not produce functional channels (Proenza *et al.*, 2002). In the same report, using yeast-two hybrid assays, it was demonstrated that the N-termini of HCN1 and HCN2 interacted, both homomerically and heteromerically (Proenza *et al.*, 2002). Deletion of the B-helix of the CNBD also produced homomeric channels which were not functional. Immunofluorescence demonstrated that these mutants were located intracellularly, whereas the wildtype was located at the cell surface (Proenza *et al.*, 2002). This may be due to alterations in the

tertiary structure of the proteins, or a second reason provided by the authors, based on work by Ma *et al.*, (2001) in COS7 cells. This showed that motifs present in inwardly rectifying K^+ (K_{ir}) channels were responsible for localisation to the plasma membrane, and similar motifs may be present in the B-helix of HCN channels.

1.2.5 Expression profile of HCN channel subunits

The successful cloning of HCN1 - 4 cDNAs enabled examination of the expression pattern of the different isoforms throughout the brain and periphery. Initial distribution studies were performed by the groups who isolated the cDNA for the HCN subunits, and since then there have been a number of more extensive studies examining the distribution of the four subunits in mouse and rat brain. Northern blots performed by Santoro *et al.*, (1998) to establish the distribution of the mouse isoforms, revealed that they all display different profiles, for example mBCNG-1 (HCN1) was solely found in the brain. However, expression of other HCN members was seen in brain, heart, liver, kidney, skeletal muscle and lung.

An extensive *in situ* hybridisation study on the distribution of HCN1-4 isoform mRNAs in mouse brain was performed by Moosmang *et al.*, (1999). This group demonstrated that the HCN1 transcript was highly expressed in cortical structures, such as the neocortex, hippocampus and cerebellum; although there were also high levels in the superior colliculus. The most ubiquitous and abundant isoform was found to be HCN2, which was present in the majority of brain structures analysed, but particularly high expression was observed in the thalamus, the olfactory bulb, hippocampus and cerebellum. HCN3 subunit mRNA expression was found at low levels throughout the brain, except from the olfactory bulb, and a similar pattern was observed for HCN4

mRNA, with the habenula and thalamus also demonstrating high expression levels (Moosmang *et al.*, 1999).

The distribution of the four HCN isoforms in rat was demonstrated to be similar to that found in mouse by Moosmang *et al.*, (1999), with HCN2 displaying the most ubiquitous and widespread profile (Monteggia *et al.*, 2000; Figure 1.3). Bender *et al.*, (2001), using *in situ* hybridisation, observed that the expression profiles of HCN1, 2 and 4 mRNA throughout the hippocampus differ significantly between adult and juvenile rats.

Immunohistochemical reports on HCN1 protein expression reveal a similar distribution to that shown by *in situ* hybridisation. These studies show protein expression on apical dendrites as well as axonal terminals of the hippocampus, less prominent in the CA3 region as compared with the CA1 (Santoro *et al.*, 2000). HCN1 immunoreactivity in apical dendrite membranes in rat hippocampus displays a 60-fold increase from somatic to distal apical dendrite membranes (Lorincz *et al.*, 2002). Additionally, the density of HCN1 immunoreactivity was found to be significantly higher in dendritic shafts than in spines, at similar distances from the soma (Lorincz *et al.*, 2002).

Figure 1.3 Representative transverse autoradiograms of HCN1-4 mRNA distribution in rat brain

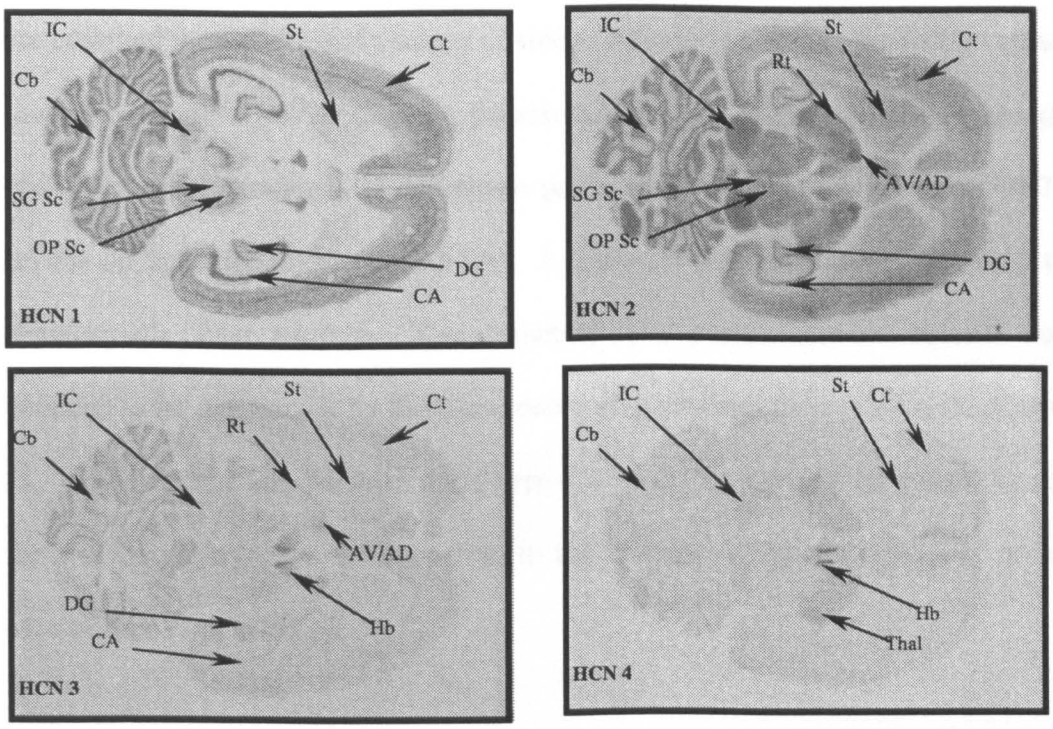

Adapted from B. Henry, (Personal communication). Abb: AD, anterodorsal thalamic nucleus, AV, anteroventral thalamic nucleus, CA, CA fields of the hippocampus, Cb, cerebellum, Ct, cortex, DG, dentate gyrus, Hb, habenula, IC, inferior colliculus, OP Sc, optic nerve layer of the superior colliculus, Rt, reticular thalamic nucleus, SG Sc, superfical grey layer of the superior colliculus, St, striatum, Thal, thalamus.

1.2.6 Physiological functions

There have been three main physiological functions attributed to I_h channels in the brain:

1. Control of the rate of rhythmic activity in neurones and neuronal networks.
2. Contribution to the resting neuronal membrane potential.
3. Contributing to the neuronal response after hyperpolarising currents.

There are numerous examples of the generation of rhythmic activity within neuronal networks (in addition to that of the heart rate mentioned previously); one such is spindle waves (McCormick *et al.*, 1997; Santoro *et al.*, 1999). These oscillations have a

frequency of 7 – 14 Hz, wax and wane within 1 - 3 s, display periodicity of 3 – 20 s and are common throughout early stages of sleep. Spindle waves are gradually replaced by lower frequency, 0.5 – 4 Hz firing patterns and neurones can switch between the two with only small alterations in membrane potential (see McCormick *et al.*, (1997) for a review on thalamocortical oscillations). I_h channels are believed to contribute to both characteristic wave patterns. The refractory time period between spindle waves is believed to be determined by the time course of I_h channel deactivation (McCormick *et al.*, 1997). Interaction between the T-type Ca^{2+}- and I_h channels is thought to generate the low frequency 0.5 – 4 Hz rhythm to the thalamic relay neurones (for review see McCormick *et al.*, (1997)).

The fact that I_h and HCN channels are positively modulated by cyclic nucleotides and PKA enables G-protein coupled receptors to alter the properties of the channels *via* regulation of cAMP- and PKA-levels. A1 adenosine (Pape, 1992; Strecker *et al.*, 2000) and μ-opioid receptors (Ingram *et al.*, 1994; Svoboda *et al.*, 1998; Ulens *et al.*, 2001b) have been demonstrated to modulate pacemaker channels through this mechanism. In a recent study utilising different 5-hydroxytryptamine (5-HT) receptor agonists, Bickmeyer *et al.*, (2002) demonstrated that 5-HT_4- and 5-HT_7-receptor activation increased the I_h current and shifted $V_{1/2}$ by + 5 mV, whereas 5-HT_{1A}-receptor activation shifted $V_{1/2}$ to more hyperpolarised potentials by 5 mV in murine hippocampus. Moreover, Ulens *et al.*, (2001b) demonstrated in *Xenopus* oocytes that G_s-coupled 5-HT_4-receptor activation modulated HCN2 *via* cAMP but had no effect on HCN1 channels, which was also the case for G_i/G_o-coupled μ-opioid receptors. This concurs with the knowledge that cAMP dramatically alters HCN2 channel properties but has very little effect on HCN1 (see Table 1.4). Therefore, HCN channels are extremely important as both primary and secondary drug targets. Unsurprisingly, due to their

involvement in rhythmic oscillations, I_h channels have been implicated in epilepsy and sleep disorders, as well as neuropsychiatric disorders, such as depression, given the altered sleep patterns observed in patients (Monteggia *et al.*, 2000; Moosmang *et al.*, 1999).

1.2.7 HCN channels and depression

Sleep disturbance is a key aspect of depression, with an estimated 75 % of patients suffering some form of sleep dysfunction (Thase, 1999). The knowledge that HCN channels contribute to the generation of spindle waves and their refractory period suggests that modulation of these channels would lead to alterations in the sleep architecture. The findings from Phase 1 clinical trials of Org 34167 have provided evidence for this hypothesis, with increased REM sleep demonstrated in healthy male volunteers (vanBerkel, Personal communication). To date, this finding, and those from preclinical animal models of depression, are the only confirmed data supporting a link between HCN channels and depression.

A recent study in crayfish muscle cells proposed another property of HCN channels; namely presynaptic facilitation of neurotransmitter release (Beaumont *et al.*, 2000). The report suggests that the mechanism through which the channels achieve this is *via* direct coupling to the vesicular release machinery, as it occurs independent of an increase in intracellular Ca^{2+} (Beaumont *et al.*, 2000). This has potential implications for a number of diseases, including depression, as all current antidepressant mechanisms of action involve, either directly or indirectly, elevating central monoamine transmitter concentrations.

1.3 Depression

1.3.1 Introduction

Over 340 million people worldwide are affected by major depression, with females comprising roughly two thirds of that number. The average age of onset is now in the 20's compared with the late 40's before World War II (Weissman *et al.*, 1996). The World Health Organisation estimate that by 2020, unipolar major depression, will become the second largest cause of global disease burden in the world, behind ischaemic heart disease (Murray *et al.*, 2001). Within the female population in the developing countries, unipolar depression is predicted to become the largest cause of disease burden (Murray *et al.*, 2001). Therefore, depression represents a major medical and social problem. Despite the last 40 years witnessing the introduction of agreed criteria e.g. Diagnostic and Statistical Manual of Mental Disorders – Fourth Edition (DSM-IV; see Table 1.6), newer, faster onset treatments and an increased understanding of the neurobiology of depression, studies indicate that roughly 30% of patients do not receive any benefit from present drugs (Doris *et al.*, 1999).

The original modern drugs used for the treatment of depression were the monoamine oxidase inhibitor (MAOI) iproniazid, and the tricyclic antidepressant (TCA) imipramine (mainly blocks noradrenaline (NA) reuptake). Both compounds were discovered fortuitously, with iproniazid being developed as a treatment for tuberculosis and imipramine as an antihistamine but tested for the treatment of schizophrenia due to the success of chlorpromazine. The discovery of these compounds' mechanisms of actions led to the catecholamine hypothesis of depression being developed in the mid-1960s. This theory stated "that some, if not all, depressions are associated with an absolute or relative deficiency of catecholamines, particularly noradrenaline (NA), at functionally

important adrenoceptor sites in the brain. Elation conversely may be associated with an excess of such amines" (Schildkraut, 1965).

Table 1.6 DSM-IV criteria for major depressive disorder

DSM-IV Criteria for Major Depressive Disorder
A. Five (or more) of the following symptoms have been present during the same 2-week period and represent a change from previous functioning; at least one of the symptoms is either (1) depressed mood or (2) loss of interest or pleasure.
(1) Depressed mood most of the day, as indicated by either subjective report (e.g. feels sad or empty) or observation made by others (e.g. appears tearful). **Note:** In children and adolescents can be irritable mood.
(2) Markedly diminished interest or pleasure in all, or almost all, activities most of the day, nearly everyday (as indicated by either subjective account or observation made by others).
(3) Significant weight loss when not dieting or weight gain (e.g. a change in more than 5 % of body weight in a month), or decrease or increase in appetite nearly everyday. **Note:** In children, consider failure to make expected weight gains.
(4) Insomnia or hypersomnia nearly every day.
(5) Psychomotor agitation or retardation nearly everyday (observable by others, not merely subjective feelings of restlessness or being slowed down).
(6) Fatigue or loss of energy nearly everyday
(7) Feelings of worthlessness or excessive or inappropriate guilt (which may be delusional) nearly everyday (not merely self-reproach or guilt about being sick).
(8) Diminished ability to think or concentrate, or indecisiveness, nearly everyday (either by subjective account or as observed by others).
(9) Recurrent thoughts of death (not just fear of dying), recurrent suicidal ideation without a specific plan, or a suicide attempt or a specific plan for committing suicide.
B. The symptoms do not meet the criteria for a mixed episode.
C. The symptoms cause clinically significant distress or impairment in social, occupational, or other important areas of functioning.
D. The symptoms are not due to the direct physiological effects of a substance (e.g. a drug of abuse, a medication) or a general medical condition (e.g. hypothyroidism).
E. The symptoms are not better accounted for by bereavement, i.e., after the loss of a loved one, the symptoms persist for longer than 2 months or are characterised by marked functional impairment, morbid preoccupation with worthlessness, suicidal ideation, psychotic symptoms or psychomotor retardation.

There is still a lack of understanding of the pathology of depression, which has hindered the development of novel therapies, and all present antidepressant therapies have a delayed onset of action with their primary action to increase the levels of monoamines in the brain. These therapies have proved very successful and remain the most widely prescribed drugs (for example, TCAs, MAOIs and uptake inhibitors). Currently, a number of novel drug targets are being examined as new antidepressants, with the hope of a more rapid onset of action and more universal effectiveness.

1.3.2 Monoamine theories of depression

The first catecholamine theory of depression was proposed by Schildkraut (1965), based mainly on the actions of reserpine (depletes catecholamine stores and to a lesser extent 5-HT), iproniazid and imipramine. It stated that a deficiency of catecholamines, particularly NA, led to some forms of depression. Evidence for this came from reserpine, a drug used in the treatment of hypertension due to its ability to decrease sympathetic activity, which was noted to cause sedation and in many instances evoke severe depression in patients. Tetrabenazine, a similar agent to reserpine, was also shown to induce depression in many patients (Lingjaerde, 1963).

In contrast, iproniazid was fortuitously noted to elevate mood in depressed patients in the early 1950s, and thereafter was shown to increase extracellular NA and 5-HT concentrations. Initially, imipramine cast doubt on the catecholamine theory because it was shown not to inhibit MAO. However, Hertting *et al.*, (1961) demonstrated that it inhibited cellular uptake of NA in peripheral tissues. This enabled imipramine to fit into the hypothesis as it, like iproniazid, elevated both mood and NA (see Figure 1.4). Moreover, both antidepressant agents were demonstrated to attenuate reserpine-induced sedation (Carlsson, 1961; Chessin *et al.*, 1957; Sulser *et al.*, 1964). Similarly,

administration of dihydrophenylalanine (DOPA; a precursor of dopamine (DA) and NA) to laboratory animals was shown to reverse reserpine-induced sedation (Carlsson *et al.*, 1957); a finding reproduced in humans (Schildkraut *et al.*, 1965). Amphetamine, which releases NA from vesicles and prevents re-uptake was also used in the treatment of depression at the time with varying success and so added further support to the catecholamine theory of depression (Schildkraut *et al.*, 1965).

Shortly after Schildkraut's catecholamine hypothesis was published, Coppen (1967) proposed that 5-HT, rather than NA, was the more important neurotransmitter in depression. This was based on similar evidence to that of the NA theory as reserpine, imipramine and iproniazid all affect the 5-HT system, in addition to the noradrenergic system (Coppen, 1967). It was also supported by work demonstrating that if catecholamine levels were depleted by up to 20 % but 5-HT neurotransmission remained unaltered, there was no sedation in animals (Brodie *et al.*, 1966). Alongside this, the main observation promoting the 5-HT theory was that administration of a MAOI in conjunction with tryptophan (precursor of 5-HT) elevated mood in control patients and potentiated the antidepressant effect of MAOI (Coppen *et al.*, 1963). Set against this, combination of a MAOI with DOPA did not produce further therapeutic benefit (Klerman *et al.*, 1963). Additionally, the therapeutic effect of MAOI and TCA drugs was later shown to be blocked by administration of 5-HT synthesis inhibitors (Shopsin *et al.*, 1976; Shopsin *et al.*, 1975).

Figure 1.4 Mechanism of NA reuptake inhibitors and α_2-adrenoceptor antagonists

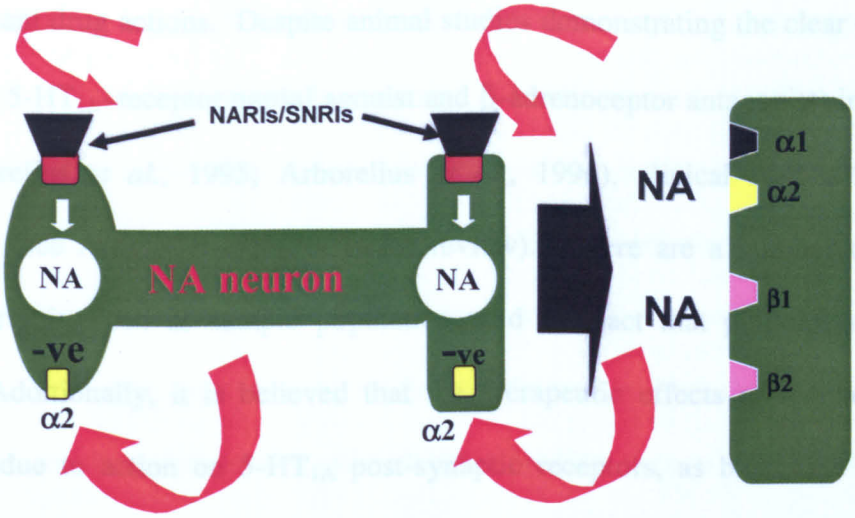

The 5-HT hypothesis gained significant weight with the introduction of the selective serotonin reuptake inhibitors (SSRI) in the mid-1980s, which soon became the main prescribed antidepressant medication. Indeed the success of SSRI's led to the role of 5-HT in depression and antidepressant therapies dominating thinking in scientific and drug company research throughout the 1980's. However, these monoamine hypotheses do not address the fact that alterations of neurotransmitters occur after acute administration of the pharmacologic agents, whereas the onset of therapeutic action requires 2-4 weeks (Doris *et al.*, 1999). Indeed, although tolerance develops to the side-effects of SSRIs, the opposite appears to be the case with their therapeutic effects continuing to grow over time (Stahl, 1998). Additionally, the fact that antidepressants do not elevate mood in healthy individuals does not fit with the original hypothesis.

The time lag in current SSRI antidepressant medications is believed, at least in part, to be due to desensitisation of 5-HT_{1A} autoreceptors, which occurs over a three to four week period (Bel *et al.*, 1993; Rutter *et al.*, 1994). The increase in 5-HT levels in response to reuptake block is partially offset by activation of these autoreceptors initially, which decreases cell firing (Gardier *et al.*, 1996). In view of this a number of

5-HT_{1A}–receptor antagonist drugs have been used in attempts to augment and accelerate antidepressant drug actions. Despite animal studies demonstrating the clear efficacy of pindolol (a 5-HT_{1A}–receptor partial agonist and β-adrenoceptor antagonist) in achieving this (Arborelius *et al.*, 1995; Arborelius *et al.*, 1996), clinical studies have been ambiguous (see Artigas *et al.*, (2001) for review). There are a number of possible reasons for this, such as sample population, and the fact that pindolol is a partial agonist. Additionally, it is believed that the therapeutic effects of increasing 5-HT levels are due to action on 5-HT_{1A} post-synaptic receptors, as buspirone (a 5-HT_{1A} agonist) displays some antidepressant properties (Rickels *et al.*, 1990; Stahl *et al.*, 1998). Therefore, the post-synaptic actions of pindolol may offset the pre-synaptic ones. A more specific compound, which only blocked somatodendritic 5-HT_{1A}-autoreceptors may be more successful in accelerating the clinical onset of current medications.

The decreased levels of NA proposed by Schildkraut, suggested that there would be a compensatory upregulation of β-adrenoceptors. Despite inconsistent findings supporting this, more consistent evidence demonstrates that chronic treatment with antidepressants and electroconvulsive therapy (ECT) decrease β-adrenoceptor density in the rat forebrain (Banerjee *et al.*, 1977; Banerjee *et al.*, 1978). This lead to the theory that β-adrenoceptor downregulation was required for clinical antidepressant efficacy (Sulser *et al.*, 1978). However, some of the newly developed antidepressants do not alter, or even increase β-adrenoceptor density (Vetulani *et al.*, 2000).

Another adrenoceptor implicated in depression is the presynaptic α_2-adrenoceptor (Leonard, 1997). Chronic desipramine (strongly inhibits NA reuptake and to a lesser extent 5-HT) treatment in rats decreased the sensitivity of α_2-adrenoceptors, a finding

supported by the fact that clonidine (α_2-adrenoceptor agonist) administration caused a significant increase in growth hormone (an indirect measure of α_2-adrenoceptor activity) although platelet studies proved inconsistent (Cheetham *et al.*, 1991). Heal *et al.*, (1991) demonstrated that chronic administration of the antidepressants, amitriptyline (inhibits catecholamine reuptake; 10 mg/kg), desipramine (10 mg/kg) or tranylcypromine (MAOI; 10 mg/kg) attenuated clonidine-induced hypoactivity and mydriasis. Moreover, post-mortem studies, performed in brains of suicide victims, demonstrate an upregulation of α_2-adrenoceptor binding sites in the prefrontal cortex (Garcia-Sevilla *et al.*, 1999), hippocampus and striatum (Callado *et al.*, 1998). These data imply a supersensitivity of α_2-adrenoceptors in depression, which has been postulated to decrease locus coeruleus (the main projection site of NA in the CNS) firing and therefore decrease NA release (Charney *et al.*, 1981; Spyraki *et al.*, 1980).

The NA theory received a major boost with the arrival of new antidepressants in the 1990s, including mirtazapine (mainly an α_2-adrenoceptor antagonist with 5-HT_2 and 5-HT_3 receptor antagonist properties), venlafaxine (inhibitor of 5-HT and NA reuptake) and in particular reboxetine (the most specific inhibitor of NA reuptake approved for treating depression). Indeed, reboxetine has been shown in clinical trials to be at least as effective as citalopram, the most specific inhibitor of 5-HT re-uptake currently available. This finding suggests that individual modulation of either NA or 5-HT neurotransmission is beneficial in treating depression. However, there is substantial interplay between the two systems, as for example, in addition to enhancing NA release, α_2-adrenoceptor antagonism also increases serotonergic neurotransmission due to blockade of α_2-adrenoceptor present on 5-HT nerve terminals (Bengtsson *et al.*, 2000).

1.3.2.1 Evidence from clinical studies:-

Post-mortem studies remain equivocal about the levels of neurotransmitters in depression and their receptors and transporters. There are numerous reports showing elevated, no alteration, or decreases in monoamine metabolite levels, monoamine receptors and uptake sites, in the studies examining them (see Cheetham *et al.,* (1991) for review). One of the more consistent findings from post-mortem brains (in addition to the α_2-adrenoceptor increase already discussed) are elevated 5-HT_2 receptor levels in the frontal cortex of suicide victims (Gross-Isseroff *et al.*, 1989; Mann *et al.*, 1986; Stanley *et al.*, 1983); a group which contains a significant proportion of depressed patients (Barraclough *et al.*, 1974). Additionally, the antidepressants mirtazapine, mianserin (non-selective 5-HT_2 receptor antagonist), trazodone (inhibits 5-HT reuptake) and nefazodone (5-HT_2 receptor antagonist and weak 5-HT reuptake inhibitor) all have 5-HT_2 receptor antagonistic properties, which decrease serotonergic side-effects associated with antidepressant treatment (de Boer, 1996; DeVane *et al.*, 2002; Fuller *et al.*, 1984; Nutt, 1997).

In order to investigate the relative mechanisms of antidepressants depletion studies have been performed over the course of the last 20 years in a further attempt to elucidate the role of NA and 5-HT and their receptors in depression. In the 1970s administration of parachlorophenylalanine (an inhibitor of tryptophan hydroxylase) produced a relapse in depressive symptoms of treated patients (Shopsin *et al.*, 1976), but it is considered too toxic for use today. Therefore, tryptophan depletion paradigms have been used to reduce 5-HT levels in the brain, and are performed by giving a drink loaded with amino acids, except tryptophan. In animals, such depletion is known to increase pain sensitivity, motor activity, aggression and decrease REM sleep, all behaviours which indicate a deficit in 5-HT function (Bel *et al.*, 1996; Kawai *et al.*, 1994; Young *et al.*,

1989). Control patients subjected to tryptophan depletion, do not demonstrate a lowering of mood (Benkelfat *et al.*, 1994; Carpenter *et al.*, 1998; Knott *et al.*, 1999). Similarly, untreated depressives subjected to this paradigm do not demonstrate any worsening of symptoms, which was a surprise as it was hypothesised that there would be a further decline in mood in response to lowering of 5-HT levels (Delgado *et al.*, 1994; Price *et al.*, 1997; Price *et al.*, 1998). This could be due to the fact that the 5-HT system is already diminished and that a further decline has no effect, or that downstream responses to 5-HT function are the main component of depression. However, in an SSRI treated group, tryptophan depletion causes a relapse in depressive symptoms and especially in those whose symptoms had remitted for under 2 weeks while having little effect on patients treated with mainly NA drugs (Bremner *et al.*, 1997; Delgado *et al.*, 1991; Nutt *et al.*, 1999). The opposite holds true for catecholamine depletion studies using α-methyl-*p*-tyrosine (an inhibitor of tyrosine hydroxylase). This is suggestive that there are subsets of patients where either 5-HT or NA is the more important neurotransmitter in depression. Additionally, patients treated with noradrenergic drugs relapse more frequently than those treated with serotonergic antidepressants (Miller *et al.*, 1996).

Figure 1.5 Mechanism of action of 5-HT reuptake inhibitors and pindolol

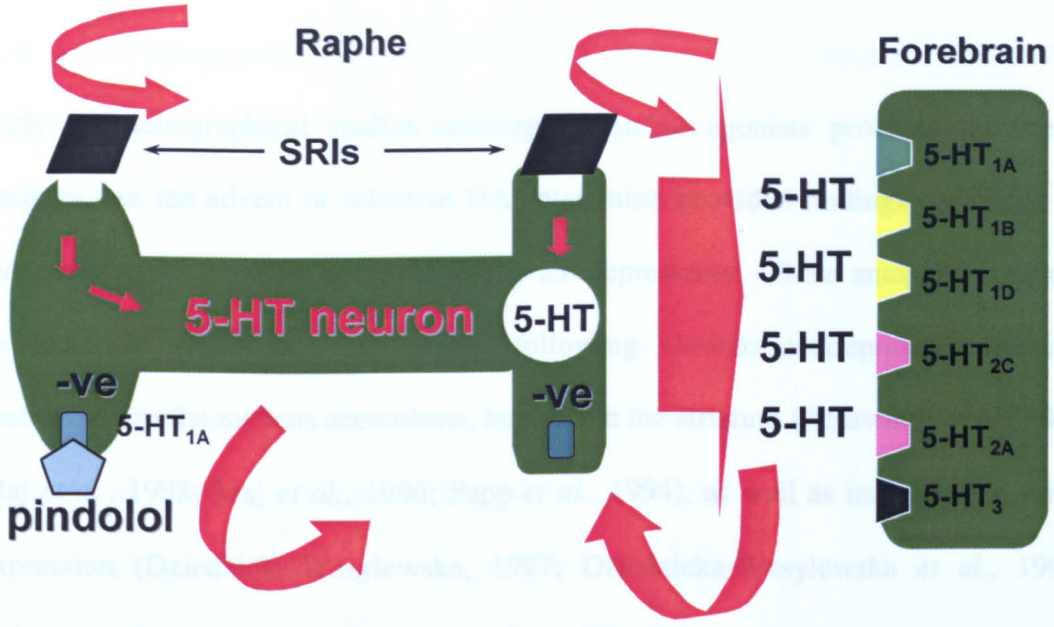

1.3.2.2 Dopamine

With discrepancies emerging regarding the NA and 5-HT theories of depression, the 1970s saw DA postulated to play a critical role in depression and antidepressant action. It had been known that drugs such as amphetamine and cocaine elevated mood as well as DA release, but not in depressed patients (Schildkraut, 1965). This knowledge, coupled with the knowledge that reserpine depletes DA, in addition to NA and 5-HT, to produce sedation and severe depression in some patients provided evidence for DA playing a significant role in depression. Additionally, Serra *et al.,* (1979) examined the role of antidepressants on dopaminergic neurotransmission, demonstrating that chronic imipramine, amitriptypline and mianserin treatment prevented or reversed the sedative effect of low doses of apomorphine (D_1- and D_2-receptor agonist). This finding has since been replicated with other antidepressants, ECT treatment and REM-sleep deprivation (Collu *et al.*, 1997; D'Aquila *et al.*, 1997; D'Aquila *et al.*, 2000). These effects are believed to reflect an increased sensitivity of postsynaptic DA receptors

induced by chronic antidepressant treatment, as opposed to the initial belief that these findings reflected a subsensitivity of D_1-autoreceptors (D'Aquila *et al.*, 2000).

Early autoradiographical studies utilising dopamine agonists provided inconsistent findings, but the advent of selective DA antagonists provided findings consistent with DA postsynaptic receptor upregulation by antidepressants. These antagonists revealed an increased D_2/D_3-receptor number following chronic antidepressant treatment, particularly in the nucleus accumbens, but also in the striatum (Ainsworth *et al.*, 1998b; Maj *et al.*, 1998; Maj *et al.*, 1996; Papp *et al.*, 1994), as well as increased D_2 mRNA expression (Dziedzicka-Wasylewska, 1997; Dziedzicka-Wasylewska *et al.*, 1997a). This may relate, in part to, the therapeutic profile of the antidepressants, given the role of the nucleus accumbens, which is impaired in depressed patients (Di Chiara, 2002; Drevets, 2000). A recent animal study by Lammers *et al.*, (2000) reported that a common effect of chronic antidepressant treatment was a selective increase in D_3 receptor gene expression in the shell of the nucleus accumbens. Desipramine, imipramine, amitriptyline and tranylcypromine all elevated D_3 mRNA in this region after 21-day treatment. Interestingly, fluoxetine following 42-day administration, despite significantly decreasing D_3 mRNA levels, prevented the down-regulation of D_3-receptors caused by handling stress, as did imipramine. ECT produced the largest increase of the treatments, both mRNA and D_3 receptor number, which is an accordance with clinical efficacy (Lammers *et al.*, 2000). This finding may have implications for depression and may provide a novel target for new antidepressants but requires further verification.

Lending weight to the DA theory of depression are a number of dopaminergic compounds, which have been successful in treating depression; bupropion (weak

inhibitor of DA, NA and 5-HT uptake; Rudorfer *et al.*, 1984), nomifensine (inhibitor of DA and NA-uptake; Feighner *et al.*, 1984; Goldstein *et al.*, 1984)) and amineptine (inhibitor of DA reuptake; Garattini, 1997). Pramipexole (D_3-receptor agonist) has been approved for use in Parkinson's disease but has also been shown in two animal models, the forced swim test and exposure to chronic stress, to be antidepressant-like (Maj *et al.*, 1997; Willner *et al.*, 1994). Although no large scale clinical trials have been performed, a small-scale trial by Ostow with 22 patients, demonstrated not only that pramipexole augmented previously ineffectual antidepressant treatments, but that it significantly improved mood alone with relatively few side-effects (Ostow, 2002). However, it is clear that a larger trial will have to be performed to validate these findings.

Another line of evidence supporting a role of DA in depression comes from Keck *et al.*, (2002), who successfully demonstrated that repetitive transcranial magnetic stimulation (rTMS) elevates DA in the hippocampus, nucleus accumbens and striatum. A previous study by Keck *et al.*, (2000) revealed an increase in DA but not in 5-HT and NA in the hippocampus, providing evidence that DA may play a role in the use of rTMS in depression. These findings have also been supported by a clinical study showing that rTMS decreased [^{11}C]raclopride (D_2, D_3 and D_4 receptor antagonist) binding (Strafella *et al.*, 2001). This evidence is suggestive of alterations in the dopaminergic system in depression, which, at least partially, are redressed by antidepressant treatments. However, it is unknown whether this is secondary to changes in other monoaminergic systems given the interaction between DA and these.

Taken as a whole, the body of literature dealing with monoamine deficits in depression does not satisfactorily provide clear evidence for one neurotransmitter being central to the aetiology. Both serotonergic and noradrenergic compounds are equally useful in

treating patients, and there are also a number of dopaminergic drugs that are successful in treating depression. This may also reflect different underlying heterogeneity of depressive disorders. It is clear that these drugs, which raise monoamine levels in the synapse, have been very successful in the treatment of depression. What still remains unclear is whether disruption of these systems initiates depressive symptoms.

Figure 1.6 Summary of monoamine drug treatment evolution

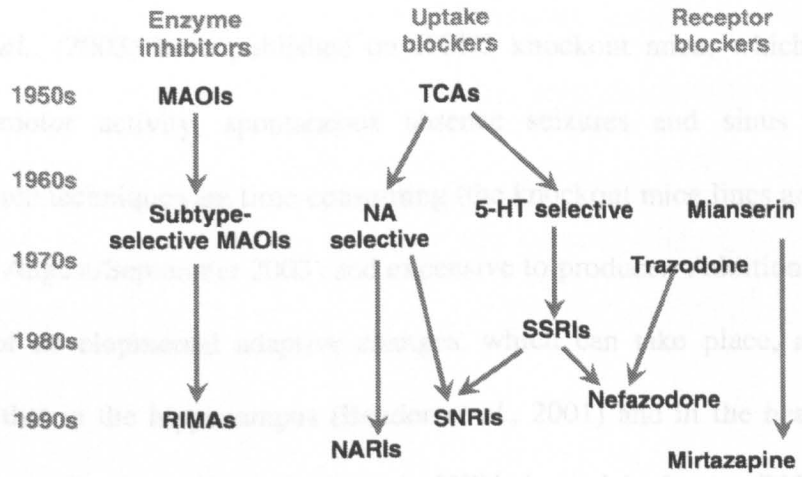

Abb: NARIs = NA selective reuptake blocker; RIMAs = Reversible inhibitor of MAO; SNRIs = 5-HT and NA selective reuptake inhibitor.

1.3.3 Novel approaches to research the proposed role of I_h channels in depression

The lack of selective ligands for I_h/HCN channels has hindered further insight into the potential role of this channel in depression, and other behaviours it may contribute to, such as epilepsy (see Chen *et al.*, (2002) for review). There are a number of genetic approaches, which are presently being taken by Organon Laboratories to address this issue, including the generation of HCN1 and HCN2 isoform knockout mice. Indeed, Ludwig *et al.*, (2003) have published on HCN2 knockout mice, which demonstrate lower locomotor activity, spontaneous absence seizures and sinus dysrhythmia. However, such techniques are time-consuming (the knockout mice lines are predicted to be ready in August/September 2003) and expensive to produce. Additionally, there are a number of developmental adaptive changes, which can take place, and given the knowledge that in the hippocampus (Bender *et al.*, 2001) and in the heart (Shi *et al.*, 1999) there are developmental alterations in HCN channel isoform mRNA expression, make interpretation of data obtained from knockout mice more complicated.

An alternative approach is the use of antisense technology, which utilises the administration of a short synthetic oligonucleotide (< 25 bases), complementary to the target gene's mRNA sequence, to specifically and reversibly inhibit gene expression (See Section 1.4). In this manner a specific HCN isoform can be targeted, and if successful down-regulation of the gene is observed *in vivo*, rats can be introduced to a variety of behavioural paradigms and biochemical assays to ascertain the effect of down-regulation of HCN protein.

1.4 Antisense oligonucleotide technology

1.4.1 Introduction to antisense

Antisense technology was first utilised by Zamenik and Stephenson (1978), who injected a complementary phosphodiester oligonucleotide to the Rous sarcoma virus, in chicken embryo fibroblasts tissue cultures, and inhibited virus production. Since then, antisense technology has expanded and become a commonly used laboratory technique to reversibly inhibit mRNA translation. With increasing knowledge of this technique, modifications to the phosphodiester structure have been implemented to improve the antisense sequence stability and lower toxicity. In theory, any mRNA sequence which is known, can be targeted to downregulate the corresponding protein expression, thereby providing a powerful tool for the study of specific gene products, both *in vitro* and *in vivo*.

1.4.2 Mechanism of antisense-mediated action

Antisense oligonucleotides are believed to exert their biological action, down-regulation of a target protein, *via* numerous mechanisms due to the complexity of mRNA. There are a number of theoretical mechanisms by which antisense oligonucleotides may act and while experimental evidence for some of these has been demonstrated the precise manner by which antisense oligonucleotides achieve their goal remains to be fully established. There are two main mechanisms, which have been demonstrated to be responsible for knockdown of the target protein; steric hindrance and RNase H-mediated degradation of the mRNA.

1.4.2.1 Steric hindrance

The majority of antisense sequences designed by early antisense workers were complementary to the initiation-encoding region of an mRNA as disruption of this vital region was believed to lead to the greatest down-regulation. The mechanism of action responsible for sequences targeted here is believed to be steric hindrance of the ribosome; a mechanism which could be employed anywhere along the entire length of the mRNA.

Figure 1.7 Example of steric hindrance of translation.

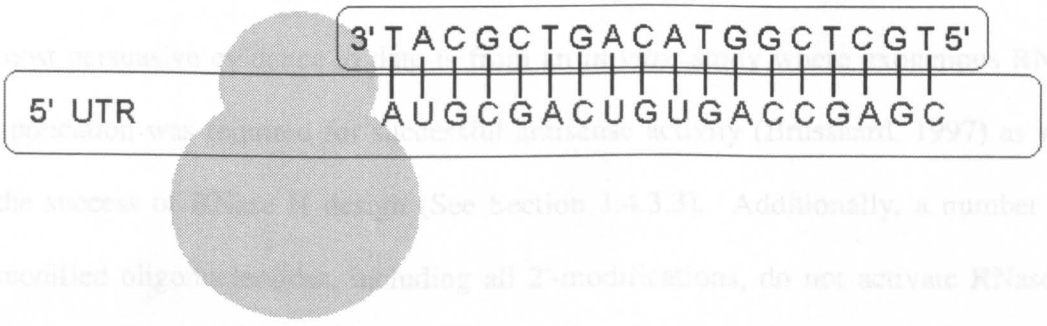

The antisense sequence targeted to the initiation-encoding region of the mRNA prevents the ribosome from binding to and scanning the message. A similar effect can occur wherever the antisense is targeted along the entire length of the mRNA. Abb: 5' UTR, 5' untranslated region

Another possible outcome of antisense binding may be to alter the overall RNA spatial structure, which in turn could prevent the binding and interaction of a number of factors such as the ribosome, or indeed even destabilise the RNA molecule (Crooke, 1999).

1.4.2.2 RNase H activated degradation

An alternative mechanism of action of antisense oligonucleotides, which has been demonstrated *in vitro,* is cleavage of the mRNA *via* activation of a ubiquitous enzyme, ribonuclease H (RNase H). This enzyme selectively cleaves the RNA strand of a RNA/DNA duplex (Zamaratski *et al.,* 2002). The cleaved RNA products then undergo

further degradation by 5' and 3' exonucleases while the antisense sequence is freed to bind to another complementary target, effectively making the process catalytic (Figure 1.8). It is this mechanism of antisense-mediated protein inhibition that makes it beneficial for oligonucleotides to comprise of DNA-like regions, such as phosphodiester or phosphorothioate linkages (see Section 1.4.4). This increases their likelihood of successful antisense activity *via* this mechanism.

Activation of RNase H has been demonstrated in numerous studies; Toulme *et al.*, (1992) demonstrated that oligonucleotides targeted at the coding region were unsuccessful unless RNase H-mediated cleavage of mRNA occurred. However, the most persuasive evidence to date is from an *in vitro* study where exogenous RNase H application was required for successful antisense activity (Brussaard, 1997) as well as the success of RNase H design (See Section 1.4.3.3). Additionally, a number of the modified oligonucleotides, including all 2'-modifications, do not activate RNase H as the cleavage reaction occurs at the 2'-OH of the RNA strand (Zamaratski *et al.*, 2001) and are less active. The only backbone modifications, which form duplexes that have been shown to activate RNase H are phosphodiester, phosphorothioates (Stein *et al.*, 1993) and boranophosphates (Rait *et al.*, 1999a; Rait *et al.*, 1999b). In fact, it has recently been implied that RNase H may play a critical role in the unravelling process of RNA enabling the oligonucleotide to bind (Zamaratski *et al.*, 2001). The extent to which RNase H activation is necessary for successful antisense application may depend on the oligonucleotide and the system used as it has been shown that RNase H activity is quite low in the cytoplasm of neurones compared to that of the nucleus (Crum *et al.*, 1988).

Figure 1.8 Example of RNase H-mediated antisense action.

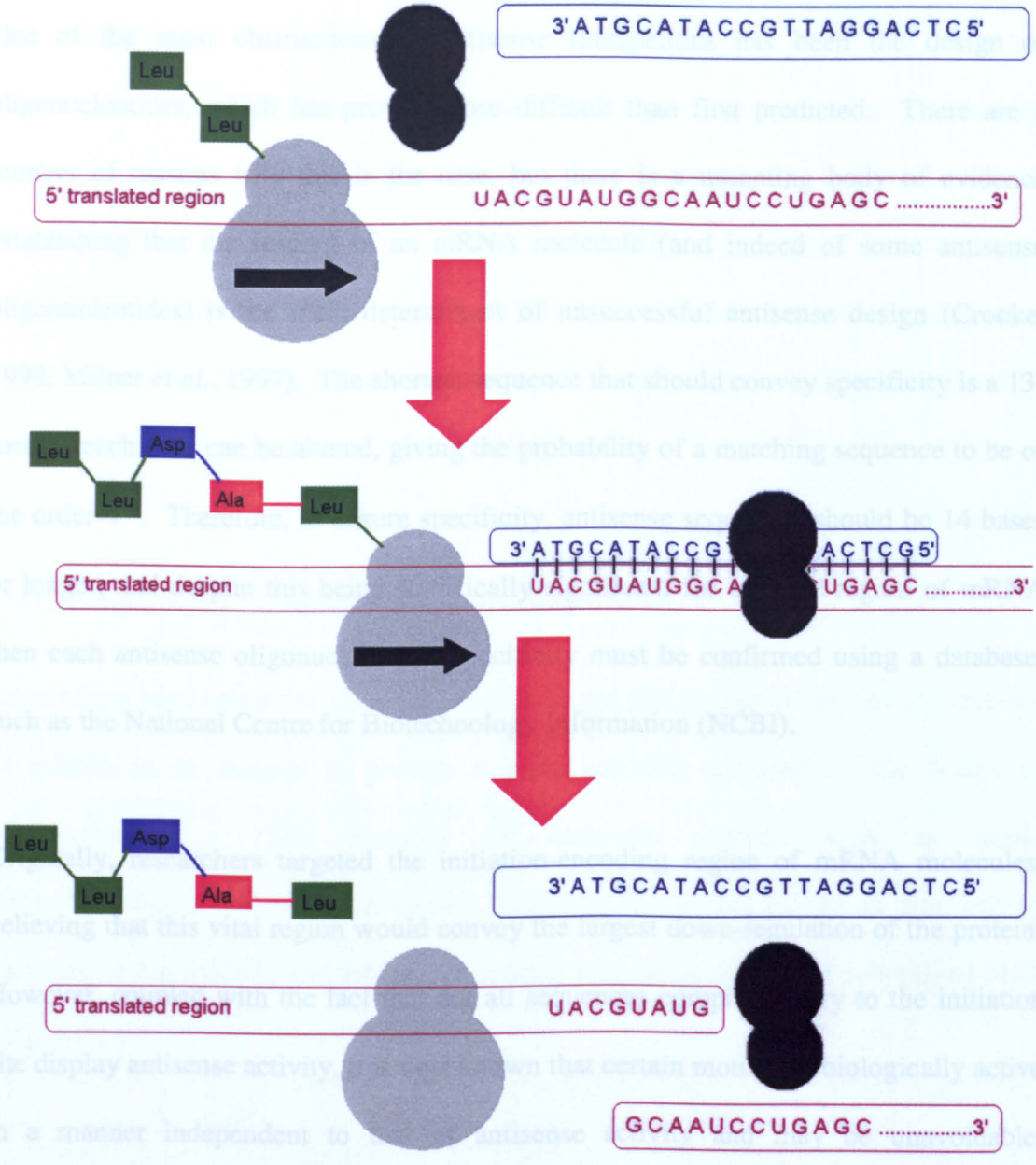

The formation of a RNA/DNA duplex activates RNase H (black) which selectively cleaves the RNA strand (red), leaving the antisense oligonucleotide free to bind to another complementary target. The resulting RNA cleavage products are further degraded by 5' and 3' exonucleases, and the growing polypeptide chain (green) is also degraded.

1.4.3 Design of antisense oligonucleotide sequences

One of the main obstructions of antisense therapeutics has been the design of oligonucleotides, which has proved more difficult than first predicted. There are a number of reasons why this is the case, but there is a mounting body of evidence establishing that the folding of an mRNA molecule (and indeed of some antisense oligonucleotides) is the main determinant of unsuccessful antisense design (Crooke, 1999; Milner *et al.*, 1997). The shortest sequence that should convey specificity is a 13-mer, as each base can be altered, giving the probability of a matching sequence to be of the order 4^{13}. Therefore, to ensure specificity, antisense sequences should be 14 bases or longer, and despite this being statistically significant for a single region of mRNA then each antisense oligonucleotide's specificity must be confirmed using a database, such as the National Centre for Biotechnology Information (NCBI).

Originally, researchers targeted the initiation-encoding region of mRNA molecules, believing that this vital region would convey the largest down-regulation of the protein. However, coupled with the fact that not all sequences complementary to the initiation site display antisense activity, it is now known that certain motifs are biologically active in a manner independent to that of antisense activity and may be unavoidable. Additionally, the initiation-encoding region is highly conserved, which may result in a loss of specificity of the sequence (Cooper *et al.*, 1999). It has been demonstrated that numerous accessible sites for antisense molecules can exist along the entire length of an mRNA, from the 5'-untranslated region to the 3'-polyadenylated tail (Agrawal *et al.*, 2000), and it is considered advantageous to test oligonucleotides over a wide region of the mRNA.

1.4.3.1 Random design

This method involves designing a large number of sequences (up to 100) that are complementary to regions along the length of the target mRNA, and then individually assessing each one. Unsurprisingly, this approach does not yield a high proportion of successful sequences, only 2 – 5 % (Sohail *et al.*, 2000) and is labour intensive, time-consuming and expensive. However, it avoids oligonucleotides that are complementary to other mRNAs and also immuno-active motifs (see Section 1.4.4.2) that may not be possible when targeting the initiation-encoding region.

1.4.3.2 Secondary structure prediction design

Researchers have employed computational packages that predict the secondary structure of mRNA in an attempt to provide a more scientific approach to the design of oligonucleotides. The majority of computer models, such as mfold (http://bioinfo.math.rpi.edu/~mfold/rna/), calculate the global minimum free energy structure of the mRNA, and returns an optimal fold and a number of suboptimal folds (Figures 1.9).

Figure 1.9 Example of a predicted mRNA secondary structure using the computer package mfold.

The chain like structures are areas where the mRNA folds back upon itself, while the circular patterns are predicted to be single-stranded and therefore areas were antisense oligonucleotides would be targeted.

Oligonucleotides can then be designed to target the regions, which are predicted to be predominantly single-stranded and then examined for antisense activity. There are a number of inherent weaknesses involved in computational prediction. These predominantly stems from the lack of understanding of RNA secondary and tertiary structure at present (Sohail *et al.*, 2001). A histogram can be generated based on all the predicted structures by plotting the single-stranded frequency of each base (see Figure 1.10) in an attempt to isolate areas, which are predicted to be predominantly single-stranded. Computer packages do not account for any tertiary folding which may occur, or interactions with cytoplasmic proteins, and instead treat the mRNA as an isolated entity, which further detract from the accuracy of the predicted folds (Stein, 1999).

Figure 1.10 Example of a single-stranded frequency histogram based on the folds predicted by mfold.

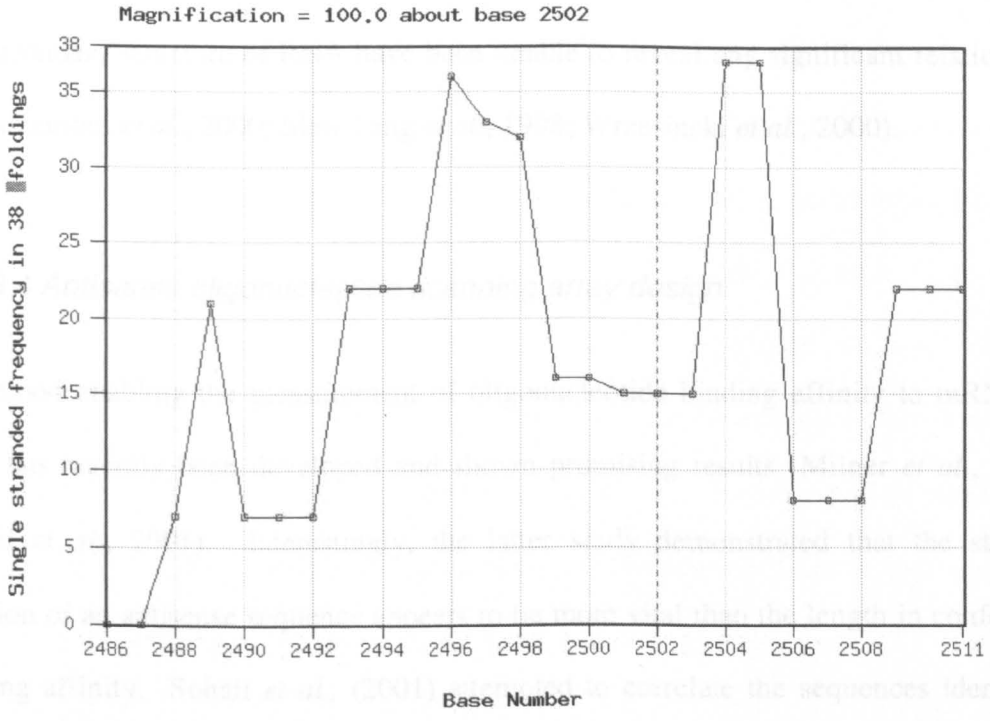

The x-axis represents the base number and the y-axis the single-stranded frequency. By analysing the entire mRNA in this way areas which are predicted to be predominantly single-stranded can utilised to design antisense oligonucleotides.

Conflicting findings on the success of oligonucleotide sequences subjected to this method have been reported (Amarzguioui *et al.*, 2000; Wrzesinski *et al.*, 2000). Although this method may represent an improvement over random design of oligonucleotides, until the computer methods employed to predict the structure of mRNA molecules are more accurate, the usefulness of this method is limited.

1.4.3.3 Ribonuclease H mapping design

The knowledge that certain oligonucleotides activate RNase H (See Section 1.4.2.2) has been incorporated into the design of antisense oligonucleotides and has shown promising results to date. A number of researchers have demonstrated that the sites identified by RNase H digestion of *in vitro* transcribed mRNA correlate to antisense

sequences, which are active *in vitro* (Matsuda *et al.*, 1998) and *in vivo* (Matveeva *et al.*, 1997). However, attempts to correlate sequences identified by RNase H mapping with the secondary structure of RNA have been unable to reveal any significant relationship (Amarzguioui *et al.*, 2000; Slew Peng *et al.*, 1998; Wrzesinski *et al.*, 2000).

1.4.3.4 Antisense oligonucleotide scanning array design

A method enabling the measurement of oligonucleotide binding affinity to mRNA *in vitro* has recently been developed and shown promising results (Milner *et al.*, 1997; Sohail *et al.*, 2001). Interestingly, the latter study demonstrated that the starting position of an antisense sequence appears to be more vital than the length in conferring binding affinity. Sohail *et al.*, (2001) attempted to correlate the sequences identified using a scanning array with mfold analysis of the secondary structure of mRNA in order to describe the specific hybridisation pattern found but could show no relationship. Alternatively, good correlation has been demonstrated between sequences predicted by RNase H digestion and those by scanning arrays and also with antisense activity *in vitro* (Milner *et al.*, 1997). Not all sites identified by hybridisation affinity translate to active antisense sequences, although there does appear to be a high level of success using this method, and this, along with RNase H mapping promise to improve oligonucleotide design.

1.4.4 Experimental controls

1.4.4.1 Introduction

Experimental controls are vital when using antisense oligonucleotides. They are required to ensure that the measured biological effect results from knockdown of the target protein and not from non-specific toxicity. Positive controls are antisense

sequences designed to be complementary to another region along the mRNA molecule. This type of control is recommended if there exists no method for directly measuring the protein level of a target gene and should alter the target mRNA levels, or demonstrate the same behavioural phenotype (Brysch, 1999). However, due to the lack of accessible sites and the number of different possible antisense mechanisms it is often difficult to design a positive control, which satisfies all the design criteria. There are a variety of negative controls, which can be designed to validate that the measured parameter of an antisense infusion is due to target gene downregulation and these must be designed to fulfil a number of criteria (see Table 1.7). To date, no one control can rule out all the other possible oligonucleotide administration factors, and therefore suitable controls for each individual experiment must be designed.

There are four main negative controls used in antisense experiments (See Table 1.8) and of these mismatch controls are the most commonly utilised. Mismatches incorporate base switches from the antisense control, and those introduced in the centre of a sequence have more effect than peripheral swaps as there are less consecutive complementary bases (Brysch, 1999). Furthermore, the bases which are swapped play a crucial role in ensuring that a mismatch sequence does not retain hybridisation affinity for the target mRNA. The general rule for base changes from greatest effect to least is G → A/T > C → A > G/C → C/G > A/T → G > A → C > A/T → T/A (A, adenine, C, cytosine, G, guanine, T, thymine; Brysch, 1999).

Table 1.7 Design criteria for antisense oligonucleotide controls

DESIGN CRITERIA FOR NEGATIVE ANTISENSE CONTROLS
The same length and modifications as the antisense oligonucleotide
Retain similar base composition as the antisense oligonucleotide
No ability (or decreased) to bind to the target mRNA or any other cellular mRNA
Avoidance of active sequence motifs, unless present in the antisense oligonucleotide

Table 1.8 Negative controls for use in antisense experiments

CONTROL	DESIGN	ADVANTAGES	DISADVANTAGES	REFERENCES
Sense	Identical to target mRNA sequence	Easily designed Retain similar base composition Good indicator of oligo administration effects	May not retain biologically active motifs Unexpectedly high level of biological activity	(Brysch, 1999) (Le Corre *et al.*, 1997) (Georgieva *et al.*, 1995)
Random	Randomise bases of antisense sequence	Easily designed Good indicator of oligo administration effects	May not retain similar base composition May not retain biologically active motifs	(Brysch, 1999)
Mismatch	Introduction of base switches to the antisense sequence	Retain large percentage of original sequence Good indicator of oligonucleotide specificity Active motifs retained	May bind to target mRNA	(Brysch, 1999)
Reverse	Alteration of 5' to 3' orientation of antisense sequence	Retain GGGG motif Retain same base composition	May be complementary to another mRNA May lose or gain biologically active motifs	(Brysch, 1999)

1.4.4.2. Biologically active sequence motifs

It has become apparent that not all sequences reported to successfully inhibit expression have achieved this 'success' *via* knockdown of the target protein. A reason for this is the presence of motifs within an antisense sequence, which cause biological effects, such as immune stimulation, unrelated target gene knockdown. These include, CG bases with a phosphorothioate linkage (CpG), which is immunostimulatory (Yu *et al.*, 2002) and GGGG, which can form tetrads and bind to a variety of proteins (Anselmet *et al.*, 2002).

1.4.5 Backbone Modifications

When Zamecnik and Stephenson (1978) first developed the idea of administering antisense to down-regulate the expression of a target protein 'natural' phosphodiester oligonucleotides were used. There have been numerous backbone modifications employed in a bid to optimise the stability and lower the toxicity of antisense administration, both *in vivo* and *in vitro*. No ideal backbone modification has been developed for use in antisense therapeutics, but a number of important properties have been identified (Table 1.9).

Table 1.9 Optimal antisense oligonucleotide properties for use *in vivo*.

DESIRED PROPERTIES OF ANTISENSE OLIGONUCLEOTIDES
Maximal cellular uptake
Protection against degradation by nucleases
High affinity for mRNA
Ability to bind specifically to target mRNA
Activation of RNase H by forming RNA/DNA duplex

1.4.5.1 Phosphodiester oligonucleotides

Phosphodiester backbone oligonucleotides (Figure 1.11) were the first generation of antisense molecules used for inhibiting protein expression. They display high affinity for target mRNA sequences and the resultant duplex activates RNase H-mediated cleavage of the mRNA strand (Agrawal *et al.*, 1990).

Figure 1.11 Example of a phosphodiester backbone.

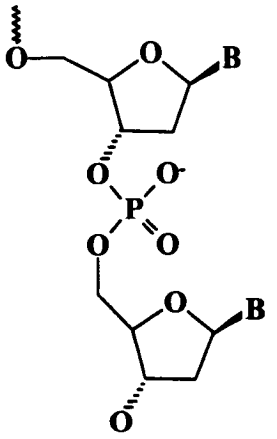

Despite the size and the polyanionic nature of phosphodiester oligonucleotides numerous studies have demonstrated that they are internalised, especially *in vivo* (Lebedeva *et al.*, 2000). However, *in vitro* uptake of all types of oligonucleotide is less effective and may require the use of a carrier system to transport the oligonucleotide into the cell and this is believed to be due to the fact that internalisation of oligonucleotides is an active process (Lebedeva *et al.*, 2000).

The rational for backbone modification was primarily to increase stability due to the rapid degradation of phosphodiester oligonucleotides by nucleases. Pharmacokinetic studies have shown that, *in vitro,* phosphodiester oligonucleotides display a half-life of ~ 5 min (Agrawal *et al.*, 1997a). This rapid breakdown of the molecules necessitates

repeated, or continuous, administration of large dose of the oligonucleotide in order to achieve a sufficient concentration inside the cell to inhibit translation. However, the brain and cerebrospinal fluid (CSF) contains relatively few nucleases and these oligonucleotides have been successfully utilised *in vivo* (Kathmann *et al.*, 1999; Kolesnikov *et al.*, 1997; Wahlestedt *et al.*, 1993).

1.4.5.2 Phosphorothioate oligonucleotides

Phosphorothioate oligonucleotides were developed in an attempt to overcome the problem of nuclease stability by substituting one of the non-bridging oxygen atoms in the phosphate backbone with a sulphur atom (Figure 1.12). The half-life of the antisense oligonucleotides containing this backbone modification is markedly improved, as a result of a 100 – 300 fold increase in nuclease resistance (Cummins *et al.*, 1995). The pharmacokinetic analysis of a single intravenous injection of phosphorothioate antisense oligonucleotides showed an initial plasma half-life of 0.95 h compared with the aforementioned 5 min half-life of phosphodiester oligonucleotides (Agrawal *et al.*, 1997a).

Figure 1.12 Example of a phosphorothioate backbone.

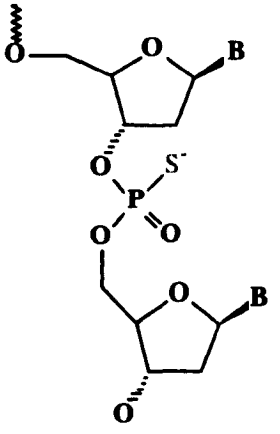

One of the non-bridging oxygen atoms is replaced by a sulphur atom.

The addition of a sulphur atom also provides another benefit, as phosphorothioate oligonucleotides demonstrate high binding affinity to a number of cell-surface proteins, which is a crucial stage before internalisation into an endocytic compartment and then into the cell nucleus (Lebedeva *et al.*, 2000). Phosphorothioate oligonucleotides retain affinity for mRNA, although not as high as that displayed by phosphodiesters (Agrawal, 1996). Phosphorothioate oligonucleotides also activate RNase H upon the formation of the duplex but to a lesser extent than phosphodiester oligonucleotides, possibly due to higher duplex stability or inhibition of RNase H catalytic activity at high concentrations (Agrawal *et al.*, 1990; Gao *et al.*, 1992).

However, the price to pay for the addition of a sulphur moiety is increased toxicity compared with phosphodiester oligonucleotides. Although, phosphorothioate antisense administration does demonstrate high tolerability in rats and mice, with an LD_{50} (lethal dose) of 500 mg/kg (Agrawal *et al.*, 1997a). However, there are a number of dose dependent side effects, including splenomegaly, thrombocytopenia and elevation of liver transaminases (see Agrawal *et al.*, (1997a) & Levin, (1999) for reviews). Intravenous injection of phosphorothioate oligonucleotides also dose-dependently causes complement activation, prolongation of activated partial thromboplastin time (Kandimalla *et al.*, 1998) and increased arterial blood pressure in monkeys (Agrawal *et al.*, 1997a). These undesirable effects can be avoided by altering the administration rate or route. These side effects are related to the polyanionic nature of phosphorothioate antisense oligonucleotides as other polyanionic molecules, such as dextran sulphate, show similar biological effects when administered (Agrawal *et al.*, 1997a).

1.4.5.3 Newer modifications and Mixed backbone oligonucleotides

The bid to optimise antisense therapeutics has led to new generation of chimeric oligonucleotides, which incorporate different modifications into one antisense oligonucleotide. The idea behind such oligonucleotides is to decrease the undesired effects of phosphorothioate oligonucleotides and introduce the favourable characteristics of other modifications, while retaining RNase H activity. Many different modifications have been attempted but 2'-O-methyl ribonucleotides and methylphosphonates are the most extensively studied due to their advantageous properties (See Table 1.10).

Mixed backbone oligonucleotides can incorporate the changes at either the 5'- or 3'-end of the sequence (End-modified) or at the centre (Centrally-modified) but at least four contiguous phosphodiester or phosphorothioate linkages are required to retain an oligonucleotide, which forms a duplex that activates RNase H (Shen *et al.*, 1998). These oligonucleotides combine the advantageous properties of each modification and the disadvantages are minimised i.e. toxicity is decreased due to less sulphur linkages and RNase H activation is incorporated. These oligonucleotides are becoming the most commonly utilised in antisense therapeutics for the reasons listed above and Table 1.10.

Table 1.10 General properties of different antisense oligonucleotide backbone modifications

BACKBONE MODIFICATION	ADVANTAGES	DISADVANTAGES	REFERENCES
2'-O-Methyl 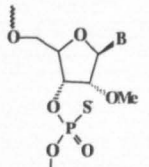	↑ nuclease stability over PO-oligo ↓ toxicity	Duplexes do not activate RNase H	(Iribarren *et al.*, 1990; Metelev *et al.*, 1994; Shen *et al.*, 1998)
Methylphosphonate 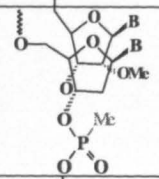	↓ toxicity ↑ nuclease stability over PO-oligo	Duplexes do not activate RNase H	(Qiuyan *et al.*, 1996; Sarin *et al.*, 1988; Shaw *et al.*, 1997)
2'-O-Methyl MBOs 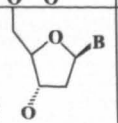	↓ toxicity ↓ binding to plasma proteins ↑ affinity for target mRNA ↑ activation of RNase H	↓ metabolic stability (unless PS-linkage in backbone)	(Agrawal *et al.*, 1997b; Agrawal *et al.*, 1999; Crooke *et al.*, 1996; Metelev *et al.*, 1994; Shaw *et al.*, 1997; Shen *et al.*, 1998)
Methylphosphonate MBOs	↓ toxicity ↑ nuclease resistance	↓ affinity for target protein ↓ RNase H activation	(Agrawal *et al.*, 1997b; Agrawal *et al.*, 1999; Giles *et al.*, 1992)

The advantages and disadvantages listed are compared to phosphorothioate oligonucleotides unless otherwise stated. Abb: PO-oligo, phosphodiester oligonucleotide, MBO, mixed backbone oligonucleotide.

1.4.6 Antisense technology in the CNS

There are numerous examples of successful application of antisense oligonucleotides directly into the CNS in the literature. These studies have utilised different chemical modifications, from unmodified phosphodiesters (*Shaker-like* Kv1.1; Kathmann *et al.*, (1999); neuronal nitric oxide synthase, Kolesnikov *et al.*, (1997); N-methyl-D-aspartate (NMDA) receptor, Wahlestedt *et al.*, (1993), phosphorothioate (m1 muscarinic receptor, Zang *et al.*, (1994); D2-receptor, Zhou *et al.*, (1994), to newer modifications including end-capped oligonucleotides; prodynorphin, Broberger *et al.*, (2000). Unlike *in vitro* assays, antisense oligonucleotide application *in vivo* does not require a carrier system, as the examples above involve administration of the oligonucleotide alone; either *via* osmotic minipumps or direct application. This repeated or continuous infusion is necessary because of the breakdown of antisense oligonucleotides by nucleases (Crooke, 1999; Sands *et al.*, 1995). As witnessed by the examples cited, antisense technology can be used to target proteins as diverse as receptors, ion channels and enzymes, and have provided valuable information regarding their *in vivo* functions. Antisense oligonucleotides are particularly beneficial for studying proteins which have no (or few) selective ligands, as is the case for I_h channels. They can provide selective and reversible knockdown of the target protein enabling behavioural and biochemical measurements to be performed (Robinson *et al.*, 2000).

1.5 The present study

Investigation of I_h channels have been limited by the lack of highly selective ligands and it is currently unknown whether Org 34167 mediates its proposed antidepressant-like action *via* these channels. Antisense oligonucleotides provide an *in vivo* technique to investigate the behavioural effects of downregulation of HCN channel isoforms in rat. It would then be possible to determine whether functional downregulation of the proposed molecular identity of I_h channels effected a similar antidepressant-like action by performing behavioural and biochemical tests. Another novel approach to assist the understanding of the effects of Org 34167 is to study the expression profile of immediate-early genes, such as *c-fos* and Egr-1. Induction of these genes is widely believed to correlate to increased neuronal activity and lead to long term alterations in cellular phenotype (Beckmann *et al.*, 1997; Chaudhuri, 1997; Herdegen *et al.*, 1998; Herrera *et al.*, 1996; Ziolkowska *et al.*, 2002). This can provide information related to brain regions that are affected by drug administration. Finally, drug treatment has been shown to modulate gene expression in a number of different systems, and can be used to determine whether chronic administration alters HCN mRNA levels. The main aims of this project were therefore:

1. To design and characterise antisense oligonucleotide sequences to the HCN 2 transcript *in vivo*, using 3- or 7-day administration to identify an antisense sequence which downregulated HCN 2 mRNA or protein expression.

2. To profile the effect of Org 34167, on *c-fos* and Egr-1 mRNA expression throughout the rat brain and compare these with known antidepressants.

3. To determine the effects of chronic administration of Org 34167 and a number of antidepressants on the expression levels of HCN 1 – 3 mRNA in the rat brain.

Chapter 2 Antisense approaches to the HCN channel

2.1 Introduction

The lack of selective ligands to modulate I_h channel has hindered insight into the functions mediated by the channel *in vivo*. Despite substantial knowledge concerning the structural and physical properties of I_h and HCN channels, relatively little is known regarding their physiological functions. As discussed in Section 1.2, I_h channels regulate rhythmicity of neuronal networks, and their interaction with Ca^{2+} channels in the thalamus generates spindle waves during sleep (McCormick *et al.*, 1997). This involvement, in the sleep-wake cycle, is to date, the main evidence (alongside Org 34167) supporting a possible role of these channels in depression, given the altered sleep patterns witnessed in depressed patients and animal models (Thase, 1999). Additionally, it has recently been proposed that these channels, couple presynaptically with the vesicular release machinery to increase neurotransmitter release, which provides another possible link (Beaumont *et al.*, 2000).

It is still unconfirmed that Org 34167's antidepressant-like activity is due to blockade of HCN channels. A possible approach to address this is the use of antisense technology, to specifically and reversibly inhibit protein expression (See Section 1.4). In this manner a specific HCN isoform can be targeted, and if successful down-regulation of the protein is achieved *in vivo*, rats can be introduced to a number of behavioural paradigms to ascertain the effects of down-regulation of the HCN isoform as well as challenging the rats with Org 34167. As the half-life of the HCN channel is unreported, both 3- and 7-day antisense infusion periods were attempted to ensure sufficient administration time to down-regulate expression. Other ion channels, such as the Na^+ channel and two subunits of the NMDA ion channel have half-lives in the range of 10 –

18 h (Chen *et al.*, 1997; Monjaraz *et al.*, 2000). It is presently unknown whether Org 34167 displays any isoform specificity, it blocks HCN1 and HCN2 in cell lines at similar concentrations of 1μM (Mason, Personal communication), and it is unclear whether one isoform is more important in the proposed antidepressant effect. Given the number of brain regions affected in depression, the HCN2 isoform was targeted, as this subtype exhibits the highest and most widespread expression level of the four HCN genes in the brain (Monteggia *et al.*, (2000); Moosmang *et al.*, (1999); Figure 1.3). The methods available for the quantification of HCN2 gene expression were *in situ* hybridisation to examine the level of HCN2 mRNA expression and [^{3}H]-Org 34167 autoradiography, which, given the *in vitro* data, is predicted to be specific for HCN channels (Ruigt, Personal communication). Organon Laboratories did commission the production of HCN1 and HCN2 antibodies but these were not validated for Western blotting or immunohistochemistry at the time of study.

The aim of the experiments performed in the current chapter was to examine the effect of i.c.v. infusion of antisense oligonucleotides targeted to HCN2 isoform mRNA. A number of different trials were performed, utilising both 3- and 7-day infusion protocols of sequences designed to target different regions along the mRNA and finally modification of the oligonucleotide chemistry (See Table 2.1 for details of the experiments performed). The reasons for these alterations were to attempt to find an efficacious antisense sequence with minimal toxicity. [^{3}H]-Org 34167 autoradiography has been performed before (Makkink, Personal communication) but further method validation was carried out during this study prior to analysis of antisense-treated brain sections.

Table 2.1 Overview of antisense experiments performed in the present study

EXPERIMENT	INFUSION TIME AND CONCENTRATION	NUMBER OF SEQUENCES	MODIFICATION	ANALYSIS PERFORMED	HISTOLOGICAL STAINING	DETAILS
Initiation-codon	3 & 7 day trials 6.5 µg/µl/h	1 antisense 1 mismatch	Fully-modified PS-oligo	[^{3}H]-Org autoradiography HCN 2 ISH	Cresyl violet	Section 2.2.1
mfold Design	3 day trial 4 µg/µl/h	6 antisense	Fully-modified PS-oligo	Behavioural observations HCN 2 ISH	Cresyl violet	Section 2.2.2
Investigation of 2 mfold sequences	3 day trial 4 µg/µl/h	2 antisense 2 mismatch	Fully-modified PS-oligo	Behavioural observations HCN 2 ISH β-actin ISH	Haematoxylin & eosin	Section 2.2.3
MBO trial	7 day trial 0.4 & 4 µg/µl/h	1 antisense 1 mismatch	PO-oligo with end-modified PS-bases	HCN 2 ISH β-actin ISH	Haematoxylin & eosin	Section 2.2.4

Abb: ISH, *in situ* hybridisation, MBO, mixed backbone oligonucleotide, PO-oligo, phosphodiester oligonucleotide, PS-oligo, phosphorothioate oligonucleotide.

2.2 Materials and methods

2.2.1 Antisense oligonucleotide infusion targeting the initiation codon of HCN2

2.2.1.1 Animals and experimental procedure

Male Wistar rats (Bantin and Kingman) weighing 230 - 250 g were housed in groups of four or five on a 12 h light/dark cycle (lights on 07:00 h) at 22 ± 2 °C. Rats were given free access to tap water and standard rat diet and allowed to habituate for 1 week prior to surgery.

The antisense sequence targeted a region of the HCN2 mRNA transcript, which included the initiation-codon. A mismatch sequence was designed incorporating two paired base switches as an experimental control. The fully-modified phosphorothioate oligonucleotides were designed and synthesised by Professor Len Hall (Biochemistry Department, University of Bristol). The oligonucleotides were administered using osmotic mini-pumps combined with a brain infusion kit (Alzet, Charles River, U.K.). The pumps were primed for 4 h in saline solution at 37 °C, with vehicle (saline), antisense or mismatch oligonucleotide where the experimenter was unaware of the contents of the mini-pump. The weight of the mini-pump was recorded before and after filling to ensure correct loading; if less than 90 % filling was achieved the pump was reloaded. Two trials were performed, a three day infusion, using Alzet osmotic minipump model 1003D, and a seven day infusion using Alzet osmotic minipump model 1007D. In both trials, antisense or mismatch oligonucleotides were administered at an infusion rate of 6.5 μg/μl/h *via* the Alzet osmotic minipumps, or vehicle (0.9 %

saline) at 1 µl/h. The rats were weighed between 08:00 - 09:00 h on the day of the surgery and each day during the infusion.

On the day of surgery rats were anaesthetised using sodium pentobarbitone (Sagatal, Rhone Mérieux) and then placed into a stereotaxic frame (Stoelting Co, Illinois, USA). The top of the rat's head was shaved and cleaned with 70 % ethanol. A sterile scalpel blade was used to cut an incision along the midline of the skull and the perioistum cleared from the surface of the skull. The blood was swabbed using cotton buds and the skin held apart using artery forceps. Blunt scissors were then used to create a subcutaneous pocket to place the osmotic minipump in the midscapular region, connected to the cannulae by 4 cm of polyethylene tubing. A stainless steel skull screw (BN650 DIN 84A, Allscrews Ltd, U.K.) was then inserted in to the skull to secure the cannula in place.

The cannula was placed directly over bregma using a cannula holder specifically designed for Alzet cannulae (Model 1766-AP, David Kopf Instruments), and the brain co-ordinates relative to bregma recorded. The cannula was then moved 0.9 mm caudal to bregma and 1.4 mm lateral, to locate it above the left lateral ventricle (Paxinos *et al.*, 1986). A small hole was drilled through the skull at these co-ordinates and the dura was pierced using a 21 gauge needle, and again any blood was swabbed using cotton buds. Superglue was applied to the bottom of the cannula, which was then lowered and secured onto the skull. Spacers on the cannula ensured its placement 2.5 mm below the surface of the dura; into the lateral ventricle (Paxinos *et al.*, 1986). The cannula holder was removed and dental cement (methyl methacrylate and acrylic, Sigma, U.K.) was placed around the cannula and the skull screw to provide extra security. The skin was then closed using surgical staples.

On the final infusion day, between 09:00 and 11:00 h, the animals were deeply anaesthetised with sodium pentobarbitone (90 mg/kg.; Sagatal, Rhone Mérieux). A midline incision, from the diaphragm to the throat, was made and then one set of ribs cut through, followed by the diaphragm, taking care to avoid the heart and lungs. The second set of ribs were then cut and the chest cavity exposed by clamping the sternum to hold the chest wall back. A transcardiac perfusion of the rat with ice-cold, phosphate buffered, physiological saline (~ 250 ml, 10 mM, pH 7.4 see Appendix A) was performed by inserting a steel cannula into the left ventricle and cutting the right ventricle. Brains were removed rapidly over ice and frozen in isopentane cooled on dry ice to -32 °C and then stored in a -80 °C freezer.

2.2.1.2 Cryostat sectioning

The brains were removed from the -80 °C freezer and allowed to thaw to -20 °C before 20 μm brain sections were cryostat-cut onto superfrost slides (BDH) from ~ 1.2 mm to ~ -2.3 mm relative to bregma in 5 series each containing 12 slides (with 3 sections on each slide). Sections were stored at -80 °C until required.

2.2.1.3 In situ hybridisation

Sections were fixed in a 4 % paraformaldehyde, 0.9 % saline solution, made using diethylpyrocarbonate (DEPC)-treated water, for 10 min, rinsed in DEPC-treated water and incubated for 10 min in a 0.25 % solution of acetic anhydride in 0.1 M triethanolamine in 0.9 % DEPC-saline (pH 8). Sections were dehydrated in ethanol (diluted in DEPC-treated water); 1 min in 70 %, 1 min in 80 %, 2 min in 95 % and 1 min in 100 %, defatted for 5 min in 100 % chloroform and then re-hydrated for 1 min in

100 % ethanol and 1 min in 95 % ethanol. Slides were then dried at room temperature and then placed in an air-tight hybridisation box containing swabs soaked in 50 % formamide / 50 % DEPC-treated water solution to maintain humidity.

Synthetic oligonucleotide probes designed to be complementary to the HCN2 transcript (see Appendix B) were synthesised by Life Technologies (Gibco, BRL, U.K.). Specificity of the sequences was assessed using the NCBI database to verify that the sequences would not hybridise to any other known sequences. Additionally, the probe was checked against the antisense sequences to ensure that it targeted a different region of the HCN2 transcript.

The oligonucleotide probes were 3'-end labelled using [^{33}P]-dATP. Each oligonucleotide probe, at a concentration of 2 pmol, was tailed by the isotope at an incubation temperature of 37 °C in a reaction containing, 20 µl terminal transferase reaction buffer, 5 µl terminal deoxynucleotide transferase (pH 7.2; Promega), 8 µl [^{33}P]-dATP (3000 Ci/mmol, NEN) and made up to a final volume of 100 µl with DEPC-treated water. The reaction mixture was heated to 70 °C for 10 min followed by 1 h incubation at 37 °C to terminate the reaction. Unlabelled probe and isotope were separated out from the labelled probe using Micro Bio-Spin chromatography columns (P-30 Tris RNase-free, Bio-Rad, U.K.) centrifuged for 4 min at 3,300 r.p.m. in a desktop centrifuge (Centrifuge 5415 D, Eppendorf UK Ltd.). To assess the efficacy of radioactive labelling, 1 µl of the probe was removed and counted by a liquid scintillation counter (Tricarb, 1500 Packard). The labelled probe was then added to 'maximalist' (Henry *et al.*, 1999) hybridisation buffer (50 % formamide, 4 x Standard Sodium Citrate (SSC), 10 % dextran sulphate, 5 x Denhardt's solution, 200 µg/µl Salmon testes DNA, 100 µg/µl Poly-adenosine (poly-A) and 2 % (10 mM) dithiothreitol

(DTT)) to give a final concentration of 0.5 pmol/ml hybridisation solution. The final hybridisation buffer was used the same day. Hybridisation solution was pipetted onto each slide in the hybridisation box (150 µl per slide), which were then covered with Hybrislips (Sigma) and incubated in a hybridisation oven at 42 °C for 18 h.

All the solutions used in the post-hybridisation stages were diluted using distilled water (dH_20) as the oligonucleotide probe / mRNA duplex is resistant to RNases (except RNase H, which selectively cleaves the RNA strand of a RNA / DNA duplex). Following the 18 h incubation, the Hybrislips were floated off using 2 x standard sodium citrate (SSC) and the slides were placed in racks for further processing. Stringent washes were carried out for 30 min at room temperature in 1 x SSC, followed by 30 min at 55 °C in 1 x SSC and finally 10 min at 55 °C in 0.1 x SSC. Sections were then dehydrated for 2 min in 70 % ethanol and 2 min in 95 % ethanol and then allowed to air dry.

Once dry the sections were placed in a hypercassette (Amersham) and exposed to X-ray film (BioMax MR-1, Kodak) under 'safe' red light conditions for the required number of days (see Appendix B) at room temperature. An autoradiographic [^{14}C] micro-scale (Amersham) of known radioactivity (range 31 – 833 nCi/g) was also placed in each cassette to allow conversion of the optical density measurements to nCi/g. The films were then developed under 'safe' light conditions for 3 min in Kodak GBX developer/replenisher (20 % aqueous), rinsed briefly in water, fixed for 5 min in Kodak GBX fixer/replenisher (20 % aqueous), and washed for 5 min in tap water, and finally air-dried.

2.2.1.4 In situ probe validation

Specificity of the oligonucleotide probes was further assessed by RNase pre-treatment of brain sections, and by the addition of 100-fold excess non-labelled probe to separate control slides. After fixation in 4 % paraformaldehyde solution and incubation in acetic anhydride, brain sections were incubated in 10 mg/ml Ribonuclease A (RNase A) solution (Sigma) in phosphate buffered saline (PBS) at 37 °C for 30 min or PBS buffer alone. The sections were then processed for *in situ* hybridisation as described in Section 2.2.1.3. For controls involving excess non-labelled probe, *in situ* hybridisation was performed as described in Section 2.2.1.3 with the addition of 50 pmol/ml of non-labelled oligonucleotide probe added to the hybridisation buffer prior to hybridisation.

2.2.1.5 Analysis of in situ hybridisation

Densitometric analysis of autoradiographs was performed using a Microcomputer Imaging Device (MCID, InterFocus, Ltd., Haverhill, Suffolk, U.K.) system. Optical density measurements were obtained by calculating the average of the three sections on each slide for each brain region examined and used to determine the mean ± s.e. mean of each treatment group (n = 4 - 5). These values were converted to nCi/g by creating a standard curve from [^{14}C]-standards. Values were calculated for the left and right hemispheres for each brain region analysed.

2.2.1.6 [^{3}H]-Org 34167 autoradiography

The conditions for [^{3}H]-Org 34167 autoradiography were based on those previously used to demonstrate binding of [^{3}H]-Org 34167 throughout the brain (Makkink, Personal communication). A number of scientists at Organon Laboratories had attempted to use this protocol but achieved a negligible level of specific binding.

Therefore, the protocol was subjected to a number of variations, utilising control rat brain sections of 20 μm. These variations included altering the concentration of [^{3}H]-Org 34167, fixation of the tissue with 4 % paraformaldehyde (dissolved in PBS) for 30 min at room temperature, buffer used, and duration of post-incubation washes. Following the post-washes, brain sections were scraped into scintillation vials using a scalpel-blade, before being counted in a liquid scintillation counter (TriCarb, 1500 Packard). The protocol which yielded the highest percentage of specific binding (See Tables 2.2 & 2.5) was then performed on the brain sections obtained from 3-day vehicle, antisense or mismatch infused rats. All slides were pre-washed for 20 min in 50 mM Tris-buffer containing 0.1 % BSA and 1 mM $MgCl_2$, or 50 mM phosphate buffer, at room temperature and then dried under a stream of constant cool air. Once dry a hydrophobic barrier was then created around the outside of the slide using an "ImmEdge" pen. The slides were incubated for 40 min at room temperature in 200 μl 1, 10, 20 or 30 nM [^{3}H]-Org34167 in the relevant buffer to determine the total radioactivity binding. Exactly the same protocol was followed to determine the non-specific binding but 20 μM Org 34167 was added to the incubation buffer. The assay was terminated by performing three post-washes in the same buffer as the incubating solution and then a final dip rinse in ice-cold distilled water. The slides were finally dried under a stream of cool air and placed into cassettes and exposed to X-ray film (BioMax MR-1 film, Kodak) for 2 weeks at 4 °C. An autoradiographic [^{3}H] micro-scale (Amersham) of known radioactivity (range 31-833 nCi/g) was also placed in each cassette. The film was then developed as described in Section 2.2.1.3.

2.2.1.7 Statistical analyses

Data from each brain region of interest in the *in situ* hybridisation and [^{3}H]-Org 34167 autoradiography experiments were analysed by One-way analysis of variance followed

by Bonferroni *post-hoc* multiple comparison test in the 3-day infusion study. The mismatch group from the 7-day trial were excluded due to an insufficient n number to perform statistical analysis, and an unpaired t-test was used to compare vehicle and antisense groups only. Significance in each statistical test was assigned when $P < 0.05$, and the analysis was performed using GraphPad Prism v3.02 (GraphPad Software Inc).

2.2.1.8 Histological staining

Slides from animals treated for both the 3- and 7- day infusions were subject to cresyl violet staining. The sections utilised for this protocol had undergone no previous manipulation except from cryostat sectioning and all washes were diluted in dH_20. Firstly, the sections were equilibrated to room temperature for 30 min, then transferred to dH_20 for 30 s and then dehydrated for 30 s in an ascending series of ethanol washes (50, 95, and 100 %). The sections were then incubated for 7 min in 0.25 % cresyl violet in 200 mM acetate buffer, pH 4 (see Appendix A), then washed for 30 s in dH_20, 70 % ethanol and then 90 % ethanol. To differentiate the staining the sections were washed for 3 min in 0.4 % glacial acetic acid in ethanol (see Appendix A) then 30 s in 95 % and 100 % ethanol. Finally, the sections were cleared in xylene for 4 min and immediately mounted in DPX mounting medium.

2.2.1.9 Drugs and chemicals

The following drugs and chemicals were all purchased from Sigma: formamide, NaCl, tri-sodium citrate, dextran sulphate, Denhardt's solution, salmon testes DNA, Poly-A, ZD 7288, DTT, DEPC, tris-HCl, ethanol, xylene, di-sodium hydrogen orthophosphate (Na_2HPO_4) and sodium di-hydrogen orthophosphate (NaH_2PO_4; all Sigma). Terminal transferase (TT) buffer, TT (Promega), sodium pentobarbitone (Sagatal; Rhone

merieux), Gill No 2 (haematoxylin), 1 % eosin solution, acetic anhydride, triethanolamine, NaOH, isopentane, cryoembed (all BDH), and halothane (Animal Unit, University of Bristol) were also used in these experiments.

2.3 Results

2.3.1 Antisense oligonucleotide infusion targeting the initiation codon of HCN2

2.3.1.1 Effect of 3- or 7-day infusion on rat body weight

Individual body weights were taken each day from each animal and meaned to give the group daily body weight. There was no significant difference between each of the treatment groups, most probably due to the large variations in weight within each group (see Figures 2.1 & 2.2). During the course of the 7-day infusion, three mismatch rats were euthanased prior to the completion of the infusion. The toxicity observed in these three rats, coupled with the weight loss meant they had to be euthanased under the Home Office licence guidelines. All rats in the 3-day study completed the i.c.v infusion.

Figure 2.1 Total weight change of rats given a 3-day i.c.v infusion of vehicle (saline), antisense (targeting the initiation codon) or mismatch oligonucleotide

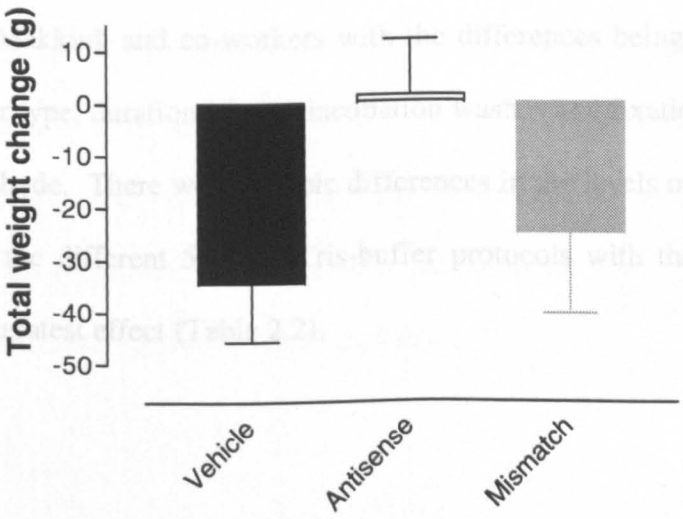

Total weight change was recorded for the 3 day infusion and 1 day baseline. Data represent means ± s.e. mean for 4 animals per group. Vehicle (■), Antisense (□) or Mismatch (▩).

Figure 2.2 Total weight change of rats given a 7-day i.c.v. infusion of vehicle (saline), antisense (targeting the initiation codon), or mismatch oligonucleotide

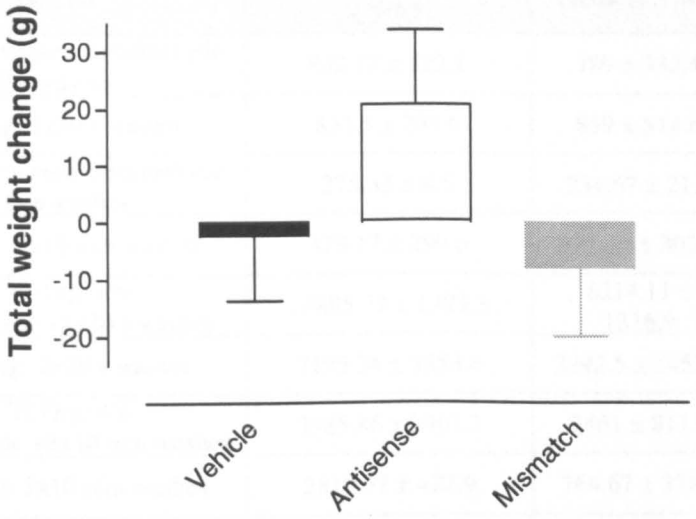

Total weight change was recorded for the 3 day infusion and 1 day baseline. Data represent means ± s.e. mean for 5 animals in the vehicle and antisense groups and an $n = 2$ shows median and range for the mismatch group. Vehicle (■), Antisense (□) or Mismatch (▩).

2.3.1.2 [^{3}H]-Org 34167 autoradiography

The results obtained using the established protocol for [^{3}H]-Org 34167 autoradiography (Makkink, Personal communication) proved difficult to reproduce at Organon Laboratories, Newhouse. Therefore, various protocols were attempted in an effort to find a viable and consistent methodology for use. All the autoradiography trials were based on that of Makkink and co-workers with the differences being concentration of radioligand, buffer type, duration of post-incubation washes and fixation of the tissue in 4 % paraformaldehyde. There were notable differences in the levels of specific binding attained between the different 50 mM Tris-buffer protocols with the duration of the wash having the greatest effect (Table 2.2).

Table 2.2 Initial 50 mM Tris-Buffer optimisation of [^{3}H]-Org 34167 autoradiography

PROTOCOL	TOTAL BINDING (CPM)	NSB (CPM)	SPECIFIC
1 nM ^{3}H-Org: 4% paraformaldehyde +2x20 s washes	802.17 ± 522.1	789 ± 332.4	2%
1 nM ^{3}H-Org: 2x20 s washes	831.5 ± 294.6	859 ± 514.6	-3%
1 nM ^{3}H-Org: 4% paraformaldehyde +3x10 min washes	275.33 ± 8.5	254.67 ± 21.9	8%
1 nM ^{3}H-Org: 3x10 min washes	479.17 ± 290.6	521.17 ± 301.4	-8%
10 nM ^{3}H-Org: 4% paraformaldehyde +2x20 s washes	13895.77 ± 1793.3	6214.11 ± 1316.9	55%
10 nM ^{3}H-Org: 2x20 s washes	7195.24 ± 3853.4	3292.5 ± 1452.3	54%
10 nM ^{3}H-Org: 4% paraformaldehyde +3x10 min washes	3985.86 ± 2901.7	2461 ± 811.3	38%
10 nM ^{3}H-Org: 3x10 min washes	2819.67 ± 422.9	764.67 ± 378.6	73%
20 nM ^{3}H-Org: 4% paraformaldehyde +2x20 s washes	34088.33 ± 44766.3	12969.17 ± 1488	62%
20 nM ^{3}H-Org: 2x20 s washes	17625.1 ± 16659	10078.51 ± 738.7	43%
20 nM ^{3}H-Org: 4% paraformaldehyde +3x10 min washes	13248 ± 834.2	3442.5 ± 988.6	74%
20 nM ^{3}H-Org: 3x10 min washes	3035.17 ± 1713.3	2134.67 ± 579.5	30%

Autoradiography scrapes of [^{3}H]-Org 34167 performed on 20 µm brain sections. Sections have been subjected to different protocols. Data represent CPM mean ± St. Dev (n = 3).

The results of the initial experiment demonstrate that fixation of the tissue in 4 % paraformaldehyde increased total binding and non-specific binding; although it did produce the protocol with the highest percentage of specific binding (20 nM, 3 x 10 min washes; Table 2.2). The concentration which provided the most consistent assay, with a high level of specific binding and low NSB was 10 nM [^{3}H]-Org 34167. Therefore, the experiment was performed again as described in section 2.2.1.4 but only at a 10 nM concentration of the radiolabel and no fixation. Additionally, a further post-incubation wash protocol (3 x 1 min washes) was added (Table 2.3).

Table 2.3 Final 50 mM Tris-Buffer optimisation of [^{3}H]-Org 34167 autoradiography

Wash Protocol	Total Binding (CPM)	NSB (CPM)	Specific
2 x 20sec washes	11030.5 ± 1159.2	3843.2 ± 1325.5	65%
3 x 1min washes	8182.7 ± 672.3	2964.8 ± 770.5	64%
3 x 10min washes	4220.6 ± 837.1	1770.2 ± 783.6	52%

Autoradiography scrapes of 10 nM [^{3}H]-Org 34167 performed on unfixed 20 µm brain sections with different post-incubation wash durations. Data represent CPM mean ± St. Dev (n = 6).

Comparison of the level of specific binding achieved using the same protocol revealed a high level of inconsistency in the assay, where 2 x 20 s washes produced 54 and 65 %, and 3 x 10 min washes, 73 and 64 % specific binding (Tables 2.2 & 2.3). Therefore, further optimisation was attempted using 50 mM phosphate buffers at varying pH and ion consistencies. Of the buffers attempted 50 mM phosphate buffer at pH 7.4 was observed to produce the highest, and most consistent across the varying ion and [^{3}H]-Org 34167 conditions (see Table 2.4). The experiment was performed again using 50 mM phosphate buffers, pH 7.4. Similar to the Tris-buffer observations, phosphate buffer produced variable specific binding at all concentrations of [^{3}H]-Org 34167 between experiments (see Tables 2.4 & 2.5).

Table 2.4 Initial 50 mM phosphate buffer optimisation of [^{3}H]-Org 34167 autoradiography

BUFFER COMPOSITION	% SPECIFIC	BUFFER COMPOSITION	% SPECIFIC	BUFFER COMPOSITION	% SPECIFIC
pH 7 No Ions 10nM	-257.38	pH 7.4 No Ions 10nM	-48.49	pH 8 No Ions 10nM	42.27
pH 7 150mM NaCl 10nM	17.35	pH 7.4 150mM NaCl 10nM	-1836.40	pH 8 150mM NaCl 10nM	-270.06
pH 7 5mM KCl 10nM	-47.94	pH 7.4 5mM KCl 10nM	0.76	pH 8 KCl 5mM 10nM	-18.42
pH 1mM $MgCl_2$ 10nM	1.63	pH 7.4 1mM $MgCl_2$ 10nM	85.01	pH 8 1mM $MgCl_2$ 10nM	-42.12
pH 7 all ions 10nM	-448.49	pH 7.4 all ions 10nM	47.62	pH 8 all ions 10nM	38.95
pH 7 no ions 20nM	12.73	pH 7.4 no ions 20nM	3.71	pH 8 no ions 20nM	12.91
pH 7 150mM NaCl 20nM	22.46	pH 7.4 150mM NaCl 20nM	3.90	pH 8 150mM NaCl 20nM	-15.76
pH 7 5mM KCl 20nM	98.34	pH 7.4 5mM KCl 20nM	-1.53	pH 8 5mM KCl 20nM	31.92
pH 7 1mM $MgCl_2$ 20nM	-52.07	pH 7.4 1mM $MgCl_2$ 20nM	16.34	pH 8 1mM $MgCl_2$ 20nM	24.84
pH 7 All ions 20nM	-105.33	pH 7.4 All ions 20nM	-6.99	pH 8 All ions 20nM	-17.28
pH 7 no ions 30nM	-8.43	pH 7.4 no ions 30nM	66.53	pH 8 no ions 30nM	65.59
pH 7 150mM NaCl 30nM	55.13	pH 7.4 150mM NaCl 30nM	8.10	pH 8 150mM NaCl 30nM	35.23
pH 7 5mM KCl 30nM	-36.09	pH 7.4 5mM KCl 30nM	11.55	pH 8 5mM KCl 30nM	12.27
pH 7 1mM $MgCl_2$ 30nM	41.69	pH 7.4 1mM $MgCl_2$ 30nM	18.91	pH 8 1mM $MgCl_2$ 30nM	-5.63
pH 7 All ions 30nM	7.73	pH 7.4 All ions 30nM	26.75	pH 8 All ions 30nM	29.52

Table 2.5 Final 50 mM phosphate buffer optimisation of [^{3}H]-Org 34167 autoradiography

PROTOCOL	TOTAL BINDING CPM	TOTAL BINDING SD	NSB CPM	NSB SD	SPECIFIC
10nM [^{3}H]-Org No ions	5559.00	± 258.10	2594.70	± 146.90	53.32
10nM [^{3}H]-Org 150mM NaCl	4594.10	± 140.70	2524.50	± 25.50	45.05
10nM [^{3}H]-Org 5mM KCl	5210.20	± 179.10	2385.20	± 120.20	54.22
10nM [^{3}H]-Org 1mM $MgCl_2$	6720.30	± 206.00	3310.00	± 181.70	50.75
20nM [^{3}H]-Org No ions	6059.00	± 73.00	2857.00	± 148.80	52.85
20nM [^{3}H]-Org 150mM NaCl	4972.80	± 140.70	2851.30	± 302.40	42.66
20nM [^{3}H]-Org 5mM KCl	5571.40	± 10.60	2495.70	± 77.60	55.21
20nM [^{3}H]-Org 1mM $MgCl_2$	7452.60	± 377.50	3389.40	± 700.00	54.52
30nM [^{3}H]-Org	15334.70	± 1013.40	5638.00	± 178.30	63.23
30nM [^{3}H]-Org 150mM NaCl	8301.10	± 252.90	4584.00	± 345.30	44.78
30nM [^{3}H]-Org 5mM KCl	8834.60	± 717.00	3984.70	± 147.90	54.90
30nM [^{3}H]-Org 1mM $MgCl_2$	11998.10	± 298.30	6535.60	± 688.90	45.53

Despite the substantial inter-assay variability in [^{3}H]-Org 34167 binding, autoradiography was performed on oligonucleotide-infused brain sections from the 3-day trial. The 50 mM Tris-buffer, using 10nM [^{3}H]-Org 34167 and 3 x 1 min post-washes protocol was performed (see Figure 2.3 for representative autoradiographs). There were significant differences between the treatment groups at the majority of brain regions analysed (Table 2.6). Both significant increases and reductions in specific binding for the same treatment group were observed at different levels examined. These inconsistencies may be due, in part, to the low level of specific binding achieved despite the optimised protocol displaying ~60% specific binding. The levels of binding are expressed in relative optical density (ROD) because the standards that were employed were not exposed to the film for sufficient time.

Table 2.6 [^{3}H]-Org 34167 autoradiography on 3-day vehicle, antisense or mismatch treated brain sections

Region		Vehicle infusion			Antisense infusion			Mismatch infusion		
		mean	±	s.e.mean	mean	±	s.e.mean	mean	±	s.e.mean
-0.7mm bregma	Left Cg ctx	0.0369	±	0.0022	0.0392	±	0.0047†	0.0128	±	0.00895*
	Left rDM Str	0.0286	±	0.0017	0.0298	±	0.0043†	0.0028	±	0.0085*
	Left rVM Str	0.0305	±	0.0008	0.0283	±	0.0032†	0.0004	±	0.0084**
	Right Cg ctx	0.0339	±	0.0021	0.0385	±	0.0031	0.0160	±	0.0099
	Right rDM Str	0.0256	±	0.0014	0.0289	±	0.0035†	0.0029	±	0.0093
	Right rVM Str	0.0273	±	0.0021	0.0297	±	0.0042	0.0061	±	0.0088
-1.5mm bregma	Left pCg ctx	0.0218	±	0.0032	0.0293	±	0.0147	0.0289	±	0.0091
	Left cDM Str	0.0115	±	0.0030	0.0205	±	0.0103	0.0167	±	0.0079
	Left cVM Str	0.0118	±	0.0024	0.0175	±	0.0088	0.0241	±	0.0091
	Right pCg ctx	0.0171	±	0.0044	0.0284	±	0.0142	0.0274	±	0.0068
	Right cDM Str	0.0134	±	0.0034	0.0151	±	0.0076	0.0183	±	0.0067
	Right cVM Str	0.0120	±	0.0017	0.0209	±	0.0105	0.0223	±	0.0090
-2.3mm bregma	Left RS Ctx	0.0086	±	0.0008	0.0209	±	0.0016**	0.0150	±	0.0023
	Left D Thal	0.0006	±	0.0027	0.0114	±	0.0044	0.0082	±	0.0009
	Right RS Ctx	0.0019	±	0.0010	0.0129	±	0.0014**	0.0109	±	0.0015**
	Right D Thal	0.0021	±	0.0014	0.0067	±	0.0023	0.0111	±	0.00195*

Quantified data for specific [^{3}H]-Org 34167 binding (10 nM) to rat brain sections following a 3-day i.c.v infusion with vehicle (saline), antisense (targeting the initiation codon) or mismatch oligonucleotide. Results represent mean specific binding ± s.e.mean (relative optical density) for 3 – 4 rats per group, three sections per animal. * $P < 0.05$, ** $P < 0.01$ oligonucleotide compared with vehicle, † $P < 0.05$ antisense compared with mismatch. Abb: c, caudal, Cg ctx, cingulate cortex, D, dorsal, DM Str, dorsomedial striatum, p, posterior, r, rostral, RS ctx, retrosplenial cortex, Thal, thalamus, VM Str, ventromedial

Figure 2.3 Representative autoradiograph images of total and NSB [^{3}H]-Org 34167 autoradiography

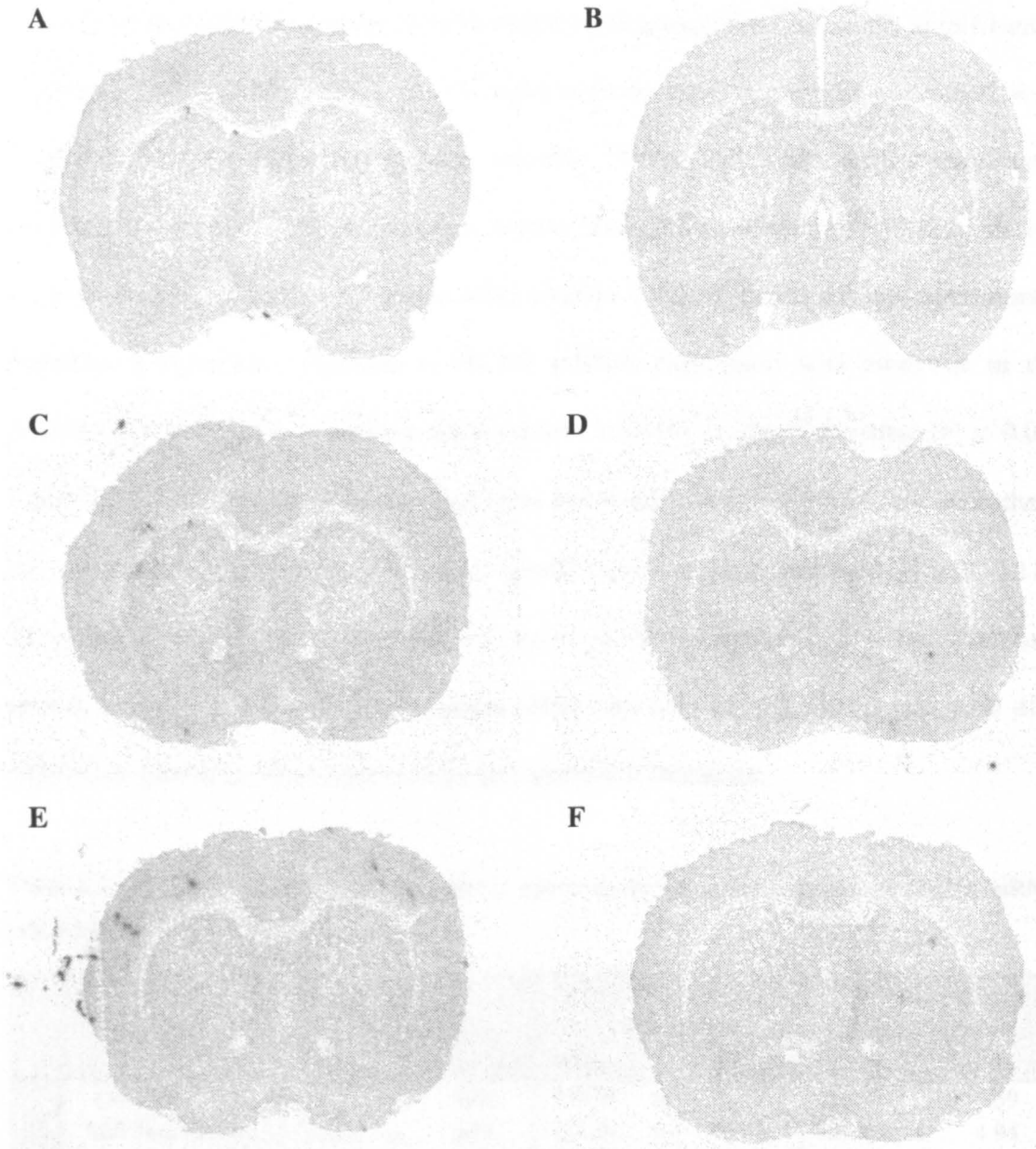

A = Vehicle treatment Total binding, B = Vehicle treatment NSB, C = Mismatch Total Binding, D = Mismatch NSB, E = Antisense treatment Total Binding and F = Antisense treatment NSB.

2.3.1.3 Effect of 3- and 7-day i.c.v. infusion on HCN2 mRNA expression

Infusion of the antisense oligonucleotide targeting the initiation codon only significantly decreased HCN2 mRNA levels in the right anterior cingulate cortex compared with mismatch infusion following a 3-day infusion (Table 2.7). No further significant differences were observed at this, or the regions analysed between 0 to -1.5 mm relative to bregma in either the 3- or 7-day studies (Tables 2.8 & 2.9). In the left anterodorsal thalamus a significant decrease in HCN2 mRNA expression was observed in the antisense-treated group compared with vehicle infusion in the 7-day trial ($P < 0.05$; Table 2.10). No significant differences were observed in the 3-day trial, nor were there any differences observed in the most caudal brain regions analysed (Table 2.11). Mismatch data from the 7-day trial are provided for information only, and therefore shown in italics. A significant antisense effect can only be regarded in the case of a significant alteration from both vehicle and mismatch infusions.

Table 2.7 Effect of 3- and 7-day i.c.v. vehicle, antisense or mismatch infusion on HCN2 mRNA expression – (~ 1 mm relative to bregma)

	Region	Vehicle infusion		Antisense infusion		Mismatch infusion	
		Mean	s.e.mean	Mean	s.e.mean	Mean	s.e.mean
3 DAY	Left Ant Cg ctx	142.37 ±	3.04	139.90 ±	7.70	154.00 ±	4.39
	Left Rost DM Str	113.55 ±	3.61	117.01 ±	11.60	133.16 ±	4.94
	Left Rost VM Str	101.22 ±	2.95	105.58 ±	11.24	120.87 ±	6.98
	Right Ant Cg ctx	141.66 ±	6.24	124.66 ±	7.88+	157.56 ±	7.93
	Right Rost DM Str	106.38 ±	3.95	112.23 ±	8.98	119.08 ±	4.99
	Right Rost VM Str	97.22 ±	2.61	100.83 ±	8.96	106.86 ±	4.81
7 DAY	Left Ant Cg ctx	162.84 ±	12.66	146.90 ±	10.28	*155.54* ±	
	Left Rost DM Str	124.28 ±	9.71	116.92 ±	6.64	*120.53* ±	
	Left Rost VM Str	107.00 ±	8.81	102.54 ±	3.75	*106.58* ±	
	Right Ant Cg ctx	165.18 ±	14.51	145.46 ±	6.74	*138.59* ±	
	Right Rost DM Str	120.48 ±	11.01	108.46 ±	6.48	*103.41* ±	
	Right Rost VM Str	107.17 ±	10.72	92.87 ±	3.13	*101.75* ±	

Data represent mean ± s.e. mean of three sections per animal ($n = 4$ rats for all groups in 3-day infusion and $n = 5$ rats for vehicle and antisense groups in 7-day infusion and $n = 2$ rats for 7-day mismatch infusion). Optical density readings have been converted to nCi/g of tissue. + $P < 0.05$ compared with mismatch. Abb: Ant Cg ctx, anterior cingulate cortex, Rost DM Str, rostral dorsomedial striatum, Rost VM Str, rostral ventromedial striatum (Paxinos *et al.*, 1986).

Table 2.8 Effect of 3- and 7-day i.c.v. vehicle, antisense or mismatch infusion on HCN2 mRNA expression – (~ 0 mm relative to bregma)

	Region	Vehicle infusion			Antisense infusion			Mismatch infusion		
		Mean		s.e.mean	Mean		s.e.mean	Mean		s.e.mean
3 DAY	Left Cg ctx	123.26	±	7.39	128.88	±	3.85	111.65	±	6.06
	Left DM Str	91.17	±	6.40	97.01	±	3.82	93.34	±	5.61
	Left VM Str	96.29	±	4.99	102.87	±	2.60	93.63	±	8.41
	Right Cg ctx	127.16	±	6.55	113.80	±	4.40	122.16	±	8.18
	Right DM Str	87.70	±	9.17	98.38	±	4.82	85.12	±	5.90
	Right VM Str	84.34	±	6.97	96.45	±	7.04	81.59	±	5.98
7 DAY	Left Cg ctx	116.55	±	3.50	110.83	±	7.29	*121.30*	±	
	Left DM Str	89.10	±	3.10	75.25	±	5.01	*82.75*	±	
	Left VM Str	80.48	±	3.02	77.19	±	2.78	*85.73*	±	
	Right Cg ctx	123.57	±	3.88	117.57	±	2.53	*117.13*	±	
	Right DM Str	84.82	±	3.96	78.84	±	5.55	*83.45*	±	
	Right VM Str	79.67	±	2.47	63.44	±	5.82	*80.27*	±	

Data represent mean ± s.e. mean of three sections per animal (n = 4 rats for all groups in 3-day infusion and n = 5 rats for vehicle and antisense groups in 7-day infusion and n = 2 rats for 7-day mismatch infusion). Optical density readings have been converted to nCi/g of tissue. Abb: Cg ctx, cingulate cortex, DM Str, dorsomedial striatum, VM Str, ventromedial striatum (Paxinos *et al.*, 1986).

Table 2.9 Effect of 3- and 7-day i.c.v. vehicle, antisense or mismatch infusion on HCN2 mRNA expression – (~ -0.7 mm relative to bregma)

	Region	Vehicle infusion			Antisense infusion			Mismatch infusion		
		Mean		s.e.mean	Mean		s.e.mean	Mean		s.e.mean
3 DAY	Left Cg ctx	115.34	±	6.44	117.14	±	8.72	113.86	±	10.24
	Left cDM Str	64.94	±	7.07	82.08	±	7.04	75.39	±	4.40
	Left cVM Str	77.39	±	5.65	89.05	±	5.17	85.58	±	6.77
	Right Cg ctx	110.21	±	5.18	106.76	±	7.41	123.07	±	6.88
	Right cDM Str	68.05	±	12.60	84.97	±	4.82	84.47	±	4.55
	Right cVM Str	69.60	±	16.01	103.18	±	7.22	96.59	±	6.08
7 DAY	Left Cg ctx	127.15	±	3.70	128.91	±	8.63	*114.73*	±	
	Left cDM Str	83.93	±	6.69	88.40	±	6.71	*75.79*	±	
	Left cVM Str	95.96	±	3.74	102.40	±	4.14	*85.51*	±	
	Right Cg ctx	131.84	±	3.50	125.59	±	4.02	*111.48*	±	
	Right cDM Str	92.62	±	2.74	90.96	±	6.26	*76.52*	±	
	Right cVM Str	100.65	±	4.12	99.76	±	6.73	*79.83*	±	

Data represent mean ± s.e. mean of three sections per animal (n = 4 rats for all groups in 3-day infusion and n = 5 rats for vehicle and antisense groups in 7-day infusion and n = 2 rats for 7-day mismatch infusion). Optical density readings have been converted to nCi/g of tissue. Abb: Cg ctx, cingulate cortex, cDM Str, caudal dorsomedial striatum, cVM Str, caudal ventromedial striatum (Paxinos *et al.*, 1986).

Table 2.10 Effect of 3- and 7-day i.c.v. vehicle, antisense or mismatch infusion on HCN2 mRNA expression – (~ -1.5 mm relative to bregma)

	Region	Vehicle infusion			Antisense infusion			Mismatch infusion		
		Mean		s.e.mean	Mean		s.e.mean	Mean		s.e.mean
3	Left Post Cg Ctx	124.33	±	3.77	124.63	±	8.65	101.30	±	11.87
D	Left AD Thal	249.49	±	8.54	224.86	±	5.98	234.49	±	18.62
A	Right Post Cg ctx	124.25	±	4.50	120.99	±	8.55	114.43	±	8.94
Y	Right AD Thal	240.68	±	13.47	230.01	±	9.68	221.02	±	15.14
7	Left Post Cg ctx	122.21	±	2.33	115.84	±	9.72	*133.91*	±	
D	Left AD Thal	220.92	±	4.95	185.71	±	9.25*	*185.24*	±	
A	Right Post Cg ctx	124.41	±	7.12	106.01	±	9.16	*129.63*	±	
Y	Right AD Thal	203.59	±	7.89	175.14	±	8.83	*162.87*	±	

Data represent mean ± s.e. mean of three sections per animal (n = 4 rats for all groups in 3-day infusion and n = 5 rats for vehicle and antisense groups in 7-day infusion and n = 2 rats for 7-day mismatch infusion). Optical density readings have been converted to nCi/g of tissue. * $P < 0.05$ compared with vehicle. Abb: Post Cg ctx, posterior cingulate cortex, AD Thal, anterodorsal thalamus (Paxinos *et al.*, 1986).

Table 2.11 Effect of 3- and 7-day i.c.v. vehicle, antisense or mismatch infusion on HCN2 mRNA expression – (~ -2.3 mm relative to bregma)

	Region	Vehicle infusion			Antisense infusion			Mismatch infusion		
		Mean		s.e.mean	Mean		s.e.mean	Mean		s.e.mean
3 D A Y	Left RS ctx	133.33	±	3.52	127.25	±	7.68	123.69	±	11.23
	Left D Thal	226.74	±	18.07	253.63	±	8.01	265.58	±	12.42
	Left CA3	208.02	±	7.97	186.11	±	10.25	213.11	±	7.35
	Right RS ctx	126.19	±	8.22	103.08	±	1.86	115.68	±	8.66
	Right D Thal	215.24	±	20.72	206.31	±	13.32	242.57	±	12.38
	Right CA3	212.73	±	5.43	185.46	±	19.83	213.33	±	16.43
7 D A Y	Left RS ctx	118.27	±	4.48	130.11	±	10.27	*125.32*	±	
	Left D Thal	241.02	±	6.11	238.40	±	15.33	*254.34*	±	
	Left CA3	207.00	±	5.17	184.63	±	17.03	*192.12*	±	
	Right RS ctx	116.50	±	5.13	122.48	±	7.44	*134.21*	±	
	Right D Thal	237.32	±	9.19	219.58	±	8.65	*241.00*	±	
	Right CA3	195.56	±	11.87	201.58	±	20.72	*205.41*	±	

Data represent mean ± s.e. mean of three sections per animal (n = 4 rats for all groups in 3-day infusion and n = 5 rats for vehicle and antisense groups in 7-day infusion and n = 2 rats for 7-day mismatch infusion). Optical density readings have been converted to nCi/g of tissue. Abb: RS ctx, anterior retrosplenial cortex, D Thal, dorsal thalamus (Paxinos *et al.*, 1986).

2.2.2 Design and investigation of six antisense sequences to the HCN2 gene

2.2.2.1 Design of six antisense sequences to the rat HCN2 gene using mfold

Utilising the secondary structure prediction computer modelling program, "mfold", antisense sequences were designed along the length of the rat HCN2 mRNA transcript (Accession number: AF247451). These sequences were then examined for possible complementarity to other known genes using the NCBI database and rejected if significant homology (5 bases) was observed. This is with the exception of other HCN genes, as Sequence 6 was complementary to HCN1, 2 and 4 and Sequences 3 and 5 to HCN2 and 3. Furthermore, the sequences were checked for any possible active motifs (see Section 1.4.3) and their percentage GC content. If active motifs were present, or the GC content too high or low (accepted between 33 – 60 %), sequences were rejected. Finally, the sequences were examined for possible hairpin loops, or self-annealing sequences, using an oligonucleotide properties calculator and rejected in either case (http://www.basic.nwu.edu/biotools/oligocalc.html). Using this selection procedure, six antisense sequences were chosen (See Table 2.12). The sequences were fully-modified phosphorothioate oligonucleotides and synthesised by MWG Biotech (Germany).

Table 2.12 Six antisense sequences designed using mfold secondary structure prediction

NAME	SEQUENCE (5' – 3')	COMPLEMENTARY BASES (AF247451)
Sequence 1	CAA GGG TCA CAA GTT GGA	2493 – 2511
Sequence 2	TTG AAG AAA GTG ATG	528 - 542
Sequence 3	GGG AGA ACT TGT TGA CG	354 – 370
Sequence 4	GGA TGA TGT AGT CT	1536 – 1553
Sequence 5	AGA TGG AGT TCT TCT	1823 – 1840
Sequence 6	CAG GTC GTA GGT CAT GTG	895 – 911

2.2.2.2 Animals and experimental procedure

Housing conditions, filling of the osmotic minipumps, and implantation of the cannula were performed as described in section 2.2.1.1 with the use of different anaesthesia. On the day of surgery rats were anaesthetised with halothane using a rodent ventilator, which maintained an O_2 flow rate of 1.5 l/min and NO_2 flow rate of 2 l/min. Anaesthesia was induced using 3 % halothane *via* a nosepiece that was connected to the rodent ventilator and a Fluovac (International Market Supply) fitted with a Cardiff Aldasorber (Shirley Aldred & Company Ltd, U.K.) to scavenge the halothane. Once anaesthetised the rat was transferred to a stereotaxic frame (Stoelting Co, Illinois, USA) with a specially adapted nosepiece, which was connected to the rodent ventilator *via* the Fluovac with 1.5 – 2 % halothane, to maintain anaesthesia for the duration of the surgery (see Figure 2.4).

Figure 2.4 Representative image of stereotaxic surgery procedure

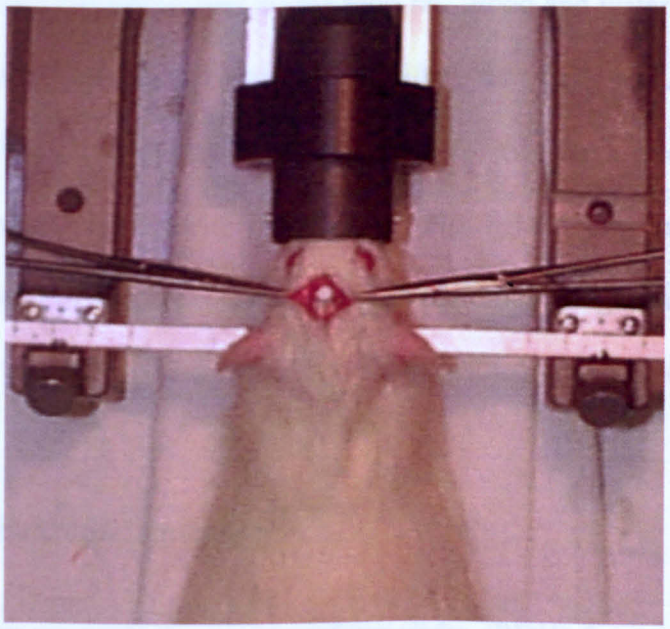

Image shows rat in sterotaxic frame with the adapted nose-piece, which maintains the halothane anaesthesia. A pair of artery forceps keeps the skin clear of the skull to enable the cannula to be implanted i.c.v. and then application of dental cement to secure the cannula to the skull and bone screw. Following surgery the rat is removed from the sterotaxic frame and the skin is stapled together to seal the surgery.

The fully-modified phosphorothioate oligonucleotides were administered at a rate of 4 μg/μl/h with two animals in each treatment group. On the final day of the 3-day infusion the rats were perfused and the brains collected and stored as described in Section 2.2.1.1.

Additionally, because no mismatch oligonucleotide control sequences were employed, behavioural observations of the rats were performed to assess potential toxicity or behavioural effects of the different antisense administration. These observations were based upon time-sampling (adapted from Reinstein & Isaacson (1977)) and were performed during the first four (07:30 – 11:30 h) and last four (15:30 -18:50 h) hours of the light-phase. The behaviour of each rat was recorded for 15 s every 60 s, for a total of 10 min in each hour. The behaviours were exclusive and only one parameter could be scored for each recording (see Table 2.13 for list of behavioural measures). The first observed behaviour was given a score in each minute meaning that the maximum score per day for any given behaviour was 80 for each rat. Food and water intake, as well as body weights, were measured immediately after the first and last behavioural observations. These observations were performed for two-days prior to surgery and two-days post-surgery (i.e. during infusion). No behavioural observations were performed on the day of surgery, only food, water and body weight measurements were recorded.

2.2.2.3 In situ hybridisation protocol

Brain sections were cryostat-cut onto superfrost slides (BDH) from ~ 0 mm bregma to ~ -2.5 mm bregma in 4 series each containing 8 slides (with 3 sections on each slide) as described in Section 2.2.1.2. Sections were stored at -80 °C until required. *In situ* hybridisation was performed, as described in Section 2.2.1.3, using the complementary

oligonucleotide to HCN2 (see Appendix B for sequence details) and one slide for each brain was subjected to cresyl violet staining as described in Section 2.2.1.9.

2.2.2.4 Statistical analyses

No statistical analyses were performed due to an insufficient n number. This was due to the preliminary nature of the experiments performed in the trial.

Table 2.13 Description of behavioural parameters measured during oligonucleotide infusion

BEHAVIOUR	DESCRIPTION
Locomotion	Movement around the home cage
Wall Climbing	Forepaws resting against the side of the cage and an elevated posture
Rearing	Elevated posture with forepaws in the air
Grooming	Any grooming of rat, with either tongue or paws
Scratching	Scratching with hind paw
Eating	Eating of standard rat diet, sawdust or faeces
Drinking	Drinking of water
ACTIVITY	Total score of all above behaviours
ST AWAKE	Stationary awake
ST ASLEEP	Stationary asleep
Sniffing	Sniffing of air or cage
Head weaving	Continuous head movement in horizontal and/or vertical planes
Arched back	Back in an elevated posture
↓ muscle tone	Decreased muscle tone (only performed during weighing of rat)
Hindlimb stretch	Stretching of hindlimbs
Tremor	Tremor
Ataxia	Uncoordinated locomotion
Wet dog shake	Whole body shake
Forepaw treading	Forepaws in the air moving consistently
Yawning	Yawning

The behaviours listed below St asleep are those which were employed to observe for signs of toxicity following oligonucleotide administration. Only one behaviour above activity could be recorded at one observation but those listed below St. asleep could be recorded at the same time as they were employed to look for signs of toxicity.

2.3.2 Design and investigation of six antisense sequences to the HCN2 gene

2.3.2.1 Body weight, food and water intake and behavioural observations

With the preliminary nature of this study no statistical analyses were performed as there was an insufficient *n* number ($n = 2$). Consequently, the data for each rat is graphically represented. Differential effects were observed on the total weight gain of rats receiving different antisense sequences targeted to varying regions along the HCN2 transcript. Sequences 1 – 3 infusions resulted in an increase in total body weight over the five-day time course, whereas Sequences 4 – 6 caused a decrease in body weight (Figure 2.5). This trend was similar to the daily food intake of the rats; although all groups displayed a marked decrease in food intake on the day of surgery. Sequence 4 and 6 infusions decreased food intake over the infusion period compared with the corresponding baseline period. Sequences 1, 2 and 3 infused rats recovered to baseline readings following surgery and Sequence 5 administration caused the least fluctuation in daily food intake (Figure 2.6). Infusions of Sequence 1, 2, 3 and 5 resulted in an increase in daily water intake for the duration of the infusion compared with the corresponding baseline recordings, whilst infusion of Sequence 4 infusion caused no apparent alteration to this parameter. Infusion of Sequence 6 resulted in decreased water intake during the infusion period compared with baseline (Figure 2.6). Median total activity scores of all antisense sequences were increased compared with vehicle infusion, with the exception of Sequence 6 where a decrease was observed (Figure 2.7).

Figure 2.5 Effect of 3-day infusion of six antisense sequences designed using mfold on total body weight

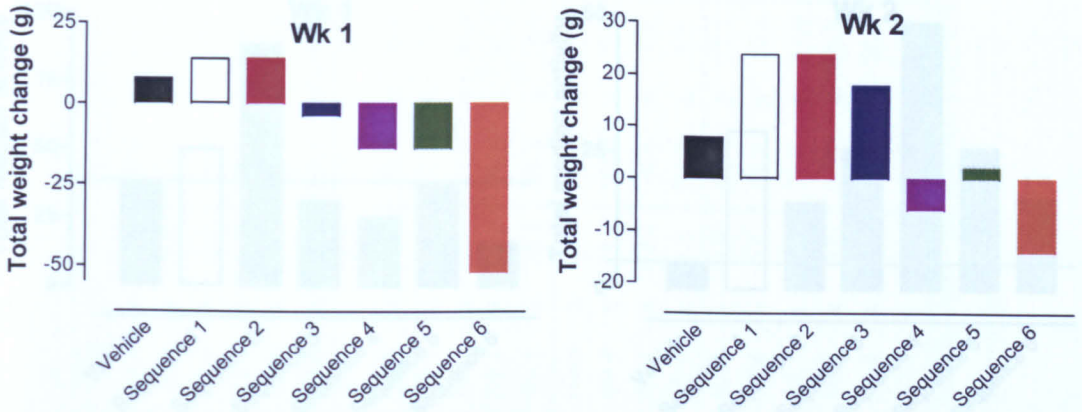

Results are shown for each of the two animals for the duration of the five day time course study. Sequence 6 displays the total weight gain for one rat, which completed the five day study (Wk 1) and one which was euthanased 1 day into the infusion (Wk 2). All other rats completed the time-course.

Figure 2.6 Effect of 3-day infusion of six antisense sequences designed using mfold on daily food and water intake

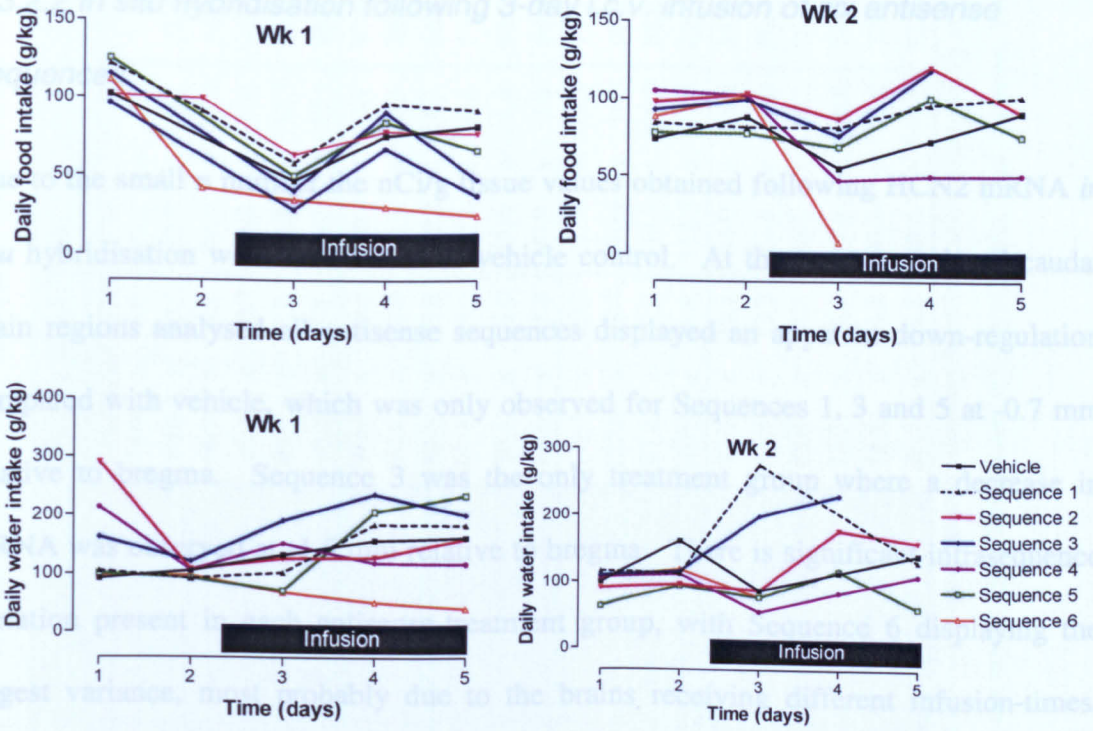

Results are shown for each of the two animals for the duration of the five day time course study. Sequence 6 displays the total parameter for one rat, which completed the five day study (Wk 1) and one which was euthanased 1 day into the infusion (Wk 2). All other rats completed the time-course.

Figure 2.7 Effect of 3-day infusion of six antisense sequences designed using mfold on total activity scores

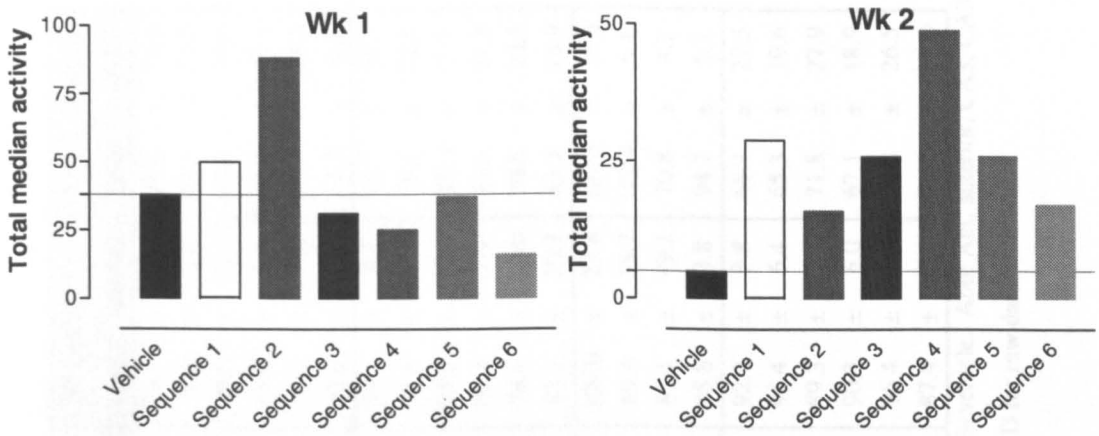

Results represent the total median activity of each rat over the course of the two days pre-surgery and two days post-surgery observations (see Table 2.13). The maximum score recordable was 320. Results are shown for each of the two animals for the duration of the five day time course study. Sequence 6 displays the total parameter for one rat, which completed the five day study (Wk 1) and one which was euthanased 1 day into the infusion (Wk 2). All other rats completed the time-course.

2.3.2.2 In situ hybridisation following 3-day i.c.v. infusion of six antisense sequences

Due to the small *n* number the nCi/g tissue values obtained following HCN2 mRNA *in situ* hybridisation were normalised to vehicle control. At the most rostral and caudal brain regions analysed all antisense sequences displayed an apparent down-regulation compared with vehicle, which was only observed for Sequences 1, 3 and 5 at -0.7 mm relative to bregma. Sequence 3 was the only treatment group where a decrease in mRNA was observed at -1.5 mm relative to bregma. There is significant intrasequence variation present in each antisense-treatment group, with Sequence 6 displaying the largest variance, most probably due to the brains receiving different infusion-times, while Sequence 4 demonstrated the least variation (see Table 2.14).

Table 2.14 Effect of 3-day infusion of six antisense sequences designed using mfold on HCN2 mRNA expression

	Region	Sequence 1			Sequence 2			Sequence 3			Sequence 4			Sequence 5			Sequence 6		
		mean		range	mean		range	mean		range	mean		range	mean		range	mean		range
0mm bregma	L Ant Cg Ctx	74.6	±	5.6	90.2	±	9.3	72.9	±	22.8	84.5	±	3.9	89.8	±	13.3	59.6	±	14.6
	R Ant Cg ctx	80.0	±	10.7	92.7	±	9.2	73.0	±	15.6	93.6	±	5.8	76.6	±	4.4	73.3	±	15.2
	L Rost VM Str	66.9	±	6.5	89.4	±	17.6	64.8	±	19.1	87.6	±	7.5	79.6	±	4.3	50.4	±	20.0
	R Rost VM Str	75.4	±	10.7	89.7	±	9.8	62.5	±	7.4	95.1	±	8.6	71.0	±	5.8	59.4	±	18.1
	L Rost DM Str	66.3	±	6.7	80.8	±	12.3	64.9	±	17.2	87.3	±	2.3	78.2	±	3.5	63.7	±	15.6
	R Rost DM Str	66.5	±	9.8	80.7	±	13.1	66.8	±	14.4	89.4	±	4.8	65.6	±	4.6	71.5	±	8.4
-0.7mm bregma	L Cg ctx	102.6	±	18.3	100.2	±	2.8	80.6	±	12.8	101.8	±	2.3	99.1	±	9.2	73.7	±	30.7
	R Cg ctx	90.4	±	17.3	98.1	±	0.3	78.7	±	9.4	104.3	±	12.1	91.6	±	7.1	78.9	±	22.5
	L VM Str	86.5	±	15.6	106.8	±	1.7	66.0	±	21.7	101.3	±	10.5	94.4	±	10.2	101.1	±	7.7
	R VM Str	97.4	±	10.9	111.4	±	6.6	73.6	±	26.8	98.3	±	5.8	99.3	±	1.9	57.6	±	31.8
	L DM Str	80.1	±	14.0	85.6	±	1.6	63.8	±	15.3	95.3	±	9.3	78.4	±	10.0	70.6	±	20.5
	R DM Str	90.6	±	21.9	90.9	±	3.6	69.1	±	10.4	103.9	±	17.0	93.2	±	20.3	85.3	±	18.9
-1.5mm bregma	L Post Cg ctx	119.5	±	20.2	127.6	±	21.9	71.1	±	19.6	101.8	±	0.0	100.0	±	23.8	107.5	±	15.5
	R Post Cg ctx	135.0	±	13.0	130.9	±	26.3	69.9	±	17.9	111.8	±	0.0	89.4	±	35.7	100.4	±	5.4
	L Ant Thal	97.4	±	7.2	114.2	±	20.0	53.6	±	4.3	151.0	±	0.0	85.1	±	49.2	70.8	±	4.2
	R Ant Thal	105.3	±	5.4	114.5	±	22.6	62.5	±	3.4	154.9	±	0.0	85.8	±	3.8	94.7	±	5.2
-2.3mm bregma	L RS ctx	83.5	±	20.1	84.0	±	14.8	87.1	±	0.2	93.7	±	19.9	92.4	±	3.8	68.7	±	27.5
	R RS ctx	84.5	±	23.3	92.6	±	14.4	90.3	±	2.0	99.2	±	6.4	95.4	±	6.4	65.3	±	19.6
	L Thal	85.4	±	15.7	85.5	±	13.2	70.5	±	0.3	89.3	±	4.4	89.3	±	7.1	71.8	±	27.9
	R Thal	83.3	±	18.4	87.5	±	16.8	71.4	±	2.1	89.7	±	7.0	90.3	±	6.0	67.1	±	18.9
	L CA3	79.9	±	13.3	90.7	±	15.6	77.0	±	6.8	99.7	±	11.1	96.4	±	5.1	71.2	±	26.5
	R CA3	79.7	±	18.1	88.1	±	10.8	81.8	±	7.7	107.3	±	11.6	87.4	±	7.0	61.8	±	25.0

Data represent mean ± range (n = 2). Optical density readings have been converted to nCi/g of tissue and then to normalised to % vehicle. Abb: Ant, anterior, CA3, CA3 field of the hippocampus, Cg, cingulate, ctx, cortex, DM, dorsomedial, RS, retrosplenial, Thal, thalamus, VM, ventromedial. See Appendix D for raw data.

2.2.3 Further investigation of two antisense sequences obtained from those designed by mfold

2.2.3.1 Animals and experimental procedure

Using the data from the first mfold trial (See Section 2.3.2), two of the most promising sequences were selected. Sequence 1 was chosen due to the behavioural observations, which demonstrated an increase in overall rat activity compared with vehicle (see Figure 2.7) and Sequence 4 was chosen after analysis of both the *in situ* hybridisation data and activity data (see Figure 2.7 & Table 2.14). Mismatch sequences were designed by incorporating two paired base switches, which were subjected to the same scrutiny as described in Section 2.2.2.1 for the antisense sequences. These sequences were namely, Mismatch 1: 5' – AAA TGG TCA CAA GTG CGG – 3' and Mismatch 4: 5' – GCG TGG TAT AAT GT – 3'. Both mismatch oligonucleotides were synthesised to the same modifications as the antisense oligonucleotides; fully-modified phosphorothioates. Similar to the previous trial (Section 2.2.2) the oligonucleotides were infused at a rate of 4 μg/μl/h, but with five rats in each treatment group.

Behavioural observation were performed as described in Section 2.2.2.2, except from rat body weight measurements, which were only taken immediately after the first behavioural observations each day. Surgical implantation of the cannula was performed as described in Section 2.2.2.2 and the osmotic minipumps used were Model 1003D, for a 3-day infusion period.

Brain sections were cryostat-cut onto superfrost slides (BDH) from ~ 0 mm bregma to ~ -2.5 mm bregma in 4 series each containing 8 slides (with 3 sections on each slide). Sections were stored at -80 °C until required. The first slide from each of the four brain

series collected was subjected to HCN2 *in situ* hybridisation and the second slide to β-actin (see Appendix B for probe details). Specificity of the oligonucleotide probes was assessed as described in Section 2.2.1.4 and the autoradiograph images are shown in Appendix C.

2.2.3.2 Histological staining (haematoxylin and eosin)

One slide from each series was subjected to haematoxylin and eosin histological staining. The haematoxylin and eosin stain was applied to brain sections which had been subjected to the pre-hybridisation washes described in Section 2.2.1.3. Sections were first re-hydrated using 95- and 70 % ethanol and then immersed in distilled water for 2 min. The sections were then incubated for between 50 - 100 s in haematoxylin (Gill No 2 Haematoxylin solution, BDH, UK) and washed in distilled water for 5 min before being immersed in 1 % eosin (BDH, UK) for 90 – 120 s. Finally, sections were dehydrated for 30 s in a series of ascending concentrations of ethanol (70, 90 and 100 %, diluted in distilled water) and then immersed in xylene for 2 min and immediately mounted in DPX mounting medium. The stained sections were then observed using a microscope connected to an image capture device (Olympus Provis AX camera linked to image analysis software, AnalySIS, Version 3.2, Soft Imaging Systems), which enabled images to be collected at x1.5 magnification.

2.3.3 Further investigation of two antisense sequences designed using mfold

2.3.3.1 Body weight, food and water intake and behavioural observations

There was a trend towards an increase in total weight gain in all of the oligonucleotide infusion groups compared with vehicle, but this did not reach significance for any group (Figure 2.8). Daily food and water intake was not significantly altered at any time point (Figure 2.9). The median total behavioural activity parameter was elevated in both Sequence 1 and Mismatch 1 infused rats compared with vehicle, whereas Sequence 4 and Mismatch 4 infusions did not cause an apparent increase in activity (Figure 2.10). All rats in the trial completed the five-day time course.

Figure 2.8 Effect of 3-day infusion of two antisense sequences on total weight gain

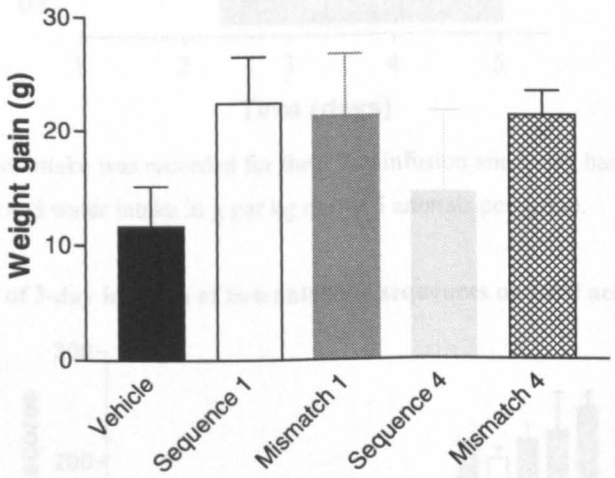

Total weight gain was recorded for the 3 day infusion and 1 day baseline. Data represent mean ± s.e. mean for 5 animals per group. Vehicle (■), Sequence 1 (□), Mismatch 1 (▩), Sequence 4 (▒), or Mismatch 4 (▒).

Figure 2.9 Effect of 3-day infusion of two antisense sequences on daily food and water intake

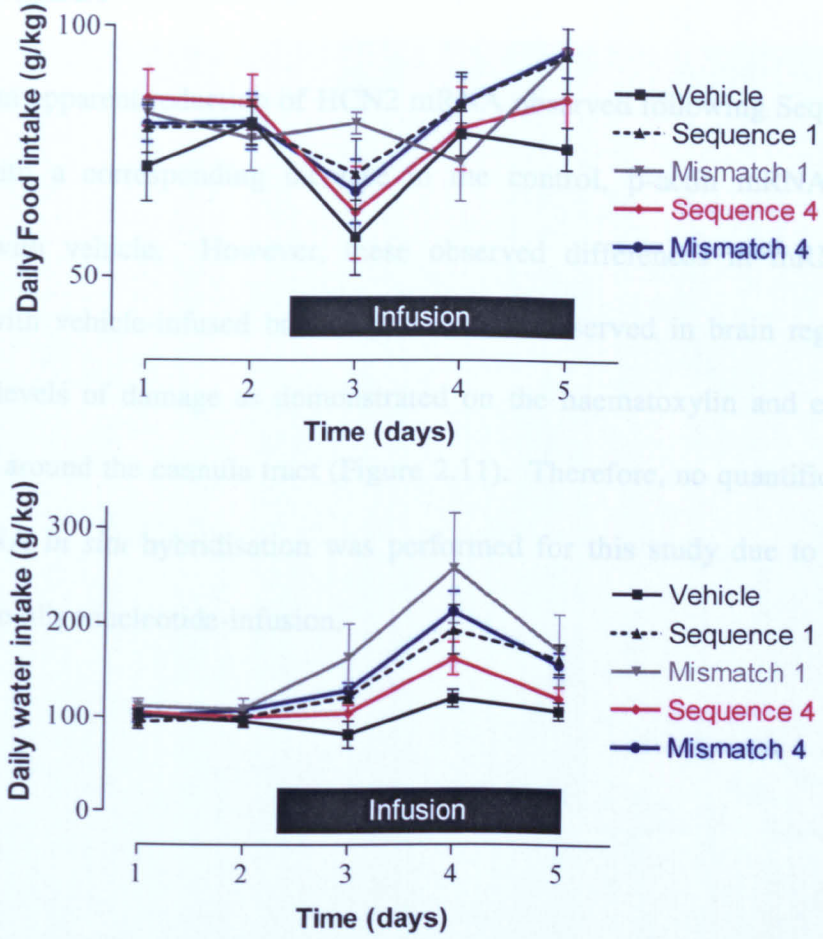

Daily food and water intake was recorded for the 3 day infusion and 1 day baseline. Data represent mean ± s.e. mean of food and water intake in g per kg rat for 5 animals per group.

Figure 2.10 Effect of 3-day infusion of two antisense sequences on total activity

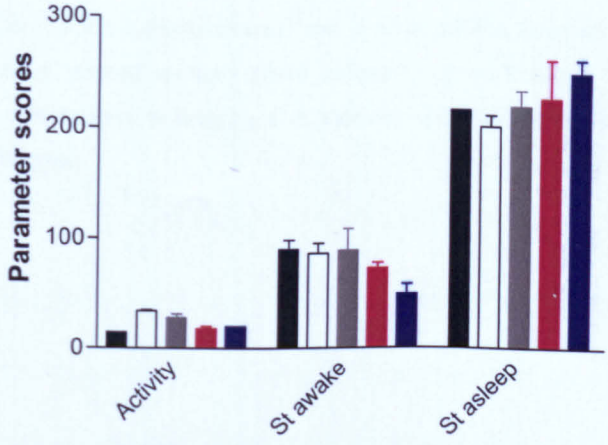

Total activity, stationary awake and stationary asleep scores for the duration of the five day time course (see Table 2.13). Data represent the median frequency score + upper range for 5 animals per group. . Vehicle (■), 0.4 µg/µl/h antisense (□), 0.4 µg/µl/h mismatch (■), 4 µg/µl/h antisense (■), or 4 µg/µl/h mismatch (■).

2.3.3.2 Effect of 3-day i.c.v. infusion of two antisense sequences on HCN2 mRNA expression

There was an apparent reduction of HCN2 mRNA observed following Sequence 1 & 4 infusion, with a corresponding increase in the control, β-actin mRNA expression compared with vehicle. However, these observed differences in mRNA patterns compared with vehicle-infused brain sections were observed in brain regions, which show high levels of damage as demonstrated on the haematoxylin and eosin stained sections i.e. around the cannula tract (Figure 2.11). Therefore, no quantification of the HCN2 mRNA *in situ* hybridisation was performed for this study due to the toxicity following the oligonucleotide-infusion.

Figure 2.11 Representative autoradiograph images of HCN2 and β-actin *in situ* hybridisation and haematoxylin and eosin stained sections

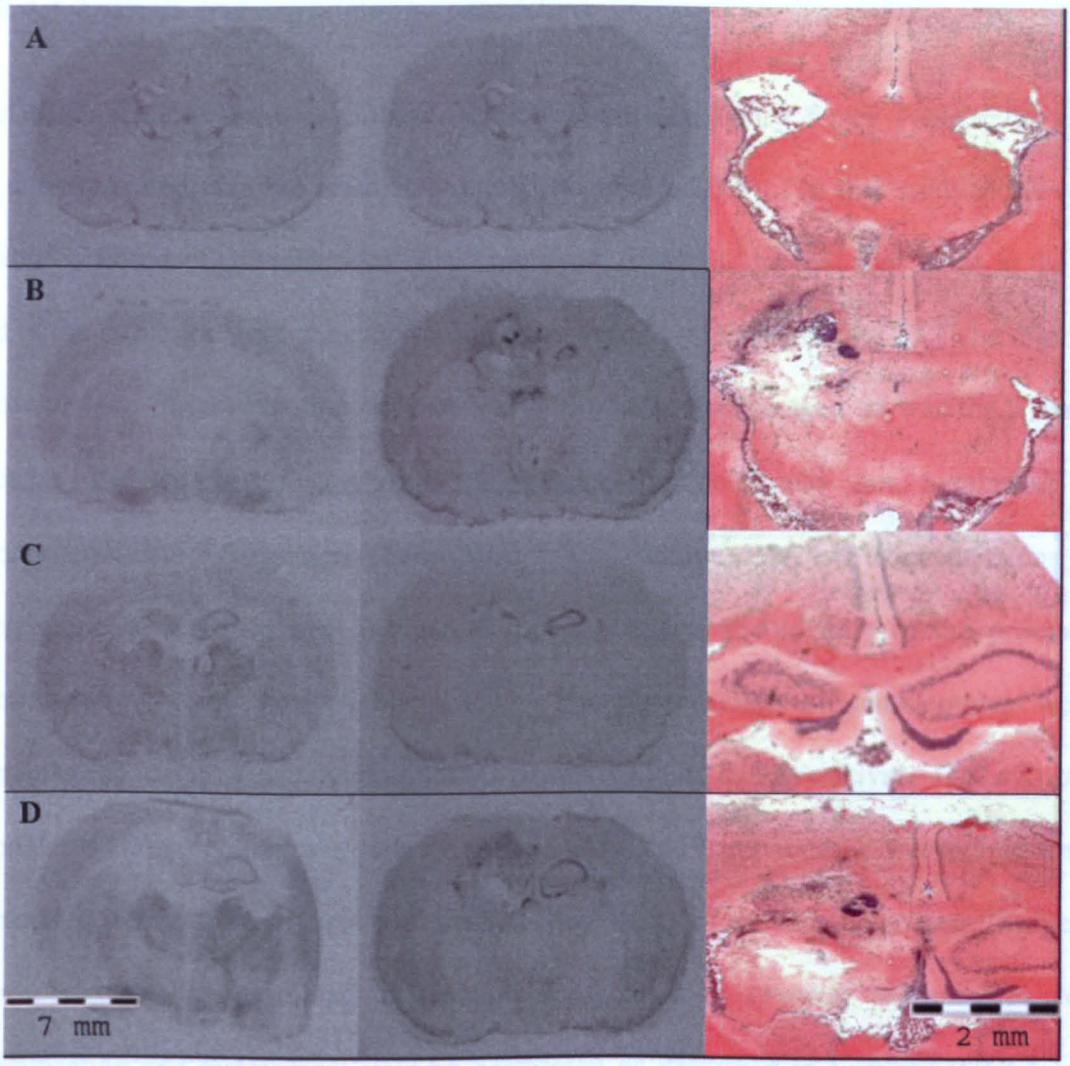

Comparison of *in situ* hybridisation autoradiographs utilising [^{33}P] – labelled oligonucleotide probes targeted against HCN 2 mRNA (first column) and β-actin mRNA (second column) and representative haematoxylin and eosin stained sections (third column). A = Vehicle, -1 mm relative to bregma, B = Sequence 1, -1 mm relative to bregma, C = Vehicle, -2.3 mm relative to bregma, D = Sequence 4, -2.3 mm relative to bregma.

2.2.4 Mixed backbone oligonucleotide infusion

2.2.4.1 Animals and experimental procedure

The oligonucleotide sequences used in this trial were Sequence 1 (see Table 2.12) and its corresponding control; Mismatch 1 (see Section 2.2.3.1). In this study however, mixed backbone oligonucleotides were employed, in which the first four bases at the 5' end of the sequence were phosphorothioate-linkages as were bases 14 – 17. The middle section of the oligonucleotide consisted of phosphodiester linkages, as was the 3'-base because the company supplying the oligonucleotide could not synthesise a phosphorothioate linkage here (GibcoBRL, UK). Additionally, two concentrations of each sequence were infused; 0.4 and 4 μg/μl/h, due to the toxicity of the previous administration study (see Figure 2.11). Phosphorothioate oligonucleotides were administered using 7-day osmotic mini-pumps (Alzet, Charles River, U.K., 1μl/h, Model 1007D) combined with a brain infusion kit. No behavioural observations were performed in this study, except for informal monitoring of rat cage behaviour. Surgery was performed as described in Section 2.2.2.2., with cryostat sections, *in situ* hybridisation and histological staining performed as described in Sections 2.2.3.1 and 2.2.3.3 respectively.

2.2.4.2 Statistical analyses

Data for each brain region of interest were analysed by one-way analysis of variance followed by Student Newman Keuls *post-hoc* multiple comparison test, as more than 3 groups were compared. Significance was assigned when $P < 0.05$ and analysis was performed using GraphPad Prism v3.02 (GraphPad Software Inc).

2.3.4 Mixed-backbone oligonucleotide infusion

2.3.4.1 Effect of 7-day infusion on rat body weight

Individual body weights were taken daily to determine the total body weight gain over the course of the study and collated to calculate the mean ± s.e. mean value for each treatment group (Figure 2.12). There was no significant difference between any of the treatment groups ($P > 0.05$). During the course of the study no animals required euthanasia, and infusion had no discernable effect on "normal" cage behaviour.

Figure 2.12 Total body weight gain for 7-day vehicle or end-modified oligonucleotide infusion.

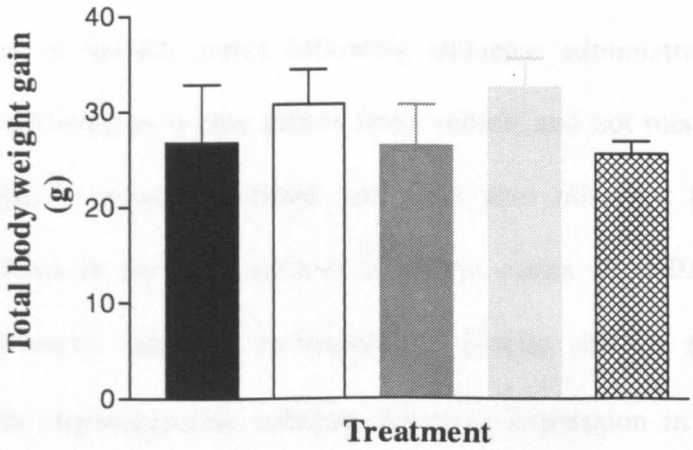

Weight gain of rats given a 7 day i.c.v. infusion of antisense to the HCN 2 transcript, mismatch oligonucleotide or vehicle (saline). Total weight gain was recorded for the 7 day infusion and 1 day baseline. Values represent means ± s.e. mean for 5 animals per group. Vehicle (■), 0.4 μg/μl/h antisense (□), 0.4 μg/μl/h mismatch (▪), 4 μg/μl/h antisense (▫), or 4 μg/μl/h mismatch (▨).

2.3.4.2 HCN2 and β-actin in situ hybridisation

A 7-day infusion of mixed backbone oligonucleotides significantly altered HCN2 and β-actin mRNA expression in a number of regions which were not confined to the unilateral hemisphere of surgery. However, this was not significant compared with both controls and cannot therefore be deemed a successful antisense effect. In the most rostral brain regions examined 0.4 μg/μl/h mismatch oligonucleotide infusion significantly increased HCN2 mRNA levels in the anterior cingulate cortex, rostral dorsal striatum and rostral ventral striatum of both hemispheres ($P < 0.001$). Infusion of 4 μg/μl/h antisense and 4 μg/μl/h mismatch oligonucleotide also significantly increased HCN2 mRNA expression in the left cortex ($P < 0.05$). Therefore, the increase in HCN2 expression observed in the left cortex following antisense administration cannot be considered to be significant as it only differs from vehicle and not mismatch infusion. Furthermore, 4 μg/μl/h antisense infused rats were also observed to significantly increase HCN2 mRNA in the right anterior cingulate cortex ($P < 0.05$). The only treatment to significantly alter the corresponding β-actin mRNA expression was 4 μg/μl/h mismatch oligonucleotide infusion, lowering expression in the left dorsal striatum and right ventral striatum ($P < 0.05$). No significant effect of oligonucleotide infusion was observed throughout the septum, thalamus or CA3 field of the hippocampus on either HCN2 or β-actin mRNA expression, as there was considerable variation within each treatment group, especially beside the cannula tract (Figures 2.13 – 2.20). β-actin mRNA levels were significantly higher following 4 μg/μl/h mismatch oligonucleotide infusion compared with saline control in the left ventral hippocampal commissure (Figures 2.17 & 2.18).

Figure 2.13 Effect of vehicle, antisense or mismatch infusion on HCN2 and β-actin mRNA expression (~ -0.3 mm relative to bregma)

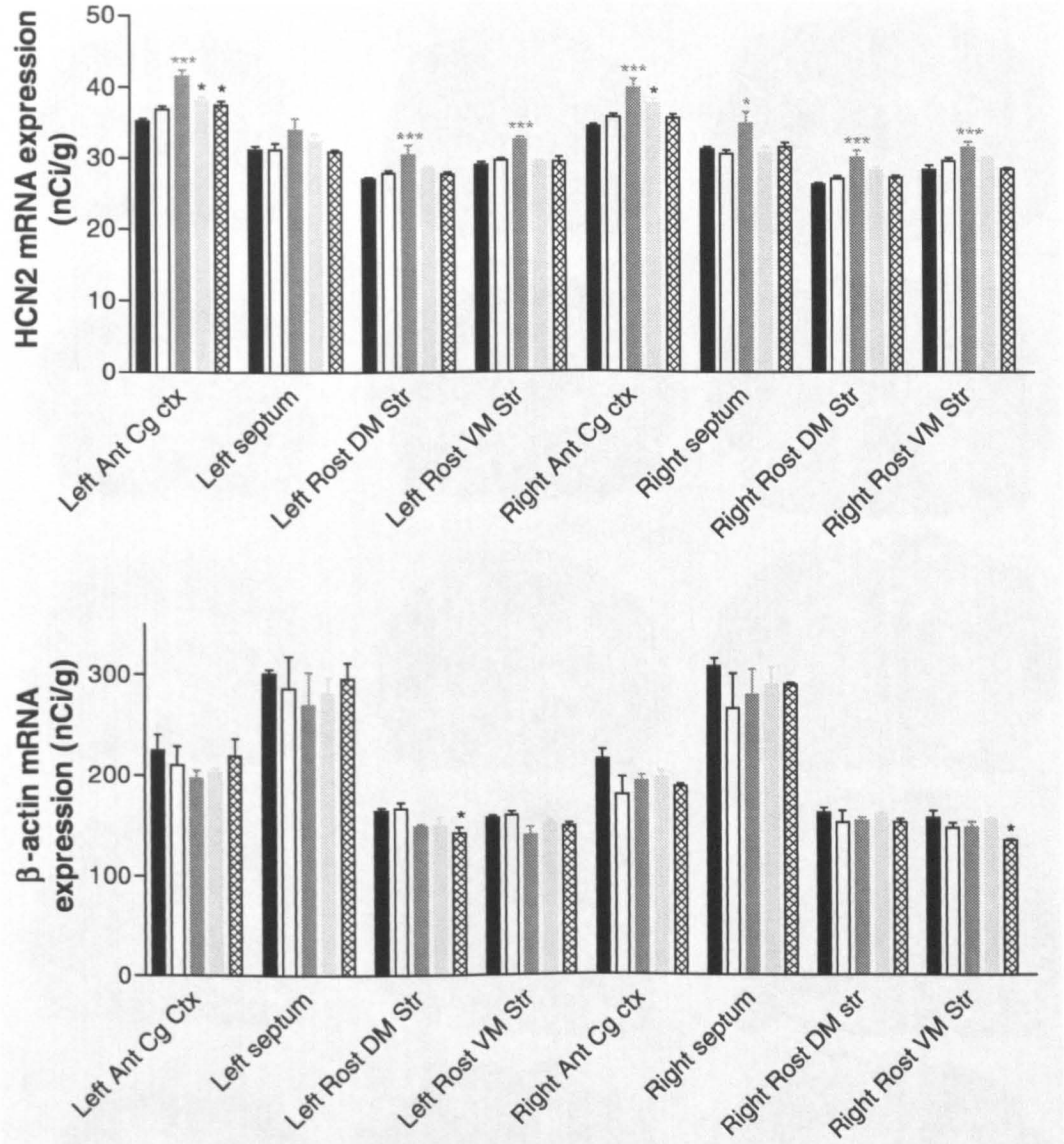

Data represent mean ± s.e. mean of three sections per animal (n = 4 - 5). Optical density readings have been converted to nCi/g of tissue. Treatment groups represented; Vehicle (■), 0.4 μg/μl/h antisense (□), 0.4 μg/μl/h mismatch (▪), 4 μg/μl/h antisense (▩) or 4 μg/μl/h mismatch (▨). One-way ANOVA with Student Newman Keuls *post-hoc* test was performed, * $P < 0.05$ and *** $P < 0.001$ compared with vehicle. Abb: Ant Cg ctx, anterior cingulate cortex, Rost DM Str, rostral dorsomedial striatum, Rost VM Str, rostral ventromedial striatum (Paxinos *et al.*, 1986).

Figure 2.14 Representative *in situ* hybridisation and haematoxylin and eosin images of vehicle, antisense and mismatch brain sections (~ -0.3 mm relative to bregma)

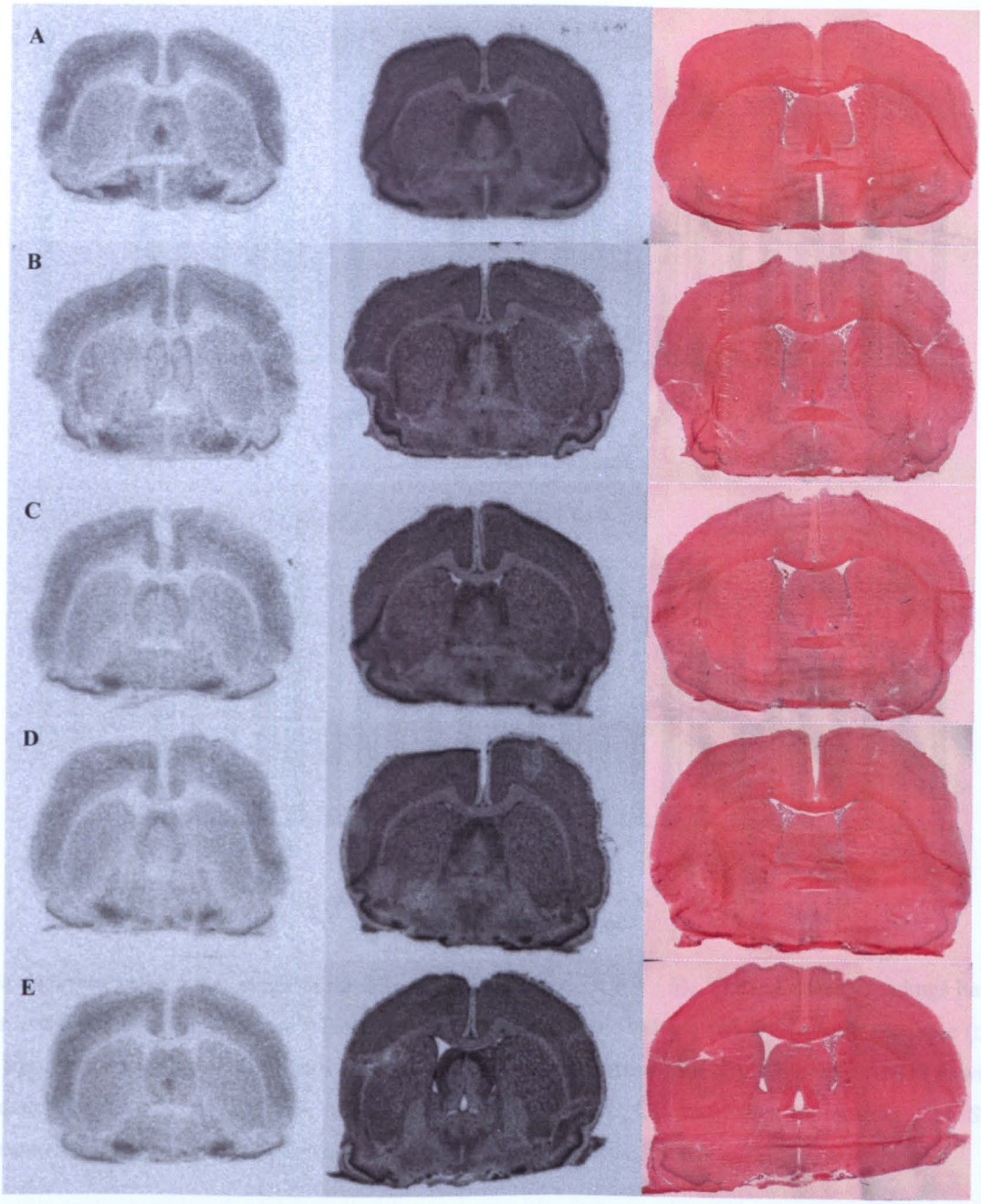

Comparison of *in situ* hybridisation autoradiographs utilising [^{33}P] – labelled oligonucleotide probes targeted against HCN 2 mRNA (first column) and β-actin mRNA (second column). Representative H & E stained sections (third column) are also shown for comparison (A = vehicle, B = 0.4 mg/ml antisense, C = 0.4 mg/ml mismatch, D = 4 mg/ml antisense and E = 4 mg/ml mismatch).

Figure 2.15 Effect of vehicle, antisense or mismatch infusion on HCN2 and β-actin mRNA expression (~ -0.8 mm relative to bregma)

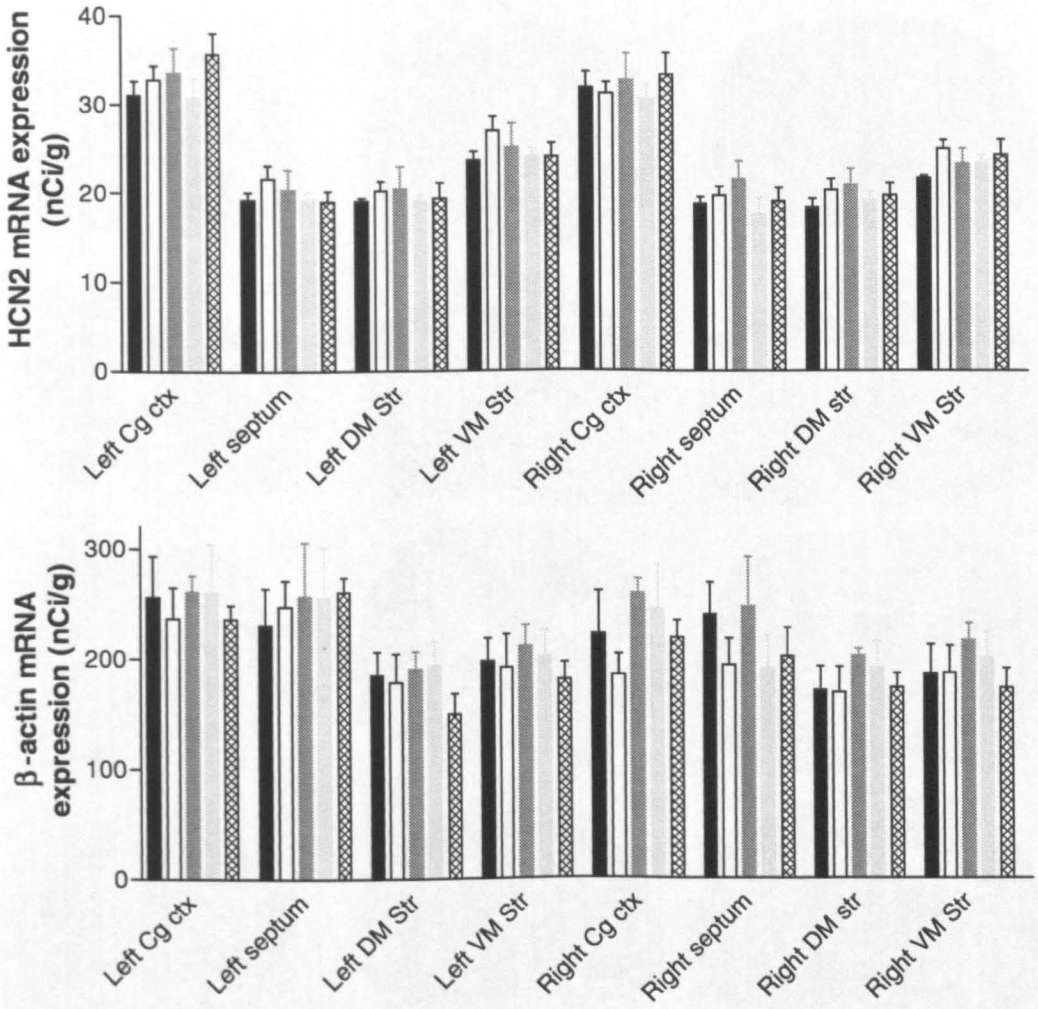

Data represent mean ± s.e. mean of three sections per animal (n = 4 - 5). Optical density readings have been converted to nCi/g of tissue. Treatment groups represented; Vehicle (■), 0.4 μg/μl/h antisense (□), 0.4 μg/μl/h mismatch (▪), 4 μg/μl/h antisense (▫) or 4 μg/μl/h mismatch (▩). One-way ANOVA with Student Newman Keuls *post-hoc* test was performed. Abb: Cg ctx, cingulate cortex, DM Str, dorsomedial striatum, VM Str, ventromedial striatum (Paxinos *et al.*, 1986).

Figure 2.16 Representative *in situ* hybridisation and haematoxylin and eosin images of vehicle, antisense and mismatch brain sections (~ -0.8 mm relative to bregma)

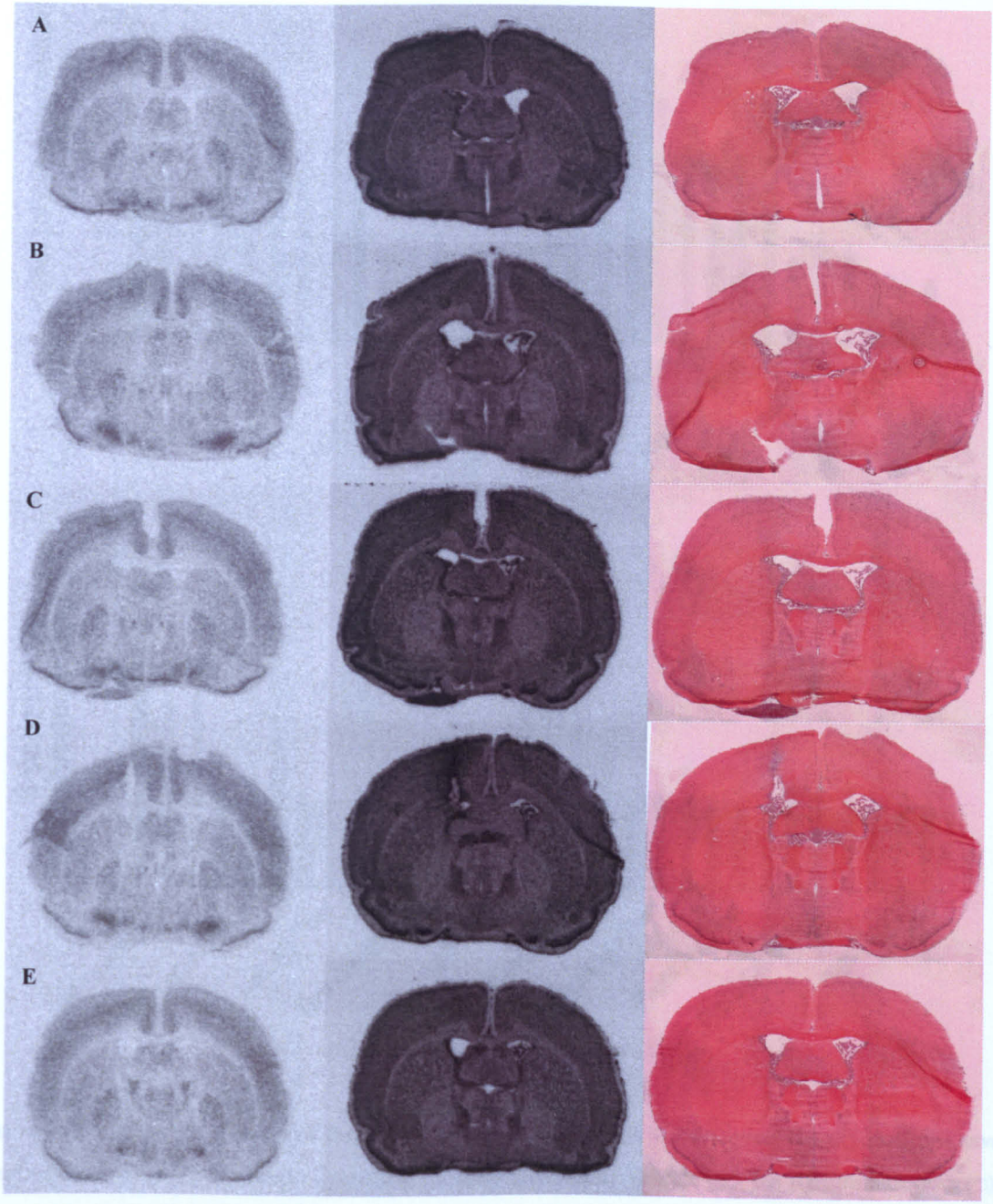

Comparison of *in situ* hybridisation autoradiographs utilising [^{33}P] – labelled oligonucleotide probes targeted against HCN 2 mRNA (first column) and β-actin mRNA (second column). Representative H & E stained sections (third column) are also shown for comparison (A = vehicle, B = 0.4 mg/ml antisense, C = 0.4 mg/ml mismatch, D = 4 mg/ml antisense and E = 4 mg/ml mismatch).

Figure 2.17 Effect of vehicle, antisense or mismatch infusion on HCN2 and β-actin mRNA expression (~ -1.5 mm relative to bregma)

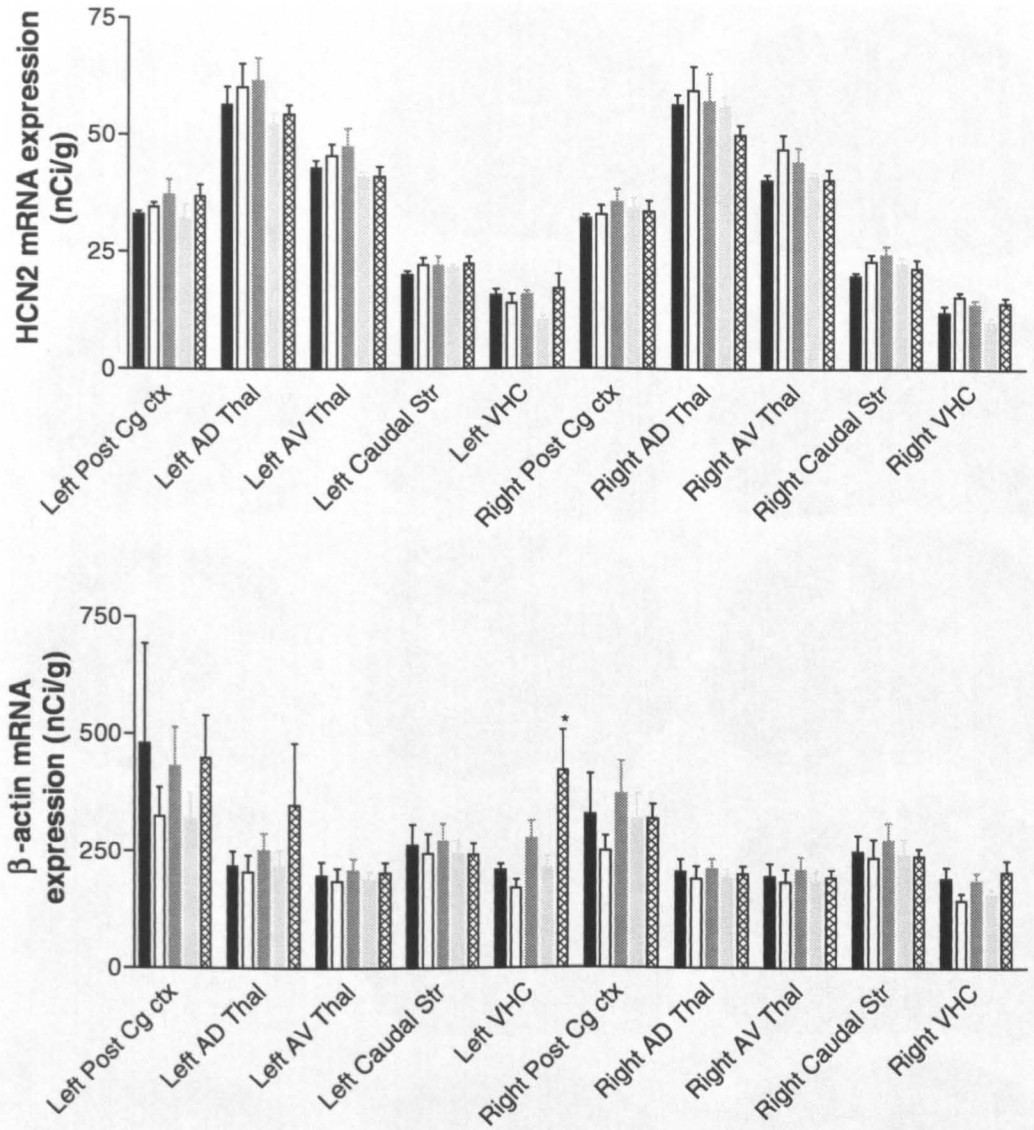

Data represent mean ± s.e. mean of three sections per animal (n = 4 - 5). Optical density readings have been converted to nCi/g of tissue. Treatment groups represented; Vehicle (■), 0.4 μg/μl/h antisense (□), 0.4 μg/μl/h mismatch (▪), 4 μg/μl/h antisense (▫) or 4 μg/μl/h mismatch (▩). One-way ANOVA with Student Newman Keuls *post-hoc* test was performed, * $P < 0.05$. Abb: AD Thal, anterodorsal thalamus, AV Thal, anteroventral thalamus, Post Cg ctx, posterior cingulate cortex, Str, striatum, VHC, ventral hippocampal commissure (Paxinos *et al.*, 1986).

Figure 2.18 Representative *in situ* hybridisation and haematoxylin and eosin images of vehicle, antisense and mismatch brain sections (~ -1.5 mm relative to bregma)

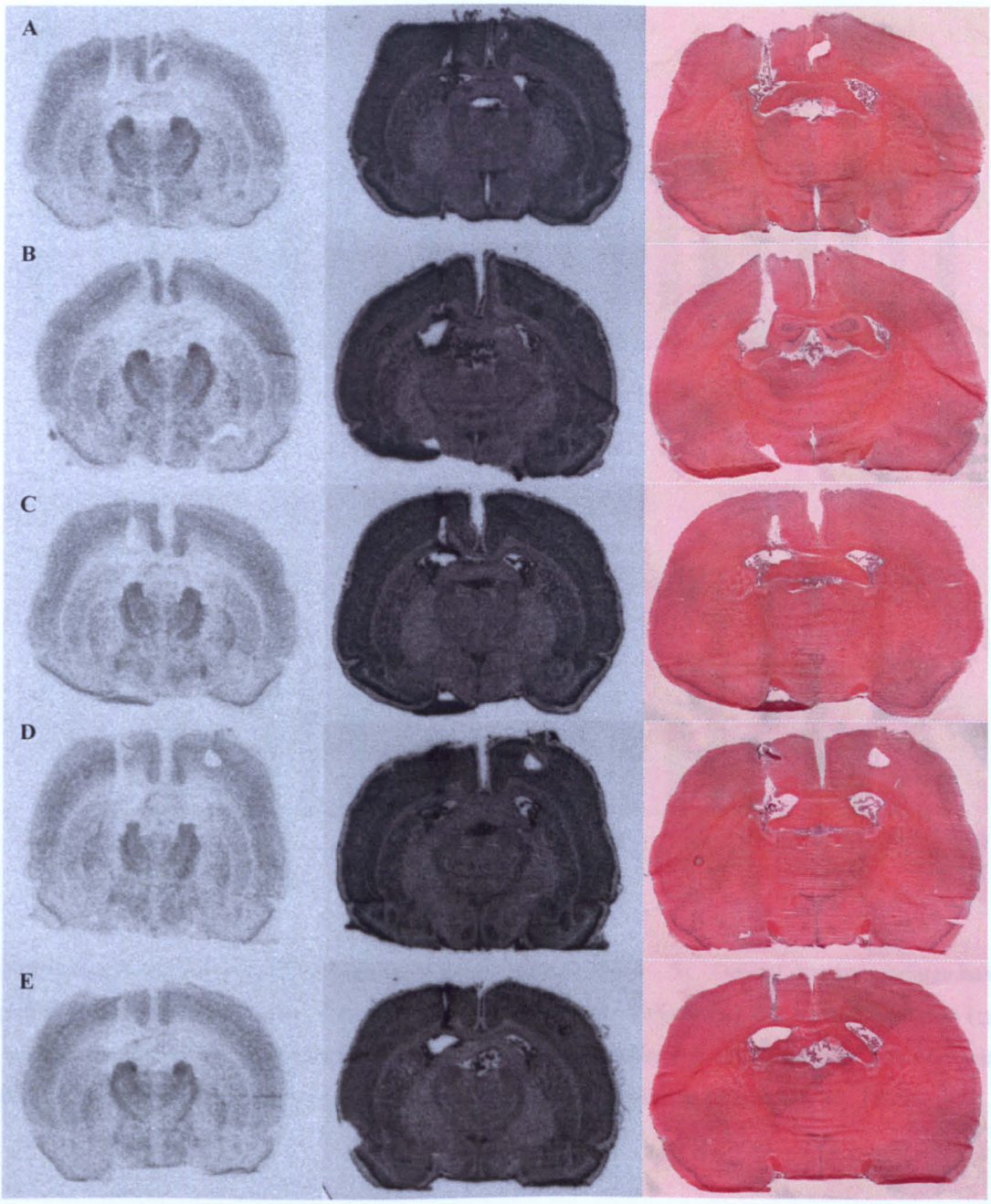

Comparison of *in situ* hybridisation autoradiographs utilising [^{33}P] – labelled oligonucleotide probes targeted against HCN 2 mRNA (first column) and β-actin mRNA (second column). Representative H & E stained sections (third column) are also shown for comparison (A = vehicle, B = 0.4 mg/ml antisense, C = 0.4 mg/ml mismatch, D = 4 mg/ml antisense and E = 4 mg/ml mismatch).

Figure 2.19 Effect of vehicle, antisense or mismatch infusion on HCN2 and β-actin mRNA expression (~ -2.3 mm relative to bregma)

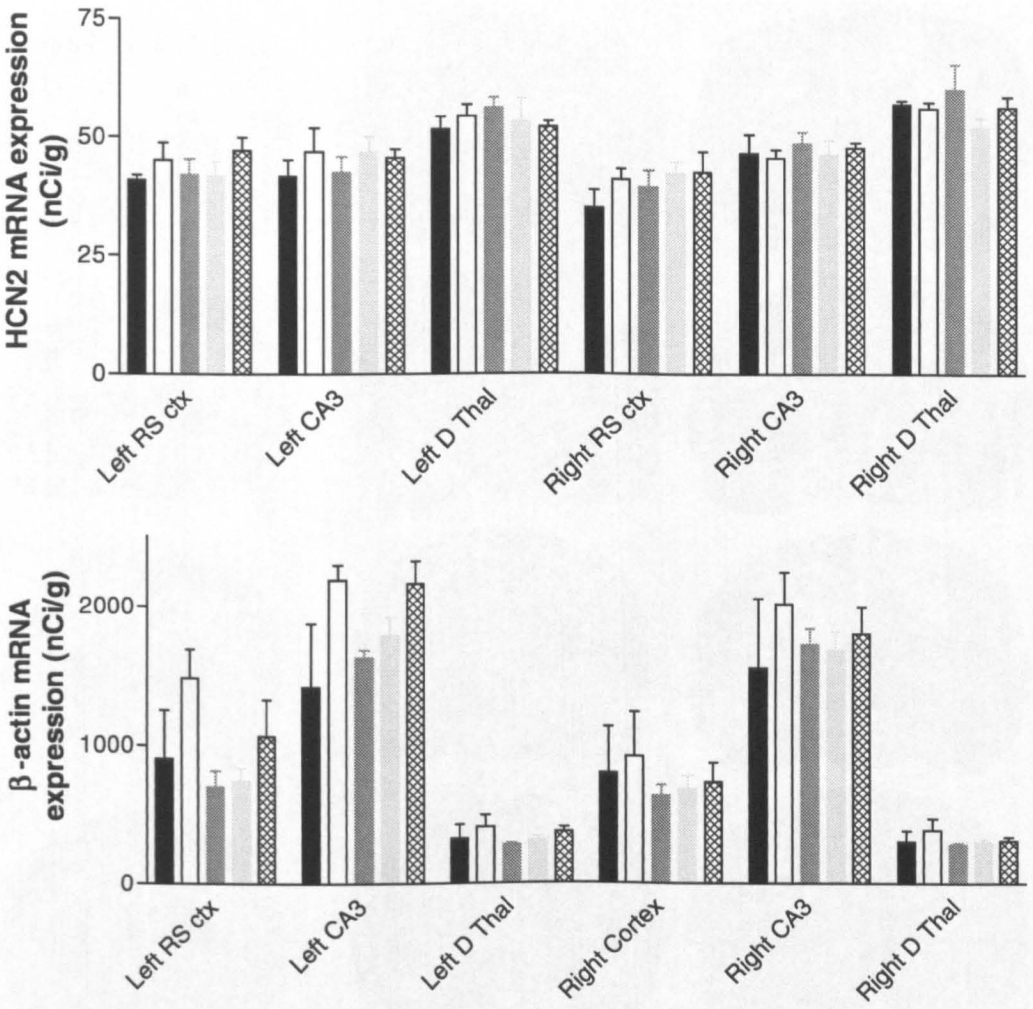

Data represent mean ± s.e. mean of three sections per animal (n = 4 - 5). Optical density readings have been converted to nCi/g of tissue. Treatment groups represented; Vehicle (■), 0.4 μg/μl/h antisense (□), 0.4 μg/μl/h mismatch (▪), 4 μg/μl/h antisense (▫) or 4 μg/μl/h mismatch (▩). One-way ANOVA with Student Newman Keuls *post-hoc* test was performed. Abb: Thal, thalamus (Paxinos *et al.*, 1986).

Figure 2.20 Representative *in situ* hybridisation and haematoxylin and eosin images of vehicle, antisense and mismatch brain sections (~ -2.3 mm relative to bregma)

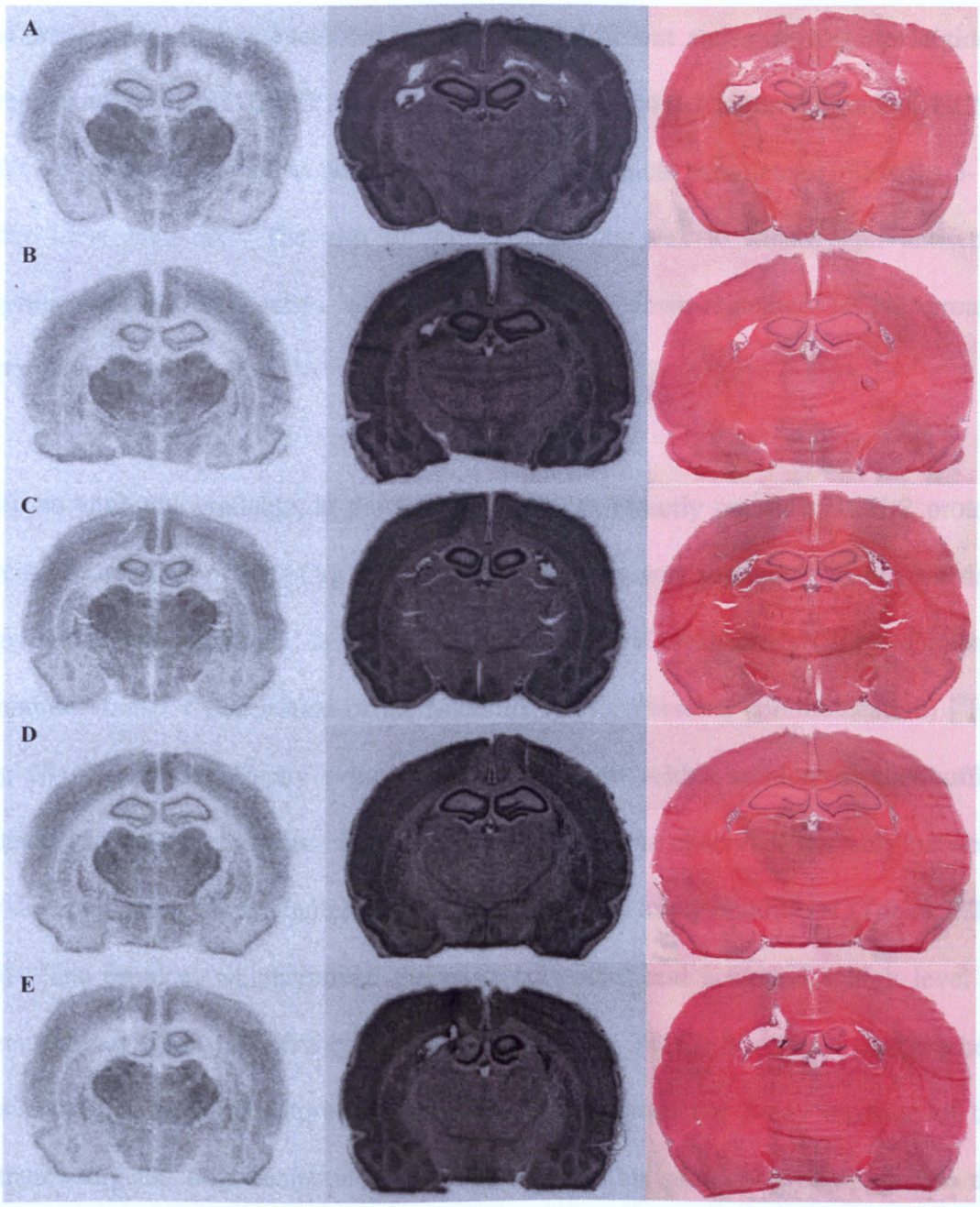

Comparison of *in situ* hybridisation autoradiographs utilising [^{33}P] – labelled oligonucleotide probes targeted against HCN 2 mRNA (first column) and β-actin mRNA (second column). Representative H & E stained sections (third column) are also shown for comparison (A = vehicle, B = 0.4 mg/ml antisense, C = 0.4 mg/ml mismatch, D = 4 mg/ml antisense and E = 4 mg/ml mismatch).

2.4 Discussion

The present chapter has examined the effects of different antisense oligonucleotides, complementary to the HCN2 transcript, on [^{3}H]-Org 34167 autoradiography, HCN2 mRNA expression, as well as behavioural and physiological parameters, following 3- or 7-day i.c.v. infusion. The aim of the experiments was to identify an antisense oligonucleotide, which when administered *in vivo,* down-regulated HCN2 protein expression.

With no antibody available, at the time of study, to directly measure HCN 2 protein levels, optimisation of [^{3}H]-Org 34167 autoradiography was attempted, as *in vitro* data suggest that this compound is a selective blocker of HCN channels (Ruigt, Personal communication). Optimisation of the Makkink *et al.,* (Personal communication) [^{3}H]-Org 34167 autoradiography protocol was performed with variation of the buffer, fixation and post-wash steps. Substantial variability was observed, not only between the different protocols attempted, but also for the same assay conditions (Tables 2.2 – 2.5). The protocol which proved the most consistent and achieved a high level of specific binding (50 mM Tris-buffer; 10 nM [^{3}H]-Org 34167; 3 x 1 min post-washes) was chosen to perform autoradiography on sections from the 3-day infusion of the initiation-targeted oligonucleotide. However, when this protocol was applied to the treated brain sections and exposed to tritium-sensitive film, negligible specific binding was achieved (Table 2.6 & Figure 2.3). This could have been as a result of the hyperfilm reaching saturation, because too high a concentration of [^{3}H]-Org 34167 was employed. However, similar negligible binding was observed when the treated sections were exposed to film for less time (results not shown). The more likely explanation is that the tritiated ligand had broken down, or the substantial inter-assay variability makes

this ligand unsuitable for autoradiographical use. Therefore, with the failure of [^{3}H]-Org 34167 to demonstrate HCN protein binding levels, and no available HCN2 antibody, only *in situ* hybridisation to study HCN2 mRNA was available to study the effect of antisense administration.

The studies, which employed an antisense oligonucleotide complementary to a region encompassing the initiation codon did not significantly alter mRNA expression. Despite the majority of early antisense experiments targeting this region, as this was believed to lead to the highest probability of success, it is now generally accepted that this is not the case (Smith *et al.*, 2000). Furthermore, a number of reportedly successful antisense experiments in the literature are now believed to be the result of non-specific antisense action (Smith *et al.*, 2000). There are two main reasons for this; firstly, sequences surrounding the initiation codon are more highly conserved than other regions (Crooke, 1999), which can result in non-specific interactions with non-homologous sequences, especially for GC-rich oligonucleotides (Lebedeva *et al.*, 2000; Smith *et al.*, 2000). Secondly, in targeting this region biologically active motifs within the sequence may be unavoidable (See Section 1.4.3); although this was not the case for any of the sequences investigated in this study. One of the newer backbone modifications, which have been utilised for antisense oligonucleotides, is the morpholino phosphorodiamidate. These oligonucleotides do not activate RNase H and achieve inhibition of translation only if targeted to a region incorporating the 5'-UTR through to 20 translated bases, solely *via* a steric mechanism (Nasevicius *et al.*, 2000; Summerton, 1999). It is possible that in targeting a similar region that the main mechanism of action of the oligonucleotide targeted to the initiation codon could be steric hindrance of the ribosome.

Therefore, with no down-regulation of HCN2 mRNA observed following infusion of a sequence targeting the initiation codon, six new sequences were designed. It has been shown that roughly 1 in 8 to 1 in 10 antisense sequences are successful at inhibiting protein expression and the main reason for this low success rate is believed to be accessibility to the targeted mRNA (Amarzguioui *et al.*, 2000; Milner *et al.*, 1997; Slew Peng *et al.*, 1998). A number of researchers have attempted to circumvent this problem by designing antisense oligonucleotides using secondary structure prediction computer modelling programs. However, these modelling programs are limited in their use, as the mechanism employed, calculation of global minimum free energy, returns numerous possible folds, especially for large sequences (see Section 1.4.2.2).

Of the sequences designed using mfold, Sequence 6 was 100 % complementary to HCN1, 2 and 4 transcripts, and when infused, severely altered rat physiological and behavioural functions. Indeed, the two rats administered with this antisense sequence demonstrated behaviours, including tremors, convulsions, weight loss and muscle wasting and were humanely killed. Similar behaviours (decreased movements and convulsions) have been observed previously when infusing mismatch oligonucleotides (Le Corre *et al.*, 1997), which may account for them in the present study. Another possibility is that this sequence knocked down HCN 1, 2 and 4 protein expression, which then lead to the observed behaviours. High doses of Org 34167 (> 0.5 mg/kg) also induce tremor and convulsions in rats, which are believed to be cerebellar in origin as they resemble harmaline-induced tremors and are linked to intentional movements (Blackburn-Munro *et al.*, Personal communication). Sequences 1, 2 and 4 were observed to elevate median daytime activity of rats compared with vehicle, while Sequences 1, 3 and 4 were noted to decrease HCN 2 mRNA in a number of brain regions analysed (Table 2.14). Furthermore, Sequence 4 infused rats were observed to

display the most consistent findings in the *in situ* hybridisation study. Sequences 2 and 5 were discarded due to an increase in behavioural signs of toxicity (Table 2.13), as was Sequence 6 due to neither rat completing the 3-day infusion. Therefore, based on these observations Sequences 1 and 4 were chosen to perform an extended trial on.

When the two sequences were subjected to a full-trial, with corresponding mismatch oligonucleotides, Sequence 1 again displayed a similar increase in total median rat behavioural activity, but there was also an increase in Mismatch 1 rat behavioural activity, suggesting this may be due to a non-specific mechanism (Figure 2.10). All oligonucleotides in this trial showed a trend towards an increase in total body weight, which was reflected in a similar trend in food and water intake during the 3-day infusion (Figures 2.8 & 2.9). This suggests a non-specific action of oligonucleotide infusion is to increase water intake, and it has previously been shown that oligonucleotide infusion caused a non-sequence-dependent suppression of food and water intake (Schobitz *et al.*, 1997). The authors hypothesised that the mechanism for the decreased food, water and locomotor parameters may be a direct result of modified nucleic acid administration, or indirectly *via* degradation products. However, phosphorothioate oligonucleotides have been demonstrated to cause brain inflammation and tissue damage, *via* granulocyte and macrophage entry into the parenchyma (Elepfandt *et al.*, 2002). This activation of the immune system by oligonucleotide infusion may provide an alternative explanation for the alteration in food and water intake. Furthermore, administration of a mismatch oligonucleotide (to an $\alpha_{2A/D}$ phosphorothioate antisense oligonucleotide) has been demonstrated to increase daily water intake (Robinson, Personal communication).

Histological staining of the 3-day i.c.v. infusion of Sequence 1 and 4 treated brain sections revealed significant tissue damage, especially in regions close to the cannula

tract. Similar damage to the brain has been reported previously following infusion of phosphorothioate oligonucleotides (Broberger *et al.*, 2000), which is mainly as a result of the incorporation of the sulphur atoms in the backbone to protect the oligonucleotide from degradation by nucleases. Therefore, no quantification of HCN2 or β-actin mRNA expression was performed because of the toxicological damage incurred following the infusion of the oligonucleotides (similar damage was observed in the mismatch control rats). This tissue damage may also explain the non-specific elevation of water intake.

A mixed backbone oligonucleotide infusion was used in an attempted to decrease the toxicity observed following oligonucleotide infusion, *via* reduction of their sulphur content. Sequence 1 was chosen for this trial due to the increase in rat behavioural activity observed in both the preliminary mfold study (Figure 2.7) and the full-trial (Figure 2.10). There was no significant alteration of HCN2 mRNA expression following 7-day antisense oligonucleotide infusion compared with both vehicle- and mismatch administration. Only the higher concentration of antisense (4 μg/μl/h) resulted in a significant change, an increase in HCN2 mRNA expression compared with vehicle, in the rostral left anterior cingulate cortex ($P < 0.05$, Figure 2.13). However, this cannot be considered a specific antisense effect as both concentrations of mismatch oligonucleotide (0.4- and 4-μg/μl/h) were observed to increase mRNA levels in this brain region ($P < 0.001$, Figures 2.13 & 2.14) and there was no significant difference compared with antisense administration. This may have been a result of tissue damage in the cingulate cortex by the cannula. Therefore, the antisense sequences administered did not result in a significant alteration in HCN 2 mRNA expression compared with both vehicle and mismatch treatment.

The second aim of lowering toxicity of oligonucleotide infusion by reducing the sulphur content of the oligonucleotides was achieved, as has been shown throughout the literature (Agrawal *et al.*, 1997b; Sands *et al.*, 1995). Comparison of the histology between the corresponding brain regions of the fully-modified oligonucleotides and the mixed-backbone oligonucleotides infusions reveals less toxic damage of the brain regions surrounding the lateral ventricle (Figure 2.11, 2.16, 2.18 & 2.20). Additionally, the fact that there was little significant alteration in the housekeeping gene, β-actin, which was employed as a control gene, suggests that the toxicity was decreased. There were a number of brain regions where expression of the housekeeping gene β-actin's mRNA was increased following infusion of the higher concentration of mismatch oligonucleotide (4 μg/μl/h) but the only region this reached significance was the ventral hippocampal commissure ($P < 0.05$; Figure 2.17). However, there was considerable variation within each treatment group, especially in regions close to the cannula tract (see Figures 2.13 – 2.20). It has previously been demonstrated that cells within 200 μm of the cannula tract are heavily labelled with fluorescent oligonucleotide (Grzanna *et al.*, 1998), which may explain some of the variation in β-actin mRNA levels. The haematoxylin and eosin staining demonstrates an increased number of nuclei around the cannula tract, which may be due to the damaged tissue resulting in an immune response. This increase in cells may therefore be the cause of the variation and increase in β-actin mRNA observed. Additionally, the histological evidence showing damage incurred when implanting the cannula may be responsible for the variation in the activation of β-actin mRNA, as some surgery may have involved more extraneous movement of the cannula.

The fact that there was no significant alteration of HCN2 mRNA expression does not necessarily lead to the conclusion that there was no antisense-mediated down-regulation

of HCN2 protein. Despite examples in the literature of successful antisense sequences down-regulating the target mRNA expression (see Table 2.15) there are also numerous reports of successful down-regulation of the target protein without a corresponding affect on the mRNA expression (see Table 2.15). All the examples in Table 2.15 use phosphodiester or phosphorothioate oligonucleotides, similar to those used in the present study, which are believed to mediate their antisense effect through two main mechanisms; RNase H activation and steric hindrance of the ribosome (see Section 1.4.2). There are a number of possible explanations for not observing a down-regulation of target mRNA expression. Firstly, and most likely, is that none of the sequences employed resulted in successful antisense-mediated down-regulation of HCN2 protein expression. This could not be confirmed at the time of study because of the lack of a specific antibody and the failure of [^{3}H]-Org 34167 autoradiography to provide meaningful results. The main obstruction for antisense therapeutics has been to overcome the problem of targeting an accessible site on the mRNA, which is devoid of secondary and tertiary structure (or at least displays minimal folding). This is believed to be the main reason why only ~ 1 in 10 sequences are successful. Despite a number of the current sequences being designed with the aid of the computer modelling program mfold (http://bioinfo.math.rpi.edu/~mfold/rna/) to target a region of the mRNA which was predicted to be predominantly single-stranded, in the optimal folds, these prediction programs are limited in predicting accurately, especially for large sequences.

Table 2.15 Literature examples of antisense oligonucleotide administration on mRNA and protein levels

TARGET	OLIGONUCLEOTIDE	EFFECT ON GENE EXPRESSION		REFERENCE
		mRNA	Protein	
NMDA-R1	Phosphodiester 18 mer i.c.v.80 µg x 4/2d	No change	↓ 35 %	(Wahlestedt *et al.*, 1993)
m1 mACh	Phosphorothioate 16 mer 5 µg/µl/h 3d	↓ 64 % in Superior cervical ganglia cells (not done in vivo)	↓ 40 %	(Zang *et al.*, 1994)
CB1	Phosphodiester 18 mer 10nM x 2/3d	No change	↓35 %	(Kathmann *et al.*, 1999)
D_2	Phosphorothioate 20 mer 16 µg i.c.v 9d	↓ 20 %	↓ 15 %	(Zhou *et al.*, 1994)
nNOS-1	Phosphodiester 20 mer 2 µl i.c.v	↓ 60 %	n.d.	(Kolesnikov *et al.*, 1997)
nNOS-2	Phosphodiester 20 mer 2 µl i.c.v.	↓ 75 %	n.d.	(Kolesnikov *et al.*, 1997)

Abb: CB1, cannabinoid-1 receptor. D_2, Dopamine$_2$-receptor. m, muscarinic. nNOS, neuronal nitric oxide synthase. n.d. = not defined.

Alternatively, it may be that these oligonucleotides' main mechanism of action is *via* steric hindrance, which would prevent translation but not cause a corresponding degradation of the mRNA by RNase H. This theory is supported by the fact that backbone modifications, including locked nucleic acids (Kurreck *et al.*, 2002) and 2'-O-methoxyethyl (Baker *et al.*, 1997) have been demonstrated to achieve down-regulation of the target protein but do not activate RNase H and therefore do not alter mRNA expression. The oligonucleotides may act by preventing transportation of the target mRNA, which similarly would prevent translation (Alama *et al.*, 1997). There may be a compensatory up-regulation of mRNA as a consequence of increased turnover of

mRNA due to digestion by RNase H and a decrease of protein levels although there is no evidence in the literature to support this. Another possible reason for detecting no change in HCN2 mRNA expression in any of the current studies is that the concentration of antisense oligonucleotide was not sufficient. As can be seen in Table 2.15 a wide range of concentrations have been used to successfully down-regulate the target protein. This is believed to relate to each individual sequence, backbone modifications and accessibility to the targeted region of the mRNA (see Crooke, (1999) for a review). A behavioural assay can be performed to assess for an antisense-mediated down-regulation of the target gene (Robinson *et al.*, 2000). However, there were no such assays available at the time of study. Electrophysiological recording of the properties of the HCN channel, in either brain slices or human HCN2 cell lines could have been performed after *in vitro* or *in vivo* administration of antisense oligonucleotide but there was no opportunity to perform such an experiment. The final option to assess for a specific antisense-effect is by performing an agonist-induced behavioural response (Robinson *et al.*, 2000). At the time of writing there are no available compounds for the HCN channel with which to perform such an experiment.

In conclusion the antisense oligonucleotides used in the present studies, despite the majority of sequences being designed with the aid of a secondary structure prediction program, were not observed to alter HCN2 mRNA expression *in vivo*. The use of an end-modified oligonucleotide resulted in a lower degree of toxicity. This is apparent from the histological images of the brain sections compared with the corresponding fully-modified oligonucleotides, as has been demonstrated throughout the literature. A successful antisense action cannot presently be completely rejected, as direct measurement of HCN2 protein expression has not been performed, or a behavioural assay examined, neither of which could be attempted at the time of study.

Chapter 3 Comparison of Org 34167 induced changes in *c-fos* expression to that of known antidepressants

3.1 Introduction

In the late 1980s, it was discovered that the Fos-oncogene, isolated from the Finkel-Biskis-Jinkins murine sarcoma virus (Curran *et al.*, 1982) was derived from a normal cellular gene (Sagar *et al.*, 1988). There are a now a number of similar genes identified; of which the Fos-, Jun- and Egr- families are the most extensively studied (Beckmann *et al.*, 1997; Cochran *et al.*, 2002). These products are classed as immediate early genes (IEG; Herdegen *et al.*, 1998; Hoffman *et al.*, 2002), or inducible transcription factors (ITF; Herdegen *et al.*, 1998); although not all IEGs function as transcription factors. Currently, four protein members of the Fos-family have been identified; c-Fos, FosB, Fra-1 and Fra-2 (Cohen *et al.*, 1990; Greenberg *et al.*, 1984; Nishina *et al.*, 1990; Zerial *et al.*, 1989).

IEGs are so called due to their rapid expression in the absence of new protein synthesis, governed by pre-existing, constitutive transcription factors (Herdegen *et al.*, 1998). Therefore, IEG induction, in response to a stimulus, represents one of the earliest cellular effects, and can be detected using *in situ* hybridisation (Ziolkowska *et al.*, 2002) or immunohistochemistry (Dragunow *et al.*, 1989). c-Fos protein, following dimerisation with a member of the Jun-family (c-Jun, JunB or JunD) form Activator protein (AP)-1, which binds to consensus DNA sequences to enhance or repress transcription (Herdegen *et al.*, 1998). This protein dimer also controls the expression of IEGs, which are synthesised in the cytoplasm and translocated to the nucleus (Herrera *et al.*, 1996).

Under basal conditions *c-fos* mRNA and protein expression are very low, displaying a widespread, but not ubiquitous, distribution. However, they are rapidly induced following a variety of stimuli (see Figure 3.1; Herrera *et al.*, 1996; Hoffman *et al.*, 2002). It is generally believed that Fos-induction can be considered to reflect neuronal activity due to it's function of controlling gene transcription (Chaudhuri, 1997; Dragunow *et al.*, 1989; Herrera *et al.*, 1996; Hoffman *et al.*, 2002). These properties have rendered Fos the most commonly utilised IEG for mapping neuronal activity. The pathways which lead to the activation of c-Fos are the best studied of the IEGs; with three main regulatory sites present on the protein (See Figure 3.1). A calcium response element (CRE) is activated *via* phosphorylation of CREB by cAMP, PKA, or Ca^{2+} entry (Herrera *et al.*, 1996; Sheng *et al.*, 1990). This appears to be the dominant pathway of *c-fos* activation, as NMDA-receptor antagonists prevent Ca^{2+} entry in to the cell and also prevent the induction of *c-fos* (Ziolkowska *et al.*, 2002). Growth factors and cytokines, *via* mitogen activated protein (MAP) kinases and Janus protein kinases (JAK), also lead to the induction of *c-fos* through serum-response factors and the signal transducer and activator of transcription (STAT) on tyrosine kinases respectively (Herrera *et al.*, 1996; Pennypacker, 1998). It is the presence of these different promoters on c-Fos, which makes it an ideal gene to study neuronal activation, as a wide variety of stimuli lead to alteration of the regulatory pathways. Induction of c-Fos is not simply related to cellular activity as a number of studies have demonstrated that alterations in Fos expression are not related to depolarisation but changes in second messenger systems caused by drug administration (Young *et al.*, 1991).

Figure 3.1 Major induction pathways of *c-fos*

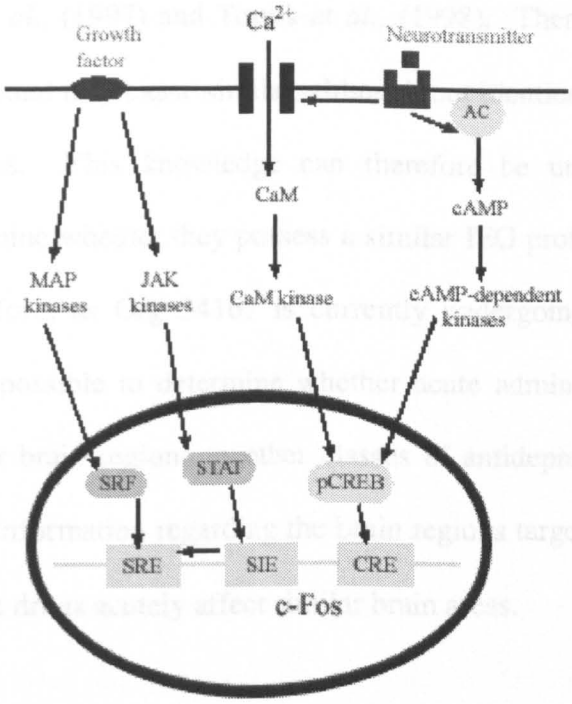

Adapted from Hoffman & Lyo (2002) and Pennypacker (1998). Abb: AC, adenylyl cyclase, cAMP, 3' 5' monophosphate, CaM, calcium calmodulin, JAK, Janus activated protein, MAP, mitogen activated protein, SRF, serum response factor, SRE, serum response element, CRE, calcium response element, STAT, signal transducer and activator of transcription.

The ability to utilise IEGs as markers of neuronal activity has been used to study both acute and chronic antidepressant administration (although the latter is normally followed by an acute challenge), and a number of animal models of depression (see Discussion). In the majority of these studies, only a few brain regions have been examined for Fos alterations, which does not enable the different classes of antidepressant to be compared with Fos neuronal activity throughout the CNS. Additionally, many of these studies have focussed on similar brain regions, for example Beck (1995) demonstrated that the central amygdala was activated by all antidepressants studied; fluoxetine (10 and 15 mg/kg, i.p.), desipramine (TCA inhibits NA reuptake and 5-HT to a lesser extent; 10 mg/kg, i.p.), bupropion (inhibits mainly DA reuptake; 20 mg/kg, i.p.), tranylcypromine (monoamine oxidase inhibitor, 7.5 mg/kg), nortriptyline (TCA, inhibits NA reuptake; 15 mg/kg, i.p), imipramine (20

mg/kg, i.p.) and citalopram (SSRI; 5 mg/kg, i.p.), findings repeated by Ducan *et al.*, (1996), Morinobu *et al.*, (1997) and Torres *et al.*, (1998). Therefore, it would appear that classes of compound may cause similar, although not identical, induction of *c-fos* in several brain regions. This knowledge can therefore be utilised to study novel compounds to determine whether they possess a similar IEG profile as drugs already in clinical use. Therefore, as Org 34167 is currently undergoing clinical trials as an antidepressant, it is possible to determine whether acute administration induces *c-fos* expression in similar brain regions to other classes of antidepressant. This could, in turn, provide useful information regarding the brain regions targeted by antidepressants and whether different drugs acutely affect similar brain areas.

There are a number of considerations to be taken in to account when using c-Fos as a neuronal activity marker. The major drawback is that in some brain regions Fos is not basally expressed, while in others studies have shown that a wide variety of stimuli do not induce the gene above basal (Chaudhuri, 1997; Labiner *et al.*, 1993). The substantia nigra is one such region in which few stimuli in rodents induce *c-fos* (Dragunow *et al.*, 1989; Labiner *et al.*, 1993). Therefore, this may be the case in other brain regions, which implies that a lack of Fos induction need not necessarily mean a lack of neuronal activity. Another consideration in the use of IEGs for neuronal activity mapping is the transient nature of their expression. Time-course studies have shown that *c-fos* mRNA is rapidly activated, within 30 – 60 min of an acute challenge with fluoxetine (Torres *et al.*, 1998), or light stimulation (Zangenehpour *et al.*, 2002). Protein levels of *c-fos* reach a peak 2 - 6 h after the stimulus, by which time mRNA expression has returned to baseline (Torres *et al.*, 1998; Zangenehpour *et al.*, 2002). The protein expression returns to baseline within 24 h following the acute stimulus (Zangenehpour *et al.*, 2002). A problem with the present study is that the rat brain does not necessarily reflect

the situation in human (Ongur *et al.*, 2000). Although chronic antidepressant administration is required to be clinically beneficial it is possible using *c-fos* neuronal mapping, to demonstrate which brain regions are activated following an acute injection. Due to the role of *c-fos* in activating or repressing gene translation, this immediate early gene marker can be considered to reflect, to a certain degree, long-term changes in cellular phenotype.

The rationale for the present study was to examine the *c-fos* mRNA expression of Org 34167 and to compare it with a number of different classes of antidepressants and a mood stabiliser. Fluoxetine, imipramine and lithium (LiCl) were chosen due to the already existing extensive literature concerning their *c-fos* induction profile, while mirtazapine was included to provide proof of concept, as there were no previous reports examining this novel antidepressant. Furthermore, as previous literature suggests that the central amygdala is a common site of antidepressant action, the current study aimed to assess this area plus a number of other brain regions associated with depression to determine whether there are additional sites of common acute antidepressant action.

3.2 Materials and methods

3.2.1 Animals and experimental procedure

Adult male Sprague-Dawley rats (Harlan Olac, U.K.) weighing 200 - 250 g were housed in groups of 6 on a 12 h light/dark cycle (lights on at 06:00 h) at 22 ± 2 °C for 7 days with access to standard rat diet and tap water *ad libitum*. Previous studies have demonstrated that habituation to handling, prior to the acute stimulus, reduces non-specific background levels of *c-fos* mRNA (Hess *et al.*, 1995). Therefore, on each day the rats were handled for 5 min and weighed to minimise handling stress.

Animals received a single intraperitonal injection of vehicle (5 % mulgofen in 0.9 % saline), LiCl (75 mg/kg), mirtazapine (2 mg/kg), fluoxetine (5 mg/kg), imipramine (15 mg/kg) or Org34167 (0.5 mg/kg), n = 6 for each treatment group. All drugs were dissolved in a 5 % mulgofen, 0.9 % saline solution, and administered at 1 ml/kg. Following the injection the rats were returned to their home-cage for 45 min. Injection of the groups was staggered between 09:30 – 12:00 h in order to maintain a 45 min sacrifice time post-injection. Rats were sacrificed in a CO_2-chamber, at a flow-rate of 6 l/min then decapitated using a guillotine. The brains were carefully removed using scissors to cut away the skull, placed on a slide (Suprafrost Plus, VWR formally BDH) and then snap frozen in isopentane cooled on dry-ice to -32 °C. The brains were then stored at -80 °C until required for cryostat sectioning. The Org 34167 dose was selected based on previous behaviourally-active concentrations (see Table 1.1) while the antidepressant doses were chosen to reflect those used in previous literature *c-fos* reports (Beck, 1995; Dahmen *et al.*, 1997; Morinobu *et al.*, 1997; Torres *et al.*, 1998). The LiCl dose was chosen to reflect the dose, which has been demonstrated to be the lowest active dose in the conditioned taste aversion paradigm (Spencer *et al.*, 2001).

3.2.2 Cryostat-sectioning

The brains were removed from -80 °C freezer and allowed to thaw to -18 ± 2 °C inside a Bright OTF cryostat for 30 min before mounting on to a Bright orientating specimen holder with Cryo-M-bed (Bright Ltd., U.K.). Once solidly mounted, the chuck was attached to the microtome, with the blade aligned at an angle of 15 ° and set to collect sections of 20 μm. Sections were thaw-mounted on to Superfrost Plus electro-statically charged nuclease-free slides (VWR, formally BDH, UK) in 7 series of 13 slides, with 3 sections per slide. The series were chosen to maximise the number of brain areas, which have been implicated in depression (See Table 3.1)

Identification of sections was performed with the aid of a rat brain atlas (Paxinos *et al.*, 1986) and also by collecting sections and performing histological staining at routine intervals. The staining comprised 1 min in 100 % ethanol, followed by 1 min in Gills No 2 haematoxylin solution (BDH) and a final dip rinse in distilled water. These two control procedures enabled accurate and consistent sectioning to be maintained throughout each of the brains. The slides were stored at -80 °C until required for *in situ* hybridisation.

Table 3.1 Brain co-ordinates of sections collected for *c-fos* study and brain regions analysed.

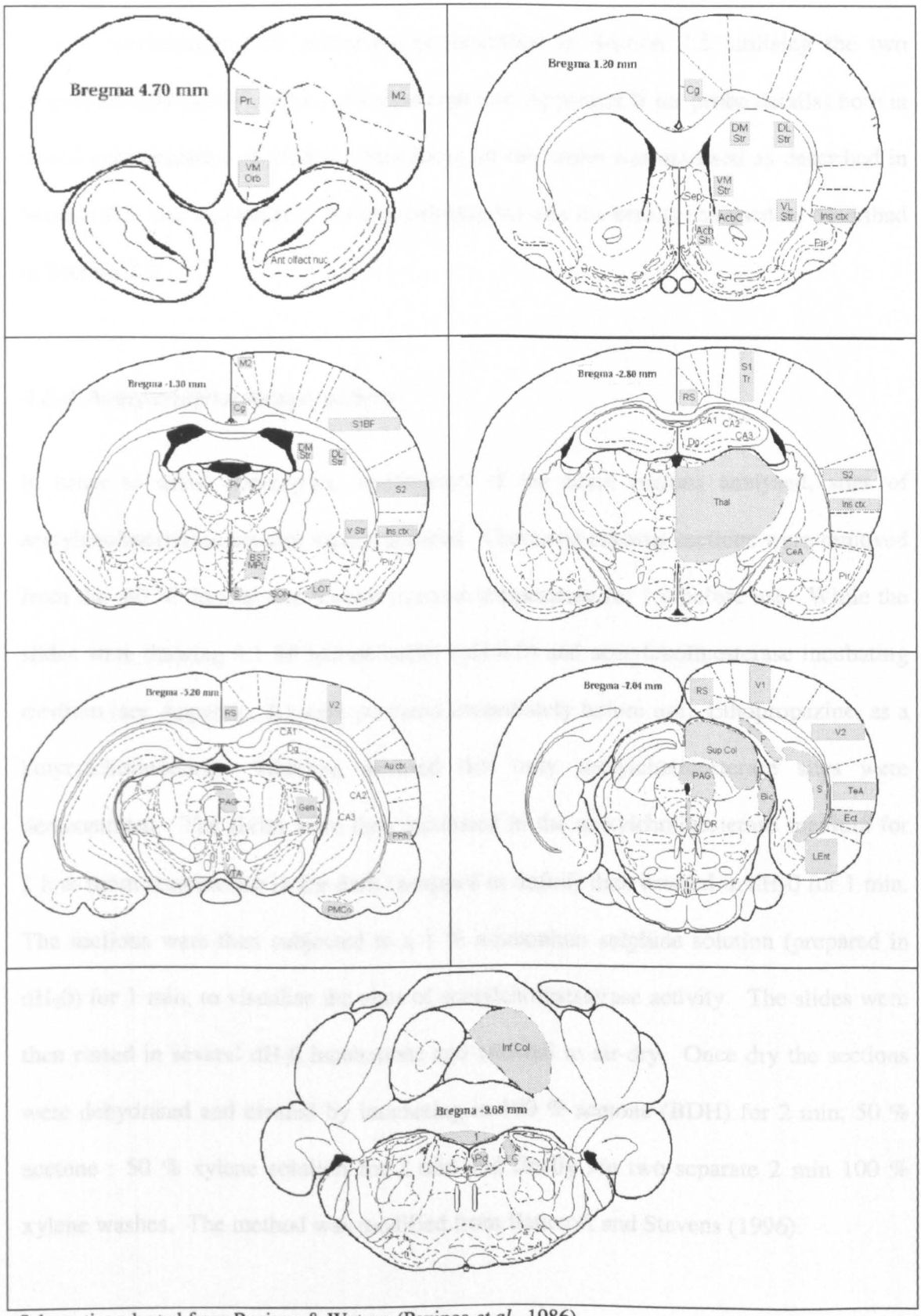

Schematics adapted from Paxinos & Watson (Paxinos *et al.*, 1986).

3.2.3 c-fos in situ hybridisation

In situ hybridisation was performed as described in Section 2.2. utilising the two complementary probes to the *c-fos* transcript (see Appendix B for probe details) both at a final concentration of 2 pmol. Specificity of the probe was assessed as described in Section 2.2. (see Appendix C for autoradiograms) and the results analysed as described in Section 2.2.

3.2.4 Acetylcholinesterase activity

In order to assist histological verification of the brain regions analysed, sites of acetylcholinesterase activity were examined. Untreated cryostat sections were removed from the -80 °C freezer and thawed to room temperature for 1 h before use. While the slides were thawing 0.1 M acetate buffer (pH 6.0) and acetylcholinesterase incubating medium (see Appendix A) were prepared immediately before use. Ethopropazine, as a butyrylcholinesterase inhibitor, ensured that only acetylcholinesterase sites were demonstrated. The slides were then incubated in the acetylcholinesterase medium for 2 h at room temperature in the dark (wrapped in tinfoil) then washed in dH_20 for 1 min. The sections were then subjected to a 1 % ammonium sulphide solution (prepared in dH_20) for 1 min, to visualise the sites of acetylcholinesterase activity. The slides were then rinsed in several dH_20 incubations and allowed to air-dry. Once dry the sections were dehydrated and cleared by incubating in 100 % acetone (BDH) for 2 min, 50 % acetone : 50 % xylene solution for 2 min and finally *via* two separate 2 min 100 % xylene washes. The method was modified from Bancroft and Stevens (1996).

Control reactions were performed as described above, but with the omission of the substrate, acetylthiocholine iodide, from the incubating medium.

3.2.5 Statistical analyses

Data for each region of interest were analysed by One-way analysis of variance followed by Student Newman-Keuls *post-hoc* multiple comparison test. Significance was assigned when $P < 0.05$ and performed using GraphPad Prism v3.02 (GraphPad Software Inc). Due to the number of comparisons performed all the statistical significance is reported as $P < 0.05$, even if the value was lower, for simplicity.

3.3 Results

3.3.1 Effect of treatment on c-fos mRNA expression

In situ hybridisation utilising two probes complementary to the rat *c-fos* transcript following acute antidepressant administration demonstrate differing expression profiles for each treatment group. In vehicle-treated animals a low level of *c-fos* mRNA expression was observed throughout the rostrocaudal extent of the rat brain as previously described (Cochran *et al.*, 2002; Dragunow *et al.*, 1989; Hoffman *et al.*, 2002). Each of the different drug-treatment groups displayed different regulation of *c-fos* mRNA expression, with both increased and decreased levels compared with all other treatment groups observed. The alteration of *c-fos* mRNA following acute drug administration is discussed by brain region relative to bregma below.

3.3.2 Effect of treatment on c-fos mRNA (4.7 to 4 mm relative to bregma)

Forty-five minutes following acute administration of Org 34167 (0.5 mg/kg) a significant increase, compared with vehicle, imipramine, mirtazapine, LiCl and fluoxetine in *c-fos* expression was observed in the anterior secondary motor cortex ($P < 0.05$; Figure 3.2 and Table 3.2). LiCl also increased *c-fos* expression compared with vehicle and fluoxetine ($P < 0.05$). Ventromedial orbital cortex *c-fos* mRNA levels were significantly elevated by fluoxetine administration compared with all other treatment groups ($P < 0.05$; Figure 3.2 and Table 3.2). No significant differences were observed in the prelimbic cortex or the anterior olfactory nucleus (Figure 3.2 and Table 3.2).

Table 3.2 Effect of acute antidepressant administration on *c-fos* mRNA expression (4.7 to 4 mm relative to bregma)

Region	Vehicle			Org34167			Imipramine			Mirtazapine			LiCl			Fluoxetine		
	Mean	±	s.e.mean	Mean	±	s.e.mean	Mean	±	s.e.mean	Mean	±	s.e.mean	Mean	±	s.e.mean	Mean	±	s.e.mean
M2 ctx	7.41	±	0.91	28.36	±	0.91*	12.11	±	1.17+	11.70	±	3.62+	16.03	±	1.57*+	9.50	±	1.59+#
PrL ctx	34.66	±	4.42	38.40	±	4.42	36.58	±	3.81	40.49	±	0.59	33.29	±	3.12	42.19	±	3.38
VM Orb ctx	71.98	±	3.50	75.80	±	3.50	72.82	±	3.19	65.50	±	1.84	66.43	±	4.38	91.40	±	7.82*+†‡#
AON	56.29	±	3.53	58.95	±	3.53	55.72	±	3.02	54.86	±	2.00	54.49	±	2.21	59.04	±	2.89

Data represent mean ± s.e.mean of three sections per animal ($n = 6$). Optical density readings have been converted to nCi/g of tissue. One-way ANOVA with Student Newman-Keuls *post-hoc* test was performed. $P < 0.05$, * compared with vehicle; + compared with Org 34167, † compared with imipramine; ‡ compared with mirtazapine; # compared with LiCl. Abb: M2 ctx, anterior secondary motor cortex, PrL ctx, prelimbic cortex, VM Orb, ventromedial orbital cortex, AON, anterior olfactory nucleus (Paxinos *et al.*, 1986).

Figure 3.2 Representative autoradiograms of acute drug administration on *c-fos* mRNA expression (4.7 to 4 mm relative to bregma)

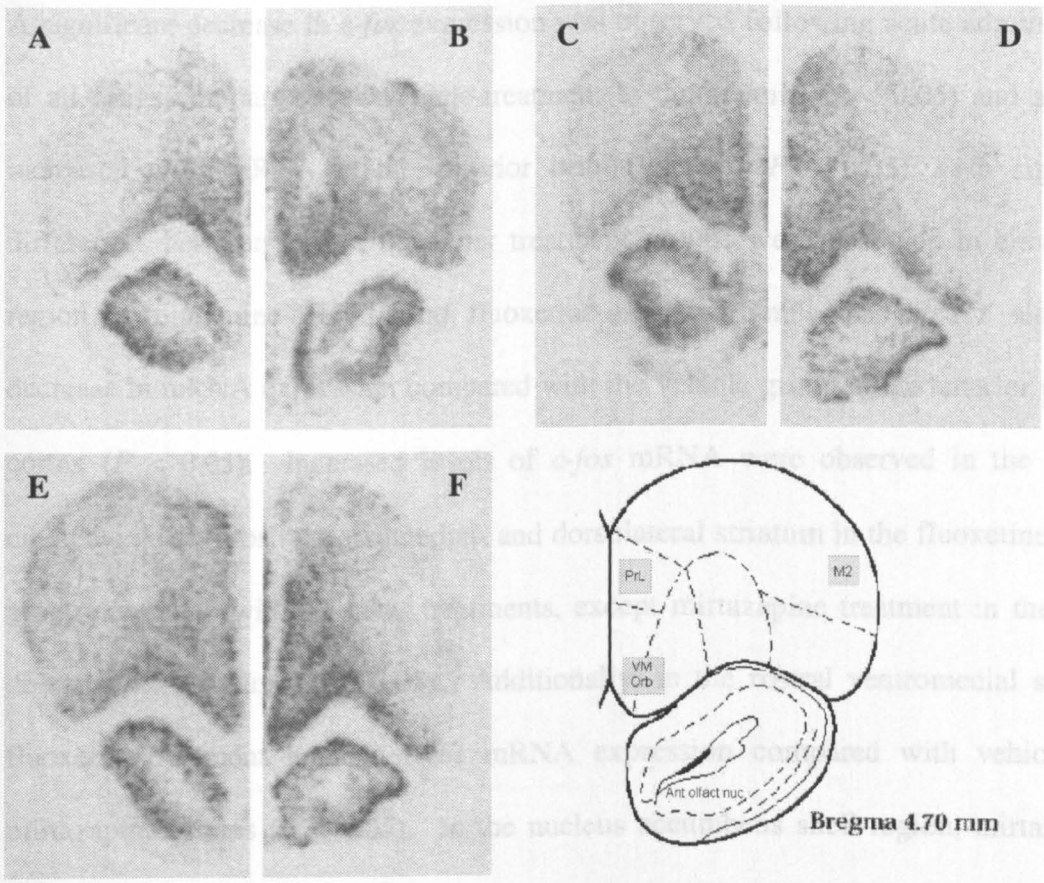

Representative autoradiographs of *in situ* hybridisation utilising ^{33}P-labelled oligonucleotide probes targeted against the *c-fos* transcript in coronal sections of rat brain following 45 min acute administration of vehicle (A), Org 34167 (0.5 mg/kg, B), imipramine (15 mg/kg, C), mirtazapine (2 mg/kg, D), LiCl (75mg/kg, E) or fluoxetine (5mg/kg, F). Also shown is a schematic representation of the brain regions analysed. Abb: M2, anterior secondary motor cortex, PrL, prelimbic cortex, VM Orb, ventro-medial orbital cortex, Ant. olfact nuc, anterior olfactory nucleus (Paxinos *et al.*, 1986).

3.3.3 Effect of treatment on c-fos mRNA (2.2 to 1.5 mm relative to bregma)

A significant decrease in *c-fos* expression was observed following acute administration of all drugs compared with vehicle-treatment in the septum ($P < 0.05$) and all drugs increased *c-fos* mRNA in the anterior insular cortex ($P < 0.05$). No significant differences between any of the other treatment groups were observed in either brain region. Imipramine-, LiCl- and fluoxetine-treated animals displayed a significant decrease in mRNA expression compared with the vehicle group in the anterior piriform cortex ($P < 0.05$). Increased levels of *c-fos* mRNA were observed in the anterior cingulate cortex, rostral dorsomedial- and dorsolateral striatum in the fluoxetine-treated group compared with all other treatments, except mirtazapine treatment in the rostral dorsomedial striatum ($P < 0.05$). Additionally, in the rostral ventromedial striatum, fluoxetine-treatment induced *c-fos* mRNA expression compared with vehicle- and mirtazapine groups ($P < 0.05$). In the nucleus accumbens shell region, mirtazapine-, LiCl- and fluoxetine-treatment induced almost a doubling of *c-fos* mRNA levels compared with vehicle-, Org 34167- and imipramine-administration ($P < 0.05$). Similar observations were demonstrated in the nucleus accumbens core, where mirtazapine-, LiCl- and fluoxetine-treatment increased *c-fos* mRNA expression compared with the vehicle control group. Mirtazapine-treatment also increased *c-fos* mRNA compared with Org 34167 and imipramine administration ($P < 0.05$). All the results are displayed in Table 3.3 and representative autoradiograms in Figure 3.3.

Table 3.3 Effect of acute antidepressant administration on *c-fos* mRNA expression (2.2 to 1.5 mm relative to bregma)

Region	Vehicle	Org34167	Imipramine	Mirtazapine	LiCl	Fluoxetine
	Mean ± s.e.mean	Mean ± s.e.mean	Mean ± s.e.mean	Mean ± s.e.mean	Mean ± s.e.mean	Mean ± s.e.mean
Septum	30.85 ± 3.05	25.68 ± 1.11*	22.10 ± 1.65*	21.63 ± 0.29*	21.71 ± 0.67*	23.82 ± 1.76*
Ant Pir ctx	89.85 ± 2.02	82.39 ± 3.50	76.79 ± 1.62*	80.35 ± 3.51	77.95 ± 2.84*	77.75 ± 3.36*
Ant Cing ctx	86.86 ± 6.48	95.52 ± 6.35	85.77 ± 5.02	78.40 ± 4.84	86.26 ± 5.93	113.12 ± 2.59*+†‡#
Ant Ins ctx	31.85 ± 4.72	47.16 ± 2.56*	43.90 ± 4.60*	48.00 ± 4.13*	44.88 ± 1.86*	51.23 ± 1.39*
Rost DM Str	23.95 ± 3.37	25.50 ± 1.73	23.74 ± 2.79	28.66 ± 2.42	27.89 ± 2.64	37.56 ± 1.85*+†‡#
Rost DL Str	10.21 ± 1.32	10.13 ± 1.40	9.75 ± 0.68	14.10 ± 1.55	11.34 ± 1.04	15.90 ± 1.57*+†#
Rost VL Str	8.41 ± 0.91	10.86 ± 1.07	8.77 ± 0.34	11.52 ± 1.31	10.07 ± 1.13	12.50 ± 1.05
Rost VM Str	17.36 ± 1.24	19.55 ± 1.84	17.61 ± 1.81	25.00 ± 2.12	23.54 ± 2.81	27.18 ± 2.67*‡
NA core	9.92 ± 1.34	11.62 ± 0.86	10.90 ± 0.95	16.33 ± 1.46*+†	14.49 ± 1.15*	15.05 ± 1.01*
NA shell	12.28 ± 1.84	14.90 ± 1.70	13.99 ± 1.59	21.90 ± 2.37*+†	27.57 ± 2.07*+†	24.29 ± 2.26*+†

Data represent mean ± s.e.mean of three sections per animal (n = 6). Optical density readings have been converted to nCi/g of tissue. One-way ANOVA with Student Newman-Keuls *post-hoc* test was performed. $P < 0.05$ * compared with vehicle; + compared with Org 34167, † compared with imipramine; ‡ compared with mirtazapine; # compared with LiCl. Abb: Ant Pir ctx, anterior piriform cortex, Ant Cing ctx, anterior cingulate cortex, Ant Ins ctx, anterior insular cortex, Rost DM Str, rostral dorsomedial striatum, Rost DL Str, rostral dorsolateral striatum, Rost VL Str, rostral ventrolateral striatum; Rost VM Str, rostral ventromedial striatum, NA, nucleus acumens (Paxinos *et al.*, 1986).

Figure 3.3 Representative autoradiograms of acute drug administration on *c-fos* mRNA expression (2.2 to 1.5 mm relative to bregma)

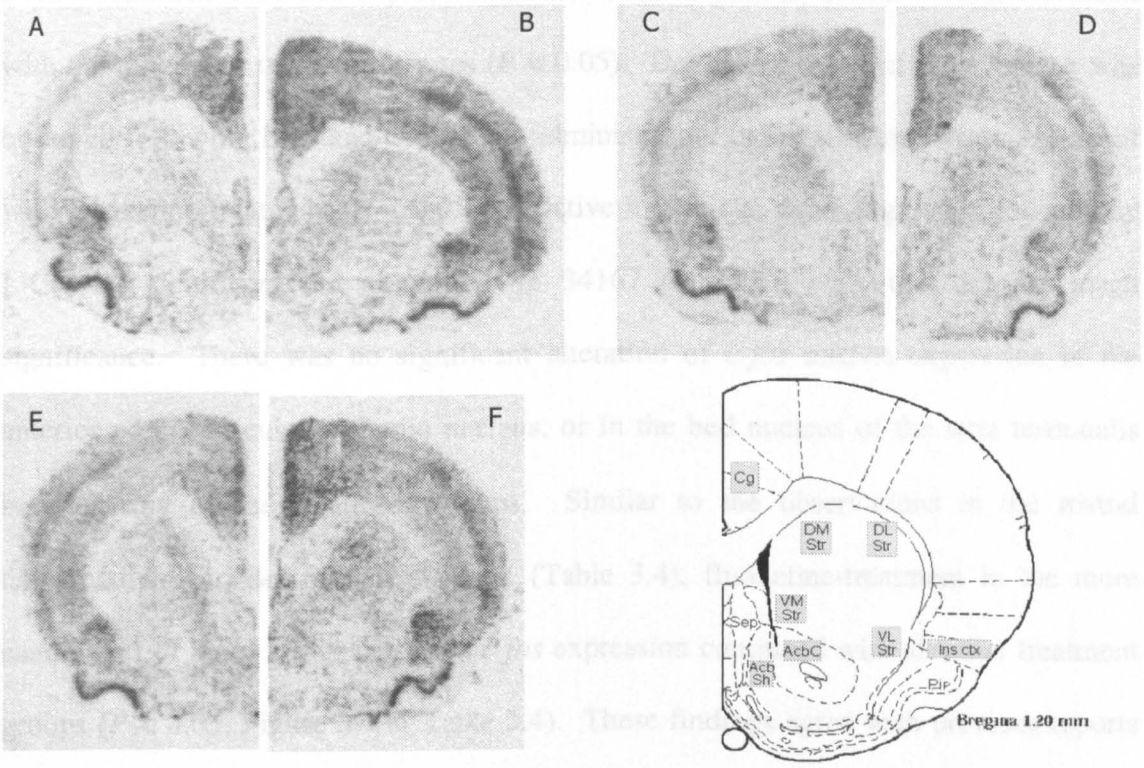

Representative autoradiographs of *in situ* hybridisation utilising ^{33}P-labelled oligonucleotide probes targeted against the *c-fos* transcript in coronal sections of rat brain following 45 min acute administration of vehicle (A), Org 34167 (0.5 mg/kg, B), imipramine (15 mg/kg, C), mirtazapine (2 mg/kg, D), LiCl (75mg/kg, E) or fluoxetine (5mg/kg, F). Also shown is a schematic representation of the brain regions analysed. Abb: Sep, septum, Cg, anterior cingulate cortex, Ins ctx, anterior insular cortex, Pir, anterior piriform cortex, DM Str, rostral dorsomedial striatum, DL Str, rostral dorsolateral striatum, VM Str, rostral ventromedial striatum, VL Str, rostral ventrolateral striatum, AcbC, nucleus acumens core, AcbSh, nucleus accumbens shell (Paxinos *et al.*, 1986).

3.3.4 Effect of treatment on c-fos mRNA (-0.8 to -1.5 mm relative to bregma)

In this more caudal region of the insular cortex a significant increase in *c-fos* mRNA expression was observed following all drug treatments ($P < 0.05$) except that of fluoxetine. Additionally, the induction of *c-fos* mRNA following Org 34167-administration was statistically greater than all other drug groups ($P < 0.05$). In every cortical region examined Org 34167-treated animals displayed a marked elevation of *c-fos* mRNA compared with all other treatment groups, with two exceptions. No

induction of *c-fos* was observed in the piriform cortex, and both fluoxetine and Org 34167-treatment increased expression in the caudal secondary motor cortex, compared with the other four treatment groups ($P < 0.05$). Down-regulation of *c-fos* mRNA was observed following LiCl and Org 34167 administration in the piriform cortex compared with fluoxetine-treatment ($P < 0.05$). Relative to vehicle, down-regulation induced by LiCl was significant but although Org 34167 decreased *c-fos* this did not reach significance. There was no significant alteration of *c-fos* mRNA expression in the anterior paraventricular thalamic nucleus, or in the bed nucleus of the stria terminalis between any of the treatment groups. Similar to the observations in the rostral dorsomedial- and dorsolateral-striatum (Table 3.4), fluoxetine-treatment in the more caudal part of these regions induced *c-fos* expression compared with all other treatment groups ($P < 0.05$; Figure 3.4 & Table 3.4). These findings agree with previous reports of 10 mg/kg fluoxetine-treatment elevating *c-fos* in neurones of the caudate putamen, mainly close to the lateral ventricle (Torres *et al.*, 1998). In the caudal ventral striatum a marked induction of *c-fos* expression was observed following Org 34167-treament compared with all other groups; with the most robust being a four-fold increase over vehicle and fluoxetine-treatment ($P < 0.05$). Imipramine-, mirtazapine- and LiCl-administration also up-regulated *c-fos* levels in the caudal ventral striatum compared with the saline controls ($P < 0.05$). All treatment groups were observed to decrease *c-fos* expression in the nucleus of the lateral olfactory tract compared with vehicle-treated animals ($P < 0.05$). The most robust increase in *c-fos* expression was observed in the supraoptic nucleus where LiCl induced a ten-fold elevation compared with saline-treatment and a five-fold increase compared with all other treatment groups ($P < 0.05$; Figure 3.4; Table 3.4). A previous study reported that fluoxetine caused a significant increase in c-Fos-like immunoreactivity (FLI) in this region (Torres *et al.*, 1998) and despite the mean values in the present study being two-fold greater for the fluoxetine-

treatment group this was not significant. There was a trend towards a down-regulation of *c-fos* in the suprachiasmatic nucleus in all treatment groups in comparison with saline controls, which reached significance for Org 34167-, mirtazapine-, and fluoxetine groups ($P < 0.05$). All the results are represented in Table 3.4 and Figure 3.4.

Table 3.4 Effect of acute antidepressant administration on *c-fos* mRNA expression (-0.8 to -1.5 mm relative to bregma)

Region	Vehicle			Org34167			Imipramine			Mirtazapine			LiCl			Fluoxetine		
	Mean	±	s.e.mean	Mean	±	s.e.mean	Mean	±	s.e.mean	Mean	±	s.e.mean	Mean	±	s.e.mean	Mean	±	s.e.mean
Cg ctx	65.39	±	5.62	113.57	±	12.26*	65.64	±	2.69+	57.90	±	2.35+	53.30	±	2.39+	65.75	±	3.07+
M2 Ctx	41.82	±	3.78	64.34	±	3.83*	43.06	±	2.12+	46.83	±	3.11+	44.54	±	1.99+	57.04	±	4.53*†‡#
S1BF	34.28	±	2.79	66.25	±	6.43*	40.37	±	3.31+	43.30	±	4.41+	37.95	±	3.06+	38.38	±	4.09+
S2 Ctx	37.21	±	1.32	75.97	±	5.69*	45.44	±	2.04+	45.77	±	3.65+	46.85	±	2.62+	47.64	±	6.33+
Ins ctx	12.50	±	1.43	42.78	±	2.83*	25.35	±	2.61*+	26.87	±	5.20*+	32.32	±	2.66*+	21.53	±	4.22+
Pir ctx	71.14	±	2.10	64.45	±	2.02	66.07	±	1.54	66.03	±	2.29	58.65	±	1.94*	73.60	±	1.93+#
PVA	48.96	±	4.81	50.03	±	3.92	48.14	±	4.07	37.45	±	2.23	35.17	±	1.48+	42.50	±	3.03
DM str	29.48	±	2.39	35.11	±	1.78	31.92	±	1.68	27.61	±	1.74	26.07	±	1.57+	39.74	±	2.88*†‡#
DL str	16.20	±	1.61	18.76	±	1.47	20.42	±	0.82	17.98	±	1.38	15.52	±	1.53	23.84	±	1.51*+†#
V str	5.90	±	1.11	20.62	±	2.09*	12.68	±	1.12*+	14.48	±	1.26*+	14.07	±	1.34*+	9.79	±	1.01+
LOT	71.80	±	3.14	60.50	±	3.78*	57.33	±	3.32*	48.48	±	2.88*	53.45	±	3.08*	53.77	±	4.23*
SON	26.83	±	3.18	32.77	±	3.94	33.60	±	2.76	44.56	±	5.47	285.89	±	37.92*+†‡	56.42	±	5.74#
BSTMPL	20.67	±	1.29	24.93	±	4.89	25.06	±	1.65	20.78	±	3.61	26.46	±	6.25	22.18	±	1.61
SCh	52.02	±	2.49	43.14	±	1.85*	47.04	±	1.30	42.23	±	1.41*	50.27	±	1.69	43.43	±	3.05*

Data represent mean ± s.e.mean of three sections per animal (n = 6). Optical density readings have been converted to nCi/g of tissue. One-way ANOVA with Student Newman-Keuls *post-hoc* test was performed. $P < 0.05$ * compared with vehicle; + compared with Org 34167, † compared with imipramine; ‡ compared with mirtazapine; # compared with LiCl. Abb: Cg ctx, cingulate cortex, M2 ctx, posterior secondary motor cortex, S1BF, primary somatosensory cortex, barrel field, S2 ctx, anterior secondary somatosensory cortex, Ins ctx, insular cortex, Pir ctx, piriform cortex, PVA, anterior paraventricular thalamic nucleus, DM Str, caudal dorsomedial striatum, DL Str, caudal dorsolateral striatum, V Str, caudal ventral striatum, LOT, nucleus of the lateral olfactory tract, SON, supra-optic nucleus, BSTMPL, nucleus of the stria terminalis, medial division, posterolateral part, SCh, suprachiasmatic nucleus (Paxinos *et al.*, 1986).

Figure 3.4 Representative autoradiograms of acute drug administration on *c-fos* mRNA expression (-0.8 to -1.5 mm relative to bregma)

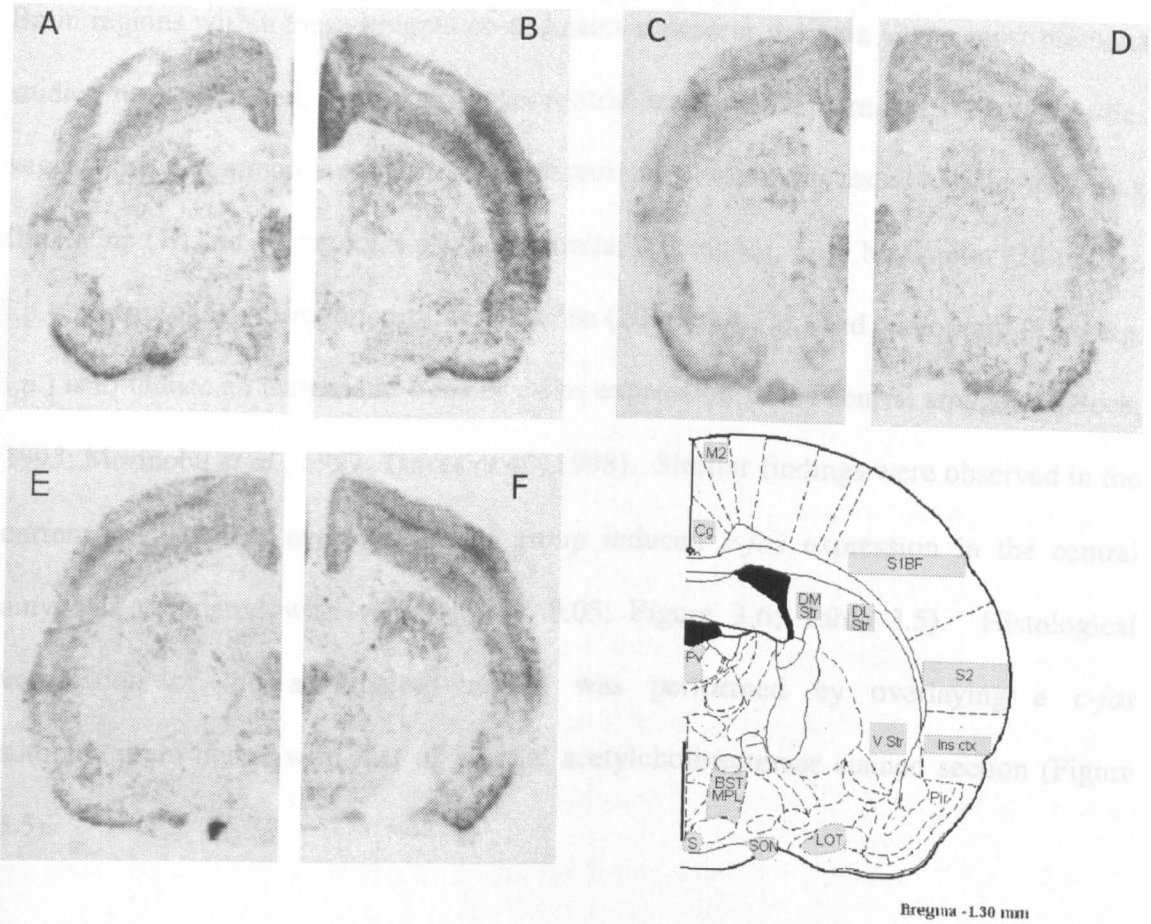

Representative autoradiographs of *in situ* hybridisation utilising ^{33}P-labelled oligonucleotide probes targeted against the c-fos transcript in coronal sections of rat brain following 45 min acute administration of vehicle (A), Org 34167 (0.5 mg/kg, B), imipramine (15 mg/kg, C), mirtazapine (2 mg/kg, D), LiCl (75mg/kg, E) or fluoxetine (5mg/kg, F). Also shown is a schematic representation of the brain regions analysed. Abb: Cg, posterior cingulate cortex, M2, posterior secondary motor cortex, S1BF, primary somatosensory cortex, barrel field, S2, anterior secondary somatosensory cortex, Ins ctx, insular cortex, Pir, piriform cortex, Pv, anterior paraventricular thalamic nucleus, DM Str, caudal dorsomedial striatum, DL Str, caudal dorsolateral striatum, V Str, caudal ventral striatum, LOT, nucleus of the lateral olfactory tract, BSTMPL, nucleus of the stria terminalis, medial division, posterolateral part, SON, supra-optic nucleus, S, suprachiasmatic nucleus (Paxinos *et al.*, 1986).

3.3.5 Effect of treatment on c-fos mRNA (-2.5 to -3.2 mm relative to bregma)

Brain regions within these bregma co-ordinates represent the area where most previous studies have focussed, particularly the central amygdaloid complex. These studies suggest that a common feature of all antidepressant compounds tested to date, including fluoxetine (10 and 15 mg/kg, i.p.), desipramine (10 mg/kg, i.p.), bupropion (20 mg/kg, i.p.), nortriptyline (15 mg/kg, i.p), imipramine (20 mg/kg, i.p.) and citalopram (5 mg/kg, i.p.) is to induce an increase in *c-fos* or c-Fos expression in the central amygdala (Beck, 1995; Morinobu *et al.*, 1997; Torres *et al.*, 1998). Similar findings were observed in the current study where every treatment group induced *c-fos* expression in the central amygdala compared with vehicle ($P < 0.05$; Figure 3.6; Table 3.5). Histological verification of the amygdaloid region was performed by overlaying a *c-fos* autoradiogram image with that of a serial acetylcholinesterase stained section (Figure 3.5).

Similar to the more rostral regions analysed, Org 34167-treatment elevated *c-fos* mRNA levels in all cortical regions analysed with the exception of the piriform cortex were no difference was observed between any treatment group ($P < 0.05$; Figure 3.6; Table 3.5). The most robust increase in *c-fos* was observed in the anterior retrosplenial cortex, where Org 34167 administration induced a two-fold increase in *c-fos* compared with all other treatments ($P < 0.05$). An increase in mRNA expression was also seen in the caudal secondary somatosensory cortex compared with all other treatments ($P < 0.05$). In the same region, a down-regulation was also observed following mirtazapine and LiCl treatment compared with vehicle and fluoxetine administration ($P < 0.05$). Acute administration of mirtazapine and LiCl also caused a down-regulation of *c-fos* in the primary somatosensory cortex compared with imipramine and fluoxetine, as well as Org 34167 treatment ($P < 0.05$). Similar to Org 34167, imipramine-treatment elevated *c-fos*

expression in the caudal insular cortex compared with vehicle, mirtazapine and LiCl but not fluoxetine ($P < 0.05$). LiCl was demonstrated to down-regulate *c-fos* compared with fluoxetine in this region ($P < 0.05$). In the rostral CA1, CA2 and dentate gyrus regions of the hippocampus, Org 34167-treated animals displayed an up-regulation of *c-fos* mRNA expression compared with all other groups, with the exception of fluoxetine in the dentate gyrus ($P < 0.05$). In the rostral CA3 field of the hippocampus Org 34167 treatment induced an increase of *c-fos* mRNA compared with mirtazapine-, LiCl- and fluoxetine-treated animals ($P < 0.05$). The level of *c-fos* expression in the thalamus produced the most varied results; Org 34167-treatment induced an increase compared with vehicle, mirtazapine-, LiCl- and fluoxetine-administration resulted in a downregulation of *c-fos* compared with both vehicle and Org 34167 groups ($P < 0.05$). Imipramine treatment, despite showing no significant difference from the saline-control group, demonstrated a decrease in *c-fos* response compared with Org 34167 but an increase compared with mirtazapine- and LiCl-treatment ($P < 0.05$).

Figure 3.5 Representative *c-fos* autoradiographic, acetylcholinesterase and overlaid images demonstrating amygdaloid region of *c-fos* induction by antidepressants.

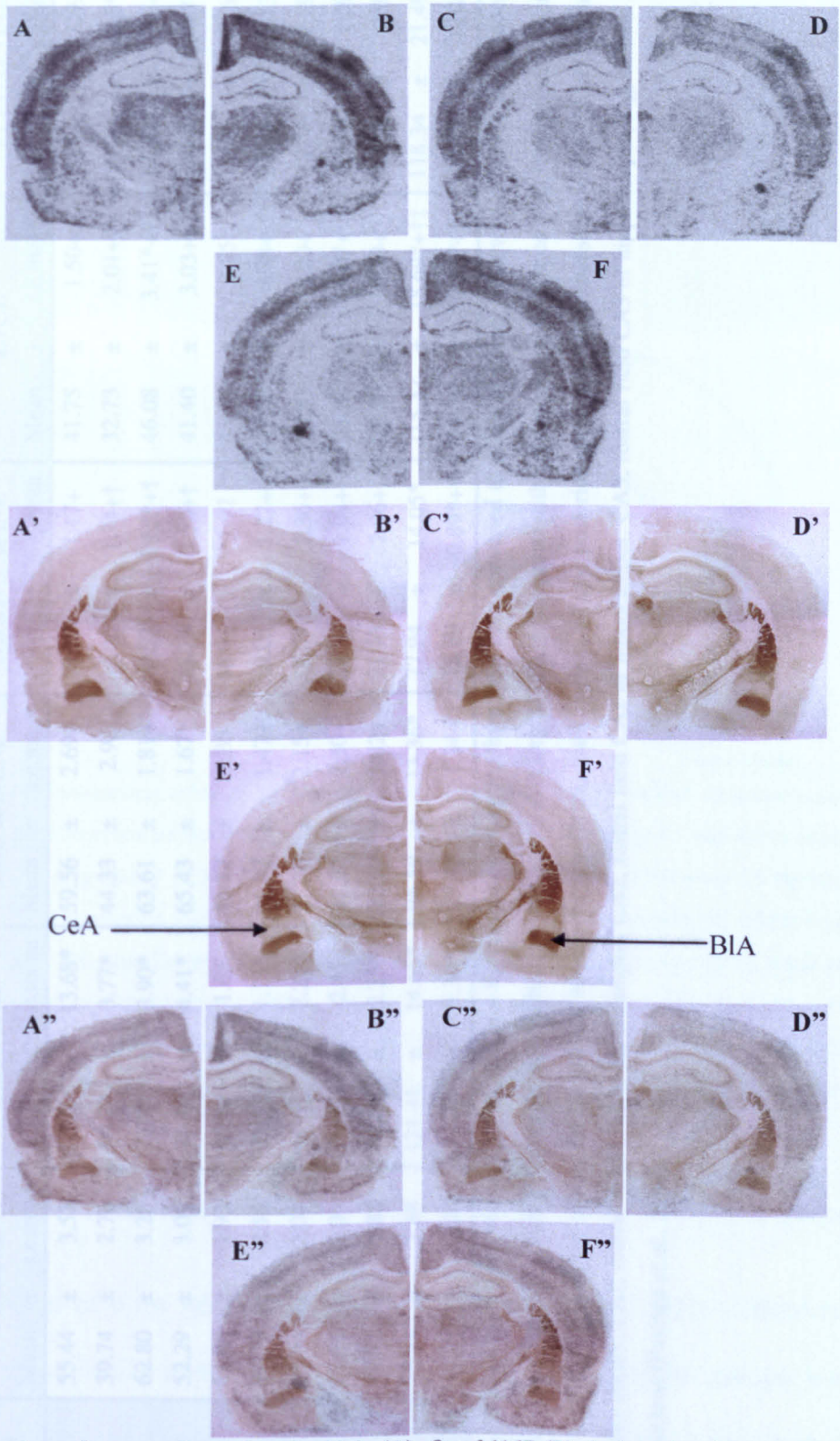

Representative *c-fos* autoradiographs of vehicle (A), Org 34167 (B), imipramine (C), mirtazapine (D), LiCl (E) or fluoxetine (F). Corresponding acetylcholinesterase images (A' – F') and overlaid images (A" – F"). The acetylcholinesterase staining enables delineation between the central amygaloid nucleus (CeA) and basolateral amygaloid nucleus (BlA), which when overlaid with the autoradiograms shows the CeA as the site of *c-fos* induction.

Table 3.5 Effect of acute antidepressant administration on *c-fos* mRNA expression (-2.5 to -3.2 mm relative to bregma)

Region	Vehicle	Org34167	Imipramine	Mirtazapine	LiCl	Fluoxetine
	Mean ± s.e.mean	Mean ± s.e.mean	Mean ± s.e.mean	Mean ± s.e.mean	Mean ± s.e.mean	Mean ± s.e.mean
RS	55.44 ± 3.53	122.21 ± 13.68*	59.56 ± 2.69+	49.19 ± 1.17+	41.75 ± 1.50+	54.61 ± 3.69+
S1Tr	39.74 ± 2.76	50.73 ± 3.77*	44.33 ± 2.92	34.66 ± 1.74+†	32.73 ± 2.01+†	50.26 ± 2.26*‡#
S2 Ctx	62.80 ± 3.28	77.99 ± 3.90*	63.61 ± 1.81+	50.57 ± 1.63*+†	46.08 ± 3.41*+†	66.81 ± 3.01+‡#
Ins Ctx	52.29 ± 3.05	71.44 ± 4.41*	65.43 ± 1.67*	45.76 ± 2.50+†	41.40 ± 3.03+†	57.64 ± 5.27+#
Pir Ctx	51.00 ± 1.93	45.70 ± 1.63	46.77 ± 2.35	46.92 ± 1.92	45.85 ± 2.75	52.29 ± 1.66
CA1	21.59 ± 2.55	33.13 ± 1.13*	21.97 ± 1.47+	19.05 ± 1.22+	17.20 ± 1.88+	20.41 ± 1.13+
CA2	35.94 ± 2.01	46.67 ± 2.21*	37.30 ± 2.15+	28.09 ± 2.36+	34.55 ± 5.20+	29.09 ± 2.69+
CA3	29.54 ± 2.04	36.13 ± 2.45	31.82 ± 2.30+	22.30 ± 1.03+	25.87 ± 4.07+	25.09 ± 1.50+
Dg	19.77 ± 1.88	32.92 ± 2.25*	22.59 ± 1.82+	21.73 ± 2.96+	22.97 ± 4.19+	25.46 ± 2.09
CeA	33.64 ± 1.68	121.41 ± 14.65*	96.59 ± 13.36*	77.94 ± 14.05*	215.37 ± 18.69*+†‡	118.34 ± 21.49*#
Thalamus	24.83 ± 2.00	31.22 ± 1.34*	23.96 ± 1.34+	18.69 ± 0.89*+†	18.39 ± 0.85*+†	20.23 ± 1.04*+

Data represent mean ± s.e.mean of three sections per animal (n = 6). Optical density readings have been converted to nCi/g of tissue. One-way ANOVA with Student Newman-Keuls *post-hoc* test was performed. $P < 0.05$ * compared with vehicle; + compared with Org 34167, † compared with imipramine; ‡ compared with mirtazapine; # compared with LiCl. Abb: RS ctx, anterior retrosplenial cortex, S1Tr, primary somatosensory cortex, trunk region, S2 ctx, posterior secondary somatosensory cortex, Ins ctx, posterior insular cortex, Pir ctx, piriform cortex, CA1, rostral field CA1 of hippocampus, CA2, rostral field CA2 of hippocampus, CA3, rostral field CA3 of hippocampus, Dg, dentate gyrus, CeA, central amygdaloid nucleus (Paxinos *et al.*, 1986).

Figure 3.6 Representative autoradiograms of acute drug administration on *c-fos* mRNA expression (-2.5 to -3.2 mm relative to bregma)

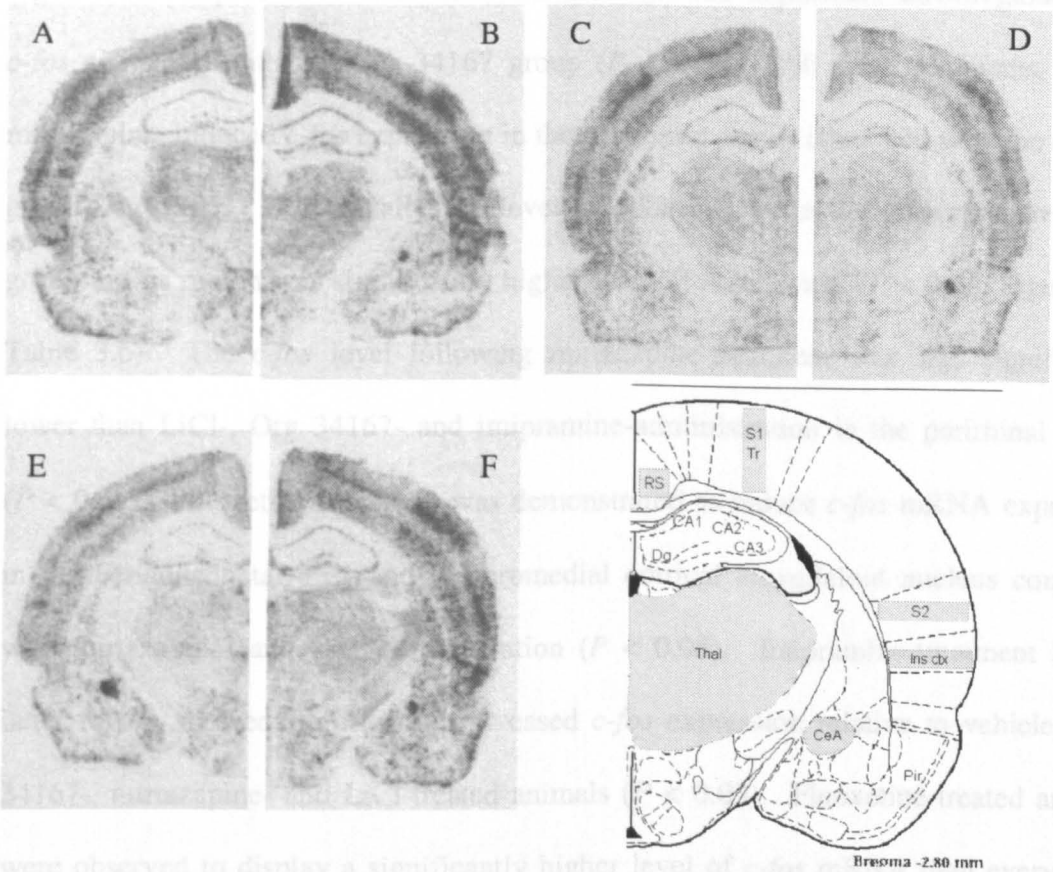

Representative autoradiographs of *in situ* hybridisation utilising ^{33}P-labelled oligonucleotide probes targeted against the c-fos transcript in coronal sections of rat brain following 45 min acute administration of vehicle (A), Org 34167 (0.5 mg/kg, B), imipramine (15 mg/kg, C), mirtazapine (2 mg/kg, D), LiCl (75mg/kg, E) or fluoxetine (5mg/kg, F). Also shown is a schematic representation of the brain regions analysed. Abb: RS, anterior retrosplenial cortex, S1Tr, primary somatosensory cortex, trunk region, S2, posterior secondary somatosensory cortex, Ins ctx, posterior insular cortex, Pir, piriform cortex, CA1, rostral field CA1 of hippocampus, CA2, rostral field CA2 of hippocampus, CA3, rostral field CA3 of hippocampus, Dg, dentate gyrus, CeA, central amygdaloid nucleus, Thal, thalamus (Paxinos *et al.*, 1986).

3.3.6 Effect of treatment on c-fos mRNA (-4.8 to -5.5 mm relative to bregma)

The elevation of *c-fos* mRNA caused by Org 34167-administration observed in the anterior retrosplenial cortex compared with all other treatment groups was again apparent in this more posterior region ($P < 0.05$; Figure 3.7; Table 3.6). There was also a strong cortical activation of *c-fos* mRNA following fluoxetine administration, in both the secondary visual cortex and primary auditory cortex, where the *c-fos* levels were

significantly higher than every other group except Org 34167 ($P < 0.05$). In these regions mirtazapine- and LiCl-treatment also showed significant downregulation of *c-fos* compared with the Org 34167 group ($P < 0.05$). All drug treatments, except mirtazapine, induced *c-fos* expression in the perirhinal cortex compared with the control group ($P < 0.05$). Additionally, the level of *c-fos* mRNA in the fluoxetine treatment group in this region was significantly higher than all other drugs ($P < 0.05$; Figure 3.7; Table 3.6). The *c-fos* level following mirtazapine-treatment was also significantly lower than LiCl-, Org 34167- and imipramine-administration in the perirhinal cortex ($P < 0.05$). Fluoxetine-treatment was demonstrated to induce *c-fos* mRNA expression in the periaqueductal grey and posteromedial cortical amygdaloid nucleus compared with mirtazapine- and LiCl-administration ($P < 0.05$). Imipramine-treatment in this latter region showed significantly increased *c-fos* expression relative to vehicle-, Org 34167-, mirtazapine- and LiCl-treated animals ($P < 0.05$). Fluoxetine-treated animals were observed to display a significantly higher level of *c-fos* mRNA than every other group in the ventral tegmental area, except imipramine ($P < 0.05$). Although no significant differences were observed between any groups in the CA2 or dentate gyrus regions of the hippocampus, a significant increase in *c-fos* mRNA expression was observed in the dorso-caudal CA1 field of the hippocampus of Org 34167-treated animals compared with all other groups ($P < 0.05$). In the caudal CA3 region a down-regulation of *c-fos* was observed following mirtazapine administration compared with all other treatment groups, and LiCl compared with Org 34167 administration ($P < 0.05$). Expression of *c-fos* in the geniculate nucleus was down-regulated following mirtazapine-, LiCl- and fluoxetine-treatment compared with both vehicle and Org 34167-treated animals ($P < 0.05$). Acute administration of imipramine was observed to increase *c-fos* expression compared with mirtazapine and LiCl treated

animals ($P < 0.05$), but to a lower level than Org 34167 ($P < 0.05$). All these results are represented in Table 3.6 and representative autoradiographs are shown in Figure 3.7.

Table 3.6 Effect of acute antidepressant administration on *c-fos* mRNA expression (-4.8 to -5.5 mm relative to bregma)

REGION	VEHICLE			ORG34167			IMIPRAMINE			MIRTAZAPINE			LICL			FLUOXETINE		
	Mean	±	s.e.mean	Mean	±	s.e.mean	Mean	±	s.e.mean	Mean	±	s.e.mean	Mean	±	s.e.mean	Mean	±	s.e.mean
RS	54.04	±	3.82	119.21	±	10.52*	50.84	±	1.77+	48.91	±	2.10+	43.22	±	2.48+	61.05	±	1.91+
V2 ctx	71.73	±	3.59	85.37	±	8.85	72.91	±	3.09	56.41	±	2.03+	57.74	±	2.62+	94.75	±	5.03*†‡#
Au ctx	92.54	±	1.84	99.03	±	3.00	90.56	±	3.32	81.97	±	2.84+	84.85	±	3.39+	107.00	±	5.28*†‡#
PRh ctx	54.12	±	1.05	68.41	±	1.70*	67.99	±	2.62*	55.49	±	1.45+†	61.82	±	2.02*‡	89.01	±	2.71*+†‡#
PAG	29.97	±	1.23	31.30	±	0.56	31.72	±	0.58	27.39	±	1.10	28.39	±	1.91	34.06	±	1.03‡#
VTA	19.00	±	1.27	19.39	±	1.09	22.51	±	2.44	18.83	±	0.79	19.66	±	1.43	28.64	±	2.15*+‡#
Gen	48.66	±	1.99	53.32	±	3.45	45.13	±	2.90+	34.63	±	0.74*+†	34.79	±	0.98*+†	40.22	±	1.83*+
CA1	29.78	±	2.32	39.31	±	2.27*	27.77	±	1.70+	28.94	±	0.56+	29.62	±	2.20+	34.09	±	0.56+
CA2	31.49	±	2.18	35.57	±	1.33	31.10	±	1.40	29.41	±	0.66	31.81	±	2.57	34.61	±	1.46
CA3	26.81	±	1.15	30.46	±	1.42	26.54	±	0.64	22.46	±	0.55*+†	26.01	±	1.51+‡	26.81	±	0.59‡
Dg	21.44	±	0.96	26.30	±	1.07	24.68	±	0.63	22.16	±	0.56	25.21	±	2.51	24.72	±	0.63
PMCo	44.88	±	1.62	42.92	±	1.22	55.75	±	2.97*+	39.77	±	3.18†	36.65	±	2.22†	50.20	±	1.31‡#

Data represent mean ± s.e.mean of three sections per animal (n = 6). Optical density readings have been converted to nCi/g of tissue. One-way ANOVA with Student Newman-Keuls *post-hoc* test was performed. . $P < 0.05$ * compared with vehicle; + compared with Org 34167, † compared with imipramine; ‡ compared with mirtazapine; # compared with LiCl. Abb: RS, retrosplenial cortex, V2 ctx, secondary visual cortex, lateral area, Au ctx, primary auditory cortex, PRh ctx, perirhinal cortex, PAG, anterior periaqueductal grey, VTA, ventral tegmental area, Gen, geniculate nucleus, CA1, dorsocaudal field CA1 of hippocampus, CA2, caudal field CA2 of hippocampus, CA3, caudal field CA3 of hippocampus, Dg, caudal dentate gyrus, PMCo, posteromedial cortical amygdaloid nucleus (Paxinos *et al.*, 1986).

Figure 3.7 Representative autoradiograms of acute drug administration on *c-fos* mRNA expression (-4.8 to -5.5 mm relative to bregma)

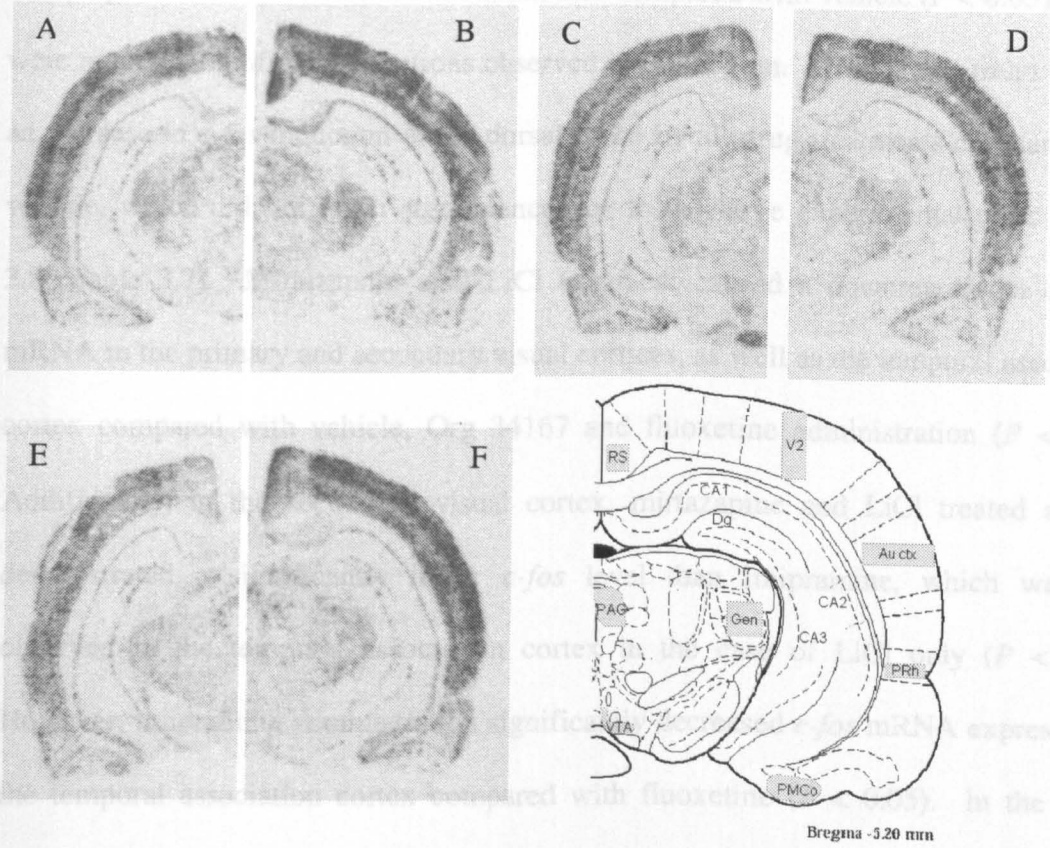

Representative autoradiographs of *in situ* hybridisation utilising ^{33}P-labelled oligonucleotide probes targeted against the *c-fos* transcript in coronal sections of rat brain following 45 min acute administration of vehicle (A), Org 34167 (0.5 mg/kg, B), imipramine (15 mg/kg, C), mirtazapine (2 mg/kg, D), LiCl (75mg/kg, E) or fluoxetine (5mg/kg, F). Also shown is a schematic representation of the brain regions analysed. Abb: RS, retrosplenial cortex, V2, secondary visual cortex, lateral area, Au ctx, primary auditory cortex, PRh, perirhinal cortex, CA1, dorsocaudal field CA1 of hippocampus, CA2, caudal field CA2 of hippocampus, CA3, caudal field CA3 of hippocampus, Dg, caudal dentate gyrus, PAG, anterior periaqueductal grey, Gen, geniculate nucleus, VTA, ventral tegmental area, PMCo, posteromedial cortical amygdaloid nucleus (Paxinos *et al.*, 1986).

3.3.7 Effect of treatment on c-fos mRNA (-6.8 to -7.5 mm relative to bregma)

As observed in the anterior and medial retrosplenial cortex, Org 34167-treatment induced *c-fos* expression in the posterior region almost two-fold compared with every other treatment group ($P < 0.05$). Org 34167 and fluoxetine administration were observed to elevate *c-fos* mRNA expression compared with the other four treatment groups in the ectorhinal cortex ($P < 0.05$). Similar to the rostral periaqueductal grey,

fluoxetine was demonstrated to activate *c-fos* in this more caudal region compared with mirtazapine- and LiCl-administration, but also compared with vehicle ($P < 0.05$). There were no other significant alterations observed in this region. There was a trend towards an increase in *c-fos* induction in the dorsal raphé by all drug treatments compared with vehicle, which did not reach significance due to the large experimental error (Figure 3.8; Table 3.7). Mirtazapine- and LiCl treatment caused a downregulation of *c-fos* mRNA in the primary and secondary visual cortices, as well as the temporal association cortex compared with vehicle, Org 34167 and fluoxetine administration ($P < 0.05$). Additionally, in the secondary visual cortex, mirtazapine and LiCl treated animals demonstrated a significantly lower *c-fos* level than imipramine, which was also observed in the temporal association cortex in the case of LiCl only ($P < 0.05$). However, imipramine administration significantly decreased *c-fos* mRNA expression in the temporal association cortex compared with fluoxetine ($P < 0.05$). In the lateral entorhinal cortex mirtazapine- and LiCl-administration were found to significantly downregulate *c-fos* mRNA compared with both vehicle and Org 34167 treatment groups ($P < 0.05$). Similar to the CA1 field of the hippocampus observations, Org 34167 was observed to activate *c-fos* expression in the subiculum and post-subiculum regions of the hippocampus compared with all other treatments ($P < 0.05$). Moreover, a down-regulation of *c-fos* expression, in comparison with vehicle, was noted for every other treatment group in these two regions ($P < 0.05$), with the exception of fluoxetine in the subiculum (Figure 3.8 and Table 3.7). The only other significant finding in these two hippocampal regions was that LiCl-treatment significantly lowered *c-fos* expression in the subiculum compared with fluoxetine ($P < 0.05$). Acute administration of Org 34167 also activated *c-fos* in the superior colliculus in comparison with vehicle, mirtazapine and LiCl ($P < 0.05$). In addition, mirtazapine and LiCl treated animal were observed to display a significantly lower expression of *c-fos* when compared with vehicle-,

imipramine- and fluoxetine administration ($P < 0.05$). Finally, LiCl treatment down-regulated *c-fos* expression in the nucleus of the brachium of the inferior colliculus compared with vehicle-, imipramine- and fluoxetine-administration ($P < 0.05$). Mirtazapine also demonstrated significantly lower *c-fos* expression in this region compared with fluoxetine ($P < 0.05$).

Table 3.7 Effect of acute antidepressant administration on *c-fos* mRNA expression (-6.8 to – 7.5 mm relative to bregma)

Region	Vehicle			Org34167			Imipramine			Mirtazapine			LiCl			Fluoxetine		
	Mean	±	s.e.mean	Mean	±	s.e.mean	Mean	±	s.e.mean	Mean	±	s.e.mean	Mean	±	s.e.mean	Mean	±	s.e.mean
RS	69.73	±	4.26	135.34	±	12.40*	73.87	±	5.40+	64.71	±	4.25+	56.00	±	7.28+	71.41	±	5.36+
V1 ctx	91.49	±	7.27	88.14	±	8.50	75.96	±	3.63	63.06	±	5.43*+	62.25	±	2.71*+	92.69	±	3.17‡#
V2 ctx	108.38	±	5.87	105.88	±	10.10	89.52	±	3.86	67.06	±	3.34*+†	66.37	±	2.43*+†	104.03	±	6.21‡#
TeA ctx	107.81	±	2.69	105.51	±	4.52	96.66	±	3.26	87.75	±	3.56*+	82.67	±	5.36*+†	113.52	±	3.43†‡#
Ect ctx	49.69	±	3.60	66.29	±	4.20*	53.52	±	2.51+	47.42	±	1.50+	44.68	±	1.87+	64.65	±	2.70*†‡#
LEnt	43.29	±	1.16	47.04	±	2.28	41.70	±	1.73	35.31	±	2.07*+	34.48	±	2.88*+	41.89	±	1.69
PAG	25.57	±	1.57	30.75	±	1.78	29.05	±	1.66	23.33	±	1.50	24.79	±	2.34	34.12	±	1.77*‡#
DR	22.55	±	2.12	30.78	±	1.97	26.53	±	1.39	24.58	±	0.90	22.70	±	2.89	27.31	±	1.58
Sup col	27.36	±	1.36	33.77	±	2.01*	30.36	±	1.54	22.84	±	1.10*+†	19.50	±	1.56*+†	30.49	±	1.35‡#
BIC	31.37	±	1.22	30.73	±	1.59	31.15	±	3.05	25.51	±	1.18	23.00	±	1.42*†	33.67	±	0.96‡#
Subic	27.32	±	0.77	35.93	±	1.18*	22.47	±	0.67*+	22.19	±	2.00*+	20.78	±	1.34*+	25.41	±	0.47+#
P Sub	61.00	±	3.25	81.43	±	3.67*	41.01	±	2.55*+	46.39	±	4.09*+	36.26	±	3.98*+	48.75	±	3.30*+

Data represent mean ± s.e.mean of three sections per animal (n = 6). Optical density readings have been converted to nCi/g of tissue. One-way ANOVA with Student Newman-Keuls *post-hoc* test was performed. . $P < 0.05$ * compared with vehicle; + compared with Org 34167, † compared with imipramine; ‡ compared with mirtazapine; # compared with LiCl. Abb: RS, posterior retrosplenial cortex, V1 ctx, primary visual cortex, V2 ctx, secondary visual cortex, TeA ctx, temporal association cortex, Ect ctx, ectorhinal cortex, LEnt, lateral entorhinal cortex, PAG, posterior periaqueductal grey, DR, dorsal raphé, Sup Col, superior colliculus, BIC, nucleus of the brachium of the inferior colliculus, Subic, subiculum, P Sub, post-subiculum (Paxinos *et al.*, 1986).

Figure 3.8 Representative autoradiograms of acute drug administration on *c-fos* mRNA expression (-6.8 to -7.5 mm relative to bregma)

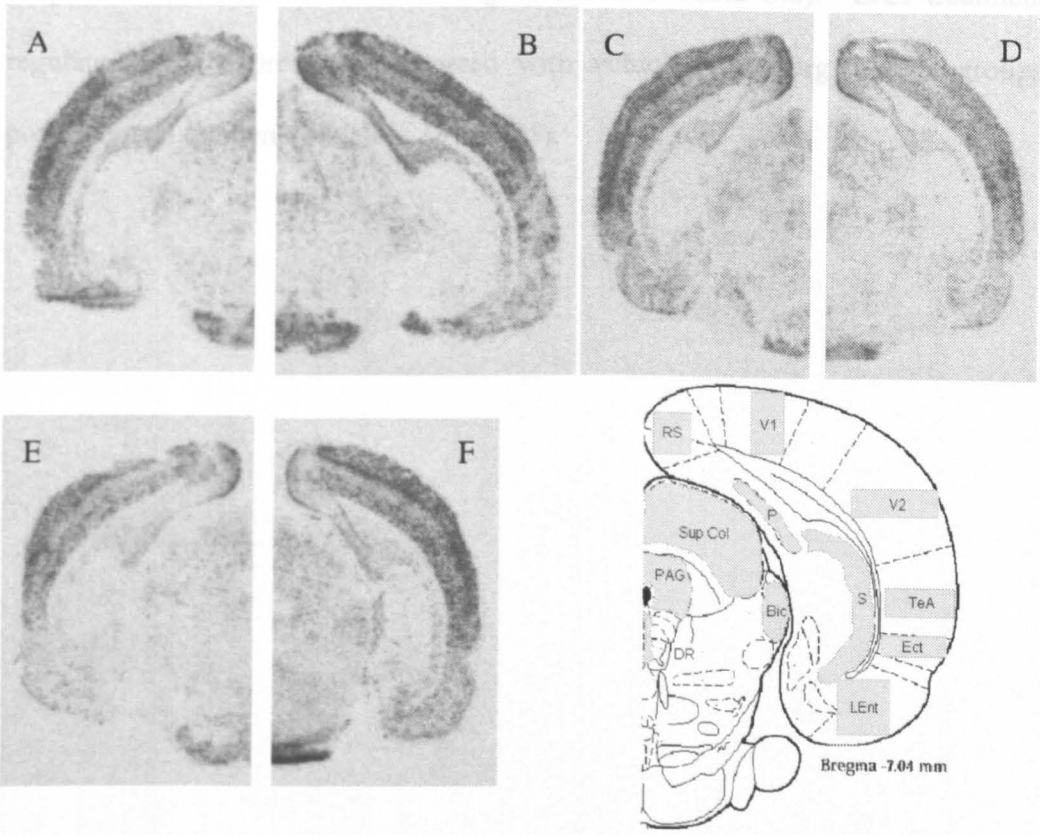

Representative autoradiographs of *in situ* hybridisation utilising ^{33}P-labelled oligonucleotide probes targeted against the *c-fos* transcript in coronal sections of rat brain following 45 min acute administration of vehicle (A), Org 34167 (0.5 mg/kg, B), imipramine (15 mg/kg, C), mirtazapine (2 mg/kg, D), LiCl (75mg/kg, E) or fluoxetine (5mg/kg, F). Also shown is a schematic representation of the brain regions analysed. Abb: RS, posterior retrosplenial cortex, V1, primary visual cortex, V2, secondary visual cortex, TeA, temporal association cortex, Ect, ectorhinal cortex, LEnt, lateral entorhinal cortex, PAG, posterior periaqueductal grey, DR, dorsal raphé, Sup Col, superior colliculus, BIC, nucleus of the brachium of the inferior colliculus, P, post-subiculum, S, subiculum (Paxinos *et al.*, 1986).

3.3.8 Effect of treatment on c-fos mRNA (-9.3 to -10 mm relative to bregma)

In this most caudal region of the rat brain examined, *c-fos* mRNA levels of Org 34167-treated animals were significantly higher compared with vehicle-, mirtazapine- and to that of LiCl-administration in the inferior colliculus ($P < 0.05$). A significantly lower *c-fos* expression was also observed in this region following LiCl-treatment compared with fluoxetine ($P < 0.05$). Despite a trend towards an increase in *c-fos* expression following all drug treatments in the locus coeruleus compared with saline control, this only

reached significance with the fluoxetine group, which was also observed over imipramine treatment ($P < 0.05$; Figure 3.9 and Table 3.8). LiCl treatment down-regulated *c-fos* expression compared with vehicle- and Org 34167- groups in the posterodorsal tegmental nucleus ($P < 0.05$).

Table 3.8 Effect of acute antidepressant administration on *c-fos* mRNA expression (-9.3 to -10 mm relative to bregma)

Region	Vehicle			Org34167			Imipramine			Mirtazapine			LiCl			Fluoxetine		
	Mean	±	s.e.mean	Mean	±	s.e.mean	Mean	±	s.e.mean	Mean	±	s.e.mean	Mean	±	s.e.mean	Mean	±	s.e.mean
Inf col	44.84	±	2.67	56.70	±	2.81*	49.63	±	2.70	45.43	±	2.16+	40.86	±	2.23+	51.04	±	1.63#
LC	35.43	±	1.98	47.66	±	2.51	38.60	±	3.08	47.47	±	3.38	42.61	±	4.93	52.79	±	3.56*†
Pd	47.26	±	1.73	48.58	±	3.58	37.80	±	5.48	37.79	±	1.19	30.66	±	1.24*+	38.67	±	1.08

Data represent mean ± s.e.mean of three sections per animal (n = 5 - 6). Optical density readings have been converted to nCi/g of tissue. One-way ANOVA with Student Newman-Keuls *post-hoc* test was performed. . $P < 0.05$ * compared with vehicle; + compared with Org 34167, † compared with imipramine; ‡ compared with mirtazapine; # compared with LiCl. Abb: Inf col, inferior colliculus, LC, locus coeruleus, Pd, posterodorsal tegmental nucleus (Paxinos *et al.*, 1986).

Figure 3.9 Representative autoradiograms of acute drug administration on *c-fos* mRNA expression (-9.3 to -10 mm relative to bregma)

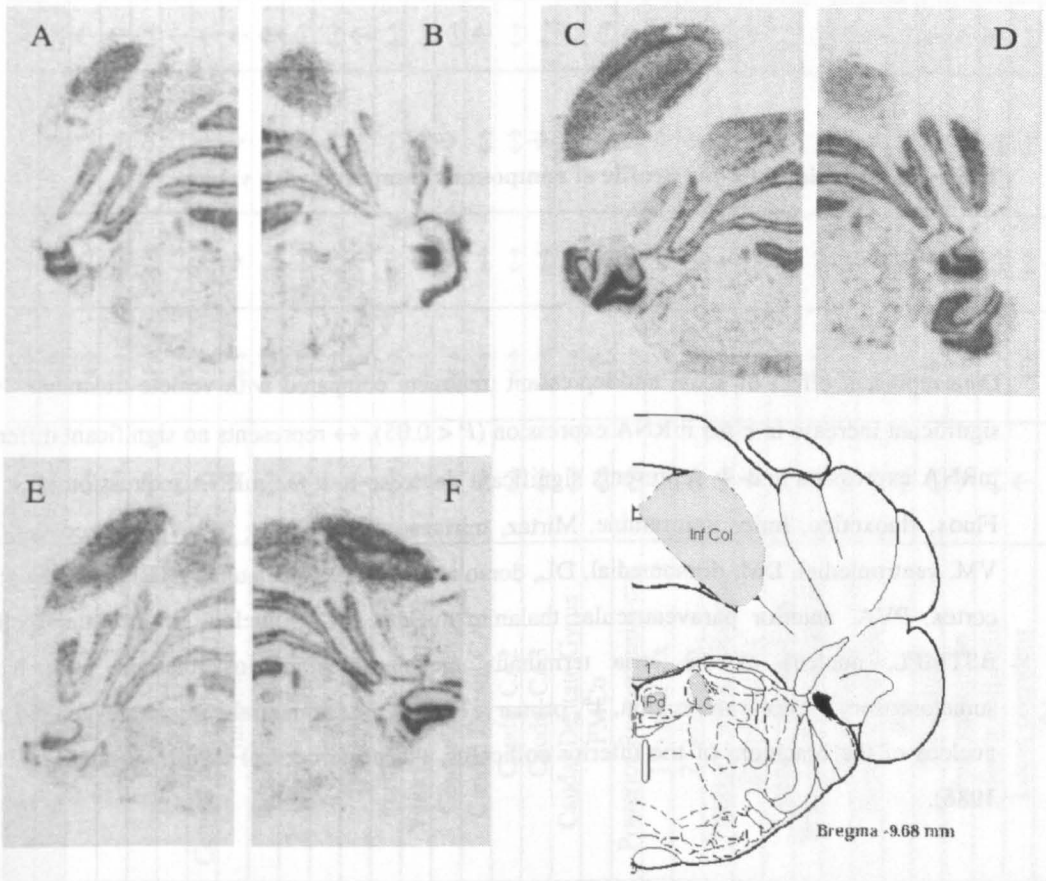

Representative autoradiographs of *in situ* hybridisation utilising ^{33}P-labelled oligonucleotide probes targeted against the *c-fos* transcript in coronal sections of rat brain following 45 min acute administration of vehicle (A), Org 34167 (0.5 mg/kg, B), imipramine (15 mg/kg, C), mirtazapine (2 mg/kg, D), LiCl (75mg/kg, E) or fluoxetine (5mg/kg, F). Also shown is a schematic representation of the brain regions analysed. Abb: Inf Col, inferior colliculus, LC, locus coeruleus, Pd, posterodorsal tegmental nucleus (Paxinos *et al.*, 1986).

All of the results from each brain region analysed, relative to vehicle administration, are provided in Table 3.9 in order to provide an overall summary.

Table 3.9 Overview of *c-fos* profile of compounds compared with vehicle

Data represent effect of acute antidepressant treatment compared with vehicle treatment. ↑ represents significant increase in *c-fos* mRNA expression ($P < 0.05$), ↔ represents no significant difference in *c-fos* mRNA expression and ↓ represents significant decrease in *c-fos* mRNA expression ($P < 0.05$). Abb: Fluox, fluoxetine, Imip, imipramine, Mirtaz, mirtazapine, Org, Org 34167, 2°, secondary, ctx, cortex, VM, ventromedial, DM, dorsomedial, DL, dorsolateral, VL, ventrolateral, S1BF, primary somatosensory cortex, PVA, anterior paraventricular thalamic nucleus, LOT, nucleus of the lateral olfactory tract, BSTMPL, nucleus of the stria terminalis medial division posterolateral part, S1Tr, primary somatosensory cortex trunk region, 1°, primary, PMCo, posteromedial cortical amygdaloid nucleus, BIC, nucleus of the brachium of the inferior colliculus, Pd, posterodorsal tegmental nucleus (Paxinos *et al.*, 1986).

Drug	Fluox	Imip	LiCl	Mirtaz	Org
Dose (mg/kg)	5	15	75	2	0.5
2° motor ctx	↔	↔	↑	↔	↑
Prelimbic ctx	↔	↔	↔	↔	↔
VM orbital ctx	↑	↔	↔	↔	↔
Anterior Olfactory nucleus	↔	↔	↔	↔	↔
Septum	↓	↓	↓	↓	↓
Anterior Piriform Ctx	↓	↓	↓	↔	↔
Anterior Cingulate Ctx	↑	↔	↔	↔	↔
Anterior Insular ctx	↑	↑	↑	↑	↑
Rostral DM striatum	↑	↔	↔	↔	↔
Rostral DL striatum	↑	↔	↔	↔	↔
Rostral VL striatum	↔	↔	↔	↔	↔
Rostral VM striatum	↑	↔	↔	↔	↔
Nucleus accumbens core	↑	↔	↑	↑	↔
Nucleus accumbens shell	↑	↔	↑	↑	↔
Cingulate Ctx	↔	↔	↔	↔	↑
Posterior 2° motor ctx	↑	↔	↔	↔	↑
S1BF	↔	↔	↔	↔	↑
Anterior 2° somatosensory ctx	↔	↔	↔	↔	↑
Insular ctx	↔	↑	↑	↑	↑
Piriform ctx	↔	↔	↓	↔	↔
PVA	↔	↔	↔	↔	↔
Caudal DM striatum	↑	↔	↔	↔	↔
Caudal DL striatum	↑	↔	↔	↔	↔
Caudal Ventral striatum	↔	↑	↑	↑	↑
LOT	↓	↓	↓	↓	↓
Supra-optic nucleus	↔	↔	↑	↔	↔
BSTMPL	↔	↔	↔	↔	↔
Suprachiasmatic nucleus	↓	↔	↔	↓	↓
Anterior Retrosplenial ctx	↔	↔	↔	↔	↑
S1Tr	↑	↔	↔	↔	↑
Posterior 2° somatosensory ctx	↔	↔	↓	↓	↑
Posterior Insular ctx	↔	↑	↔	↔	↑
Piriform Ctx	↔	↔	↔	↔	↔

Drug	Fluox	Imip	LiCl	Mirtaz	Org
Dose (mg/kg)	5	15	75	2	0.5
Rostral CA1	↔	↔	↔	↔	↑
Rostral CA2	↔	↔	↔	↔	↑
Rostral CA3	↔	↔	↔	↔	↔
Dentate Gyrus	↔	↔	↔	↔	↑
Central Amygdaloid nucleus	↑	↑	↑	↑	↑
Thalamus	↓	↔	↓	↓	↑
Retrosplenial cortex	↔	↔	↔	↔	↑
2° visual ctx, lateral area	↑	↔	↔	↔	↔
1° auditory ctx	↑	↔	↔	↔	↔
Perirhinal ctx	↑	↑	↑	↔	↑
Periaqueductal grey	↔	↔	↔	↔	↔
Ventral tegmental area	↑	↔	↔	↔	↔
Geniculate nucleus	↓	↔	↓	↓	↔
Caudal Dorsal CA1	↔	↔	↔	↔	↑
Caudal CA2	↔	↔	↔	↔	↔
Caudal CA3	↔	↔	↔	↓	↔
Caudal Dentate Gyrus	↔	↔	↔	↔	↔
PMCo	↔	↑	↔	↔	↔
Posterior Retrosplenial ctx	↔	↔	↔	↔	↑
1° visual ctx	↔	↔	↓	↓	↔
2° visual ctx	↔	↔	↓	↓	↔
Temporal association ctx	↔	↔	↓	↓	↔
Ectorhinal ctx	↑	↔	↔	↔	↑
Lateral entorhinal ctx	↔	↔	↓	↓	↔
Posterior Periaqueductal	↑	↔	↔	↔	↔
Dorsal Raphé	↔	↔	↔	↔	↔
Superior colliculus	↔	↔	↓	↓	↑
BIC	↔	↔	↓	↔	↔
Subiculum	↔	↓	↓	↓	↑
Post subiculum	↓	↓	↓	↓	↑
Inferior colliculus	↔	↔	↔	↔	↑
Locus coeruleus	↑	↔	↔	↔	↔
Pd	↔	↔	↓	↔	↔

3.4 Discussion

The aim of the present study was to examine the effects on *c-fos* mRNA expression, of antidepressants from different classes and a mood stabiliser, after acute administration (a single i.p. injection). Overall, some of the brain regions shared a common *c-fos* profile following acute antidepressant administration but a number of individual differences between the drugs were identified. All drugs tested, including the novel antidepressant Org 34167, induced *c-fos* expression in the central amygdala and anterior insular cortex ($P < 0.05$; Tables 3.3 & 3.5). A downregulation of *c-fos* mRNA, compared with vehicle, was observed for all treatment groups in the septum and nucleus of the lateral olfactory tract ($P < 0.05$; Table 3.3). The first three of these areas have been implicated in depression, with human neuro-imaging studies showing an abnormal increase in metabolic activity in the insula and amygdala (Drevets, 2000). Additionally, in the case of the amygdala, Beck (1995) and Duncan *et al.*, (1996) previously reported that this was the only brain region were an increase in *c-fos* expression was observed following all different antidepressant administrations. These alterations in *c-fos* expression underline long-term changes in cellular phenotype, which provide insight into the brain regions that these antidepressants are acting.

The principle behind the present study was to determine whether the *c-fos* profile of the novel antidepressants Org 34167 and mirtazapine corresponded with the profile of known antidepressants. The *c-fos* profile of mirtazapine was observed to be most similar to that of imipramine (see Table 3.9). Mirtazapine is a noradrenergic and specific serotonergic antidepressant (NaSSA), which results in increased NA and 5-HT_1 transmission (de Boer, 1996). Imipramine also increases available NA and 5-HT by blocking reuptake, therefore, both drugs increase available NA and 5-HT although

their mechanisms of action are different. The fact that mirtazapine (previously undocumented) induces *c-fos* expression in the central amygdala and anterior insular cortex, which all other antidepressants in the present study and in the literature (see Beck, (1995)) provides proof of concept for the use of neural activity mapping with *c-fos* as a technique to characterise novel compounds.

The orbitofrontal circuit has been shown to be present in rats, monkeys and humans (Ongur *et al.*, 2000) and has been implicated in depression. This circuit consists of direct pathways from the orbital cortex to the ventral striatum (including the nucleus accumbens), then to the globus pallidus and finally to the mediodorsal thalamic nucleus (Ongur *et al.*, 2000; Tekin *et al.*, 2002). This system interacts with the anterior cingulate cortex, which projects to the caudate, then to the substantia nigra, which projects to the ventroanterior thalamus. The thalamic areas in each pathway provide reciprocal connections with their respective cortical origins (Tekin *et al.*, 2002; See Figure 3.10). Results presented here for fluoxetine suggest that these circuits are activated.

Figure 3.10 Orbito-frontal circuitry

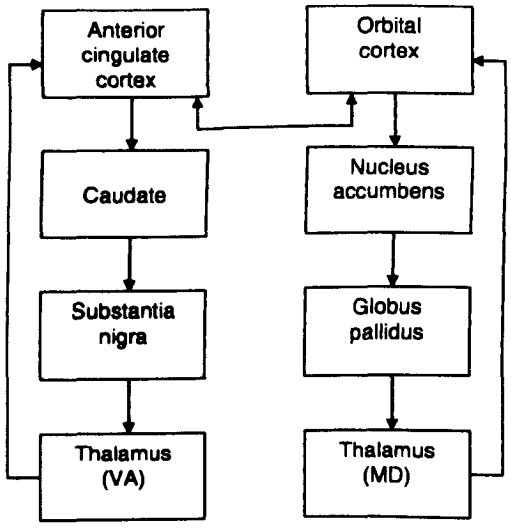

Adapted from (Tekin *et al.*, 2002).

The orbitofrontal circuit has been implicated in mood disorders by animal and human studies. Lesions of the orbital cortex are associated with social apathy (Tekin *et al.*, 2002) and cause animals to lose their position in the social hierarchy or become solitary (reviewed by Ongur *et al.*, (2000)). Human neuroimaging studies have shown that in familial major depressive disorder there is abnormally elevated cerebral blood flow and glucose metabolism in the orbital, ventral anterior cingulate cortex, anterior insular cortex, ventral striatum, amygdala and medial thalamus (see Drevets, (2000) for review). The orbital cortex has extensive reciprocal connections with limbic structures, including the amygdala, subiculum and CA1 field of the hippocampus, and the entorhinal and perirhinal cortices (reviewed by Ongur *et al.*, (2000)). In all of these structures, as well as the direct orbitofrontal circuit, only fluoxetine administration was observed to induce *c-fos* expression compared with vehicle, with the exception of the subiculum and CA1 (the globus pallidus, substantia nigra and mediodorsal thalamic nucleus were not analysed). Particularly strong activation was noted throughout the striatum, including the nucleus accumbens core and shell regions (Tables 3.3 and 3.4). The ventral striatum also projects to the VTA and PAG, in which *c-fos* induction following fluoxetine administration was observed (Table 3.6).

Figure 3.11 Reciprocal anatomical connections of the orbital cortex

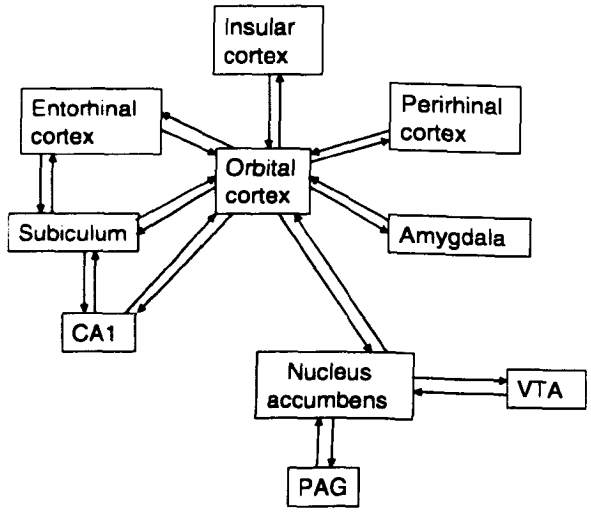

Although previous reports have demonstrated an increase in *c-fos* in the amygdala following acute fluoxetine (15 mg/kg) administration (Beck, 1995; Duncan *et al.*, 1996; Morinobu *et al.*, 1997) there are no reports concerning the other regions in the circuit. The current findings are suggestive that fluoxetine, one of the most commonly prescribed antidepressants, targets a number of brain regions after acute administration, which are abnormal in depression. The induction of *c-fos* leads to long-term alterations in gene transcription *via* the AP-1 complex. However, despite substantial knowledge regarding the activation of *c-fos* (See Herrera and Robertson (1996) for review), and the availability of a verified antisense oligonucleotide targeting the *c-fos* transcript, little is known regarding the genes which are targeted by AP-1 (Hoffman *et al.*, 2002). It is also possible that fluoxetine administration only targets a few of the brain regions in this circuitry but due to the reciprocal connections shared between them, the increase in neuronal activity in one region affects others. This is a possibility as it has been demonstrated that *c-fos* can be activated in neurones removed from the site of direct neuronal stimulus (Ziolkowska *et al.*, 2002). Nevertheless, it is striking that fluoxetine (when given acutely) targets so many brain regions associated with depression, especially as very few structures other than those mentioned were observed to be altered

by fluoxetine compared with vehicle (piriform cortex, suprachiasmatic nucleus, primary somatosensory cortex, secondary visual cortex, auditory cortex, see Table 3.9).

In addition to the increase in *c-fos* expression by fluoxetine in the majority of the regions associated with the orbitofrontal circuit, the other administered antidepressants were also observed to induce *c-fos* in a number of these areas. All drugs induced *c-fos* in the central amygdala compared with vehicle (Figure 3.6 and Table 3.5). Beck (1995) observed that this was the only brain region of those examined, in which all antidepressants (fluoxetine (10 and 15 mg/kg, i.p.), desipramine (10 mg/kg, i.p.), bupropion (20 mg/kg, i.p.), nortriptyline (15 mg/kg, i.p), imipramine (20 mg/kg, i.p.) and citalopram (5 mg/kg, i.p.)) induced *c-fos* expression. Therefore, that Org 34167 and mirtazapine (both previously undocumented) also display this attribute, adds support to the idea that a common mechanism of antidepressant administration is to alter activity in the central amygdala. This is also supported by the fact that chronic antidepressant treatment normalises the hyperactivity of the amygdala in rat and human (see Drevets (1999) for review). This adds further evidence in support of Org 34167 as a novel antidepressant; although non-antidepressants have also been reported to induce *c-fos* mRNA expression in this brain region, including diazepam (modulates $GABA_A$ receptor, 10 mg/kg; Salminen *et al.*, (1996)), haloperidol (D_2-receptor antagonist, 0.1 & 1 mg/kg; Morelli *et al.*, (1999); Sebens *et al.*, (1996)), clozapine (broad spectrum antagonist acting at $D_{1\text{-}5}$ receptors; also antagonistic at 5-HT_{2A} and $_{2C}$, α_1 and α_2-adrenoceptors, histamine H_1, and acetylcholine M_1 receptors, 10 & 20 mg/kg; Morelli *et al.*, (1999); Sebens *et al.*, (1996)), cocaine (inhibits DA reuptake, 15 mg/kg; Day *et al.*, (2001)) and amphetamine (inhibits NA and DA reuptake, 2 & 5 mg/kg; Day *et al.*, (2001); Engber *et al.*, (1998)).

The insular cortex is another brain region in which all drug treatments were observed to increase *c-fos* expression compared with the saline control. This increase was significant for all drugs in the anterior region (Table 3.3) and all except fluoxetine in the medial region (Table 3.4). As described above, the insular cortex is a region which is abnormally activated in patients with depression (Drevets, 2001; Drevets, 2000) and the fact that all these antidepressants induce neuronal activation in this region suggests that this is a region where they exert their influence. Similarly, all antidepressants, with the exception of mirtazapine significantly induced *c-fos* expression compared with vehicle in the perirhinal cortex (Table 3.6). The perirhinal cortex has been demonstrated to have reciprocal connections with the frontal cortex in rat and damage to this region impairs familiar object recognition in rats (Mumby *et al.*, 2002).

Fluoxetine treatment induced *c-fos* expression in the anterior cingulate cortex compared with all other groups (Table 3.3). While this has previously been demonstrated for other antidepressants, it has also been shown in all studies involving the psychostimulants amphetamine (2.5 & 5 mg/kg; Turgeon *et al.*, (2001)), PCP (0.8 & 8.6 mg/kg; Gao *et al.*, (1993)) and MK-801 (antagonist at NMDA receptors, 0.2 & 0.4 mg/kg; Wedzony *et al.*, (1996), where the anterior cingulate cortex has been analysed. However, in the cingulate cortex, Org 34167 treatment induced *c-fos* mRNA expression compared with all other groups with no other significant alterations between the remaining drugs (Table 3.3); a finding similar to that observed following psychostimulant administration (Gao *et al.*, (1993); Turgeon *et al.*, (2001); Wedzony *et al.*, (1996)). Intriguingly, at these bregma co-ordinates, for all cortical areas examined, with the exception of the piriform cortex, Org 34167 induced *c-fos* mRNA expression significantly compared with all other treatments, except fluoxetine in the caudal

secondary motor cortex (Table 3.4). This strong cortical induction of *c-fos* is more akin to that observed in studies involving psychostimulants as discussed above. Doses of Org 34167 similar to those used in the present study have been demonstrated to be active in the rat intracranial self-stimulation (Ruigt, Personal communication) and this pattern of *c-fos* induction provides some insight as to why this may be the case. The cortical increase in *c-fos* was most apparent throughout the retrosplenial cortex, where Org 34167 administration resulted in a doubling of *c-fos* expression compared with all other treatment groups, at the anterior, medial and posterior areas analysed (Tables 3.5 – 3.7). It has previously been observed that the head-weaving behaviour following MK-801 administration is correlated with the level of *c-fos* induction in the retrosplenial cortex (O'Neill *et al.*, 1998). Org 34167-administration also produces head-weaving in rats (0.01 mg/kg i.c.v.) and the similar activation of *c-fos* in the retrosplenial cortex may indicate the possible mechanism of action. The strong cortical activation of *c-fos* following Org 34167-treatment mirrors the distribution of brain regions in which both HCN1 and HCN2 mRNA expressions are high (Table 3.9 & 3.10; Monteggia *et al.*, 2000; Moosmang *et al.*, 1999). Therefore, it is possible that the reason for the consistently high induction of *c-fos* is due to the presence of high expression of HCN1 and HCN2 isoforms in the cortex (See Table 3.10).

The septum is also believed to be an important brain region in animal models of depression. The helpless behaviour in learned helplessness is thought to be related to 5-HT levels in the septum, as microinjection of 5-HT into the lateral septal nucleus reverses learned helplessness (Sherman *et al.*, 1980). A recent study reported decreased c-Fos in the lateral septal nucleus of learned helpless rats, and it was hypothesised that this may represent the deficient 5-HT transmission of these rats (Steciuk *et al.*, 1999). Another animal model of depression, the forced swim test, has been demonstrated to

increase c-Fos in the lateral septum (Duncan *et al.*, 1996), which is reversed by pre-treatment with antidepressants (Duncan *et al.*, 1996). Therefore, the fact that all drugs in the present study decreased *c-fos* mRNA expression in the septum would appear to contradict the findings from the learned-helplessness study but corroborate those of the forced-swim test.

In the frontal cortex, both Org 34167 and LiCl-treatment induced *c-fos* expression in the anterior secondary motor cortex (Table 3.2). However, the only other component of the motor circuit analysed, the dorso-lateral striatum, did not differ significantly from vehicle (Tables 3.3. and 3.4). Interestingly, Org 34167 elevated *c-fos* significantly compared with all other treatment groups in the secondary motor cortex ($P < 0.05$). This induction has been demonstrated previously for psychostimulants, including cocaine (3 & 30 mg/kg; Johansson *et al.*, (1994)) and amphetamine (2 & 5 mg/kg; Badiani *et al.*, (1998); Johansson *et al.*, (1994)). Additionally, increased locomotor activity after low doses of Org 34167, manifested in adverse effects, such as tremor, head-weaving and forepaw treading is observed (Ruigt, Personal communication). The induction of *c-fos* was also observed in the posterior secondary motor cortex following Org 34167 administration but did not reach significance in the case of LiCl (Table 3.4). Fluoxetine-administration also induced *c-fos* in the posterior secondary motor cortex compared with all treatments, except Org 34167, which is interesting as fluoxetine increased mRNA in the dorsolateral striatum compared with all treatments. Therefore, fluoxetine increases neuronal activity in two regions of the motor circuit, whilst Org 34167 only does so in one.

The most robust induction of *c-fos* mRNA observed was in the supraoptic nucleus following LiCl administration (Table 3.4). A ten-fold increase compared with vehicle,

and five-fold compared with all other drug-treatments was seen. A likely explanation for this comes from the knowledge that the supraoptic nucleus is sensitive to osmotic balance (see Hussy *et al.*, (2000) for a review) and the injection of a large number of Li^+ ions disrupts this balance. Despite a trend towards an increase following fluoxetine treatment, as previously reported by immunohistochemical studies (Torres *et al.*, 1998) this did not reach significance compared with vehicle (Table 3.4).

The *c-fos* profile of Org 34167 may also give some insight into a number of the side-effects, which were reported during Phase 1 clinical trials. Visual disturbances were the most frequently cited adverse effect following administration, and Org 34167 induces *c-fos* mRNA in the superior colliculus compared with vehicle, mirtazapine and LiCl ($P < 0.05$; Table 3.7). The superior colliculus is involved in the control of orientation, by use of eye and head movements, in many different species, including rats, monkeys and humans (see Guitton (1999) for review). Therefore, it is possible that Org 34167 alters this control region, leading to the visual disturbances. No significant alterations were observed in the primary or secondary visual cortices compared with vehicle (Table 3.7). Additionally, I_h channels are abundant in the retina and it is possible that the impairment in vision is due to Org 34167 acting directly on these channels; however, the retina was not examined in the present study. Furthermore, in the superior colliculus and the primary and secondary visual cortices, mirtazapine and LiCl-administration downregulated *c-fos* mRNA compared with vehicle, and although visual disturbances are not reported as a side-effect of mirtazapine administration, lithium toxicity is associated with blurred vision.

Imipramine administration resulted in little significant alteration from vehicle treatment out-with those areas already discussed, where the *c-fos* profile of all antidepressants

were similar (see Table 3.9). In addition to the anterior and medial insular cortex, imipramine induced *c-fos* expression in the posterior insular cortex, which is similar to the findings of Org 34167. This is consistent with the theory that the abnormalities observed in patients with familial major depression in the insular cortex (Drevets, 2001) are acutely targeted by antidepressant administration. Interestingly, imipramine induced *c-fos* expression in the posteromedial cortical amygdaloid nucleus (Table 3.6 & Figure 3.7). This structure forms part of the vomeronasal system, which is implicated in the control of reproductive behaviour and in males contains a greater number of neurones than in females (Vinader-Caerols *et al.*, 2000). One of the side-effects of imipramine is the interference of sexual function, which can be manifest in testicular enlargement. Recently, Vinader-Caerols *et al.*, (2000) demonstrated that estradiol aromatisation from circulating testosterone masculinises this brain region. This may represent a possible explanation for the side-effects of imipramine, as this system conveys olfactory information related to reproductive behaviour, especially considering that imipramine also decreased *c-fos* expression throughout the piriform cortex, which is important in olfaction (Bouret *et al.*, 2002).

As previously stated fluoxetine-treatment did not significantly alter *c-fos* expression in the subiculum compared with vehicle. However, Org 34167 treatment significantly induced *c-fos*, compared with all groups, whereas imipramine, mirtazapine and LiCl-administration significantly decreased *c-fos* compared with vehicle, Org 34167 and fluoxetine (Table 3.7). In other areas of the hippocampal complex, Org 34167 induced *c-fos* expression compared with all other groups, including the post-subiculum, rostral CA1 and CA2 fields, and in the caudal CA1 field (Tables 3.5 & 3.6). Similar to the strong cortical activation, the only previous compounds, which induced *c-fos* expression in the hippocampus were the psychostimulants PCP (40 mg/kg; Sharp, (1997)) and

caffeine (50 mg/kg; Singewald *et al.*, (2003)). Therefore, it appears that the *c-fos* profile of Org 34167 is a combination of that observed for antidepressants and that for psychostimulants. The similarity of the *c-fos* profile of Org 34167 to that of psychostimulant compounds (as discussed above) may partially explain the antidepressant-like properties of Org 34167, as amphetamine and cocaine were originally used to treat depression (see Section 1.3.2). Additionally, NMDA antagonists have been shown to have antidepressant-like activity. Trullas & Skolnick (1990) demonstrated that 2-aminophosphonoheptanoic acid (a competitive NMDA antagonist), 1-aminocyclopropanecarboxylic acid (ACPC; a glycine partial agonist) and MK-801 (a use-dependent channel blocker) all reduced immobility time in the forced-swim test, as well as competitive NMDA antagonists displaying antidepressant-like activity in the Willner chronic mild stress model (Papp *et al.*, 1994). Therefore, the cortical and hippocampal activation following acute Org 34167 may represent brain regions required for its proposed antidepressant activity.

Hippocampal expression of HCN1 and HCN2 mRNA is high, as was discussed concerning the cortex, adding further evidence that the brain regions in which strong induction of *c-fos* is observed following Org 34167 administration is associated with the presence of either, or both, of these isoforms (see Table 3.10). Furthermore, the high level of neuronal activity observed following Org 34167 administration suggests that the dose used in the present study acts throughout the CNS. Similar findings have been demonstrated with lithium, where a dose of 20 mg/kg (comparable with the human dose) only elevated c-Fos in the central amygdala, while 100 mg/kg induced Fos in a number of brain regions (Hamamura *et al.*, 2000). Therefore, it would be interesting to perform a dose-response relationship to determine whether Org 34167 displays a similar characteristic.

Table 3.10 Distribution of HCN1-4 mRNA isoforms

BRAIN REGION	HCN 1	HCN 2	HCN 3	HCN 4
Prefrontal cortex	++++	+++	+	-
Nucleus accumbens	+	++	-	-
Caudate putamen	+	+++	-	-
Thalamus	-	++++	-	++
Amygdala	+++	++(+)	+	-
Hippocampus	+++	++++	+	-
Ventral tegmental area	+++	++	+	+
Subiculum	++++	+++	++++	++++
Locus coeruleus	+++	++++	+++	+++
Dorsal Raphé	+++	++++	+	-

Data adapted from (Monteggia *et al.*, 2000; Moosmang *et al.*, 1999).

In the nucleus accumbens (core and shell regions), mirtazapine, LiCl and fluoxetine administration increased *c-fos* mRNA expression compared with vehicle, Org 34167 and imipramine (Table 3.3). This has previously been noted following bupropion (20 mg/kg; Beck, (1995)) and fluoxetine (10 mg/kg; Cruise, Personal communication)). Patients with depression exhibit decreased cerebral blood flow and metabolism in this region (Drevets *et al.*, 1992), which coupled with the role of the accumbens in emotion suggests it is possible that antidepressant treatment normalises the metabolism in this region. All antipsychotics and psychostimulants (where this region has been analysed) elevate *c-fos* in the nucleus accumbens (Badiani *et al.*, (1998); Castner *et al.*, (1996); Johansson *et al.*, (1994); Morelli *et al.*, (1999); Sebens *et al.*, (1996); Singewald *et al.*, 2003)). The nucleus accumbens plays a role in reinforcing stimuli, such as food and sex, as well as mediating the reinforcement of drugs of abuse (Di Chiara, 2002). Therefore, it is unsurprising that all psychostimulants induce *c-fos* here, which would lead, in turn, to long-lasting gene alterations. While all antidepressants induce *c-fos* in the central amygdala, the nucleus accumbens appears to be the defining brain region of antipsychotic administration; being the only area activated by all.

Another important brain region in depression is the locus coeruleus, which is the major origin of noradrenergic projections in the CNS (Holets, 1990). Although all antidepressant groups elevated *c-fos* mRNA expression in this region, only the fluoxetine-evoked increase was significant (Table 3.8). Previous studies, which have analysed this brain region, have shown that the antidepressants desipramine (10mg/kg; Beck, (1995)), tranylcypromine (7.5 mg/kg; Beck, (1995)) and bupropion (20 mg/kg; Beck, (1995)) significantly elevate *c-fos*. That all antidepressants show a trend towards an increase in neuronal activity in this region is unsurprising given that most increase noradrenergic neurotransmission. Similar findings were observed in the dorsal raphé, with all drugs except LiCl displaying a trend towards an increase in *c-fos* expression. However, no previous reports concerning the dorsal raphé have come to light.

In conclusion, the *c-fos* profile of Org 34167 shows a strong cortical and subcortical nature, which is similar to literature findings for psychostimulants. Additionally, this profile correlates with regions with high expression of both HCN1 and HCN2 mRNA, which given the *in vitro* data is suggestive that Org 34167 is blocking HCN channels, which in turn causes *c-fos* induction. All compounds tested in the present trial induced *c-fos* in the anterior insular cortex and central amygdala, and decreased *c-fos* in the septum and the nucleus of the lateral olfactory tract. Previous studies have shown that all antidepressants induce *c-fos* in the central amygdala, which was repeated in the present study, and shown for the first time for mirtazapine and Org 34167; two previously undocumented compounds. Additionally, all compounds in the present study induced *c-fos* expression in the anterior insular cortex, a region linked with depression. These findings confirm the antidepressant profile of the clinically validated compound mirtazapine and provide an indication to the potential antidepressant profile of Org 34167. Furthermore, fluoxetine administration induced *c-fos* expression in every

region of the orbitofrontal circuit analysed, and a number of brain areas which possess reciprocal connections with the orbital cortex and nucleus accumbens. This circuit is altered in patients with depression and demonstrates that fluoxetine acutely targets these brain regions implicated in depression.

Chapter 4 Comparison of Org 34167 induced changes in Egr-1 expression to that of known antidepressants

4.1 Introduction

The previous chapter detailed the effect of acute administration of antidepressants, and a mood stabiliser, on the expression of the immediate early gene, *c-fos,* throughout the rat CNS. It is now becoming a common practice to examine more than one immediate early gene in such experiments, due to the fact that only a subset of neurones express *c-fos* (Ziolkowska *et al.*, 2002). Other genes utilised include members of the Jun family, such as c-jun, which dimerises with *c-fos* to form AP-1 (Herdegen *et al.*, 1998). However, the similarity of these gene families is resulting in more researchers examining a different ITF family; namely the Early growth response (Egr) family. To date there are four known Egr protein members (Egr 1 – 4), which are characterised by containing three zinc finger motifs, which recognise a 9 base-pair segment of DNA (Leah *et al.*, 2002).

The most commonly utilised Egr gene for mapping neuronal activation is Egr-1 (also termed *zif268*, Krox-24, NGFI-A, TIS8 and ZENK), which displays a widespread distribution in the CNS, with high expression throughout the cortex, hippocampus, striatum and amygdala (Schlingensiepen *et al.*, 1991). Unlike *c-fos,* Egr-1 is characterised by high basal expression level (Leah *et al.*, 2002). Basal Egr-1 expression appears to be, at least partially, under the control of NMDA-, dopamine- and noradrenergic- receptors. (Gass *et al.*, 1993a; Gass *et al.*, 1993b; O'Donovan *et al.*, 1999). Like *c-fos*, which has shown to be dependent upon Ca^{2+} entry into the neuron, L-type voltage-sensitive Ca^{2+} antagonists block basal and kainate-induced Egr-1 expression (Murphy *et al.*, 1991). The strong cortical expression of Egr-1 is at least

partially under noradrenergic control, as lesioning of NA input decreases basal expression (O'Donovan *et al.*, 1999) . Therefore, different subsets of neurones to that of *c-fos* may be activated by the same stimuli, given the different signal transduction pathways involved (see Figure 4.1). The temporal expression of Egr-1 is also different to that of *c-fos,* while mRNA expression reaches a peak level after 30 – 60 min, the mRNA expression can remain near peak after 6 h (Zangenehpour *et al.*, 2002).

Figure 4.1 The major pathways involved in the induction of Egr-1

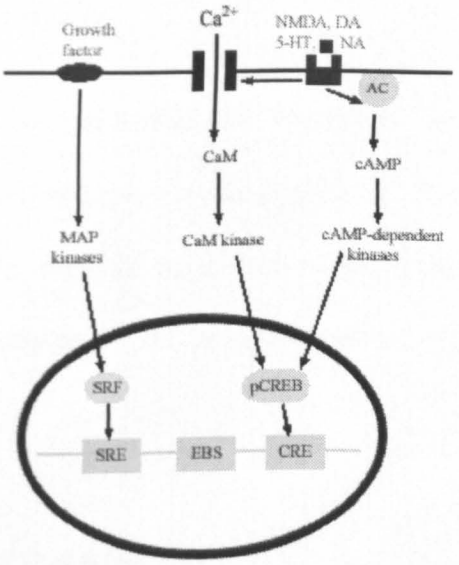

The effect of a number of different antidepressants on Egr-1 expression has been examined. Acute desipramine (10 or 25 mg/kg i.p.) has been shown to increase Egr-1 expression in the hippocampus (Dahmen *et al.*, 1997), as have acute electroconvulsive seizures in the rat frontal cortex (Morinobu *et al.*, 1997). LiCl stress induces Egr-1 in the nucleus tractus solitarus, parabrachial nucleus, paraventricular nucleus and central nucleus of the amygdala (Lamprecht *et al.*, 1995). However, to date there have been no reports concerning the affect of a wide-range of antidepressants on Egr-1 expression throughout the CNS.

The aim of the experiments performed in this chapter was to examine the effect of a number of different classes of antidepressant on Egr-1 mRNA expression levels, to determine which brain regions each affect. Comparison of Org 34167's Egr-1 profile with that of known antidepressants was peformed to determine whether similar brain regions were affected. Mirtazapine was included to discern whether it activated brain regions similar to those of other well-described classes of antidepressants.

4.2 Materials and methods

4.2.1 Animals and experimental protocol

See Section 3.2.1 for animal and experimental protocol. The same animals as used in the *c-fos* study were used for the present study.

4.2.2 Cryostat sectioning

See Section 3.2.2 for details of cryostat sectioning.

4.2.3 Egr-1 *in situ hybridisation*

In situ hybridisation was performed as described in Section 2.2 utilising a complementary probe to the *rattus norvegius* Egr-1 transcript at a final concentration of 2 pmol (see Appendix B for details). Specificity of the probe was assessed as described in Section 2.2 (See Appendix C for autoradiograms) and the results analysed as described in Section 2.2.

4.2.4 Acetylcholinesterase activity

See Section 3.2.4 for protocol used for demonstrating sites of acetylcholinesterase activity.

4.2.5 Statistical analyses

Data for each region of interest were analysed by one-way analysis of variance followed by Student Newman-Keuls *post-hoc* multiple comparison test. Significance was assigned when $P < 0.05$ and analysis was performed using GraphPad Prism v3.02 (GraphPad Software Inc).

4.3 Results

4.3.1 Effect of acute administration on Egr-1 mRNA expression

Unlike the low expression of *c-fos* mRNA observed in vehicle-treated rats, Egr-1 expression is much more prominent; displaying a pronounced rostral-caudal decline (Figures 4.2 – 4.8). Similar to the *c-fos* study there are alterations in the expression of this immediate early gene between each of the different treatment groups throughout the brain regions examined.

4.3.2 Effect of treatment on Egr-1 mRNA (4.7 to 4 mm relative to bregma)

Acute administration of Org 34167 was observed to significantly induce Egr-1 mRNA expression, compared with all other treatments, in the anterior olfactory nucleus ($P < 0.05$; Figure 4.2 and Table 4.2), and every group with the exception of fluoxetine in the secondary motor cortex ($P < 0.05$). This is similar to the *c-fos* findings in the secondary motor cortex where Org 34167 administration resulted in an elevation compared with every other group. LiCl-administration significantly lowered Egr-1 mRNA levels in the ventromedial orbital cortex compared with Org 34167 and imipramine treatment ($P < 0.05$). No significant differences were found between any treatments in the prelimbic cortex.

4.3.3 Effect of treatment on Egr-1 mRNA (2.2 to 1.5 mm relative to bregma)

Acute administration of Org 34167 significantly induced Egr-1 mRNA, compared with all other groups, in all cortical regions (piriform, anterior cingulate and anterior insular), as well as the rostral dorso- and ventro-medial striatum ($P < 0.05$; Figure 4.3, Table 4.2). This trend was observed in the nucleus accumbens core, rostral dorso- and ventro-

lateral striatum regions but only reached significance in the rostral ventro-lateral striatum compared with vehicle, mirtazapine and LiCl treatment ($P < 0.05$). No significant variation in Egr-1 mRNA expression was observed in the septum or nucleus accumbens shell between any treatments.

4.3.4 Effect of treatment on Egr-1 *mRNA (-0.8 to -1.5 mm relative to bregma)*

The strong cortico-striatal activation of Egr-1 expression following Org 34167 was again apparent at this more caudal region. Acute administration of the novel antidepressant induced Egr-1 expression compared with all other groups in the cingulate cortex and caudal dorsomedial striatum ($P < 0.05$). Imipramine-treated rats were observed to increase Egr-1 expression compared with mirtazapine and LiCl in the caudal dorsomedial striatum ($P < 0.05$). In the caudal secondary motor cortex, Org 34167 induced Egr-1 expression compared with every other treatment group except fluoxetine ($P < 0.05$), which is similar to the *c-fos* observations. In both the insular cortex and caudal ventral striatum, Org 34167 administration increased Egr-1 expression significantly compared with vehicle ($P < 0.05$). In the somatosensory cortices, mirtazapine administration demonstrated a significantly lower level of Egr-1 compared with Org 34167 in both the primary and secondary regions, and vehicle in the secondary somatosensory cortex ($P < 0.05$). In the piriform cortex and caudal dorsolateral striatum, LiCl administration resulted in significantly lower Egr-1 expression compared with Org 34167 ($P < 0.05$). Acute administration of mirtazapine decreased Egr-1 mRNA compared with Org 34167 in the caudal dorsolateral striatum ($P < 0.05$). No significant differences in Egr-1 mRNA levels in the anterior paraventricular thalamic nucleus, nucleus of the lateral olfactory tract or bed nucleus of the stria terminalis were observed. All these results are summarised in Table 4.3 and representative autoradiograph images are shown in Figure 4.4.

4.3.5 Effect of treatment on Egr-1 *mRNA (-2.5 to -3.2 mm relative to bregma)*

As was observed in the corresponding *c-fos* study, Org 34167 administration induced Egr-1 mRNA compared with vehicle control in every cortical area examined, with the exception of the posterior piriform cortex ($P < 0.05$). Furthermore, each drug treatment induced Egr-1 mRNA, compared with vehicle, in the central amygdala, which was also observed with *c-fos* mRNA expression. LiCl-treatment significantly increased Egr-1 mRNA compared with all other groups in the central amygdala ($P < 0.05$) and Org 34167 significantly higher than all other treatments except LiCl ($P < 0.05$). Similar to the increased expression of *c-fos* observed following Org 34167 administration in the anterior retrosplenial cortex, Egr-1 expression was also significantly increased compared with all other treatments ($P < 0.05$). Mirtazapine- and LiCl-treated rats displayed lower Egr-1 expression in the primary somatosensory cortex compared with Org 34167 ($P < 0.05$). Org 34167 and imipramine Egr-1 mRNA levels were significantly higher than those following vehicle, mirtazapine and LiCl administration in the secondary somatosensory- and posterior insular cortices ($P < 0.05$). Rostral CA1 Egr-1 mRNA expression was significantly increased following Org 34167 administration compared with all other treatments ($P < 0.05$), as was *c-fos* mRNA (Table 3.5). No significant variations in Egr-1 mRNA levels were observed in the posterior piriform cortex, rostral CA2, CA3 or dentate gyrus brain regions (Table 4.4). Thalamic Egr-1 mRNA expression was significantly higher following imipramine and fluoxetine administration than all other treatment groups ($P < 0.05$), although there was no significant difference between these two drugs. All these results are summarised in Table 4.4 and representative autoradiograph images are shown in Figure 4.5.

4.3.6 Effect of treatment on Egr-1 *mRNA (-4.8 to -5.5 mm relative to bregma)*

The observation that Org 34167 administration elevated Egr-1 mRNA levels in the anterior retrosplenial cortex compared with all other treatments is replicated at this more caudal level of the brain ($P < 0.05$; Figure 4.6 & Table 4.5). However, the strong cortical activation is not apparent, with only mirtazapine and LiCl administration resulting in lower mRNA expression than Org 34167, and this only in the secondary visual cortex, where they were also significantly lower than fluoxetine-treated rats ($P < 0.05$). The only other significant differences, following drug treatment, were observed in the posteromedial cortical amygaloid nucleus where LiCl-treated animals were observed to have lower Egr-1 levels than vehicle and imipramine treatment groups ($P < 0.05$).

4.3.7 Effect of treatment on Egr-1 *mRNA (-6.8 to -7.5 mm relative to bregma)*

Acute administration of Org 34167 significantly induced Egr-1 mRNA expression, at these bregma co-ordinates, in almost every region analysed compared with saline control; only the primary visual cortex, periaqueductal grey and superior colliculus did not reach statistical significance (Figure 4.7 & Table 4.6). As was observed in the *c-fos* study, Org 34167-treated rats demonstrated significantly higher mRNA levels than all other treatment groups in the retrosplenial cortex, subiculum and post-subiculum ($P < 0.05$). Imipramine and LiCl treatment also down-regulated Egr-1 mRNA expression compared with vehicle in the post-subiculum ($P < 0.05$). In both the primary and secondary visual cortices, mirtazapine- and LiCl-treatment decreased Egr-1 mRNA compared with vehicle, Org 34167 and imipramine administration, as well as fluoxetine in the primary visual cortex ($P < 0.05$). Org 34167 administration resulted in significantly higher Egr-1 expression than mirtazapine, LiCl and fluoxetine treatment in

the temporal association cortex, ectorhinal cortex and lateral entorhinal cortex ($P < 0.05$). Ectorhinal cortex levels of Egr-1 mRNA were also induced following imipramine treatment compared with mirtazapine and LiCl administration ($P < 0.05$). Mirtazapine, LiCl and fluoxetine treatment resulted in lower Egr-1 mRNA expression in the dorsal raphé compared with vehicle and imipramine administration ($P < 0.05$). In the superior colliculus, Org 34167 administration induced Egr-1 mRNA compared with mirtazapine and LiCl treatment, as did imipramine relative to LiCl ($P < 0.05$). Acute administration of vehicle, mirtazapine and LiCl resulted in decreased Egr-1 mRNA in the nucleus of the brachium of the inferior colliculus compared with Org 34167- and imipramine-treated rats ($P < 0.05$). Fluoxetine administration resulted in elevated Egr-1 expression compared with LiCl-treatment ($P < 0.05$). No significant effects of treatment were observed in the periaqueductal grey.

4.3.8 Effect of treatment on Egr-1 *mRNA (-9.3 to -10 mm relative to bregma)*

In the most caudal of the brain regions examined, acute administration of Org 34167 was observed to induce Egr-1 mRNA expression in the posterodorsal tegmental nucleus compared with all other treatments ($P < 0.05$). The only other significant differences observed were decreased levels of Egr-1 mRNA in the inferior colliculus of mirtazapine and LiCl-treated rats compared with Org 34167 ($P < 0.05$; Figure 4.8 and Table 4.7).

Table 4.1 Effect of acute antidepressant administration on Egr-1 mRNA expression (4.7 to 4 mm relative to bregma)

Region	Vehicle			Org34167			Imipramine			Mirtazapine			LiCl			Fluoxetine		
	Mean	±	s.e.mean	Mean	±	s.e.mean	Mean	±	s.e.mean	Mean	±	s.e.mean	Mean	±	s.e.mean	Mean	±	s.e.mean
M2 ctx	144.17	±	11.75	193.96	±	14.46*	141.13	±	9.39+	143.36	±	9.09+	147.99	±	11.12+	176.01	±	13.50
PrL ctx	178.86	±	14.03	223.24	±	10.67	185.68	±	8.03	185.02	±	9.36	180.04	±	12.52	201.29	±	17.11
VM Orb ctx	319.52	±	11.32	351.49	±	21.07	353.42	±	11.17	299.41	±	13.51	274.59	±	12.25+†	317.20	±	14.91
AON.	285.31	±	14.49	373.75	±	25.80*	304.35	±	5.84+	256.48	±	16.34+	267.85	±	9.32+	260.69	±	13.32+

Data represent mean ± s.e. mean of three sections per animal ($n = 6$). Optical density readings have been converted to nCi/g of tissue. One-way ANOVA with Student Newman-Keuls *post-hoc* test was performed. $P < 0.05$ * compared with vehicle; + compared with Org 34167, † compared with imipramine; ‡ compared with mirtazapine; # compared with LiCl. Abb: M2 ctx, anterior secondary motor cortex, PrL ctx, prelimbic cortex, VM Orb, ventromedial orbital cortex, AON., anterior olfactory nucleus (Paxinos *et al.*, 1986).

Figure 4.2 Representative autoradiograms of acute drug administration on Egr-1 **mRNA expression (4.7 to 4 mm relative to bregma)**

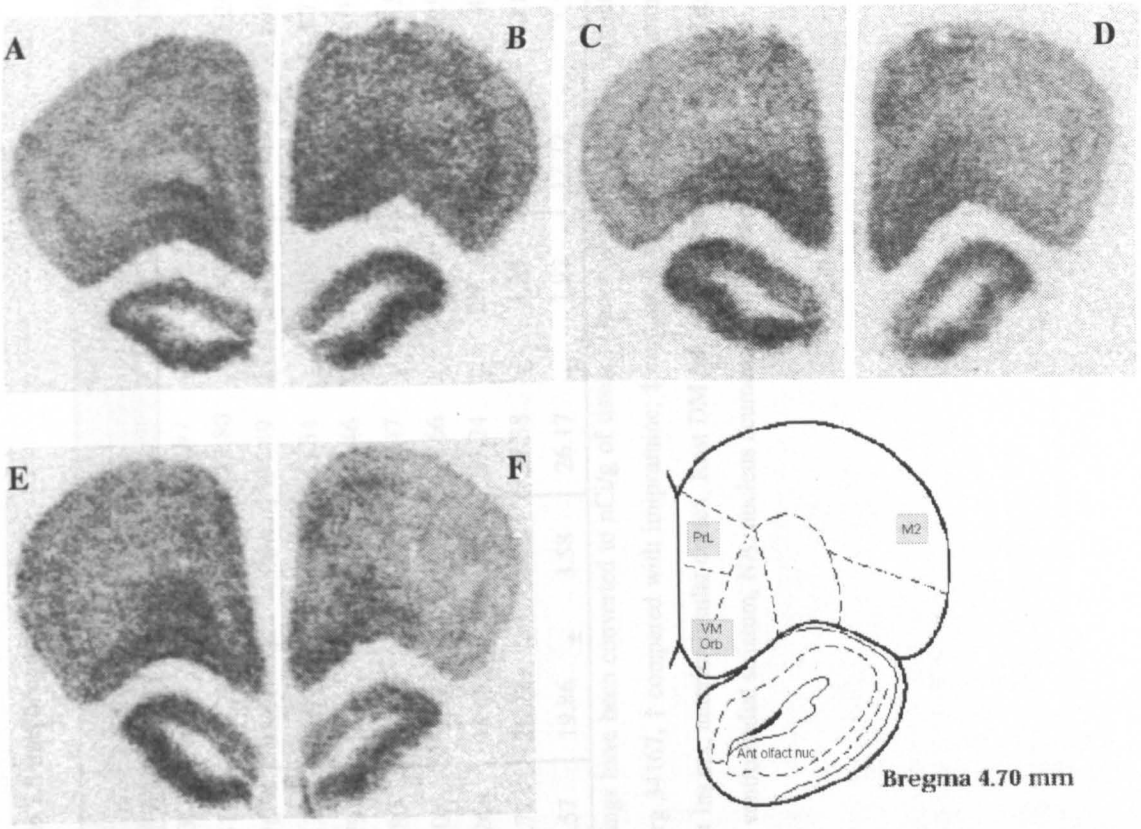

Representative autoradiographs of *in situ* hybridisation utilising a ^{33}P-labelled oligonucleotide probe targeted against the Egr-1 transcript in coronal sections of rat brain following 45 min acute administration of vehicle (A), Org 34167 (0.5 mg/kg, B), imipramine (15 mg/kg, C), mirtazapine (2 mg/kg, D), LiCl (75mg/kg, E) or fluoxetine (5mg/kg, F). Also shown is a schematic representation of the brain regions analysed. Abb: M2, anterior secondary motor cortex, PrL, prelimbic cortex, VM Orb, ventro-medial orbital cortex, Ant. olfact nuc, anterior olfactory nucleus (Paxinos *et al.*, 1986).

Table 4.2 Effect of acute antidepressant administration on Egr-1 mRNA expression (2.2 to 1.5 mm bregma)

REGION	VEHICLE			ORG34167			IMIPRAMINE			MIRTAZAPINE			LICL			FLUOXETINE		
	Mean	±	s.e.mean	Mean	±	s.e.mean	Mean	±	s.e.mean	Mean	±	s.e.mean	Mean	±	s.e.mean	Mean	±	s.e.mean
Septum	33.26	±	2.75	34.98	±	1.63	33.33	±	0.33	30.38	±	1.34	32.97	±	0.74	31.13	±	1.70
Ant Pir ctx	118.60	±	7.94	150.42	±	5.52*	124.75	±	7.31+	108.78	±	6.30+	113.80	±	3.04+	103.63	±	5.26+
Ant Cing ctx	97.75	±	9.01	130.39	±	5.13*	112.79	±	4.76+	91.61	±	4.00+	94.49	±	5.02+	104.61	±	6.43+
Ant Ins ctx	41.55	±	3.02	70.67	±	4.23*	49.26	±	3.12+	44.91	±	3.01+	45.34	±	2.10+	45.69	±	3.71+
Rost DM Str	40.20	±	2.39	57.68	±	2.02*	48.71	±	1.79+	38.04	±	2.59+†	36.46	±	2.39+†	42.70	±	3.75+
Rost DL Str	36.57	±	3.36	45.64	±	2.93	42.06	±	1.80	35.49	±	2.28	35.47	±	2.01	40.33	±	4.52
Rost VL Str	30.75	±	3.55	48.24	±	3.43*	37.40	±	3.07	31.27	±	2.26+	34.66	±	1.69+	35.31	±	3.97
Rost VM Str	37.01	±	4.35	52.16	±	3.69*	42.31	±	2.26+	35.65	±	2.52+	33.24	±	2.71+	36.91	±	1.48+
NA core	25.11	±	3.78	36.17	±	2.55	26.66	±	2.77	26.22	±	2.71	27.38	±	1.23	27.09	±	2.82
NA shell	19.92	±	2.65	19.18	±	4.11	17.70	±	2.57	19.86	±	3.58	26.17	±	1.92	17.72	±	1.32

Data represent mean ± s.e. mean of three sections per animal (n = 6). Optical density readings have been converted to nCi/g of tissue. One-way ANOVA with Student Newman-Keuls post-hoc test was performed. $P < 0.05$ * compared with vehicle; + compared with Org 34167, † compared with imipramine; ‡ compared with mirtazapine; # compared with LiCl. Abb: Ant Pir ctx, anterior piriform cortex, Ant Cing ctx, anterior cingulate cortex, Ant Ins ctx, anterior insular cortex, Rost DM Str, rostral dorsomedial striatum, Rost DL Str, rostral dorsolateral striatum, Rost VL Str, rostral ventrolateral striatum; Rost VM Str, rostral ventromedial striatum, NA, nucleus acumens (Paxinos *et al.*, 1986).

Figure 4.3 Representative autoradiograms of acute drug administration on Egr-1 **mRNA expression (2.2 to 1.5 mm relative to bregma)**

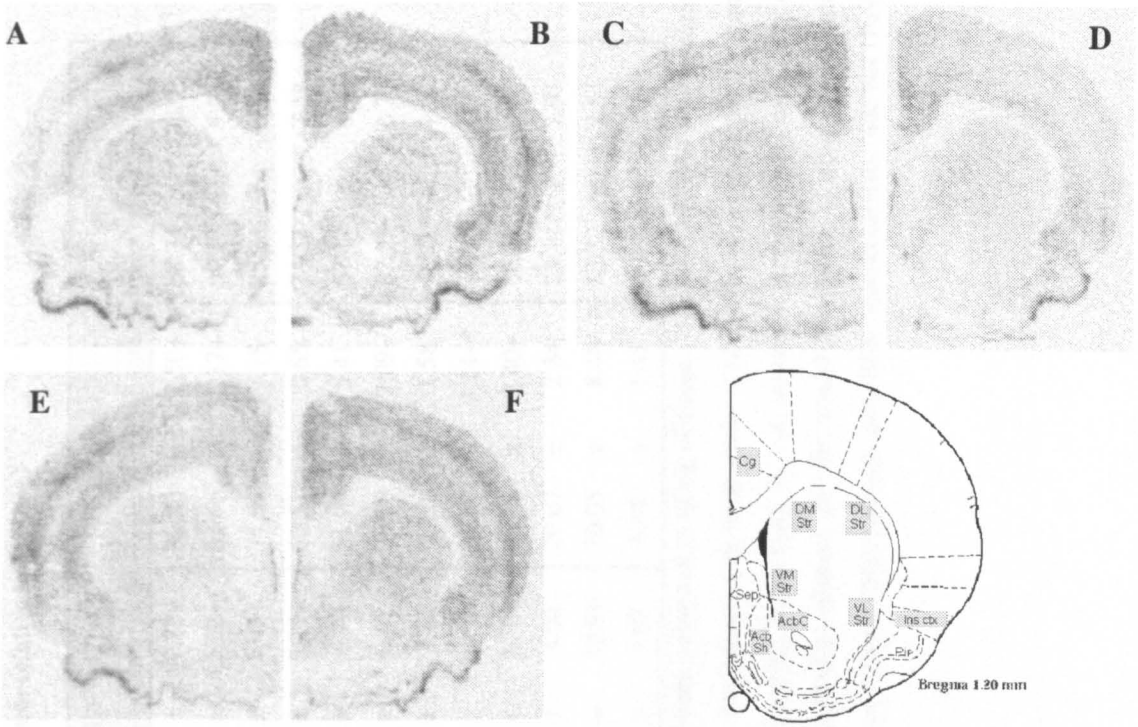

Representative autoradiographs of *in situ* hybridisation utilising a ^{33}P-labelled oligonucleotide probe targeted against the Egr-1 transcript in coronal sections of rat brain following 45 min acute administration of vehicle (A), Org 34167 (0.5 mg/kg, B), imipramine (15 mg/kg, C), mirtazapine (2 mg/kg, D), LiCl (75mg/kg, E) or fluoxetine (5mg/kg, F). Also shown is a schematic representation of the brain regions analysed. Abb: Sep, septum, Cg, anterior cingulate cortex, Ins ctx, anterior insular cortex, Pir, anterior piriform cortex, DM Str, rostral dorsomedial striatum, DL Str, rostral dorsolateral striatum, VM Str, rostral ventromedial striatum, VL Str, rostral ventrolateral striatum, AcbC, nucleus acumens core, AcbSh, nucleus accumbens shell (Paxinos *et al.*, 1986).

Table 4.3 Effect of acute antidepressant administration on Egr-1 mRNA expression (-0.8 to -1.5 mm relative to bregma)

Region	Vehicle			Org34167			Imipramine			Mirtazapine			LiCl			Fluoxetine		
	Mean	±	s.e.mean	Mean	±	s.e.mean	Mean	±	s.e.mean	Mean	±	s.e.mean	Mean	±	s.e.mean	Mean	±	s.e.mean
Cg ctx	73.98	±	7.34	125.55	±	8.72*	92.27	±	4.21+	70.40	±	2.22+	80.80	±	7.50+	88.34	±	7.79+
M2 ctx	69.57	±	3.93	111.21	±	11.76*	77.22	±	6.56+	76.17	±	5.58+	83.46	±	5.17+	99.12	±	8.91
S1BF	76.06	±	1.71	105.30	±	10.73	86.16	±	9.83	71.22	±	7.45+	75.81	±	3.18	85.38	±	6.76
S2 ctx	52.59	±	3.18	87.91	±	12.19*	69.03	±	6.38	58.88	±	5.21+	61.51	±	2.65	74.34	±	7.19
Ins ctx	35.52	±	3.64	66.36	±	9.25*	54.01	±	5.19	46.21	±	6.79	51.94	±	5.41	52.17	±	4.70
Pir ctx	89.28	±	4.04	99.24	±	3.22	82.89	±	3.97	80.80	±	6.41	76.76	±	2.09+	82.33	±	6.20
PVA	5.96	±	0.97	8.39	±	1.41	11.42	±	1.21	6.15	±	2.12	5.10	±	1.58	8.95	±	1.82
DM Str	46.39	±	2.84	61.12	±	3.83*	49.94	±	1.67+	34.31	±	1.95+†	36.50	±	3.14+†	43.30	±	5.52+
DL Str	31.60	±	1.25	41.75	±	2.38	38.81	±	2.48	27.91	±	2.70+	29.22	±	2.40+	36.22	±	4.55
V Str	22.77	±	2.16	37.65	±	3.53*	31.45	±	2.54	28.52	±	3.00	29.07	±	2.34	28.14	±	2.91
LOT	85.67	±	4.62	87.85	±	4.49	74.66	±	8.19	71.30	±	10.99	70.05	±	8.46	82.32	±	2.54
BSTMPL	9.27	±	1.66	9.89	±	1.30	12.25	±	0.88	6.36	±	2.07	6.43	±	1.41	9.47	±	1.11

Data represent mean ± s.e. mean of three sections per animal ($n = 6$). Optical density readings have been converted to nCi/g of tissue. One-way ANOVA with Student Newman-Keuls *post-hoc* test was performed. $P < 0.05$ * compared with vehicle; + compared with Org 34167, † compared with imipramine; ‡ compared with mirtazapine; # compared with LiCl. Abb: Cg ctx, cingulate cortex, M2 ctx, secondary motor cortex, S1BF, primary somatosensory cortex, barrel field, S2 ctx, secondary somatosensory cortex, Ins ctx, insular cortex, Pir ctx, piriform cortex, PVA, anterior paraventricular thalamic nucleus, DM Str, caudal dorsomedial striatum, DL Str, caudal dorsolateral striatum, V Str, caudal ventral striatum, LOT, nucleus of the lateral olfactory tract, BSTMPL, nucleus of the stria terminalis, medial division, posterolateral part, SCh, suprachiasmatic nucleus (Paxinos *et al.*, 1986).

Figure 4.4 Representative autoradiograms of acute drug administration on Egr-1 **mRNA expression (-0.8 to -1.5 mm relative to bregma)**

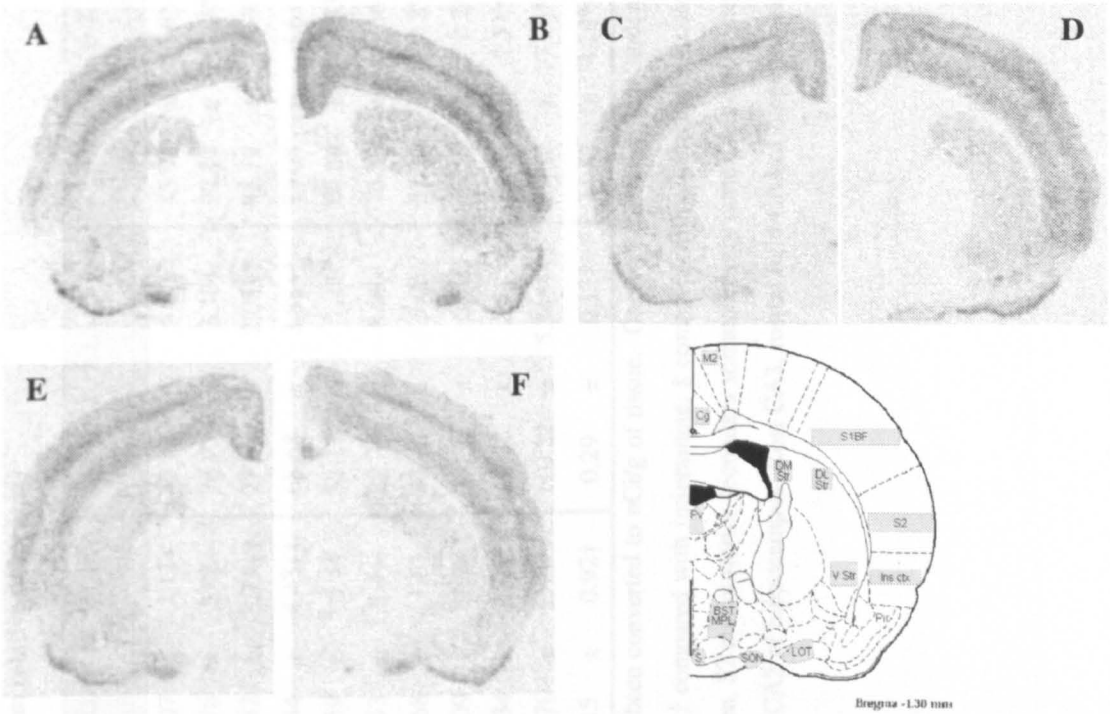

Representative autoradiographs of in situ hybridisation utilising a ^{33}P-labelled oligonucleotide probe targeted against the Egr-1 transcript in coronal sections of rat brain following 45 min acute administration of vehicle (A), Org 34167 (0.5 mg/kg, B), imipramine (15 mg/kg, C), mirtazapine (2 mg/kg, D), LiCl (75mg/kg, E) or fluoxetine (5mg/kg, F). Also shown is a schematic representation of the brain regions analysed. Abb: Cg, cingulate cortex, M2, secondary motor cortex, S1BF, primary somatosensory cortex, barrel field, S2, secondary somatosensory cortex, Ins ctx, insular cortex, Pir, piriform cortex, Pv, anterior paraventricular thalamic nucleus, DM Str, caudal dorsomedial striatum, DL Str, caudal dorsolateral striatum, V Str, caudal ventral striatum, LOT, nucleus of the lateral olfactory tract, BSTMPL, nucleus of the stria terminalis, medial division, posterolateral part, SON, supra-optic nucleus, S, suprachiasmatic nucleus (Paxinos *et al.*, 1986).

Table 4.4 Effect of acute antidepressant administration on Egr-1 mRNA expression (-2.5 to -3.2 mm relative to bregma)

Region	Vehicle			Org34167			Imipramine			Mirtazapine			LiCl			Fluoxetine		
	Mean	±	s.e.mean	Mean	±	s.e.mean	Mean	±	s.e.mean	Mean	±	s.e.mean	Mean	±	s.e.mean	Mean	±	s.e.mean
Ant RS ctx	40.73	±	2.78	93.29	±	8.16*	44.94	±	4.21+	39.07	±	2.12+	31.81	±	1.77+	45.98	±	2.63+
S1Tr	76.21	±	5.49	103.05	±	6.57*	94.62	±	3.89	77.76	±	3.96+	78.77	±	3.10+	92.12	±	5.75
S2 Ctx	80.74	±	4.40	103.69	±	5.25*	101.83	±	3.92*	80.42	±	3.73+†	77.97	±	2.05+†	95.12	±	6.40
Ins Ctx	73.16	±	3.40	100.83	±	5.02*	91.39	±	3.50*	68.44	±	4.43+†	68.68	±	3.88+†	79.08	±	7.61+
Pir Ctx	55.79	±	2.74	58.50	±	3.69	61.19	±	4.12	58.59	±	5.44	53.14	±	1.45	60.89	±	4.33
Rost CA1	85.29	±	6.41	116.39	±	8.11*	80.75	±	5.14+	73.53	±	3.44+	82.36	±	8.09+	76.49	±	4.36+
Rost CA2	55.28	±	4.36	58.85	±	7.74	56.27	±	3.02	54.68	±	1.63	45.62	±	5.00	57.33	±	2.29
Rost CA3	32.04	±	2.85	37.31	±	2.43	38.83	±	1.89	32.09	±	1.78	39.36	±	8.70	37.58	±	2.24
Rost Dg	18.71	±	2.55	22.80	±	2.96	27.25	±	1.02*	18.34	±	1.05†	18.32	±	2.51†	28.36	±	1.51*‡#
CeA	14.42	±	1.67	84.02	±	5.06*	47.18	±	5.76*+	44.70	±	5.48*+	110.22	±	5.54*+†‡	57.22	±	7.29*+#
Thalamus	0.55	±	0.39	0.25	±	0.15	9.90	±	1.38*+	2.15	±	0.92†	0.29	±	0.13†	14.57	±	4.18*+‡#

Data represent mean ± s.e. mean of three sections per animal ($n = 6$). Optical density readings have been converted to nCi/g of tissue. One-way ANOVA with Student Newman-Keuls *post-hoc* test was performed. $P < 0.05$ * compared with vehicle; + compared with Org 34167, † compared with imipramine; ‡ compared with mirtazapine; # compared with LiCl. Abb: Ant RS ctx, anterior retrosplenial cortex, S1Tr, primary somatosensory cortex, trunk region, S2 ctx, posterior secondary somatosensory cortex, Ins ctx, posterior insular cortex, Pir ctx, piriform cortex, Rost CA1, rostral field CA1 of hippocampus, Rost CA2, rostral field CA2 of hippocampus, Rost CA3, rostral field CA3 of hippocampus, Rost Dg, dentate gyrus, CeA, central amygdaloid nucleus (Paxinos *et al.*, 1986).

Figure 4.5 Representative autoradiograms of acute drug administration on Egr-1 **mRNA expression (-2.5 to -3.2 mm relative to bregma)**

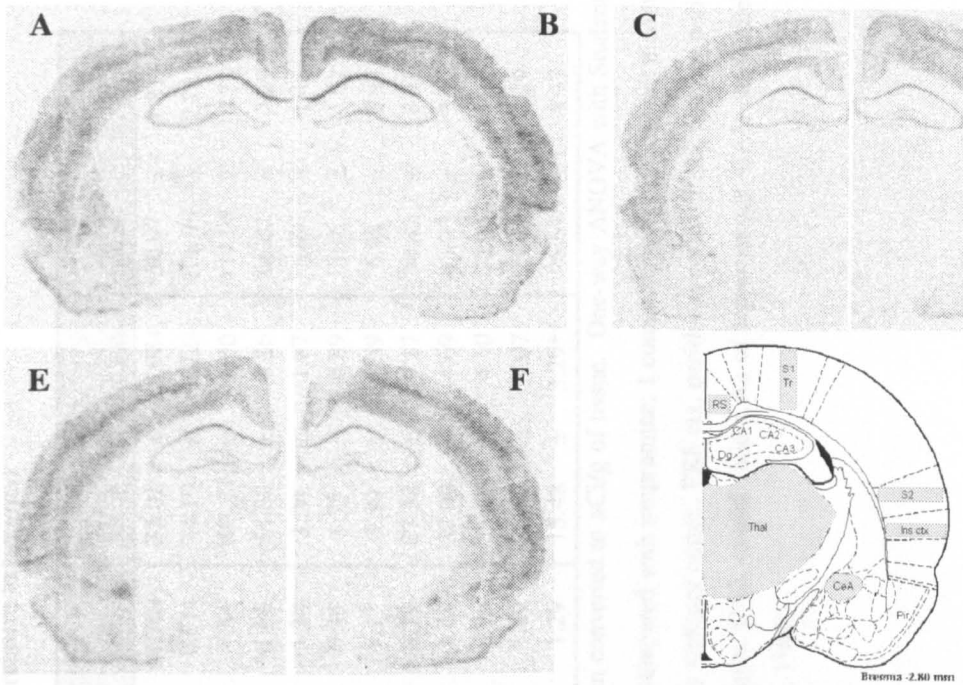

Representative autoradiographs of in situ hybridisation utilising a ^{33}P-labelled oligonucleotide probe targeted against the Egr-1 transcript in coronal sections of rat brain following 45 min acute administration of vehicle (A), Org 34167 (0.5 mg/kg, B), imipramine (15 mg/kg, C), mirtazapine (2 mg/kg, D), LiCl (75mg/kg, E) or fluoxetine (5mg/kg, F). Also shown is a schematic representation of the brain regions analysed. Abb: RS, anterior retrosplenial cortex, S1Tr, primary somatosensory cortex, trunk region, S2, posterior secondary somatosensory cortex, Ins ctx, posterior insular cortex, Pir, piriform cortex, CA1, rostral field CA1 of hippocampus, CA2, rostral field CA2 of hippocampus, CA3, rostral field CA3 of hippocampus, Dg, dentate gyrus, CeA, central amygdaloid nucleus, Thal, thalamus (Paxinos *et al.*, 1986).

Table 4.5 Effect of acute antidepressant administration on Egr-1 mRNA expression (-4.8 to -5.5 mm relative to bregma)

Region	Vehicle			Org34167			Imipramine			Mirtazapine			LiCl			Fluoxetine		
	Mean	±	s.e.mean	Mean	±	s.e.mean	Mean	±	s.e.mean	Mean	±	s.e.mean	Mean	±	s.e.mean	Mean	±	s.e.mean
RS ctx	40.30	±	6.23	86.55	±	14.05*	53.18	±	4.47+	45.60	±	1.70+	35.02	±	3.98+	50.97	±	1.81+
V2 ctx	85.53	±	6.48	115.52	±	9.66	102.45	±	6.91	72.24	±	0.87+	74.10	±	6.22+	106.79	±	12.22‡#
Au ctx	104.81	±	4.15	116.98	±	7.24	110.72	±	2.31	100.54	±	4.84	103.77	±	6.10	117.08	±	4.73
PRh ctx	50.97	±	1.38	65.39	±	5.47	64.96	±	3.56	49.04	±	1.66	54.82	±	6.86	66.02	±	2.29
PAG	3.10	±	1.44	5.37	±	1.70	5.76	±	1.55	3.64	±	1.38	3.96	±	1.87	6.99	±	1.45
VTA	0.89	±	0.47	0.59	±	0.26	3.62	±	0.97	1.05	±	0.39	1.75	±	0.89	3.16	±	1.07
Gen	3.56	±	1.55	4.10	±	1.01	5.85	±	1.31	2.94	±	1.17	3.50	±	1.59	6.98	±	1.94
CA1	95.99	±	3.05	116.31	±	7.80	97.95	±	5.52	90.03	±	3.79	87.38	±	9.17	96.42	±	8.43
CA2	50.09	±	2.98	54.36	±	4.47	44.68	±	5.07	45.08	±	1.48	37.09	±	4.69	43.27	±	3.50
CA3	30.60	±	2.90	34.32	±	3.51	32.75	±	2.91	27.10	±	0.95	28.46	±	4.10	32.94	±	2.18
DG	20.29	±	3.10	22.70	±	3.81	23.95	±	1.82	22.46	±	1.89	20.62	±	4.07	27.48	±	2.29
PMCo	31.71	±	2.07	25.21	±	1.60	32.97	±	4.55	21.10	±	1.29	15.48	±	3.29*†	26.67	±	4.47

Data represent mean ± s.e. mean of three sections per animal ($n = 6$). Optical density readings have been converted to nCi/g of tissue. One-way ANOVA with Student Newman-Keuls *post-hoc* test was performed. . $P < 0.05$ * compared with vehicle; + compared with Org 34167, † compared with imipramine; ‡ compared with mirtazapine; # compared with LiCl. Abb: RS, medial retrosplenial cortex, V2 ctx, secondary visual cortex, lateral area, Au ctx, primary auditory cortex, PRh ctx, perirhinal cortex, PAG, anterior periaqueductal grey, VTA, ventral tegmental area, Gen, geniculate nucleus, CA1, dorsocaudal field CA1 of hippocampus, CA2, caudal field CA2 of hippocampus, CA3, caudal field CA3 of hippocampus, Dg, caudal dentate gyrus, PMCo, posteromedial cortical amygdaloid nucleus (Paxinos *et al.*, 1986).

Figure 4.6 Representative autoradiograms of acute drug administration on Egr-1 **mRNA expression (-4.8 to -5.5 mm relative to bregma)**

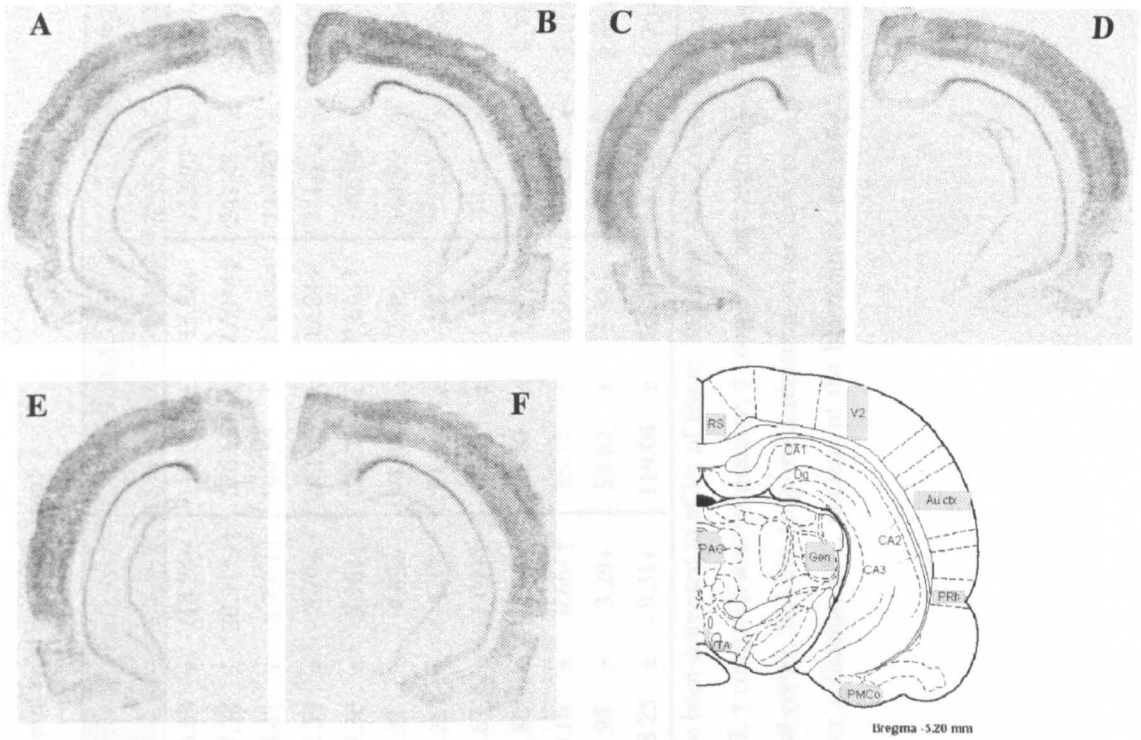

Representative autoradiographs of *in situ* hybridisation utilising a ^{33}P-labelled oligonucleotide probe targeted against the Egr-1 transcript in coronal sections of rat brain following 45 min acute administration of vehicle (A), Org 34167 (0.5 mg/kg, B), imipramine (15 mg/kg, C), mirtazapine (2 mg/kg, D), LiCl (75mg/kg, E) or fluoxetine (5mg/kg, F). Also shown is a schematic representation of the brain regions analysed. Abb: RS, retrosplenial cortex, V2, secondary visual cortex, lateral area, Au ctx, primary auditory cortex, PRh, perirhinal cortex, CA1, dorsocaudal field CA1 of hippocampus, CA2, caudal field CA2 of hippocampus, CA3, caudal field CA3 of hippocampus, Dg, caudal dentate gyrus, PAG, anterior periaqueductal grey, Gen, geniculate nucleus, VTA, ventral tegmental area, PMCo, posteromedial cortical amygdaloid nucleus (Paxinos *et al.*, 1986)

Table 4.6 Effect of acute antidepressant administration on Egr-1 mRNA expression (-6.8 to -7.5 mm relative to bregma)

Region	Vehicle			Org34167			Imipramine			Mirtazapine			LiCl			Fluoxetine		
	Mean	±	s.e.mean	Mean	±	s.e.mean	Mean	±	s.e.mean	Mean	±	s.e.mean	Mean	±	s.e.mean	Mean	±	s.e.mean
RS	142.85	±	25.15	235.25	±	20.33*	153.30	±	14.19+	123.83	±	13.24+	117.55	±	13.88+	123.90	±	13.47+
V1 ctx	244.03	±	18.91	277.29	±	16.28	272.21	±	8.20	177.38	±	20.31*+†	176.68	±	7.60*+†	241.48	±	20.10‡#
V2 ctx	253.44	±	20.69	306.02	±	15.12*	281.04	±	11.50	193.48	±	8.79*+†	199.55	±	7.31*+†	237.90	±	20.96+
TeA ctx	260.05	±	28.83	330.71	±	17.38*	309.00	±	10.85	242.59	±	8.70+	242.63	±	12.84+	241.37	±	15.50+
Ect ctx	140.11	±	17.42	195.63	±	10.35*	174.72	±	8.43	128.30	±	5.76+†	129.70	±	7.63+†	140.59	±	6.11+
LEnt	106.42	±	7.61	138.69	±	9.21*	119.72	±	4.12+	98.93	±	4.83+	94.69	±	7.36+	101.99	±	3.90+
PAG	23.63	±	3.38	25.98	±	0.70	25.71	±	0.91	20.25	±	1.37	19.36	±	1.84	22.72	±	0.89
DR	17.18	±	3.01	24.33	±	0.83*	20.15	±	1.07	13.67	±	1.09+†	12.75	±	1.10+†	14.65	±	1.01+†
Sup col	25.51	±	3.68	31.45	±	1.39	29.79	±	1.20	22.80	±	1.06+	19.40	±	1.19+†	24.87	±	0.77
BIC	41.15	±	3.27	50.29	±	1.09*	51.20	±	3.42*	40.16	±	0.66+†	35.13	±	1.54+†	44.69	±	2.71#
Subic	74.09	±	9.09	100.29	±	7.93*	72.92	±	4.58+	64.98	±	3.29+	59.62	±	3.62+	67.26	±	2.66+
P Sub	167.82	±	14.48	225.54	±	16.93*	118.51	±	10.85*+	128.25	±	9.31+	119.04	±	6.65*+	137.88	±	9.70+

Data represent mean ± s.e. mean of three sections per animal ($n = 6$). Optical density readings have been converted to nCi/g of tissue. One-way ANOVA with Student Newman-Keuls *post-hoc* test was performed. . $P < 0.05$ * compared with vehicle; + compared with Org 34167, † compared with imipramine; ‡ compared with mirtazapine; # compared with LiCl. Abb: RS, posterior retrosplenial cortex, V1 ctx, primary visual cortex, V2 ctx, secondary visual cortex, TeA ctx, temporal association cortex, Ect ctx, ectorhinal cortex, LEnt, lateral entorhinal cortex, PAG, posterior periaqueductal grey, DR, dorsal raphé, Sup Col, superior colliculus, BIC, nucleus of the brachium of the inferior colliculus, Subic, subiculum, P Sub, post-subiculum (Paxinos *et al.*, 1986).

Figure 4.7 Representative autoradiograms of acute drug administration on Egr-1 **mRNA expression (-6.8 to -7.5 mm relative to bregma)**

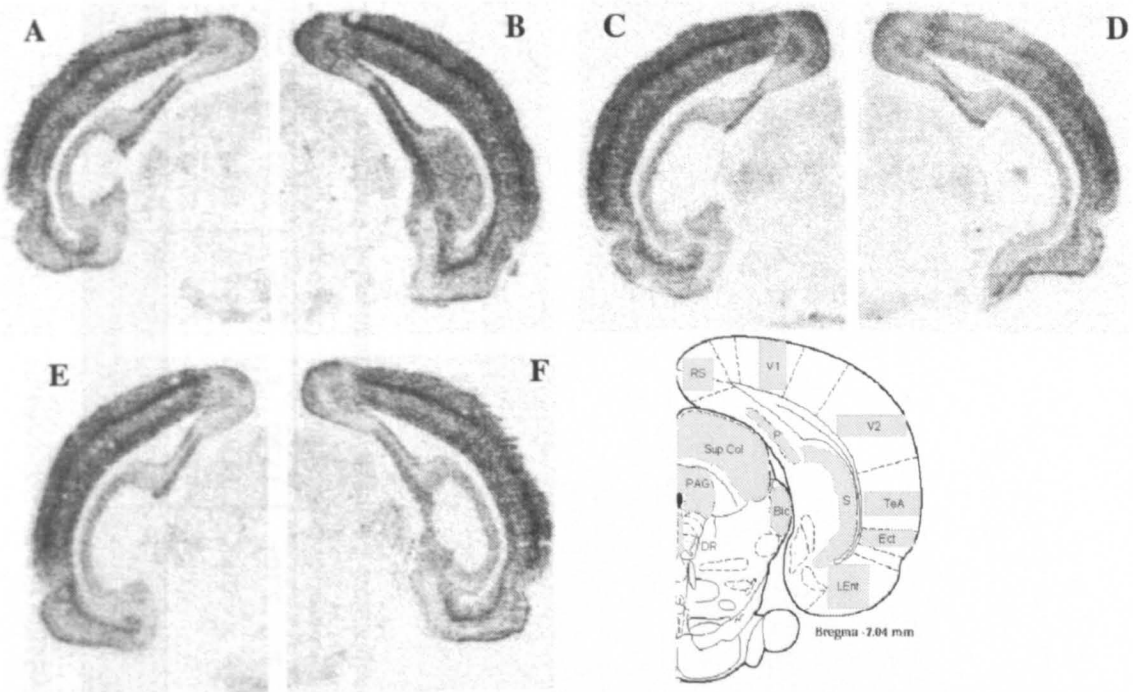

Representative autoradiographs of *in situ* hybridisation utilising a ^{33}P-labelled oligonucleotide probe targeted against the Egr-1 transcript in coronal sections of rat brain following 45 min acute administration of vehicle (A), Org 34167 (0.5 mg/kg, B), imipramine (15 mg/kg, C), mirtazapine (2 mg/kg, D), LiCl (75mg/kg, E) or fluoxetine (5mg/kg, F). Also shown is a schematic representation of the brain regions analysed. Abb: RS, posterior retrosplenial cortex, V1, primary visual cortex, V2, secondary visual cortex, TeA, temporal association cortex, Ect, ectorhinal cortex, LEnt, lateral entorhinal cortex, PAG, posterior periaqueductal grey, DR, dorsal raphé, Sup Col, superior colliculus, BIC, nucleus of the brachium of the inferior colliculus, P, post-subiculum, S, subiculum (Paxinos *et al.*, 1986).

Table 4.7 Effect of acute antidepressant administration on Egr-1 mRNA expression (-9.3 to -10 mm relative to bregma)

Region	Vehicle			Org34167			Imipramine			Mirtazapine			LiCl			Fluoxetine		
	Mean	±	s.e.mean	Mean	±	s.e.mean	Mean	±	s.e.mean	Mean	±	s.e.mean	Mean	±	s.e.mean	Mean	±	s.e.mean
Inf col	80.72	±	3.51	100.93	±	5.39	84.72	±	6.65	74.51	±	6.08+	68.76	±	5.32+	80.62	±	5.25
LC	12.01	±	1.13	20.76	±	3.16	13.53	±	2.08	17.43	±	3.00	15.33	±	1.56	14.62	±	1.91
Pd	26.32	±	2.27	37.25	±	2.14*	20.62	±	2.50+	25.42	±	5.10+	17.90	±	1.55+	20.65	±	2.53+

Data represent mean ± s.e. mean of three sections per animal ($n = 5 - 6$). Optical density readings have been converted to nCi/g of tissue. One-way ANOVA with Dunnett's *post-hoc* test was performed. $P < 0.05$ * compared with vehicle; + compared with Org 34167, † compared with imipramine; ‡ compared with mirtazapine; # compared with LiCl. Abb: Inf Col, inferior colliculus, LC, locus coeruleus, Pd, posterodorsal tegmental nucleus (Paxinos *et al.*, 1986).

Figure 4.8 Representative autoradiograms of acute drug administration on Egr-1 **mRNA expression (-9.3 to -10 mm relative to bregma)**

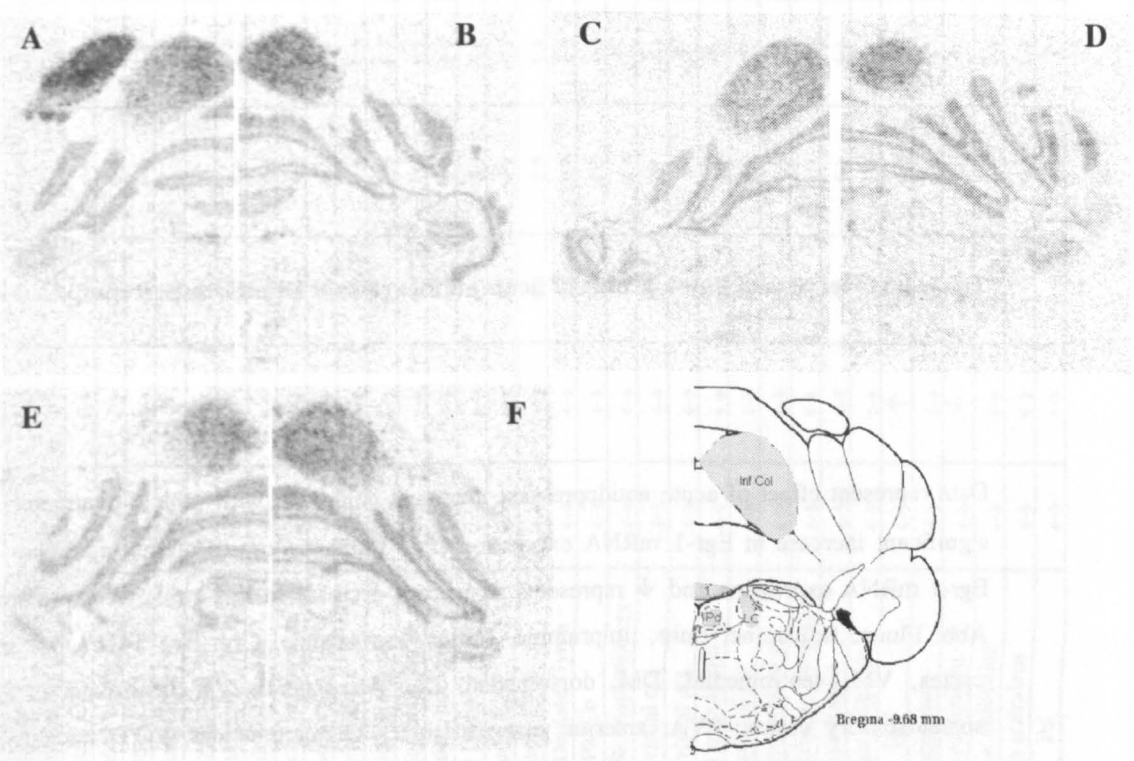

Representative autoradiographs of *in situ* hybridisation utilising a ^{33}P-labelled oligonucleotide probe targeted against the Egr-1 transcript in coronal sections of rat brain following 45 min acute administration of vehicle (A), Org 34167 (0.5 mg/kg, B), imipramine (15 mg/kg, C), mirtazapine (2 mg/kg, D), LiCl (75mg/kg, E) or fluoxetine (5mg/kg, F). Also shown is a schematic representation of the brain regions analysed. Abb: Inf Col, inferior colliculus, LC, locus coeruleus, Pd, posterodorsal tegmental nucleus (Paxinos *et al.*, 1986).

Table 4.8 Overview of Egr-1 profile of acute antidepressant administration compared with vehicle

Data represent effect of acute antidepressant treatment compared with vehicle treatment. ↑ represents significant increase in Egr-1 mRNA expression ($P < 0.05$), ↔ represents no significant difference in Egr-1 mRNA expression and ↓ represents significant decrease in Egr-1 mRNA expression ($P < 0.05$). Abb: Fluox, fluoxetine, Imip, imipramine, Mirtaz, mirtazapine, Org, Org 34167, 2°, secondary, ctx, cortex, VM, ventromedial, DM, dorsomedial, DL, dorsolateral, VL, ventrolateral, S1BF, primary somatosensory cortex, PVA, anterior paraventricular thalamic nucleus, LOT, nucleus of the lateral olfactory tract, BSTMPL, nucleus of the stria terminalis medial division posterolateral part, S1Tr, primary somatosensory cortex trunk region, 1°, primary, PMCo, posteromedial cortical amygdaloid nucleus, BIC, nucleus of the brachium of the inferior colliculus, Pd, posterodorsal tegmental nucleus (Paxinos *et al.*, 1986).

Drug	Fluox	Imip	LiCl	Mirtaz	Org
Dose (mg/kg)	5	15	75	2	0.5
2° motor ctx	↔	↔	↔	↔	↑
Prelimbic ctx	↔	↔	↔	↔	↔
VM orbital ctx	↔	↔	↔	↔	↔
Anterior Olfactory nucleus	↔	↔	↔	↔	↑
Septum	↔	↔	↔	↔	↔
Anterior Piriform Ctx	↔	↔	↔	↔	↔
Anterior Cingulate Ctx	↔	↔	↔	↔	↑
Anterior Insular ctx	↔	↔	↔	↔	↑
Rostral DM striatum	↔	↔	↔	↔	↑
Rostral DL striatum	↔	↔	↔	↔	↔
Rostral VL striatum	↔	↔	↔	↔	↑
Rostral VM striatum	↔	↔	↔	↔	↑
Nucleus accumbens core	↔	↔	↔	↔	↔
Nucleus accumbens shell	↔	↔	↔	↔	↔
Cingulate Ctx	↔	↔	↔	↔	↑
Posterior 2° motor ctx	↔	↔	↔	↔	↑
S1BF	↔	↔	↔	↔	↔
Anterior 2° somatosensory	↔	↔	↔	↔	↑
Insular ctx	↔	↔	↔	↔	↑
Piriform ctx	↔	↔	↔	↔	↔
PVA	↔	↔	↔	↔	↔
Caudal DM striatum	↔	↔	↔	↔	↑
Caudal DL striatum	↔	↔	↔	↔	↔
Caudal Ventral striatum	↔	↔	↔	↔	↑
LOT	↔	↔	↔	↔	↔
Supra-optic nucleus	nd	nd	nd	nd	nd
BSTMPL	↔	↔	↔	↔	↔
Suprachiasmatic nucleus	nd	nd	nd	nd	nd
Anterior Retrosplenial ctx	↔	↔	↔	↔	↑
S1Tr	↔	↔	↔	↔	↑
Posterior 2° somatosensory	↔	↑	↔	↔	↑
Posterior Insular ctx	↔	↑	↔	↔	↑
Piriform Ctx	↔	↔	↔	↔	↔

Drug	Fluox	Imip	LiCl	Mirtaz	Org
Dose (mg/kg)	5	15	75	2	0.5
Rostral CA1	↔	↔	↔	↔	↑
Rostral CA2	↔	↔	↔	↔	↔
Rostral CA3	↔	↔	↔	↔	↔
Dentate Gyrus	↑	↑	↔	↔	↔
Central Amygdaloid nucleus	↑	↑	↑	↑	↑
Thalamus	↑	↑	↔	↔	↔
Retrosplenial cortex	↔	↔	↔	↔	↑
2° visual ctx, lateral area	↔	↔	↔	↔	↔
1° auditory ctx	↔	↔	↔	↔	↔
Perirhinal ctx	↔	↔	↔	↔	↔
Periaqueductal grey	↔	↔	↔	↔	↔
Ventral tegmental area	↔	↔	↔	↔	↔
Geniculate nucleus	↔	↔	↔	↔	↔
Caudal Dorsal CA1	↔	↔	↔	↔	↔
Caudal CA2	↔	↔	↔	↔	↔
Caudal CA3	↔	↔	↔	↔	↔
Caudal Dentate Gyrus	↔	↔	↔	↔	↔
PMCo	↔	↔	↓	↔	↔
Posterior Retrosplenial ctx	↔	↔	↔	↔	↑
1° visual ctx	↔	↔	↓	↓	↔
2° visual ctx	↔	↔	↓	↓	↑
Temporal association ctx	↔	↔	↔	↔	↑
Ectorhinal ctx	↔	↔	↔	↔	↑
Lateral entorhinal ctx	↔	↔	↔	↔	↑
Posterior Periaqueductal grey	↔	↔	↔	↔	↔
Dorsal Raphé	↔	↔	↔	↔	↔
Superior colliculus	↔	↔	↔	↔	↔
BIC	↔	↑	↔	↔	↑
Subiculum	↔	↔	↔	↔	↑
Post subiculum	↔	↓	↔	↓	↑
Inferior colliculus	↔	↔	↔	↔	↔
Locus coeruleus	↔	↔	↔	↔	↔
Pd	↔	↔	↔	↔	↑

4.4 Discussion

The aim of the present study was to examine the effect of a single i.p. injection of several antidepressants and a mood stabiliser on Egr-1 mRNA expression. Similar to previous studies a high level of Egr-1 mRNA was observed in the cortex, hippocampus and striatum (Beckmann *et al.*, 1997; Cochran *et al.*, 2002; Thiriet *et al.*, 2001), with a decrease along the rostrocaudal gradient. Each drug provoked differential Egr-1 mRNA expression throughout the brain regions analysed. In contrast to the corresponding *c-fos* study, drug-administration produced fewer significant alterations in Egr-1 compared with vehicle; with the exception of Org 34167, which induced the immediate early gene in the majority of cortical areas analysed. All drug treatments induced Egr-1 in the central amygdala compared with vehicle, a finding which has been shown following acute administration of LiCl (Lamprecht *et al.*, 1995). A less extensive literature exists concerning drug modulation of Egr-1 mRNA than is available for *c-fos*; however, these studies demonstrate that Org 34167 displays characteristics akin to those of antidepressant and psychostimulant compounds.

The general low induction of Egr-1 mRNA in the present study has also been reported in previous studies examining more than one immediate early gene (Cochran *et al.*, 2002). The likely explanation for this is the different intracellular pathways by which, *c-fos* and Egr-1 are induced. As stated before, Egr-1 tends to be used as a marker following sensory stimuli, whereas *c-fos* is used more extensively in both sensory and drug administration paradigms.

The only site of common action of all the drugs in the current study was in the central amygdala, where all induced Egr-1 expression compared with vehicle (Table 4.4).

Previous studies have demonstrated that LiCl (Lamprecht *et al.*, 1995), acute electroconvulsive shocks and tranylcypromine, but not 15 mg/kg imipramine (Morinobu *et al.*, 1997), induce Egr-1 expression in this region. Therefore, similar to *c-fos,* it appears that the central amygdala may be a region of common antidepressant action, as all compounds in the present study were observed to induce Egr-1 expression. However, methamphetamine (40 mg/kg; Thiriet *et al.*, 2001), diazepam (2.5 & 5 mg/kg; Malkani *et al.*, 2000) and kainic acid induced seizures (Gass *et al.*, 1993b) are other compounds, which induce Egr-1 expression in the central amygdala. The induction evoked by LiCl-administration was significantly greater than all other treatments, as was observed in the corresponding *c-fos* study. The reason for this is unclear, it is not simply due to stress, as restraint stress does not affect *c-fos* or Egr-1 expression in the central amygdala (Thiriet *et al.*, 2001). Spencer *et al.*, (2001) demonstrated that LiCl induced *c-fos* as well as another transcription factor, inducible cAMP early repressor (ICER) mRNA, in the central amygdala, which is suggestive of a cAMP-dependent pathway. However, LiCl injection has been shown to phosphorylate MAP kinase in murine insular cortex and central amygdala 30 min after injection, which would lead to activation of the SRE in the promoter region of *c-fos* and Egr-1 genes. This may explain the high induction of the IEGs by LiCl in the central amygdala, as other antidepressants would be expected to only activate the cAMP-dependent elements in the immediate early gene promoters. Despite a trend of an increase in Egr-1 expression in the insular cortex following LiCl-treatment this did not reach significance.

Similar to the *c-fos* study, Org 34167-treatment induced a robust expression of Egr-1 in the majority of cortical regions examined (Figures 4.2 - 4.8 and Tables 4.2 - 4.7). The two-fold increase in *c-fos* observed in the retrosplenial cortex was apparent for Egr-1 throughout this region, compared with all other treatment groups (Tables 4.4 – 4.6).

MK-801 (0.3 & 3 mg/kg) has been demonstrated to induce the expression of both IEGs in this cortical region (Gass *et al.*, 1993a). The cingulate cortex and dorsomedial thalamic nuclei are further areas that MK-801 induces Egr-1 protein (Gass *et al.*, 1993a; Gass *et al.*, 1993b), which were activated by Org 34167 in the present study. Therefore, the Egr-1 profile of this novel antidepressant bears resemblance to that of psychostimulants, as was observed for the *c-fos* profile.

The only treatment group, which induced Egr-1 mRNA expression in striatal regions, was the novel antidepressant Org 34167 (Tables 4.2 & 4.3). In the rostral and caudal dorsomedial and ventral striatum, with the exception of the nucleus accumbens core and shell regions, Org 34167 induced Egr-1 mRNA compared with all other treatments. This is in contrast to the *c-fos* observations, where Org 34167 only induced *c-fos* in the caudal striatum (Table 3.4). Previous studies that have reported an induction of Egr-1 mRNA in the striatum include apomorphine (2 mg/kg) in reserpine (5 mg/kg) pretreated rats (Bhat *et al.*, 1992a; Bhat *et al.*, 1992b), as well as amphetamine (0.5 – 15 mg/kg) and cocaine (5, 10 & 25 mg/kg; Moratalla *et al.*, 1992) and haloperidol (1 mg/kg; Cochran *et al.*, 2002). This is similar to agents, which induce *c-fos* expression in the striatum; mainly dopaminergic compounds. However, *in vitro* testing demonstrated that Org 34167 possessed low affinity for monoamine receptors and transporters, including dopamine (Ruigt, Personal communication). Therefore, it is possible that Org 34167, by blocking I_h channels, alters the dopaminergic system in the striatum, which in turn gives rise to the induction of *c-fos* and Egr-1 mRNA. However, the appropriate experiments to verify this hypothesis, such as microdialysis, have not been performed to date.

The magnitude and widespread, induction of Egr-1 mRNA expression following acute Org 34167 administration, may be explained by the presence of HCN1 and HCN2 mRNA throughout the cortex (Monteggia *et al.*, 2000; Moosmang *et al.*, 1999). In fact, all the areas in which Egr-1 mRNA was induced by Org 34167 administration show high levels of HCN2 and HCN1 mRNA, with the only exception being the striatum, where levels of HCN1 mRNA are relatively low (Monteggia *et al.*, 2000; Moosmang *et al.*, 1999). In the ventral tegmental area and nucleus of the stria terminalis, HCN1 mRNA is high and HCN2 expression is low and in these regions no alteration in Egr-1 mRNA was observed; suggestive that Org 34167 effects HCN1 more than HCN2. This coupled with the knowledge that monoamines alter the gating properties of the HCN channel, and also regulate the basal expression of Egr-1 in the cortex, may indicate a possible mechanism for the cortical induction. Another possibility is that Org 34167, by interacting with HCN channels, alters intracellular Ca^{2+} levels, as the channel sets the resting membrane potential (Ludwig *et al.*, 1998; Pape, 1996; Santoro *et al.*, 1998).

In conclusion, the findings of this study corroborate those of the parallel *c-fos* study, supporting a role of Org 34167 as both an antidepressant and psychostimulant. Furthermore, the only common site of action of all drugs examined was the central amygdala, where an induction of Egr-1 mRNA was observed. This provides further evidence supporting the use of immediate early gene mapping for the classification of novel compounds and identification of brain regions affected by acute drug administration.

Chapter 5 Chronic Org 34167 and antidepressant alteration of HCN mRNA

5.1 Introduction

Chronic drug treatment is often associated with alteration in the target receptor density and mRNA expression. This has been shown following chronic treatment with a number of different antidepressant drugs. Increases in glucocorticoid- and mineralocorticoid- receptor mRNA in the hippocampus after amitriptyline administration (10 mg/kg/21d; Johansson *et al.*, 1998). Imipramine (2x 10 mg/kg/14d), citalopram (2x 10 mg/kg/14d) and lithium (6 mEq/kg/14d) treatments have been demonstrated to increase D_2-receptor mRNA levels in the caudate putamen and nucleus accumbens (Dziedzicka-Wasylewska *et al.*, 1996; Dziedzicka-Wasylewska, 1997). Recently, it has been demonstrated that chronic imipramine (10 mg/kg/14d) or electroconvulsive shock (150 mA, 0.5 s, 14d) results in an upregulation of α_{1A}-adrenoceptor mRNA expression (Nalepa *et al.*, 2002). Furthermore, paroxetine (a SSRI) and fluoxetine (both 5 mg/kg) produced a significant downregulation of 5-HT_{1B} receptor mRNA in the dorsal raphé (Anthony *et al.*, 2000). Therefore, these examples provide evidence that it is possible to discern alterations at the level of mRNA, and not only protein, following chronic drug treatment.

Given the knowledge that *in vitro,* Org 34167 only demonstrated affinity and efficacy for HCN channels, it may be that chronic *in vivo* administration leads to alteration in their expression. Furthermore, if I_h modulation is a common mechanism of antidepressant action it is possible that chronic administration of currently prescribed antidepressants affects these channels. Acute administration of fluoxetine does not alter HCN1 or HCN2 channel properties in human cell lines, as determined by

electrophysiological recordings (Mason, Personal communication). However, with the knowledge that direct binding of cAMP, and PKA, modulate the properties of HCN and I_h channels (See Section 1.2.3) it is possible to hypothesise that chronic fluoxetine, which increases both cAMP and PKA (Edgar *et al.,* 1999) may alter HCN channel function *in vivo*. Moreover, it has been demonstrated that 5-HT-receptor activation alters the properties of HCN channels; 5-HT-$_4$ and 5-HT-$_7$ receptor agonists shift the $V_{1/2}$ to more positive potentials, whereas 5-HT_{1A} receptor activation shifts the gating to more hyperpolarised potentials (Bickmeyer *et al.*, 2002).

The rationale for the present study was to determine whether chronic treatment of rats with fluoxetine, mirtazapine, lithium, or Org 34167 altered HCN channel expression. With no available antibody to study HCN isoform expression, *in situ* hybridisation utilising probes complementary to the different isoforms were used to determine whether there is a change at the mRNA level. This was examined in the corresponding brain regions assessed for neuronal activation in the previous *c-fos* and Egr-1 studies (Chapters 3 and 4 respectively). Additionally, the effect of chronic antidepressant treatment on 5-HT_{1A} receptor mRNA expression was assessed. This was included to determine whether chronic Org 34167 administration had similar, or differential effect on 5-HT_{1A} mRNA compared with other antidepressants, as no data concerning its effect on 5-HT were known. 5-HT_{1A} receptor function is known to be modulated by antidepressant administration with chronic fluoxetine, desensitising 5-HT_{1A} receptor function in the dorsal raphé (Hensler *et al.,* 2003). In contrast Hervas *et al.,* (2001) demonstrated that chronic fluoxetine (3 mg/kg/2wk) administration had no significant affect on 5-HT_{1A} receptor mRNA or protein expression in the dorsal raphé or hippocampus. Similar findings have been reported following chronic imipramine treatment (5 mg/kg/8wk) in the dorsal raphé (Burnet *et al.*, 1994). Therefore, if Org

34167 is acting *via* a novel mechanism it may differentially regulate 5-HT_{1A} mRNA expression to that of current antidepressants.

5.2 Materials and Methods

5.2.1 Animals and experimental procedure

Study A – Vehicle, fluoxetine and mirtazapine

Male Sprague-Dawley rats (Harlan Olac, U.K.) weighing 230 – 250 g were housed in groups of 6 on a 12 h light/dark cycle (lights on at 06:00 h) at 22 ± 2 °C and given free access to tap water and food. Rats were allowed to habituate to the conditions for 7 days prior to the start of the experiment.

Rats received administration of fluoxetine (5 mg/kg) or mirtazapine (2 mg/kg) dissolved in a 5 % mulgofen, 0.9 % NaCl solution, or an equal volume of vehicle (5 % mulgofen dissolved in 0.9 % NaCl) at a dose of 1 ml/kg i.p. once daily for 21 consecutive days (between 09:00 – 10:00 h). One day after the last injection the rats were sacrificed in a CO_2-chamber with a flow-rate of 6 l/min then decapitated using a guillotine. The treatment was performed by the Pharmacology Support Unit (PSU) at Organon Laboratories.

Study B – Vehicle and Org 34167 treatment

Male Sprague-Dawley rats (Harlan Olac, U.K.) weighing 210 – 240 g were housed in groups of 6 on a 12 h light/dark cycle (lights on at 06:00 h) at 22 ± 2 °C and given free access to tap water and food. Rats were allowed to habituate to the conditions for 7 days prior to the start of the experiment.

Rats received an i.p. dose of Org 34167 (0.5 mg/kg) or an equal 1 ml/kg injection of vehicle (5 % mulgofen dissolved in 0.9 % NaCl) once daily, between 09:00 – 10:00 h,

for 28 consecutive days. One day after the last injection the rats were sacrificed in a CO_2-chamber with a flow-rate of 6 l/min then decapitated using a guillotine. The experiment was performed by the Pharmacology Support Unit (PSU) at Organon Laboratories.

Study C – Vehicle and lithium chloride treatment

Male Sprague-Dawley rats (Harlan Olac, U.K.) weighing 210 – 240 g were housed in groups of 6 on a 12 h light/dark cycle (lights on at 06:00 h) at 22 ± 2 °C and given free access to tap water and food. Rats were allowed to habituate to the conditions for 7 days prior to the start of the experiment rats received either vehicle (0.9 % NaCl solution) or LiCl (75 mg/kg/day) *via* Alzet osmotic minipumps planted subcutaneously, under halothane anaesthesia, for 28 days at a rate of 1 µl/h. At the end of the infusion the rats were sacrificed by halothane overdose and then cervical and the brains immediately removed and frozen in isopentane cooled on dry-ice to -32 °C and stored in a -80 °C freezer until required. This study was performed by Dr Caroline Stewart at the Department of Psychiatry, Dundee University.

5.2.2 Cryostat sectioning

The brains were removed from -80 °C freezer and allowed to thaw to -18 ± 2 °C inside a Bright OTF cryostat for 30 min before mounting on to a Bright orientating specimen holder with Cryo-M-Bed (Bright Ltd., U.K.). Once solidly mounted, the chuck was attached to the microtome, with the blade aligned at an angle of 15 ° and set to collect sections of 20 µm. Sections were thaw-mounted on to Superfrost Plus electro-statically charged nuclease-free slides (VWR, formerly BDH, UK) and 4 series of 12 superfrost slides (BDH) with 3 sections on each slide were collected.

Table 5.1 Approximate bregma co-ordinates sectioned following chronic treatment and brain regions analysed.

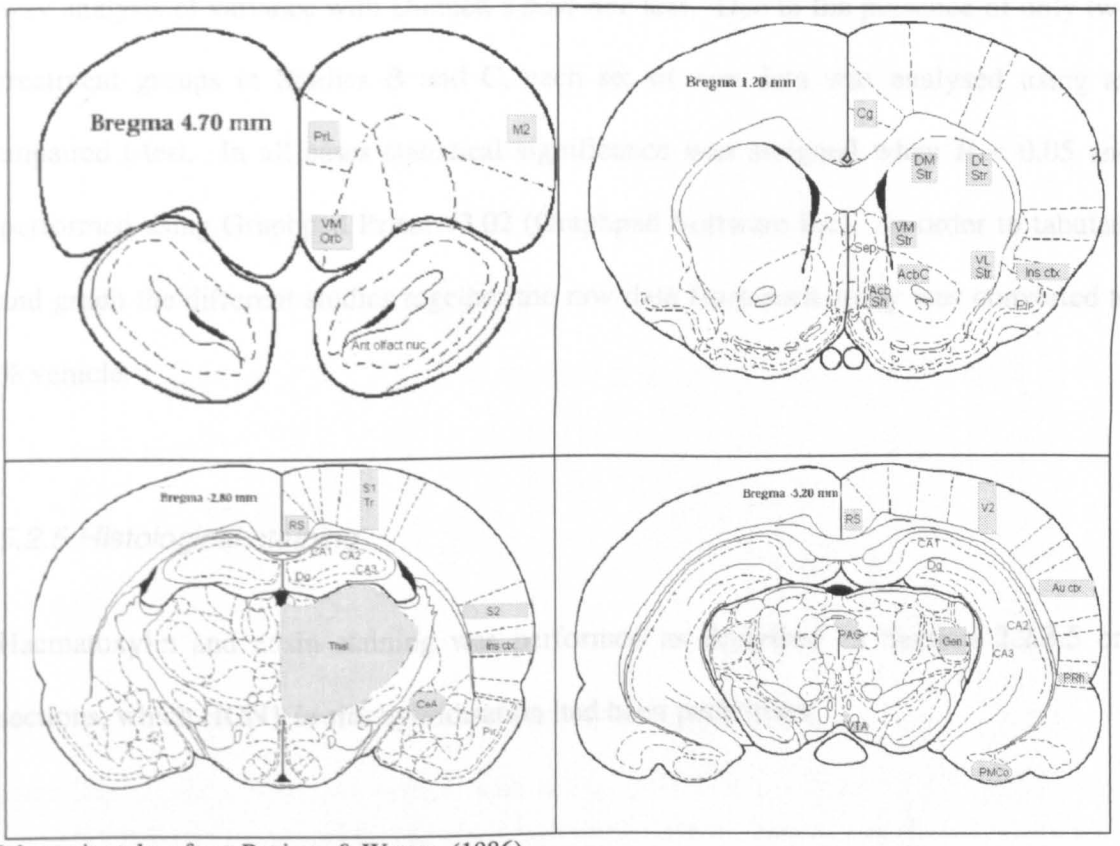

Schematics taken from Paxinos & Watson (1986).

The cryostat sectioning was performed by Fiona Adams and Joyce van de Leemput (both of Organon Laboratories Ltd). For Study C only 4.7 to 4 mm and -2.5 to -3.2 mm relative to bregma series of slides were available for *in situ* hybridisation.

5.2.3 In situ hydridisation study

In situ hybridisation was performed as described in Section 2.2.1.3 using probes complementary to the HCN1 – 3 and 5-HT_{1A} transcripts (see Appendix B for probe details). The probes were validated as described in Section 2.2.1.4 (see Appendix C for autoradiograms) and analysis of the resultant autoradiograms performed as described in Section 2.2.1.5.

5.2.4 Statistical analyses

The raw data from each brain region recorded in Study A were analysed using a One-way analysis of variance with Dunnett's *post-hoc* test. Due to the presence of only two treatment groups in Studies B and C, each set of raw data was analysed using an unpaired t-test. In all cases statistical significance was assigned when $P < 0.05$ and performed using Graphpad Prism v3.02 (Graphpad Software Inc). In order to tabulate and graph the different studies together the raw data from each study was converted to % vehicle.

5.2.5 Histological staining

Haematoxylin and eosin staining was performed as described in Section 2.2.3.5 on sections, which HCN1 *in situ* hybridisation had been performed.

5.2.6 Drugs and chemicals

Org 34167, fluoxetine and mirtazapine were synthesised by Organon Laboratories Ltd. See Section 2.2.1.9 for other drugs and chemicals used.

5.3 Results

5.3.1 In situ hybridisation following chronic drug treatment

In situ hybridisation utilising probes complementary to the HCN1 – 3 and 5-HT_{1A} transcripts following chronic drug treatment revealed differential expression levels for each of the different mRNAs analysed. Vehicle-treated rats were observed to display low expression levels of HCN3 (Monteggia *et al.*, 2000; Moosmang *et al.*, 1999) and 5-HT_{1A} mRNA (Hervas *et al.*, 2001), as previously described, while HCN1 and 2 mRNA levels were high.

4.7 to 4 mm relative to bregma

Chronic Org 34167 administration (0.5 mg/kg/28d) upregulated 5-HT_{1A} mRNA in the secondary motor cortex, compared with vehicle ($P < 0.05$; Figure 5.1). No further significant alterations of 5-HT_{1A} mRNA were observed at these bregma co-ordinates. Fluoxetine and mirtazapine treatments (5 and 2 mg/kg/21d, respectively) significantly downregulated HCN1 mRNA in all areas of the frontal cortex and the anterior olfactory nucleus ($P < 0.001$; Figure 5.1). Org 34167 and LiCl treatment did not significantly affect HCN 1 mRNA at any region analysed. Similarly no significant effect of LiCl or Org 34167 administration on HCN2 mRNA was observed in any region. However, fluoxetine and mirtazapine downregulated mRNA expression in all cortical areas ($P < 0.05$; Figure 5.1). Chronic fluoxetine and mirtazapine administration upregulated HCN 3 mRNA expression in the anterior olfactory nucleus ($P < 0.05$) but no further significant differences were observed (Figure 5.1).

Figure 5.1 Effect of chronic antidepressant drug treatment on 5-HT$_{1A}$ and HCN1-3 mRNA expression (4.7 to 4 mm relative to bregma)

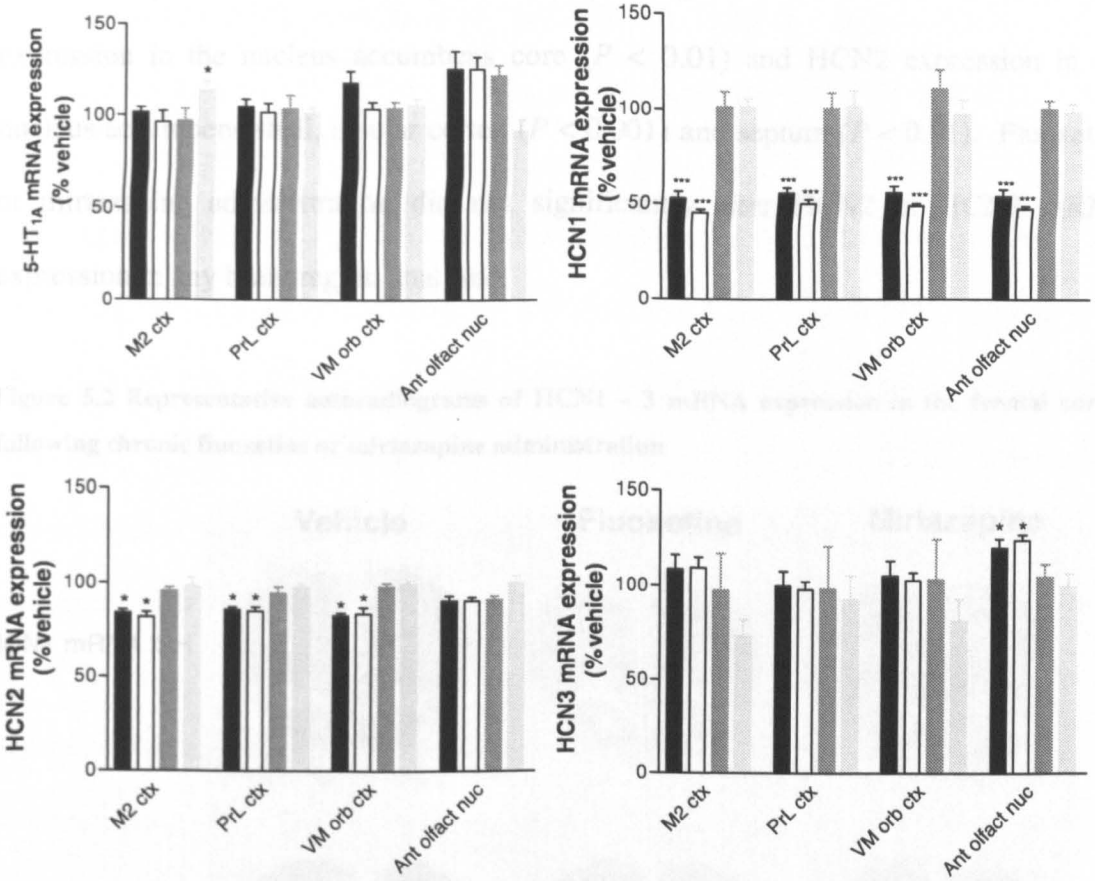

Data represent mean ± s.e.mean of three sections per animal (n = 6) were optical density readings have been converted to nCi/g of tissue. These values have then been converted to represent % vehicle mRNA expression to enable the different studies to be put into one graph. Treatment groups represented; fluoxetine (5 mg/kg, 21-day ■), mirtazapine (2 mg/kg, 21-day □), LiCl (75 mg/kg, 28-day ▩), Org 34167 (0.5 mg/kg, 28-day ▨). One-way ANOVA with Dunnett's *post-hoc* test was performed for vehicle, fluoxetine and mirtazapine study. t-test was performed for vehicle and LiCl study, and for vehicle and Org 34167 study. * $P < 0.05$, *** $P < 0.001$. All statistical analyses were performed using the raw data and against the appropriate vehicle control. Abb: M2 ctx, secondary motor cortex, PrL ctx, prelimbic cortex, VM Orb, ventromedial orbital cortex, Ant. Olfact nuc, anterior olfactory nucleus (Paxinos and Watson, 1982).

2.2 to 1.5 mm relative to bregma

In this more caudal region of the rat brain, chronic mirtazapine administration significantly upregulated 5-HT$_{1A}$ in the dorsolateral and ventrolateral striatum ($P < 0.001$) and in the nucleus accumbens shell region ($P < 0.05$; Figure 5.3). There were no significant alterations at any other brain region analysed or following fluoxetine

or Org 34167 administration on 5-HT_{1A} or HCN1 mRNA expression (Figure 5.3). Chronic Org 34167-treatment significantly downregulated HCN2 and HCN3 mRNA expression in the nucleus accumbens core ($P < 0.01$) and HCN2 expression in the nucleus accumbens shell, insular cortex ($P < 0.001$) and septum ($P < 0.01$). Fluoxetine or mirtazapine administration did not significantly alter HCN2 or HCN3 mRNA expression in any brain region analysed.

Figure 5.2 Representative autoradiograms of HCN1 – 3 mRNA expression in the frontal cortex following chronic fluoxetine or mirtazapine administration

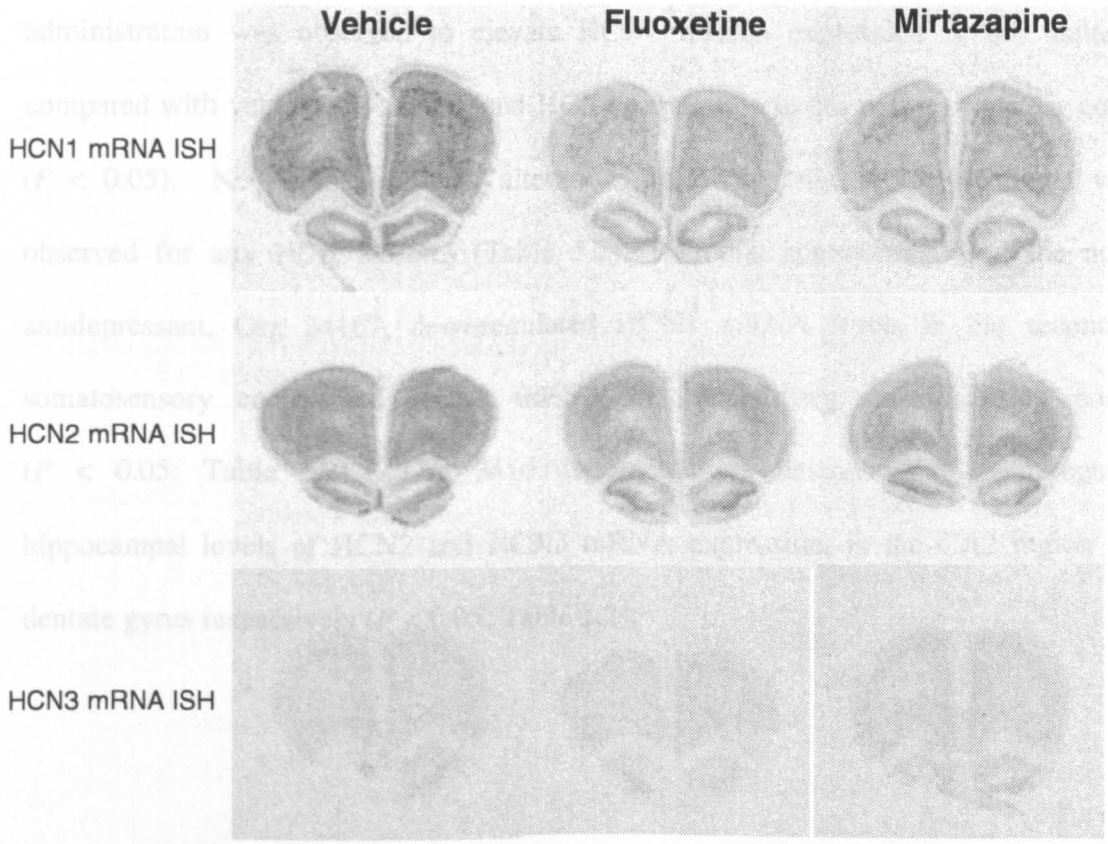

-2.5 to -3.2 mm relative to bregma

In situ hybridisation demonstrated that lithium chloride administration did not significantly affect HCN1 – 3 or 5-HT_{1A} mRNA expression levels (Table 5.2), similar to the results obtained in the frontal cortex (Figures 5.1 & 5.2). Fluoxetine or mirtazapine administration increased 5-HT_{1A} in the primary somatosensory cortex, and in the thalamus the latter case only ($P < 0.05$; Table 5.2). Org 34167 did not alter 5-HT_{1A} mRNA in any brain region analysed and fluoxetine-treatment did not significantly affect any of the HCN isoform mRNAs examined (Table 5.2). Chronic mirtazapine administration was observed to elevate HCN1 mRNA expression in the thalamus compared with vehicle ($P < 0.05$), and HCN2 expression in the posterior insular cortex ($P < 0.05$). No other significant alterations following mirtazapine treatment were observed for any HCN isoform (Table 5.2). Chronic administration of the novel antidepressant, Org 34167, downregulated HCN1 mRNA levels in the secondary somatosensory cortex and HCN2 mRNA in the primary somatosensory cortex ($P < 0.05$; Table 5.2). Org 34167-treatment was demonstrated to upregulate hippocampal levels of HCN2 and HCN3 mRNA expression, in the CA2 region and dentate gyrus respectively ($P < 0.05$; Table 5.2).

Figure 5.3 Effect of chronic treatment on 5-HT_{1A} and HCN1-3 mRNA expression (2.2 to 1.5 mm relative to bregma)

Data represent mean ± s.e.mean of three sections per animal (n = 6) were optical density readings have been converted to nCi/g of tissue. These values have then been converted to represent % vehicle mRNA expression to enable the different studies to be put into one graph. Treatment groups represented; fluoxetine (5 mg/kg, 21-day ■), mirtazapine (2 mg/kg, 21-day □), Org 34167 (0.5 mg/kg, 28-day). One-way ANOVA with Dunnett's *post-hoc* test was performed for vehicle, fluoxetine and mirtazapine study. t-test was performed for the vehicle and Org 34167 study. ** $P < 0.01$, *** $P < 0.001$. All statistical analyses were performed on the raw data and against the appropriate vehicle control. Abb: Cing ctx, cingulate cortex, Ins ctx, Insular cortex, Pir ctx, piriform cortex, DM Str, dorsomedial striatum, VL Str, ventrolateral striatum, VM Str, ventromedial striatum, AcbC, nucleus accumbens core region, AcbSh, nucleus accumbens shell region (Paxinos and Watson, 1982).

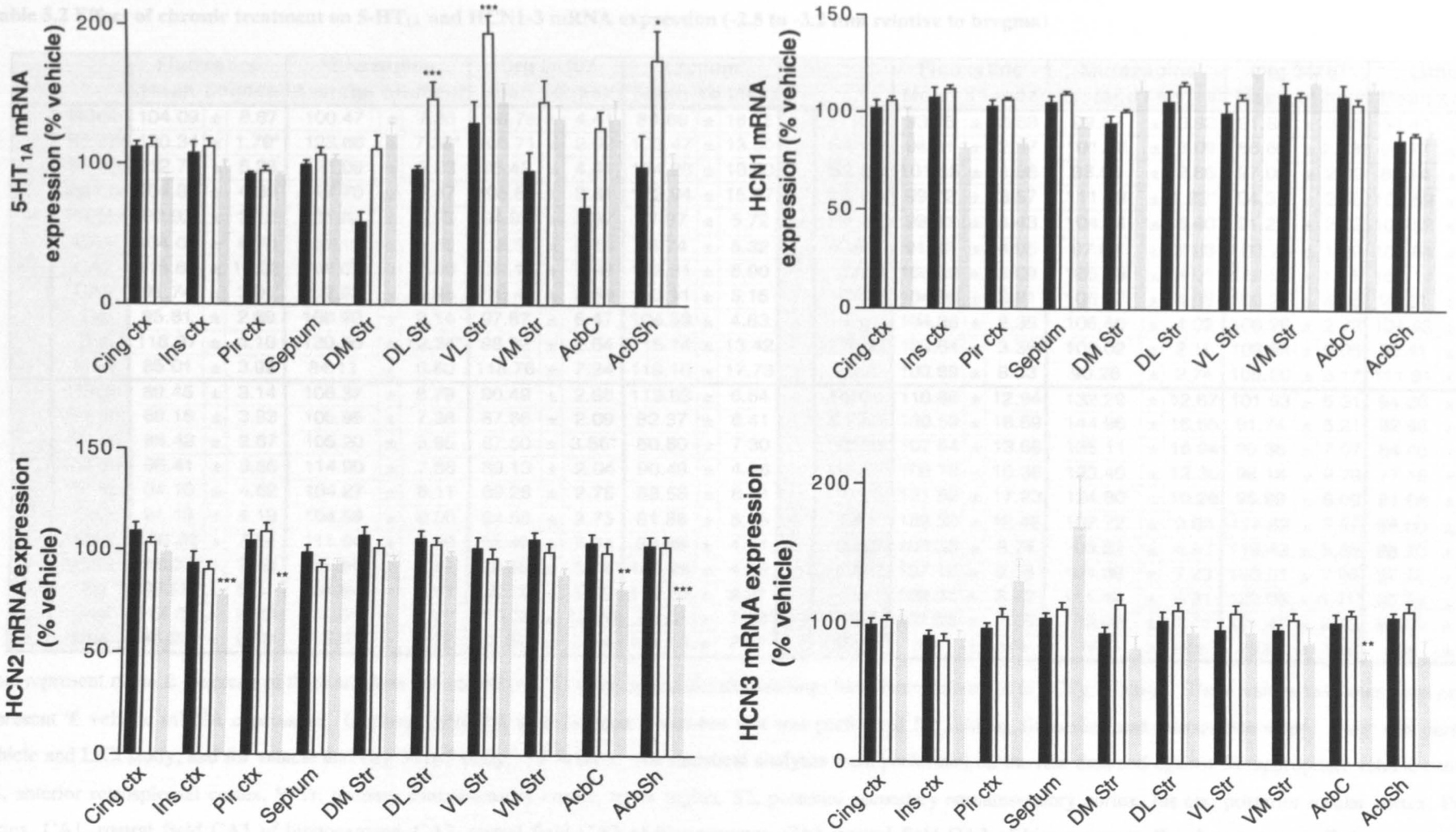
5-HT1A mRNA expression (% vehicle)
HCN1 mRNA expression (% vehicle)
HCN2 mRNA expression (% vehicle)
HCN3 mRNA expression (% vehicle)
Cing ctx
Ins ctx
Pir ctx
Septum
DM Str
DL Str
VL Str
VM Str
AcbC
AcbSh

Table 5.2 Effect of chronic treatment on 5-HT_{1A} and HCN1-3 mRNA expression (-2.5 to -3.2 mm relative to bregma)

		Fluoxetine			Mirtazapine			Org 34167			Lithium		
		Mean	±	s.e.mean	Average	±	s.e.mean	Mean	±	s.e.mean	Mean	±	s.e.mean
5-HT_{1A}	RSGb	104.09	±	8.67	100.47	±	7.35	108.75	±	4.41	89.66	±	18.75
	S1 ctx	120.34	±	1.79*	123.86	±	7.38*	105.71	±	2.02	103.47	±	13.30
	S2 ctx	112.79	±	5.28	121.09	±	6.93	95.43	±	4.41	104.28	±	10.40
	Ins ctx	104.89	±	4.86	117.70	±	6.47	105.81	±	3.81	122.94	±	15.17
	Pir ctx	92.92	±	2.18	101.82	±	3.93	94.98	±	5.87	97.97	±	5.72
	CA1	104.09	±	8.70	107.13	±	3.65	115.34	±	5.18	98.74	±	5.32
	CA2	116.85	±	11.02	109.03	±	7.40	122.14	±	9.08	102.81	±	5.90
	CA3	91.74	±	3.01	102.82	±	4.95	116.48	±	2.56	113.91	±	5.15
	Dg	95.81	±	2.69	106.20	±	2.14	97.87	±	6.47	104.89	±	4.83
	Thal	118.37	±	4.10	130.06	±	12.34*	98.92	±	2.54	115.14	±	13.42
	MeA	85.01	±	3.92	84.11	±	6.60	118.76	±	7.24	119.10	±	17.73
HCN 1	RSGb	89.45	±	3.14	106.37	±	8.79	90.49	±	2.86	113.83	±	6.64
	S1 ctx	89.15	±	3.93	105.95	±	7.38	87.66	±	2.09	82.37	±	8.41
	S2 ctx	88.42	±	2.67	105.20	±	5.95	87.50	±	3.56*	80.80	±	7.30
	Ins ctx	98.41	±	3.55	114.90	±	7.66	89.13	±	2.04	90.49	±	4.36
	Pir ctx	94.10	±	4.62	104.27	±	8.11	89.28	±	2.78	88.58	±	8.54
	CA1	94.13	±	4.19	104.59	±	8.00	94.58	±	2.75	81.88	±	5.48
	CA2	106.23	±	7.74	111.54	±	8.50	95.49	±	7.34	98.68	±	4.51
	CA3	95.02	±	3.10	99.36	±	5.37	89.85	±	5.74	105.25	±	4.32
	Dg	93.26	±	6.51	104.64	±	9.58	102.02	±	5.82	113.26	±	8.21
	Thal	117.06	±	9.20	141.01	±	7.41*	110.39	±	15.66	79.72	±	7.13
	MeA	95.23	±	2.59	115.05	±	9.72	92.57	±	2.94	101.13	±	7.47

		Fluoxetine			Mirtazapine			Org 34167			Lithium		
		Mean	±	s.e.mean	Average	±	s.e.mean	Mean	±	s.e.mean	Mean	±	s.e.mean
HCN 2	RSGb	93.75	±	3.68	99.57	±	3.93	91.84	±	3.31	86.46	±	3.96
	S1 ctx	94.31	±	2.37	101.66	±	3.09	88.65	±	2.43*	94.77	±	3.08
	S2 ctx	101.55	±	4.86	98.99	±	2.86	97.06	±	2.09	89.14	±	3.54
	Ins ctx	99.72	±	3.57	111.98	±	1.92*	94.37	±	2.95	100.69	±	6.36
	Pir ctx	99.61	±	4.43	104.54	±	5.40	91.23	±	2.62	108.52	±	7.10
	CA1	91.32	±	4.95	97.63	±	7.63	100.79	±	1.22	100.84	±	5.62
	CA2	108.02	±	3.69	105.40	±	4.01	112.83	±	1.74*	101.17	±	7.17
	CA3	104.28	±	3.91	106.27	±	4.08	108.27	±	4.05	90.81	±	4.44
	Dg	104.35	±	2.35	106.40	±	4.02	106.26	±	2.72	104.42	±	6.70
	Thal	103.64	±	3.35	105.02	±	2.15	108.88	±	5.05	90.41	±	5.29
	MeA	100.89	±	8.33	90.26	±	2.74	108.20	±	5.17	111.91	±	6.24
HCN 3	RSGb	110.89	±	12.94	132.29	±	12.67	101.53	±	5.31	94.86	±	10.22
	S1 ctx	130.59	±	18.59	144.96	±	16.65	91.74	±	5.21	92.98	±	10.86
	S2 ctx	107.54	±	13.68	135.11	±	16.04	95.36	±	7.07	84.46	±	10.24
	Ins ctx	108.78	±	10.36	123.40	±	13.35	98.18	±	9.79	77.18	±	8.67
	Pir ctx	121.52	±	17.23	124.80	±	10.28	95.99	±	6.00	81.68	±	7.63
	CA1	108.30	±	12.46	107.72	±	9.69	117.82	±	7.27	88.00	±	6.50
	CA2	106.38	±	9.74	109.82	±	4.57	119.43	±	9.88	88.70	±	9.48
	CA3	107.12	±	9.08	101.38	±	7.23	116.01	±	7.90	87.39	±	11.01
	Dg	109.04	±	8.42	111.44	±	6.91	122.03	±	6.41*	90.63	±	9.37
	Thal	107.06	±	7.05	113.02	±	7.71	121.47	±	9.47	84.81	±	5.90
	MeA	n/a	±	n/a	n/a	±	n/a	n/a	±	n/a	n/a	±	n/a

Data represent mean ± s.e.mean of three sections per animal ($n = 6$) were optical density readings have been converted to nCi/g of tissue. These values have then been converted to represent % vehicle mRNA expression. One-way ANOVA with Dunnett's *post-hoc* test was performed for vehicle, fluoxetine and mirtazapine study. t-test was performed for vehicle and LiCl study, and for vehicle and Org 34167 study. * $P < 0.05$. All statistical analyses were performed on the raw data and against the appropriate vehicle control. Abb: RS, anterior retrosplenial cortex, S1Tr, primary somatosensory cortex, trunk region, S2, posterior secondary somatosensory cortex, Ins ctx, posterior insular cortex, Pir, pirform cortex, CA1, rostral field CA1 of hippocampus, CA2, rostral field CA2 of hippocampus, CA3, rostral field CA3 of hippocampus, Dg, dentate gyrus, CeA, central amygdaloid nucleus, Thal, thalamus (Paxinos and Watson, 1982).

-4.8 to -5.6 mm relative to bregma

In the most caudal brain regions analysed neither, chronic fluoxetine or Org 34167, significantly affected HCN1 – 3 mRNA expression (Table 5.3). Chronic mirtazapine administration significantly downregulated HCN2 mRNA levels in the CA2 field of the hippocampus ($P < 0.05$) and increased HCN3 mRNA expression in the ventral tegmental area ($P < 0.05$; Table 5.3). No further significant alterations in HCN1 – 3 or 5-HT_{1A} mRNA levels were observed following mirtazapine treatment. Chronic Org 34167 administration significantly increased 5-HT_{1A} mRNA expression in the retrosplenial cortex by 27 % ($P < 0.01$; Table 5.3), and the only other alteration in 5-HT_{1A} mRNA levels was in an increase in the dentate gyrus following fluoxetine-treatment ($P < 0.05$).

Figure 5.4 Representative pseudocolour representations of HCN 2 *in situ* hybridisation autoradiograms in the caudal hippocampus following chronic mirtazapine treatment

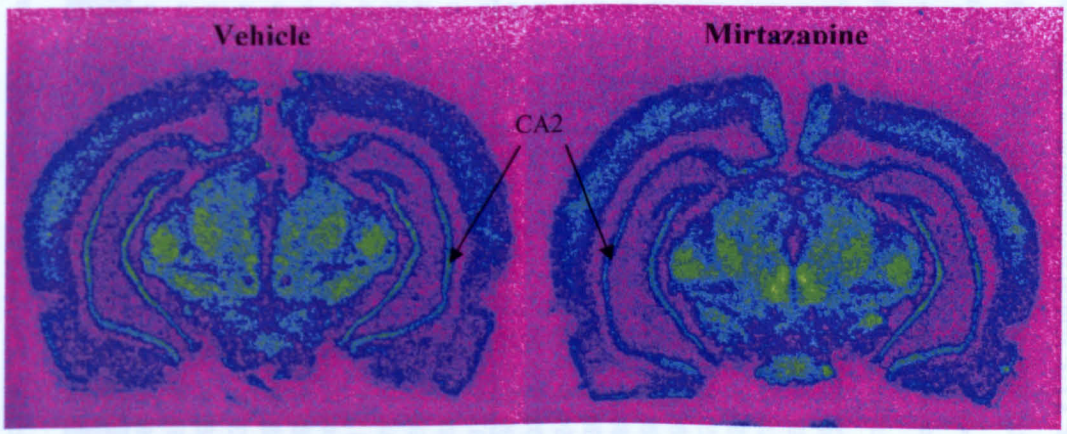

Table 5.3 Effect of chronic treatment on 5-HT_{1A} and HCN1-3 mRNA expression (-4.8 to -5.6 mm relative to bregma)

		Fluoxetine Mean	s.e.mean	Mirtazapine Mean	s.e.mean	Org 34167 Average	s.e.mean
5-HT_{1A}	RS ctx	93.68	± 2.12	97.04	± 4.92	127.04	± 5.58**
	V2 ctx	105.21	± 2.08	103.01	± 3.45	104.11	± 2.71
	Au ctx	91.29	± 3.25	92.02	± 3.11	105.51	± 4.31
	Prh ctx	89.53	± 2.14	96.09	± 1.24	104.81	± 4.13
	PAG	85.49	± 3.57	90.50	± 2.55	94.95	± 3.84
	Gen	94.39	± 3.85	96.48	± 3.63	98.21	± 7.43
	VTA	76.74	± 7.40	84.53	± 13.80	116.15	± 14.53
	PMCo	104.17	± 4.64	102.21	± 4.88	96.65	± 5.17
	CA1	102.78	± 2.80	99.15	± 2.11	101.21	± 4.49
	CA2	114.20	± 12.22	116.73	± 8.33	100.75	± 6.13
	CA3	106.63	± 3.28	100.39	± 2.95	87.03	± 4.22
	Dg	107.37	± 0.76*	105.26	± 1.22	90.88	± 2.50
HCN 1	RS ctx	105.36	± 2.68	91.78	± 3.75	101.42	± 8.11
	V2 ctx	104.03	± 2.04	89.51	± 4.68	102.60	± 9.58
	Au ctx	100.24	± 2.80	89.47	± 4.69	102.48	± 9.50
	Prh ctx	104.80	± 3.27	86.78	± 6.16	100.05	± 9.58
	PAG	102.82	± 9.07	84.75	± 9.19	95.72	± 9.25
	Gen	75.29	± 9.63	65.33	± 12.18	100.39	± 6.29
	VTA	87.99	± 9.41	83.10	± 8.45	104.81	± 10.88
	PMCo	84.02	± 4.83	82.20	± 7.00	100.58	± 11.22
	CA1	99.92	± 5.76	100.78	± 4.46	92.64	± 3.39
	CA2	106.78	± 5.69	105.55	± 7.93	91.57	± 2.97
	CA3	97.96	± 6.39	96.86	± 5.46	97.26	± 2.77
	Dg	101.98	± 4.59	97.92	± 3.51	97.66	± 1.44

		Fluoxetine Mean	s.e.mean	Mirtazapine Mean	s.e.mean	Org 34167 Average	s.e.mean
HCN 2	RS ctx	100.54	± 3.60	99.95	± 1.49	104.43	± 2.88
	V2 ctx	101.50	± 3.43	100.37	± 0.66	103.83	± 4.39
	Au ctx	105.26	± 4.29	100.42	± 1.93	105.60	± 4.50
	Prh ctx	105.20	± 4.10	94.21	± 2.58	104.39	± 4.02
	PAG	97.89	± 3.90	98.79	± 2.82	98.34	± 7.69
	Gen	106.63	± 4.67	108.46	± 1.79	115.47	± 7.74
	VTA	105.98	± 3.62	97.01	± 2.58	99.74	± 3.70
	PMCo	100.50	± 3.16	104.94	± 2.64	113.03	± 7.35
	CA1	99.84	± 3.04	95.86	± 1.70	98.14	± 1.02
	CA2	95.49	± 2.10	86.29	± 2.44*	100.38	± 2.34
	CA3	97.38	± 2.56	92.28	± 1.53	98.19	± 1.10
	Dg	103.64	± 2.84	97.84	± 0.90	102.05	± 1.58
HCN 3	RS ctx	101.16	± 6.45	111.78	± 3.43	108.92	± 11.99
	V2 ctx	103.55	± 5.50	115.38	± 8.26	101.87	± 10.12
	Au ctx	102.36	± 4.79	114.70	± 5.46	109.73	± 11.52
	Prh ctx	106.03	± 4.20	116.02	± 6.10	109.72	± 10.91
	PAG	94.72	± 4.46	105.36	± 4.76	121.50	± 13.39
	Gen	105.39	± 4.59	118.27	± 5.81	105.01	± 10.15
	VTA	107.73	± 5.16	121.55	± 3.64*	112.24	± 9.99
	PMCo	97.80	± 4.62	115.10	± 6.27	112.98	± 10.92
	CA1	101.39	± 4.47	115.00	± 4.98	111.14	± 12.78
	CA2	99.06	± 6.26	112.69	± 6.47	122.49	± 14.12
	CA3	100.10	± 3.75	114.45	± 4.96	121.39	± 14.11
	Dg	104.01	± 4.16	114.71	± 4.14	113.09	± 11.80

Data represent mean ± s.e.mean of three sections per animal ($n = 6$) were optical density readings have been converted to nCi/g of tissue. These values have then been converted to represent % vehicle mRNA expression. One-way ANOVA with Dunnett's *post-hoc* test was performed for vehicle, fluoxetine and mirtazapine study and a t-test was performed for vehicle and Org 34167 study. * $P < 0.05$, ** $P < 0.01$. Abb: RS, retrosplenial cortex, V2, secondary visual cortex, lateral area, Au ctx, primary auditory cortex, PRh, perirhinal cortex, CA1, dorsocaudal field CA1 of hippocampus, CA2, caudal field CA2 of hippocampus, CA3, caudal field CA3 of hippocampus, Dg, caudal dentate gyrus, PAG, anterior periaqueductal grey, Gen, geniculate nucleus, VTA, ventral tegmental area, PMCo, posteromedial cortical amygdaloid nucleus (Paxinos and Watson, 1982).

5.4 Discussion

The aim of the current study was to determine whether chronic antidepressant treatment altered HCN channel mRNA expression in a number of brain regions. Chronic fluoxetine, mirtazapine or Org 34167 differentially regulated HCN isoform mRNA expression compared with vehicle, whereas lithium administration had no significant affects.

Chronic administrations of fluoxetine, or mirtazapine, were observed to downregulate HCN1 and HCN2 mRNA in all regions of the frontal cortex analysed (Figures 5.1 & 5.2). As discussed in Chapters 3 and 4, the frontal cortex has been implicated in depression, particularly the orbital cortex (Drevets, 2000; Tekin *et al.*, 2002). Acute fluoxetine has been demonstrated to be inactive in electrophysiological studies involving Chinese Hamster Ovary cells overexpressing HCN 1 (Mason, Personal communication) but there are a number of possible reasons to explain the current findings. The main factors believed to modulate ion channel gene expression include, repetitive activity, depolarisation, protein kinase activation or elevation of intracellular Ca^{2+} (Kang *et al.*, 1997; Roden *et al.*, 1994). HCN channels are positively modulated by PKA and cAMP, which fluoxetine has been demonstrated to increase (Edgar *et al.*, 1999). Moreover, it has been shown that 5-HT receptor activation alters the properties of HCN 2 channels; 5-HT_4- and 5-HT_7-receptor agonists shift the $V_{1/2}$ to more depolarised potentials, whereas 5-HT_{1A}-receptor activation shifts gating to more hyperpolarised membrane potentials. This could explain the downregulation of HCN 2 mRNA observed following chronic fluoxetine or mirtazapine administration, as both drugs increase in 5-HT release (de Boer, 1996; Hervas *et al.*, 2001), which could then lead to an overactivation of HCN channels.

The fact that HCN1 channels are poorly modulated by cAMP (Table 1.4), is suggestive of a different mechanism behind the downregulation in mRNA expression. It is possible that if chronic fluoxetine or mirtazapine administration alter the properties of HCN2 isoforms to increase cell firing, there is a concurrent increase in HCN1 channel opening, which display faster kinetics than HCN2 channels. Another possibility is that heteromeric HCN1 and HCN2 channels are present in the frontal cortex, as has been demonstrated in cells expressing both isoforms (Ulens *et al.*, 2001a). If heteromeric channels were the case, it would may expected that alteration of either isoform would be reflected in the other.

This regulation of HCN channel isoform expression in the frontal cortex by fluoxetine and mirtazapine may represent a therapeutic action, which is exploited by the direct blocker Org 34167. The fact that Org 34167 does not alter HCN channel expression in the frontal cortex, suggests that fluoxetine and mirtazapine modulate the channel *via* an indirect action in the frontal cortex. Additionally, the fact that fluoxetine or mirtazapine administration did not alter 5-HT_{1A} or HCN3 mRNA expression in these regions implies that the downregulation of HCN1 and HCN2 is a specific effect. This may have implications regarding the delayed onset of action of these current antidepressants. It is believed that adaptive changes underlie the delay in antidepressant action and this modulation of HCN isoforms following chronic treatment may represent one such adaptive response to chronic drug treatment. If this were the case it may be that by directly targeting HCN channels with drugs such as Org 34167 that a faster onset of clinical benefit may be achieved. If part of the antidepressant profile of fluoxetine and mirtazapine is to chronically downregulate HCN expression, Org 34167, by directly

blocking the channel would negate the requirement of chronic downregulation of the channel by acting there immediately.

Org 34167-treated rats display an upregulation of 5-HT_{1A} expression in the secondary and retrosplenial cortices (Figure 5.1 and Table 5.3), as was demonstrated for *c-fos* and Egr-1 mRNA. Activation of postsynaptic 5-HT_{1A} receptors is associated with head-weaving (Hoyer *et al.*, 2002), as is the retrosplenial cortex, which has been implicated as the region responsible for MK-801 associated head-weaving (Wozniak *et al.*, 1996). Taken as a whole, this is suggestive that Org 34167 indirectly activates 5-HT_{1A}-receptors which results in head-weaving behaviour.

Org 34167 treatment resulted in a downregulation of HCN2 mRNA expression in the anterior insular and piriform cortices and the nucleus accumbens core and shell regions, as well as HCN3 in the accumbens core (Figure 5.3). The anterior insular cortex and nucleus accumbens are important regions in emotion, and as previously discussed display altered metabolism in patients with depression (Drevets, 2000). It is possible therefore, that Org 34167 is acting in these two brain regions to normalise brain activity *via* HCN channel modulation. The finding that the antagonist Org 34167 downregulates the expression of HCN2 mRNA, is similar to the administration of α_2-adrenoceptor antagonists, which are known to downregulate α_2-adrenoceptor expression (Heal, 1990). Furthermore, the striatum is predominantly comprised of HCN2 mRNA, which may imply that Org 34167 treatment reduces the number of functional channels in the accumbens. This could be delineated by measuring protein expression with an antibody.

Org 34167 treatment significantly downregulated HCN1 and HCN2 mRNA expression in the secondary and primary somatosensory cortices, respectively, compared with vehicle (Table 5.2). The somatosensory cortex projects to the striatum and is involved in the control and sequencing of movements, including grooming, head and forelimb co-ordination (Hoover *et al.*, 2003). I_h channels are of highest density in apical dendrites in layer V pyramidal cells (Berger *et al.*, 2001; Santoro *et al.*, 1997). Therefore, modulation of HCN isoform expression in these regions may partially explain the tremorogenic side-effects observed following Org 34167 administration (Blackburn-Munro *et al.*, Personal communication). Interestingly, fluoxetine and mirtazapine were demonstrated to elevate 5-HT_{1A} receptor mRNA expression in the primary somatosensory cortex (Table 5.2), which may be a compensatory adaptation to chronic desensitisation of the receptors. Le Poul *et al.*, (2000) previously demonstrated that chronic fluoxetine treatment (8 mg/kg/21d, i.p.) did not affect 5-HT_{1A} mRNA expression in the forebrain. However, this finding was performed on total RNA extract, whereas the present study used Densitometric analysis of individual brain regions.

Hippocampal HCN mRNA was differentially regulated by mirtazapine and Org 34167 treatment. The former downregulated HCN2 mRNA in the caudal CA2 region, and Org 34167 upregulating HCN2 expression in the rostral CA2 field and HCN3 levels in the dentate gyrus (Tables 5.2 and 5.3). The differential regulation of hippocampal HCN expression is interesting, as I_h activation has been associated with hippocampal long term potentiation (Chevaleyre *et al.*, 2002; Mellor *et al.*, 2002). Additionally, Brewester *et al.*, (2002) demonstrated that kainate-induced seizures in immature rats resulted in elevated HCN2 expression in all hippocampal fields and decreased HCN1 mRNA in the CA1 field in the adults. This is similar to the HCN2 mRNA increase observed following Org 34167 administration, which produces tremors in adult rats at

the same dose as used in the present study (0.5 mg/kg). Increased HCN2 mRNA expression, if translated to active channels would lead to enhanced depolarisation in the hippocampus, which would in turn cause LTP (Chevaleyre *et al.*, 2002; Mellor *et al.*, 2002). No treatment significantly altered 5-HT_{1A} receptor mRNA expression in the hippocampus, as has been shown previously following fluoxetine administration (3 mg/kg, i.p., 14d; Hervas *et al.*, 2001).

Chronic mirtazapine administration was demonstrated to increase both 5-HT_{1A}-receptor and HCN1 mRNA expression in the thalamus (Table 5.2), which is an important brain region in the control of sleep organisation. I_h channels in the thalamus are believed to play a crucial role in sleep *via* modulation of spindle wave duration and frequency in the thalamus (McCormick *et al.*, 1997). Therefore, it is possible that mirtazapine, by increasing the expression of HCN1 mRNA alters the properties of these oscillations, which then has a rebound effect on sleep organisation.

In conclusion, chronic treatment with a variety of antidepressants differentially modulates HCN mRNA expression in the rat brain. Fluoxetine and particularly mirtazapine were observed to alter HCN channel expression in a number of brain areas, including the frontal cortex. This has potential implications in their mechanisms of action due to the role that I_h channels play in neuronal activity and organisation of neuronal networks and may represent an adaptive change underlying antidepressant action. Org 34167 treatment also altered HCN isoform expression, in the anterior insular cortex and nucleus accumbens, two regions implicated in depression, and may represent a basis for it's antidepressant profile. Additionally, if the adaptive changes observed following fluoxetine and mirtazapine are required for clinical benefit, directly targeting I_h channels with Org 34167 may provide a faster onset of action.

Chapter 6 General discussion

The fact that the mechanism of action of currently prescribed antidepressants are modulation of the monoamine system has lead to increasing difficulty to find new drugs to attain approval. This has increased interest and research into potential antidepressants with novel mechanisms of action in a bid to improve efficacy and onset of clinical benefit. The focus of this thesis has been on one such novel antidepressant; Org 34167, which is presently entering Phase II clinical trials. Prior to entering clinical trials, the compound was subject to a battery of assays, which demonstrated that the compound displayed high affinity for I_h channels (Ruigt, Personal communication). However, a lack of selective pharmacological tools to study the behavioural effects of I_h channels *in vivo* has hindered further insight into the channels potential role in depression. It is unknown whether blockade of I_h channels is responsible for the antidepressant-like effect of Org 34167 in pre-clinical animal models. In order to address this, a number of different approaches have been performed in the course of this thesis to examine Org 34167 and a number of clinically used antidepressants.

Antisense oligonucleotides have been employed to inhibit numerous specific proteins to improve the understanding of their function and were used in the current studies in an attempt to elucidate the mechanism of action of Org 34167. It was unknown, which, if any, HCN isoform is responsible for the antidepressant-like effect of Org 34167, with electrophysiological studies revealing that the compound inhibits HCN1, 2 and 4 homomeric channels with similar affinity (Mason, Personal communication). The HCN2 isoform was initially targeted due to both its widespread distribution and high expression throughout the rat CNS (Monteggia *et al.*, 2000). Despite designing numerous antisense sequences complementary to regions along the length of the HCN2

transcript and altering the backbone chemistry of the oligonucleotides no successful sequence was demonstrated. However, with the radioligand [^{3}H]-Org 34167 proving unsuitable for autoradiography and no available HCN2 antibody at the time of experiments only mRNA expression was quantified. Although antisense technology is an extremely powerful tool, it has been proved more difficult than expected to design efficient sequences. There are numerous reasons for this, the main one of which is the believed inaccessibility of the oligonucleotide to the folded RNA molecule. Indeed, it is estimated that only 1 in 10 antisense sequences cause downregulation of the target protein (Smith *et al.*, 2000). Additional problems with toxicity, which the introduction of phosphorothioate oligonucleotides causes, also hindered design of a successful sequence (see Chapter 2 discussion).

The recent discovery of the phenomenon of RNA interference (RNAi) may provide a possible alternative to antisense oligonucleotide infusion. RNAi is a process, which achieves gene silencing *via* complementary double-stranded RNA (dsRNA) sequences of 21 – 23 nt termed short-interfering RNAs (siRNA; Fire *et al.*, (1998); Tabara *et al.*, (1999)). One strand of siRNA then forms an RNA-induced silencing protein complex (RISC) which then cleaves the complementary mRNA (Elbashir *et al.*, 2001; Martinez *et al.*, 2002). It may be that when Zamecnik & Stephenson (1978) used phosphodiester oligonucleotides that they had accidentally stumbled across an artificial RNAi process. In a recent study, Bertrand *et al.*, (2002) demonstrated that after 5 and 20 h incubations siRNA was more efficient than its complementary antisense sequence. Therefore, it is possible that a siRNA to the HCN2 antisense sequences used in the present studies would produce an effective downregulation of the HCN2 isoform. However, the major limiting factor with siRNA at present is their use *in vivo* which is the final step to overcome before their widespread employment.

A method, which has gained increasing prominence in gaining insight into the mechanism of drug effects is immediate early gene (IEG) neuronal activity mapping. Examination of the IEG profiles of numerous psycho-active drugs, suggest that related classes of drug evoke a similar expression pattern (See Chapters 3 & 4 Discussion). Therefore, in addition to determining which brain regions a compound acutely affects, it appears that it may represent a pre-clinical method for characterising novel compounds before they undergo expensive behavioural screening. In an attempt to characterise the novel antidepressant, Org 34167, a range of antidepressant classes were subjected to IEG mapping throughout the rat CNS. Previous studies using fluoxetine, imipramine and LiCl only focussed on a small number of brain regions, such as the amygdala, striatum and hippocampus (Beck, 1995; Duncan *et al.*, 1996; Lamprecht *et al.*, 1995), which necessitated their inclusion in the present trial. Additionally, IEG mapping studies are sensitive to environmental factors and show circadian oscillations (Hess *et al.*, 1995; Ziolkowska *et al.*, 2002) therefore employing all the drugs in the same laboratory and within a tight timeframe maximises experimental control. As discussed in Chapters 3 and 4, all the compounds differed in their IEG profile but there were a number of common findings in brain regions implicated in depression. All drugs similarly affected *c-fos* expression in the central amygdala, which had previously been demonstrated for fluoxetine, imipramine (*c-fos*; Beck, (1995); Duncan *et al.*, (1996) and LiCl (Egr-1; Lamprecht *et al.*, 1995). Furthermore, in two more regions associated with depression, the septum and anterior insular cortex, all drugs had a similar effect on *c-fos* expression (Table 3.3). However, in the corresponding Egr-1 study only the central amygdala was demonstrated as a site of common manipulation by acute drug treatment and in general, substantially fewer brain regions showed altered expression compared with vehicle (see Table 4.8). This is with the exception of Org 34167, which

significantly increased Egr-1 in the majority of cortical regions examined (Table 4.8). Interestingly, this was also witnessed in the corresponding *c-fos* study, with fluoxetine being the only other drug to show cortical *c-fos* induction, but in fewer regions (Table 3.9). The strong cortical induction of IEGs by Org 34167 is interesting, as throughout the cortex, HCN1 and 2 expression is high (Lorincz *et al.*, 2002; Monteggia *et al.*, 2000; Moosmang *et al.*, 1999), which is suggestive of the presence of a high density of channels. Indeed, the majority of sub-cortical regions in which an induction of IEG expression was observed also possess high levels of HCN 1 and 2 expression, with the exception of the striatum where HCN 2 is the dominant isoform (Monteggia *et al.*, 2000; Moosmang *et al.*, 1999). This is suggestive, given the *in vitro* data (Ruigt, Personal communication), that HCN 1 and 2 isoforms play a prominent role in the mechanism underlying this induction. Clearly more experiments are required to substantiate this hypothesis, and a similar experiment could be performed using HCN knockout mice.

The widespread activation of IEG expression caused by Org 34167 (0.5 mg/kg) implies that this dose evokes a widespread activation of these genes. A previous study examining two doses of LiCl demonstrated that, while c-Fos was only significantly induced in the amygdala with a low dose (20 mg/kg), a much more widespread induction was observed with a higher dose (100 mg/kg; Hamamura *et al.*, (2000)). It would be interesting to discern whether Org 34167 displays a similar dose relationship. However, the dose used in the present study was that established to display antidepressant-like properties in the DRL 72 and ACSO animal model paradigms and lower doses may not retain the antidepressant profile (Ruigt, Personal communication). Analysis of previous *c-fos* neuronal mapping studies reveals that this strong cortical induction is akin to psychostimulant drugs, such as amphetamine, cocaine, MK-801 and PCP (See Section 3.4). Despite fewer studies involving Egr-1, similar cortical

activation has been demonstrated with psycho-stimulants (Saffen *et al.*, 1988). Therefore, despite the novel antidepressant Org 34167 displaying characteristics of current clinically used antidepressants (in the central amygdala, anterior insular cortex and septum) it also shares a similar profile to that of psychostimulants. The similarity of the IEG profile to that of psychostimulants is interesting, especially as the dose used is active in the rat intracranial self-stimulation paradigm (Ruigt, Personal communication). Obviously if this were to translate into human studies it warrants further investigation. A number of pre-clinical behavioural tests could be performed to establish the validity of this hypothesis. However, this psychostimulant profile may account for Org 34167's antidepressant-like properties as NMDA antagonists also display antidepressant properties (Berman *et al.*, 2000; Trullas *et al.*, 1990).

The current studies demonstrate that Org 34167 acutely activates brain regions associated with antidepressant drug administration and implicates the HCN channel in depression. Chronic treatment (21-day) with Org 34167, fluoxetine or mirtazapine, but not LiCl altered HCN isoform mRNA expression in a number of brain regions (see Chapter 5). If these alterations in HCN mRNA expression were mirrored in protein levels, it would indicate a potentially important mechanism of action of current antidepressants and also provide further evidence of these channels roles in depression. Fluoxetine has been demonstrated to be less selective for 5-HT reuptake inhibition than first thought, displaying affinity for 5-HT reuptake transporter and delayed rectifier K(v) potassium currents (Choi *et al.*, 1999; Yeung *et al.*, 1999). It also alters mRNA or protein expression of μ-opioid, D_2, D_3, CRF and glucocorticoid receptors (Ainsworth *et al.*, 1998a; De Gandarias *et al.*, 1999; Dziedzicka-Wasylewska *et al.*, 1997b; Torres *et al.*, 1998). Alteration in HCN channel density and/or isoforms would lead to large changes in both gating and subsequent transmitter release. With evidence suggesting that HCN channels are directly coupled to presynaptic vesicular machinery (Beaumont

et al., 2000), modulation of HCN channels may alter neurotransmitter release, which may be an important component of antidepressant drug action. The fact that in Phase I clinical trials Org 34167 prolonged REM sleep in healthy volunteers (vanBerkel, Personal communication) and the importance of I_h channels in thalamic sleep-wake organisation (McCormick *et al.*, 1997) indicates another potential link between the channels and depression.

The observations described in this thesis have helped to characterise the novel antidepressant Org 34167 and have provided a link between I_h (HCN) channels and depression. There is also insight into current antidepressants, revealing which brain regions they acutely target and evidence supporting a link between current antidepressants and HCN channel expression following chronic treatment. These observations strengthen the rational for targeting I_h channels to treat depression.

Chapter 7 References

AGRAWAL, S. (1996). Antisense oligonucleotides: towards clinical trials. *Trends in Biotechnology*, **14,** 376-387.

AGRAWAL, S. & IYER, R.P. (1997a). Perspectives in antisense therapeutics. *Pharmacology & Therapeutics*, **76,** 151-160.

AGRAWAL, S., JIANG, Z., ZHAO, Q., SHAW, D., CAI, Q., ROSKEY, A., CHANNAVAJJALA, L., SAXINGER, C. & ZHANG, R. (1997b). Mixed-backbone oligonucleotides as second generation antisense oligonucleotides: In vitro and in vivo studies. *Proceedings of the National Academy of Sciences of the United States of America*, **94,** 2620-2625.

AGRAWAL, S. & KANDIMALLA, E.R. (2000). Antisense therapeutics: is it as simple as complementary base recognition? *Molecular Medicine Today*, **6,** 72-81.

AGRAWAL, S. & KANDIMALLA, E.R. (1999). Medicinal chemistry of antisense oligonucleotides. In *Antisense technology in the central nervous system*. eds Leslie, R.A., Hunter, A.J. & Robertson, H.A. pp. 108-136: Oxford University Press.

AGRAWAL, S., MAYRAND, S.H., ZAMECNIK, P.C. & PEDERSON, T. (1990). Site-specific excision from RNA by RNase H and mixed-phosphate-backbone oligodeoxynucleotides. *Proceedings of the National Academy of Sciences of the United States of America*, **87,** 1401-1405.

AINSWORTH, K., SMITH, S.E. & SHARP, T. (1998a). Repeated administration of fluoxetine, desipramine and tranylcypromine increases dopamine D_2-like but not D_1-like receptor function in the rat. *Journal of Psychopharmacology*, **12,** 252-7.

AINSWORTH, K., SMITH, S.E., ZETTERSTROM, T.S., PEI, Q., FRANKLIN, M. & SHARP, T. (1998b). Effect of antidepressant drugs on dopamine D_1 and D_2 receptor expression and dopamine release in the nucleus accumbens of the rat. *Psychopharmacology*, **140,** 470-7.

ALAMA, A., BARBIERI, F., CAGNOLI, M. & SCHETTINI, G. (1997). Antisense oligonucleotides as therapeutic agents. *Pharmacological Research.*, **36,** 171-178.

AMARZGUIOUI, M., BREDE, G., BABAIE, E., GROTLI, M., SPROAT, B. & PRYDZ, H. (2000). Secondary structure prediction and in vitro accessibility of mRNA as tools in the selection of target sites for ribozymes. *Nucleic Acids Research.*, **28,** 4113-4124.

ANSELMET, A., MAYAT, E., WIETEK, S., LAYER, P.G., PAYRASTRE, B. & MASSOULIE, J. (2002). Non-antisense cellular responses to oligonucleotides. *FEBS Letters*, **510,** 175-180.

ANTHONY, J.P., SEXTON, T.J. & NEUMAIER, J.F. (2000). Antidepressant-induced regulation of 5-HT(1B) mRNA in rat dorsal raphe nucleus reverses rapidly after drug discontinuation. *Journal of Neuroscience Research.*, **61,** 82-87.

ARBORELIUS, L., NOMIKOS, G.G., GRILLNER, P., HERTEL, P., HOOK, B.B., HACKSELL, U. & SVENSSON, T.H. (1995). 5-HT_{1A} receptor antagonists increase the activity of serotonergic cells in the dorsal raphe nucleus in rats treated acutely or chronically with citalopram. *Naunyn-Schmiedebergs Archives of Pharmacology*, **352,** 157-65.

ARBORELIUS, L., NOMIKOS, G.G., HERTEL, P., SALMI, P., GRILLNER, P., HOOK, B.B., HACKSELL, U. & SVENSSON, T.H. (1996). The 5-HT_{1A} receptor antagonist (S)-UH-301 augments the increase in extracellular concentrations of 5-HT in the frontal cortex produced by both acute and chronic treatment with citalopram. *Naunyn-Schmiedebergs Archives of Pharmacology*, **353,** 630-40.

ARTIGAS, F., CELADA, P., LARUELLE, M. & ADELL, A. (2001). How does pindolol improve antidepressant action? [see comments.]. *Trends in Pharmacological Sciences*, **22,** 224-8.

ATTWELL, D. & WILSON, M. (1980). Behaviour of the rod network in the tiger salamander retina mediated by membrane properties of individual rods. *Journal of Physiology*, **309,** 287-315.

BADER, C.R. & BERTRAND, D. (1984). Effect of changes in intra- and extracellular sodium on the inward (anomalous) rectification in salamander photoreceptors. *Journal of Physiology*, **347,** 611-31.

BADIANI, A., OATES, M.M., DAY, H.E., WATSON, S.J., AKIL, H. & ROBINSON, T.E. (1998). Amphetamine-induced behavior, dopamine release, and c-fos mRNA expression: modulation by environmental novelty. *Journal of Neuroscience*, **18,** 10579-93.

BAKER, B.F., LOT, S.S., CONDON, T.P., CHENG-FLOURNOY, S., LESNIK, E.A., SASMOR, H.M. & BENNETT, C.F. (1997). 2'-O-(2-methoxy)ethyl-modified anti-intercellular adhesion molecule 1 (ICAM-1) oligonucleotides selectively increase the ICAM-1 mRNA level and inhibit formation of the ICAM-1 translation initiation complex in human umbilical vein endothelial cells. *Journal of Biological Chemistry*, **272,** 11994-12000.

BANCROFT, J.D. & STEVENS, A. (1996). *Theory and Practice of Histological Techniques (4th edition).* New York: Churchill Livingstone.

BANERJEE, S.P., KUNG, L.S., RIGGI, S.J. & CHANDA, S.K. (1977). Development of beta-adrenergic receptor subsensitivity by antidepressants. *Nature*, **268,** 455-6.

BANERJEE, S.P., SHARMA, V.K., KUNG, L.S. & CHANDA, S.K. (1978). Amphetamine induces beta-adrenergic receptor supersensitivity. *Nature*, **271,** 380-1.

BARNES, S. & HILLE, B. (1989). Ionic channels of the inner segment of tiger salamander cone photoreceptors. *Journal of General Physiology*, **94,** 719-43.

BARRACLOUGH, B., BUNCH, J., NELSON, B. & SAINSBURY, P. (1974). A hundred cases of suicide: clinical aspects. *British Journal of Psychiatry*, **125,** 355-73.

BEAUMONT, V. & ZUCKER, R.S. (2000). Enhancement of synaptic transmission by cyclic AMP modulation of presynaptic Ih channels. *Nature Neuroscience*, **3,** 133-41.

BECK, C.H.M. (1995). Acute treatment with antidepressant drugs selectively increases the expression of c-fos in the rat brain. *Journal of Psychiatry & Neuroscience.*, **20,** 25-32.

BECKMANN, A.M. & WILCE, P.A. (1997). Egr transcription factors in the nervous system. *Neurochemistry International.*, **31,** 477-510.

BEL, N. & ARTIGAS, F. (1993). Chronic treatment with fluvoxamine increases extracellular serotonin in frontal cortex but not in raphe nuclei. *Synapse*, **15,** 243-5.

BEL, N. & ARTIGAS, F. (1996). Reduction of serotonergic function in rat brain by tryptophan depletion: effects in control and fluvoxamine-treated rats. *Journal of Neurochemistry*, **67,** 669-76.

BENDER, R.A., BREWSTER, A., SANTORO, B., LUDWIG, A., HOFMANN, F., BIEL, M. & BARAM, T.Z. (2001). Differential and age-dependent expression of hyperpolarization-activated, cyclic nucleotide-gated cation channel isoforms 1-4 suggests evolving roles in the developing rat hippocampus. *Neuroscience*, **106,** 689-98.

BENGTSSON, H.J., KELE, J., JOHANSSON, J. & HJORTH, S. (2000). Interaction of the antidepressant mirtazapine with alpha2-adrenoceptors modulating the release of 5-HT in different rat brain regions in vivo. *Naunyn-Schmiedeberg's Archives of Pharmacology*, **362,** 406-412.

BENKELFAT, C., ELLENBOGEN, M.A., DEAN, P., PALMOUR, R.M. & YOUNG, S.N. (1994). Mood-lowering effect of tryptophan depletion. Enhanced susceptibility in young men at genetic risk for major affective disorders. *Archives of General Psychiatry*, **51,** 687-97.

BERGER, T., LARKUM, M.E. & LUSCHER, H.R. (2001). High I(h) channel density in the distal apical dendrite of layer V pyramidal cells increases bidirectional attenuation of EPSPs. *Journal of Neurophysiology*, **85,** 855-68.

BERMAN, R.M., CAPPIELLO, A., ANAND, A., OREN, D.A., HENINGER, G.R., CHARNEY, D.S. & KRYSTAL, J.H. (2000). Antidepressant effects of ketamine in depressed patients. *Biological Psychiatry*, **47,** 351-354.

BERTRAND, J.R., POTTIER, M., VEKRIS, A., OPOLON, P., MAKSIMENKO, A. & MALVYA, C. (2002). Comparison of antisense oligonucleotides and siRNAs in cell culture and in vivo. *Biochemical & Biophysical Research Communications*, **296,** 1000-1004.

BHAT, R.V. & BARABAN, J.M. (1992a). High basal expression of zif268 in cortex is dependent on intact noradrenergic system. *European Journal of Pharmacology-Molecular Pharmacology Section.*, **227,** 447-448.

BHAT, R.V., WORLEY, P.F., COLE, A.J. & BARABAN, J.M. (1992b). Activation of the zinc finger encoding gene krox-20 in adult rat brain: Comparison with zif268. *Molecular Brain Research.*, **13,** 263-266.

BICKMEYER, U., HEINE, M., MANZKE, T. & RICHTER, D.W. (2002). Differential modulation of Ih by 5-HT receptors in mouse CA1 hippocampal neurons. *European Journal of Neuroscience*, **16,** 209-218.

BIEL, M., LUDWIG, A., ZONG, X. & HOFMANN, F. (1999). Hyperpolarization-activated cation channels: a multi-gene family. *Reviews of Physiology Biochemistry & Pharmacology*, **136,** 165-81.

BLACKBURN-MUNRO, R., MACLACHLAN, F. & DRINKENBURG, P. (Personal communication). Investigation of the tremorigenic effects of Org 34167 in rats. Research and Development Subject Report.

BOSMITH, R.E., BRIGGS, I. & STURGESS, N.C. (1993). Inhibitory actions of ZENECA ZD7288 on whole-cell hyperpolarization activated inward current (If) in guinea-pig dissociated sinoatrial node cells. *British Journal of Pharmacology*, **110,** 343-9.

BOURET, S. & SARA, S.J. (2002). Locus coeruleus activation modulates firing rate and temporal organization of odour-induced single-cell responses in rat piriform cortex. *European Journal of Neuroscience*, **16,** 2371-2382.

BREMNER, J.D., INNIS, R.B., SALOMON, R.M., STAIB, L.H., NG, C.K., MILLER, H.L., BRONEN, R.A., KRYSTAL, J.H., DUNCAN, J., RICH, D., PRICE, L.H., MALISON, R., DEY, H., SOUFER, R. & CHARNEY, D.S. (1997). Positron emission tomography measurement of cerebral metabolic correlates of tryptophan depletion-induced depressive relapse. *Archives of General Psychiatry*, **54,** 364-74.

BREWSTER, A. & BENDER, R.A. (2002). Activity-dependent regulation of the expression of hippocampal HCN subunits. In *32nd Society of Neuroscience Meeting*. Orlando, U.S.A.

BROBERGER, C., NYLANDER, I., GELIER, T., TERENIUS, L., HOKFELT, T. & GEORGIEVA, J. (2000). Differential effects of intrastriatally infused fully and endcap phosphorothioate antisense oligonucleotides on morphology, histochemistry and prodynorphin expression in rat brain. *Molecular Brain Research*, **75,** 25-45.

BRODIE, B.B., COMER, M.S., COSTA, E. & DLABAC, A. (1966). The role of brain serotonin in the mechanism of the central action of reserpine. *Journal of Pharmacology & Experimental Therapeutics*, **152,** 340-9.

BROWN, H.F., DIFRANCESCO, D. & NOBLE, S.J. (1979a). How does adrenaline accelerate the heart? *Nature*, **280,** 235-6.

BROWN, H.F., DIFRANCISCO, D. & NOBLE, S.J. (1979b). Adrenaline action on rabbit sino-atrial node [proceedings]. *Journal of Physiology*, **290,** 31P-32P.

BRUSSAARD, A.B. (1997). Antisense oligonucleotides induce functional deletion of ligand gated ion channels in cultured neurons and brain explants. *Journal of Neuroscience Methods*, **71,** 55-64.

BRYSCH, W. (1999). The design of appropriate control experiments to ensure specificity in antisense oligonucleotide function. In *Antisense Technology in the Central Nervous System.* eds Leslie, R.A., Hunter, A.J. & Robertson, H.A. pp. 21-41. Oxford: Oxford University Press.

BUCCHI, A., BARUSCOTTI, M. & DIFRANCESCO, D. (2002). Current-dependent Block of Rabbit Sino-Atrial Node I(f) Channels by Ivabradine. *The Journal of General Physiology*, **120,** 1-13.

BURNET, P.W.J., MICHELSON, D., SMITH, M.A., GOLD, P.W. & STERNBERG, E.M. (1994). The effect of chronic imipramine administration of the densities of 5-HT1A and 5-HT2 receptors and the abundancies of 5-HT receptor and transporter mRNA in the cortex, hippocampus and dorsal raphe of three strains of rat. *Brain Research.*, **638,** 311-324.

CALLADO, L.F., MEANA, J.J., GRIJALBA, B., PAZOS, A., SASTRE, M. & GARCIA-SEVILLA, J.A. (1998). Selective increase of alpha(2A)-adrenoceptor agonist binding sites in brains of depressed suicide victims. *Journal of Neurochemistry.*, **70,** 1114-1123.

CARLSSON, A. (1961). Brain monoamines and psychotropic drugs. *Neuropsychopharmacology*, **2,** 417.

CARLSSON, A., LINDQVIST, M. & MAGNUSSON, T. (1957). 3,4-Dihydroxyphenylalanine and 5-hydroxytryptophan as reserpine antagonists. *Nature*, **180,** 1200.

CARPENTER, L.L., ANDERSON, G.M., PELTON, G.H., GUDIN, J.A., KIRWIN, P.D., PRICE, L.H., HENINGER, G.R. & MCDOUGLE, C.J. (1998). Tryptophan depletion during continuous CSF sampling in healthy human subjects. *Neuropsychopharmacology*, **19,** 26-35.

CASTNER, S.A. & BECKER, J.B. (1996). Sex differences in the effect of amphetamine on immediate early gene expression in the rat dorsal striatum. *Brain Research*, **712,** 245-57.

CHARNEY, D.S., HENINGER, G.R., STERNBERG, D.E., REDMOND, D.E., LECKMAN, J.F., MAAS, J.W. & ROTH, R.H. (1981). Presynaptic adrenergic receptor sensitivity in depression. The effect of long-term desipramine treatment. *Archives of General Psychiatry*, **38,** 1334-40.

CHAUDHURI, A. (1997). Neural activity mapping with inducible transcription factors. *NeuroReport.*, **8,** v-ix.

CHEETHAM, S.C., KATONA, C.L.E. & HORTON, R.W. (1991). Post-mortem studies of neurotransmitter biochemistry in depression and suicide. *Biological Aspects of Affective Disorders*, 192-221.

CHEN, K., ARADI, I., SANTHAKUMAR, V. & SOLTESZ, I. (2002). H-channels in epilepsy: new targets for seizure control? *Trends in Pharmacological Sciences*, **23,** 552-557.

CHEN, X., FERRINGTON, D.A., BIGELOW, D.J. & MICHAELIS, E.K. (1997). Protein half-lives of two subunits of an NMDA receptor-like complex, the 71-kDa glutamate-binding and the 80-kDa CPP-binding protein. *Biochemical & Biophysical Research Communications.*, **241,** 132-135.

CHESSIN, M., KRAMER, E.R. & SCOTT, C.T. (1957). Modifications of the pharmacology of reserpine and serotonin by iproniazid. *Journal of Pharmacology & Experimental Therapeutics*, **119,** 453-460.

CHEVALEYRE, V. & CASTILLO, P.E. (2002). Assessing the role of Ih channels in synaptic transmission and mossy fiber LTP. *Proceedings of the National Academy of Sciences of the United States of America*, **99,** 9538-9543.

CHOI, J.S., HAHN, S.J., RHIE, D.J., YOON, S.H., JO, Y.H. & KIM, M.S. (1999). Mechanism of fluoxetine block of cloned voltage-activated potassium channel Kv1.3. *Journal of Pharmacology & Experimental Therapeutics*, **291,** 1-6.

CLAPHAM, D.E. (1998). Not so funny anymore: pacing channels are cloned. *Neuron*, **21,** 5-7.

COCHRAN, S.M., MCKERCHAR, C.E., MORRIS, B.J. & PRATT, J.A. (2002). Induction of differential patterns of local cerebral glucose metabolism and immediate-early genes by acute clozapine and haloperidol. *Neuropharmacology.*, **43,** 394-407.

COHEN, D.R. & CURRAN, T. (1990). Analysis of dimerization and DNA binding functions in Fos and Jun by domain-swapping: Involvement of residues outside the leucine zipper/basic region. *Oncogene.*, **5,** 929-939.

COLLU, M., POGGIU, A.S., DEVOTO, P. & SERRA, G. (1997). Behavioural sensitization of mesolimbic dopamine D2 receptors in chronic fluoxetine-treated rats. *European Journal of Pharmacology*, **322,** 123-7.

COOPER, S.R., TAYLOR, J.K., MIRAGLIA, L.J. & DEAN, N.M. (1999). Pharmacology of Antisense Oligonucleotide Inhibitors of Protein Expression. *Pharmacology & Therapeutics*, **82,** 427-435.

COPPEN, A. (1967). The biochemistry of affective disorders. *British Journal of Psychiatry*, **113,** 1237-64.

COPPEN, A., SHAW, D.M. & FARRELL, J.P. (1963). Potentiation of the antidepressive effect of a monoamine oxidase inhibitor by trytophan. *Lancet*, **i,** 79.

CROOKE, S.T. (1999). Molecular mechanisms of action of antisense drugs. *Biochimica et Biophysica Acta - Gene Structure and Expression*, **1489,** 31-43.

CROOKE, S.T., GRAHAM, M.J., ZUCKERMAN, J.E., BROOKS, D., CONKLIN, B.S., CUMMINS, L.L., GREIG, M.J., GUINOSSO, C.J., KORNBRUST, D., MANOHARAN, M., SASMOR, H.M., SCHLEICH, T., TIVEL, K.L. & GRIFFEY, R.H. (1996). Pharmacokinetic properties of several novel oligonucleotide analogs in mice. *Journal of Pharmacology & Experimental Therapeutics.*, **277,** 923-937.

CRUISE, L. (Personal communication). Induction of *c-fos* by fluoxetine.

CRUM, C., JOHNSON, J., NELSON, A. & ROTH, D. (1988). Complementary oligodeoxynucleotide mediated inhibition of tobacco mosaic virus RNA translation in vitro. *Nucl. Acids. Res.*, **16,** 4569-4581.

CUMMINS, L.L., OWENS, S.R., RISEN, L.M., LESNIK, E.A., FREIER, S.M., MCGEE, D., GUINOSSO, C.J. & COOK, P.D. (1995). Characterization of fully 2'-modified oligoribonucleotide hetero- and homoduplex hybridization and nuclease sensitivity. *Nucleic Acids Research.*, **23,** 2019-2024.

CURRAN, T. & TEICH, N.M. (1982). Candidate product of the FBJ murine osteosarcoma virus oncogene: Characterization of a 55,000-dalton phosphoprotein. *Journal of Virology.*, **42,** 114-122.

DAHMEN, N., FEHR, C., REUSS, S. & HIEMKE, C. (1997). Stimulation of immediate early gene expression by desipramine in rat brain. *Biological Psychiatry.*, **42,** 317-323.

D'AQUILA, P.S., COLLU, M., GESSA, G.L. & SERRA, G. (1997). Role of D1 and alpha1 receptors in the enhanced locomotor response to dopamine D2-like receptor stimulation induced by repeated electroconvulsive shock. *Journal of Psychopharmacology*, **11,** 41-4.

D'AQUILA, P.S., COLLU, M., GESSA, G.L. & SERRA, G. (2000). The role of dopamine in the mechanism of action of antidepressant drugs. *European Journal of Pharmacology*, **405,** 365-73.

DAY, H.E., BADIANI, A., USLANER, J.M., OATES, M.M., VITTOZ, N.M., ROBINSON, T.E., WATSON, S.J.J. & AKIL, H. (2001). Environmental novelty differentially affects c-fos mRNA expression induced by amphetamine or cocaine in subregions of the bed nucleus of the stria terminalis and amygdala. *Journal of Neuroscience*, **21,** 732-40.

DE BOER, T. (1996). The pharmacologic profile of mirtazapine. *Journal of Clinical Psychiatry*, **57,** 19-25.

DE GANDARIAS, J.M., ECHEVARRIA, E., ACEBES, I., ABECIA, L.C., CASIS, O. & CASIS, L. (1999). Effects of fluoxetine administration on mu-opoid receptor immunostaining in the rat forebrain. *Brain Research*, **817,** 236-240.

DELGADO, P.L., PRICE, L.H., MILLER, H.L., SALOMON, R.M., AGHAJANIAN, G.K., HENINGER, G.R. & CHARNEY, D.S. (1994). Serotonin and the neurobiology of depression. Effects of tryptophan depletion in drug-free depressed patients. *Archives of General Psychiatry*, **51,** 865-74.

DELGADO, P.L., PRICE, L.H., MILLER, H.L., SALOMON, R.M., LICINIO, J., KRYSTAL, J.H., HENINGER, G.R. & CHARNEY, D.S. (1991). Rapid serotonin depletion as a provocative challenge test for patients with major depression: relevance to antidepressant action and the neurobiology of depression. *Psychopharmacology Bulletin*, **27,** 321-30.

DEVANE, C.L., GROTHE, D.R. & SMITH, S.L. (2002). Pharmacology of antidepressants: focus on nefazodone. *Journal of Clinical Psychiatry*, **63,** 10-7.

DI CHIARA, G. (2002). Nucleus accumbens shell and core dopamine: Differential role in behavior and addiction. *Behavioural Brain Research.*, **137,** 75-114.

DIFRANCESCO, D. (1981a). A new interpretation of the pace-maker current in calf Purkinje fibres. *Journal of Physiology*, **314,** 359-76.

DIFRANCESCO, D. (1981b). A study of the ionic nature of the pace-maker current in calf Purkinje fibres. *Journal of Physiology*, **314,** 377-93.

DIFRANCESCO, D. & TORTORA, P. (1991). Direct activation of cardiac pacemaker channels by intracellular cyclic AMP. *Nature*, **351,** 145-7.

DORIS, A., EBMEIER, K. & SHAJAHAN, P. (1999). Depressive illness. *Lancet*, **354,** 1369-1375.

DRAGUNOW, M. & FAULL, R. (1989). The use of c-fos as a metabolic marker in neuronal pathway tracing. *Journal of Neuroscience Methods.*, **29,** 261-265.

DREVETS, W.C. (2001). Neuroimaging and neuropathological studies of depression: implications for the cognitive-emotional features of mood disorders. *Current Opinion in Neurobiology*, **11,** 240-249.

DREVETS, W.C. (2000). Neuroimaging studies of mood disorders. *Biological Psychiatry*, **48,** 813-829.

DREVETS, W.C. (1999). Prefrontal cortical-amygdalar metabolism in major depression. *Annals of the New York Academy of Sciences*, **877**.

DREVETS, W.C., VIDEEN, T.O., PRICE, J.L., PRESKORN, S.H., CARMICHAEL, S.T. & RAICHLE, M.E. (1992). A functional anatomical study of unipolar depression. *Journal of Neuroscience.*, **12,** 3628-3641.

DUNCAN, G.E., KNAPP, D.J., JOHNSON, K.B. & BREESE, G.R. (1996). Functional classification of antidepressants based on antagonism of swim stress-induced fos-like immunoreactivity. *Journal of Pharmacology & Experimental Therapeutics.*, **277,** 1076-1089.

DUNCAN, G.E., MOY, S.S., KNAPP, D.J., MUELLER, R.A. & BREESE, G.R. (1998). Metabolic mapping of the rat brain after subanesthetic doses of ketamine: potential relevance to schizophrenia. *Brain Research*, **787,** 181-90.

DZIEDZICKA-WASYLEWSKA, M., MAKOWIAK, M., FIJAT, K. & WEDZONY, K. (1996) Adaptive changes in the rat dopaminergic transmission following repeated lithium administration. *Journal of Neural Transmission* **103,** 765-76.

DZIEDZICKA-WASYLEWSKA, M. (1997). The effect of imipramine on the amount of mRNA coding for rat dopamine D_2 autoreceptors. *European Journal of Pharmacology*, **337,** 291-6.

DZIEDZICKA-WASYLEWSKA, M., ROGOZ, R., KLIMEK, V. & MAJ, J. (1997a). Repeated administration of antidepressant drugs affects the levels of mRNA coding for D_1 and D_2 dopamine receptors in the rat brain. *Journal of Neural Transmission - General Section*, **104,** 515-24.

DZIEDZICKA-WASYLEWSKA, M., WILLNER, P. & PAPP, M. (1997b). Changes in dopamine receptor mRNA expression following chronic mild stress and chronic antidepressant treatment. *Behavioural Pharmacology*, **8,** 607-18.

EDGAR, V.A., STERIN-BORDA, L., CREMASCHI, G.A. AND GENARO, A.M. (1999) Role of protein kinase C and cAMP in fluoxetine effects on human T-cell proliferation *European Journal of Pharmacology* **372,** 65-73.

ELBASHIR, S.M., MARTINEZ, J., PATKANIOWSKA, A., LENDECKEL, W. & TUSCHL, T. (2001). Functional anatomy of siRNAs for mediating efficient RNAi in Drosophila melanogaster embryo lysate. *EMBO Journal.*, **20,** 6877-6888.

ELEPFANDT, P., RUPPRECHT, S., SCHONING-BURKHARDT, B., VOLK, H.D., WOICIECHOWSKY, C. (2002) Oligodeoxynucleotides induce brain inflammation in rats when infused intracerebroventricularly. *Neuroscience Letters*, **322,** 107-10

ENGBER, T.M., KOURY, E.J., DENNIS, S.A., MILLER, M.S., CONTRERAS, P.C. & BHAT, R.V. (1998). Differential patterns of regional c-Fos induction in the rat brain by amphetamine and the novel wakefulness-promoting agent modafinil. *Neuroscience Letters*, **241,** 95-8.

FEIGHNER, J.P., MERIDETH, C.H. & CLAGHORN, J.L. (1984). Multicenter placebo-controlled evaluation of nomifensine treatment in depressed outpatients. *Journal of Clinical Psychiatry*, **45,** 47-51.

FIRE, A., XU, S., MONTGOMERY, M.K., KOSTAS, S.A., DRIVER, S.E. & MELLO, C.C. (1998). Potent and specific genetic interference by double-stranded RNA in caenorhabditis elegans. *Nature.*, **391,** 806-811.

FRACE, A.M., MARUOKA, F. & NOMA, A. (1992). Control of the hyperpolarization-activated cation current by external anions in rabbit sino-atrial node cells. *Journal of Physiology*, **453,** 307-18.

FULLER, R.W., SNODDY, H.D. & COHEN, M.L. (1984). Interactions of trazodone with serotonin neurons and receptors. *Neuropharmacology*, **23,** 539-44.

GAO, W.Y., HAN, F.S., STORM, C., EGAN, W. & CHENG, Y.C. (1992). Phosphorothioate oligonucleotides are inhibitors of human DNA polymerases and RNase H: Implications for antisense technology. *Molecular Pharmacology.*, **41,** 223-229.

GAO, X.M., HASHIMOTO, T. & TAMMINGA, C.A. (1993). Induction and suppression of immediate early genes in specific rat brain regions by the non-competitive N-methyl-D-aspartate receptor antagonist MK-801. *Neuroscience*, **53,** 749-58.

GARATTINI, S. (1997). Pharmacology of amineptine, an antidepressant agent acting on the dopaminergic system: a review. *International Clinical Psychopharmacology*, **12,** S15-9.

GARCIA-SEVILLA, J.A., ESCRIBA, P.V., OZAITA, A., LA HARPE, R., WALZER, C., EYTAN, A. & GUIMON, J. (1999). Up-regulation of immunolabeled alpha(2A)-adrenoceptors, G(i) coupling proteins, and regulatory receptor kinases in the prefrontal cortex of depressed suicides. *Journal of Neurochemistry.*, **72,** 282-291.

GARDIER, A.M., MALAGIE, I., TRILLAT, A.C., JACQUOT, C. & ARTIGAS, F. (1996). Role of 5-HT_{1A} autoreceptors in the mechanism of action of serotoninergic antidepressant drugs: recent findings from in vivo microdialysis studies. *Fundamental & Clinical Pharmacology*, **10,** 16-27.

GASPARINI, S. & DIFRANCESCO, D. (1997). Action of the hyperpolarization-activated current (I(h)) blocker ZD 7288 in hippocampal CA1 neurons. *Pflugers Archiv European Journal of Physiology*, **435,** 99-106.

GASS, P., HERDEGEN, T., BRAVO, R. & KIESSLING, M. (1993a). Induction and suppression of immediate early genes in specific rat brain regions by the non-competitive N-methyl-D-aspartate receptor antagonist MK-801. *Neuroscience.*, **53,** 749-758.

GASS, P., HERDEGEN, T., BRAVO, R. & KIESSLING, M. (1993b). Spatiotemporal induction of immediate early genes in the rat brain after limbic seizures: Effects of NMDA receptor antagonist MK-801. *European Journal of Neuroscience.*, **5,** 933-943.

GAUSS, R. & SEIFERT, R. (2000). Pacemaker oscillations in heart and brain: a key role for hyperpolarization-activated cation channels. *Chronobiology International*, **17,** 453-69.

GAUSS, R., SEIFERT, R. & KAUPP, U.B. (1998). Molecular identification of a hyperpolarization-activated channel in sea urchin sperm. *Nature*, **393,** 583-7.

GEORGIEVA, J., HEILIG, M., NYLANDER, I., HERRERO-MARSCHITZ, M. & TERENIUS, L. (1995). In vivo antisense inhibition of prodynorphin expression in rat striatum: Dose-dependence and sequence specificity. *Neuroscience Letters.*, **192,** 69-71.

GHAMARI-LANGROUDI, M. & BOURQUE, C.W. (2000). Excitatory role of the hyperpolarization-activated inward current in phasic and tonic firing of rat supraoptic neurons. *Journal of Neuroscience*, **20,** 4855-63.

GILES, R.V. & TIDD, D.M. (1992). Increased specificity for antisense oligodeoxynucleotide targeting of RNA cleavage by RNase H using chimeric methylphosphonodiester/phosphodiester structures. *Nucleic Acids Research.*, **20,** 763-770.

GOETHALS, M., RAES, A. & VAN BOGAERT, P.P. (1993). Use-dependent block of the pacemaker current I(f) in rabbit sinoatrial node cells by zatebradine (UL-FS 49). On the mode of action of sinus node inhibitors. *Circulation*, **88,** 2389-401.

GOLDSTEIN, B.J., BRAUZER, B., KENTSMITH, D., ROSENTHAL, S. & CHARALAMPOUS, K.D. (1984). Double-blind placebo-controlled multicenter evaluation of the efficacy and safety of nomifensine in depressed outpatients. *Journal of Clinical Psychiatry*, **45,** 52-5.

GREENBERG, M.E. & ZIFF, E.B. (1984). Stimulation of 3T3 cells induces transcription of the c-fos proto-oncogene. *Nature.*, **311,** 433-438.

GROSS-ISSEROFF, R., ISRAELI, M. & BIEGON, A. (1989). Autoradiographic analysis of tritiated imipramine binding in the human brain post mortem: effects of suicide. *Archives of General Psychiatry*, **46,** 237-41.

GRZANNA, R., DUBIN, J.R., DENT, G.W., JI, Z., ZHANG, W., SIEW PENG, H. & HARTIG, P.R. (1998). Intrastriatal and intraventricular injections of oligodeoxynucleotides in the rat brain: Tissue penetration, intracellular distribution and c-fos antisense effects. *Molecular Brain Research.*, **63,** 35-52.

GUITTON, D. (1999). Gaze shifts in three-dimensional space: A closer look at the superior colliculus. *Journal of Comparative Neurology.*, **413,** 77-82.

HALLIWELL, J.V. & ADAMS, P.R. (1982). Voltage-clamp analysis of muscarinic excitation in hippocampal neurons. *Brain Research*, **250,** 71-92.

HAMAMURA, T., LEE, Y., OHASHI, K., FUJIWARA, Y., MIKI, M., SUZUKI, H. & KURODA, S. (2000). A low dose of lithium chloride selectively induces Fos protein in the central nucleus of the amygdala of rat brain. *Progress in Neuro-Psychopharmacology & Biological Psychiatry.*, **24,** 285-294.

HARRIS, N.C. & CONSTANTI, A. (1995). Mechanism of block by ZD 7288 of the hyperpolarization-activated inward rectifying current in guinea pig substantia nigra neurons in vitro. *Journal of Neurophysiology*, **74,** 2366-78.

HEAL, D.J. (1990) The pharmacology of noradrenaline in the central nervous system. Eds: D.J. Heal and C.A. Marsden

HEAL, D.J., PROW, M.R. & BUCKETT, W.R. (1991). Effects of antidepressant drugs and electroconvulsive shock on pre- and postsynaptic alpha2-adrenoceptor function in the brain: Rapid down-regulation by sibutramine hydrochloride. *Psychopharmacologia.*, **103,** 251-257.

HENRY, B., CROSSMAN, A.R. & BROTCHIE, J.M. (1999). Effect of repeated L-DOPA, bromocriptine, or lisuride administration on preproenkephalin-A and preproenkephalin-B mRNA levels in the striatum of the 6-hydroxydopamine-lesioned rat. *Experimental Neurology.*, **155,** 204-220.

Hensler, J.G. (2003) Regulation of 5-HT1A receptor function in brain following agonist or antidepressant administration *Life Sciences* **72,** 1665-82.

HERDEGEN, T. & LEAH, J.D. (1998). Inducible and constitutive transcription factors in the mammalian nervous system: Control of gene expression by Jun, Fos and Krox, and CREB/ATF proteins. *Brain Research - Brain Research Reviews.*, **28,** 370-490.

HERRERA, D.G. & ROBERTSON, H.A. (1996). Activation of c-fos in the brain. *Progress in Neurobiology.*, **50,** 83-107.

HERTTING, G., AXELROD, J. & WHITBY, L.G. (1961). Effect of drugs on the uptake and metabolism of H^3-Norepinephrine. *Journal of Pharmacology & Experimental Therapeutics*, **134,** 146-153.

HERVAS, I., VILARO, M.T., ROMERO, L., SCORZA, M.C., MENGOD, G. & ARTIGAS, F. (2001). Desensitization of 5-HT(1A) autoreceptors by a low chronic fluoxetine dose effect of the concurrent administration of WAY-100635. *Neuropsychopharmacology.*, **24,** 11-20.

HESS, U.S., LYNCH, G. & GALL, C.M. (1995). Regional patterns of c-fos mRNA expression in rat hippocampus following exploration of a novel environment versus performance of a well-learned discrimination. *Journal of Neuroscience.*, **15,** 7796-7809.

HO, W.K., BROWN, H.F. & NOBLE, D. (1994). High selectivity of the i(f) channel to Na+ and K+ in rabbit isolated sinoatrial node cells. *Pflugers Archiv - European Journal of Physiology*, **426,** 68-74.

HOFFMAN, G.E. & LYO, D. (2002). Anatomical markers of activity in neuroendocrine systems: Are we all 'Fos-ed out'? *Journal of Neuroendocrinology.*, **14,** 259-268.

HOLETS, V.R. (1990). The anatomy and function of noradrenaline in the mammalian brain. In *Pharmacology of noradrenaline in the central nervous system.* eds Heal, D.J. & Marsden, C.A. pp. 1-40.

HOOVER, J.E., HOFFER, Z.S. & ALLOWAY, K.D. (2003). Projections from primary somatosensory cortex to the neostriatum: The role of somatotopic continuity in corticostriatal convergence. *Journal of Neurophysiology*, **89,** 1576-1587.

HOYER, D., HANNON, J.P. & MARTIN, G.R. (2002). Molecular, pharmacological and functional diversity of 5-HT receptors. *Pharmacology Biochemistry and Behavior*, **71,** 533-554.

HUSSY, N., DELEUZE, C., DESARMENIEN, M.G. & MOOS, F.C. (2000). Osmotic regulation of neuronal activity: A new role for taurine and glial cells in a hypothalamic neuroendocrine structure. *Progress in Neurobiology.*, **62,** 113-134.

INGRAM, S.L. & WILLIAMS, J.T. (1994). Opioid inhibition of Ih via adenylyl cyclase. *Neuron*, **13,** 179-86.

IRIBARREN, A.M., SPROAT, B.S., NEUNER, P., SULSTON, I., RYDER, U. & LAMOND, A.I. (1990). 2'-O-alkyl oligoribonucleotides as antisense probes. *Proceedings of the National Academy of Sciences of the United States of America*, **87,** 7747-7751.

ISHII, T.M., TAKANO, M., XIE, L.H., NOMA, A. & OHMORI, H. (1999). Molecular characterization of the hyperpolarization-activated cation channel in rabbit heart sinoatrial node. *Journal of Biological Chemistry*, **274,** 12835-9.

JOHANSSON, B., LINDSTROM, K. & FREDHOLM, B.B. (1994). Differences in the regional and cellular localization of c-fos messenger RNA induced by amphetamine, cocaine and caffeine in the rat. *Neuroscience*, **59,** 837-49.

JOHANSSON, I.-M., BJARTMAR, L., MARCUSSON, J., ROSS, S.B., SECKL, J.R. & OLSSON, T. (1998). Chronic amitriptyline treatment induces hippocampal NGFI-A, glucocorticoid receptor and mineralocorticoid receptor mRNA expression in rats. *Molecular Brain Research*, **62,** 92-95.

KANDIMALLA, E.R., SHAW, D.R. & AGRAWAL, S. (1998). Effects of phosphorothioate oligodeoxyribonucleotide and oligoribonucleotides on human complement and coagulation. *Bioorganic and Medicinal Chemistry Letters*, **8,** 2103-8.

KANG, J.X., LI, Y. & LEAF, A. (1997). Regulation of sodium channel gene expression by class I antiarrhythmic drugs and n - 3 polyunsaturated fatty acids in cultured neonatal rat cardiac myocytes. *Proceedings of the National Academy of Sciences of the United States of America*, **94,** 2724-2728.

KATHMANN, M., BAUER, U. & SCHLICKER, E. (1999). CB1 receptor density and CB1 receptor-mediated functional effects in rat hippocampus are decreased by an intracerebroventricularly administered antisense oligodeoxynucleotide. *Naunyn-Schmiedebergs Archives of Pharmacology.*, **360,** 421-427.

KAUPP, U.B. & SEIFERT, R. (2001). Molecular diversity of pacemaker ion channels. *Annual Review of Physiology*, **63,** 235-57.

KAWAI, K., YOKOTA, N. & YAMAWAKI, S. (1994). Effect of chronic tryptophan depletion on the circadian rhythm of wheel-running activity in rats. *Physiology & Behavior*, **55,** 1005-13.

KECK, M., WELT, T., MULLER, M., ERHARDT, A., OHL, F., TOSCHI, N., HOLSBOER, F. & SILLABER, I. (2002). Repetitive transcranial magnetic stimulation increases the release of dopamine in the mesolimbic and mesostriatal system. *Neuropharmacology*, **43,** 101.

KECK, M.E., SILLABER, I., EBNER, K., WELT, T., TOSCHI, N., KAEHLER, S.T., SINGEWALD, N., PHILIPPU, A., ELBEL, G.K. & WOTJAK ET, A. (2000). Acute transcranial magnetic stimulation of frontal brain regions selectively modulates the release of vasopressin, biogenic amines and amino acids in the rat brain. *The European Journal of Neuroscience*, **12,** 3713-3720.

KHAKH, B.S. & HENDERSON, G. (1998). Hyperpolarization-activated cationic currents (Ih) in neurones of the trigeminal mesencephalic nucleus of the rat. *Journal of Physiology*, **510,** 695-704.

KLERMAN, G.L., SCHILDKRAUT, J.J., HASENBUSH, L.L., GREENBLATT, M. & FRIEND, D.G. (1963). Clinical experience with dihydroxyphenylalanine (Dopa) in depression. *Journal of Psychiatric Research*, **1,** 289.

KNOTT, V.J., HOWSON, A.L., PERUGINI, M., RAVINDRAN, A.V. & YOUNG, S.N. (1999). The effect of acute tryptophan depletion and fenfluramine on quantitative EEG and mood in healthy male subjects. *Biological Psychiatry*, **46,** 229-38.

KOLESNIKOV, Y.A., PAN, Y.X., BABEY, A.M., JAIN, S., WILSON, R. & PASTERNAK, G.W. (1997). Functionally differentiating two neuronal nitric oxide synthase isoforms through antisense mapping: Evidence for opposing NO actions on morphine analgesia and tolerance. *Proceedings of the National Academy of Sciences of the United States of America*, **94,** 8220-8225.

KURRECK, J., WYSZKO, E., GILLEN, C. & ERDMANN, V.A. (2002). Design of antisense oligonucleotides stabilized by locked nucleic acids. *Nucleic Acids Research.*, **30,** 1911-1918.

LABINER, D.M., BUTLER, L.S., CAO, Z., HOSFORD, D.A., SHIN, C. & MCNAMARA, J.O. (1993). Induction of c-fos mRNA by kindled seizures: Complex relationship with neuronal burst firing. *Journal of Neuroscience.*, **13,** 744-751.

LAMMERS, C.H., DIAZ, J., SCHWARTZ, J.C. & SOKOLOFF, P. (2000). Selective increase of dopamine D_3 receptor gene expression as a common effect of chronic antidepressant treatments. *Molecular Psychiatry*, **5,** 378-88.

LAMPRECHT, R. & DUDAI, Y. (1995). Differential modulation of brain immediate early genes by intraperitoneal LiCl. *NeuroReport.*, **7,** 289-293.

LE CORRE, S.M., BURNET, P.W.J., MELLER, R., SHARP, T. & HARRISON, P.J. (1997). Critical issues in the antisense inhibition of brain gene expression in vivo:Experiences targetting the 5-$HT_{(1A)}$ receptor. *Neurochemistry International*, **31,** 349-362.

LE POUL, E., BONI, C., HANOUN, N., LAPORTE, A.M., LAARIS, N., CHAUVEAU, J., HAMON, M. & LANFUMEY, L. (2000). Differential adaptation of brain 5-HT(1A) and 5-HT(1B) receptors and 5-HT transporter in rats treated chronically with fluoxetine. *Neuropharmacology*, **39,** 110-122.

LEAH, J. & WILCE, P.A. (2002). The Egr transcription factors and their utility in mapping brain functioning. In *Handbook of Chemical Neuroanatomy*. eds Kaczmarek, L.K. & Robertson, H.A. pp. 309-328: Elsevier.

LEBEDEVA, I., BENIMETSKAYA, L., STEIN, C.A. & VILENCHIK, M. (2000). Cellular delivery of antisense oligonucleotides. *European Journal of Pharmaceutics and Biopharmaceutics*, **50,** 101-119.

LEONARD, B.E. (1997). The role of noradrenaline in depression: A review. *Journal of Psychopharmacology*, **11,** S39-S47.

LEVIN, A.A. (1999). A review of issues in the pharmacokinetics and toxicology of phosphorothioate antisense oligonucleotides. *Biochimica et Biophysica Acta (BBA) - Gene Structure and Expression*, **1489,** 69-84.

LINGJAERDE, O. (1963). Tetrabenazine (Nitoman) in the treatment of Psychoses. *Acta Psychiatrica Scandinavica*, **39,** 1-109.

LORINCZ, A., NOTOMI, T., TAMAS, G., SHIGEMOTO, R. & NUSSER, Z. (2002). Polarized and compartment-dependent distribution of HCN1 in pyramidal cell dendrites. *Nature Neuroscience*, **5,** 1185-1193.

LUDWIG, A., BUDDE, T., STIEBER, J., MOOSMANG, S., WAHL, C., HOLTHOFF, K., LANGEBARTELS, A., WOTJAK, C., MUNSCH, T., ZONG, X., FEIL, S., FEIL, R., LANCEL, M., CHIEN, K.R., KONNERTH, A., PAPE, H.C., BIEL, M. & HOFMANN, F. (2003). Absence epilepsy and sinus dysrhythmia in mice lacking the pacemaker channel HCN2. *EMBO Journal.*, **22,** 216-224.

LUDWIG, A., ZONG, X., JEGLITSCH, M., HOFMANN, F. & BIEL, M. (1998). A family of hyperpolarization-activated mammalian cation channels. *Nature*, **393,** 587-91.

LUDWIG, A., ZONG, X., STIEBER, J., HULLIN, R., HOFMANN, F. & BIEL, M. (1999). Two pacemaker channels from human heart with profoundly different activation kinetics. *EMBO Journal*, **18,** 2323-9.

LUTHI, A. & MCCORMICK, D.A. (1998). Periodicity of thalamic synchronized oscillations: the role of Ca2+-mediated upregulation of Ih. *Neuron*, **20,** 553-63.

MA, D., ZERANGUE, N., LIN, Y.F., COLLINS, A., YU, M., JAN, Y.N. & JAN, L.Y. (2001). Role of ER export signals in controlling surface potassium channel numbers. *Science*, **291,** 316-9.

MAJ, J., DZIEDZICKA-WASYLEWSKA, M., ROGOZ, R. & ROGOZ, Z. (1998). Effect of antidepressant drugs administered repeatedly on the dopamine D_3 receptors in the rat brain. *European Journal of Pharmacology*, **351,** 31-7.

MAJ, J., DZIEDZICKA-WASYLEWSKA, M., ROGOZ, R., ROGOZ, Z. & SKUZA, G. (1996). Antidepressant drugs given repeatedly change the binding of the dopamine D_2 receptor agonist, [^{3}H]N-0437, to dopamine D_2 receptors in the rat brain. *European Journal of Pharmacology*, **304,** 49-54.

MAJ, J., ROGOZ, Z., SKUZA, G. & KOLODZIEJCZYK, K. (1997). The behavioural effects of pramipexole, a novel dopamine receptor agonist. *European Journal of Pharmacology*, **324,** 31-7.

MAKKINK, K. (Personal communication). Localisation of Org 34167 binding sites in the rat.

MALKANI, S. & ROSEN, J.B. (2000). Differential expression of EGR-1 mRNA in the amygdala following diazepam in contextual fear conditioning. *Brain Research*, **860,** 53-63.

MANN, J.J., STANLEY, M., MCBRIDE, P.A. & MCEWEN, B.S. (1986). Increased serotonin2 and beta-adrenergic receptor binding in the frontal cortices of suicide victims. *Archives of General Psychiatry*, **43,** 954-9.

MARTINEZ, J., PATKANIOWSKA, A., URLAUB, H., LUHRMANN, R. & TUSCHL, T. (2002). Single-stranded antisense siRNAs guide target RNA cleavage in RNAi. *Cell.*, **110,** 563-574.

MASON, A. (Personal communication). Electrophysiological properties of Org 34167.

MATSUDA, Y., KAMIYA, K. & UCHIDA, K. (1998). Prediction of an antisense-effective target site on VEGFmRNA by using RNase H and a library of random oligonucleotides. *Analytica Chimica Acta.*, **365,** 55-58.

MATVEEVA, O., FELDEN, B., AUDLIN, S., GESTELAND, R.F. & ATKINS, J.F. (1997). A rapid in vitro method for obtaining RNA accessibility patterns for complementary DNA probes: Correlation with an intracellular pattern and known RNA structures. *Nucleic Acids Research.*, **25,** 5010-5016.

MAYER, M.L. & WESTBROOK, G.L. (1983). A voltage-clamp analysis of inward (anomalous) rectification in mouse spinal sensory ganglion neurones. *Journal of Physiology*, **340,** 19-45.

McCormick, D.A. & Bal, T. (1997). Sleep and arousal: thalamocortical mechanisms. *Annual Review of Neuroscience*, **20,** 185-215.

McCormick, D.A. & Pape, H.C. (1990a). Noradrenergic and serotonergic modulation of a hyperpolarization-activated cation current in thalamic relay neurones. *Journal of Physiology*, **431,** 319-42.

McCormick, D.A. & Pape, H.C. (1990b). Properties of a hyperpolarization-activated cation current and its role in rhythmic oscillation in thalamic relay neurones. *Journal of Physiology*, **431,** 291-318.

Mellor, J., Nicoll, R.A. & Schmitz, D. (2002). Mediation of hippocampal mossy fiber long-term potentiation by presynaptic I_h channels. *Science*, **295,** 143-147.

Metelev, V., Lisziewicz, J. & Agrawal, Sudhir (1994). Study of antisense oligonucleotide phosphorothioates containing segments of oligodeoxynucleotides and 2'-o- methyloligoribonucleotides. *Bioorganic & Medicinal Chemistry Letters*, **4,** 2929-2934.

Miller, H.L., Delgado, P.L., Salomon, R.M., Berman, R., Krystal, J.H., Heninger, G.R. & Charney, D.S. (1996). Clinical and biochemical effects of catecholamine depletion on antidepressant-induced remission of depression. *Archives of General Psychiatry*, **53,** 117-28.

Milner, N., Mir, K.U. & Southern, E.M. (1997). Selecting effective antisense reagents on combinatorial oligonucleotide arrays. *Nature Biotechnology.*, **15,** 537-541.

Mir, K.U. & Southern, E.M. (1999). Determining the influence of structure on hybridization using oligonucleotide arrays. *Nature Biotechnology.*, **17,** 788-792.

Monjaraz, E., Navarrete, A., Lopez-Santiago, L.F., Vega, A.V., Arias-Montano, J.A. & Cota, G. (2000). L-type calcium channel activity regulates sodium channel levels in rat pituitary GH3 cells. *Journal of Physiology.*, **523,** 45-55.

Monteggia, L.M., Eisch, A.J., Tang, M.D., Kaczmarek, L.K. & Nestler, E.J. (2000). Cloning and localization of the hyperpolarization-activated cyclic nucleotide-gated channel family in rat brain. *Brain Research. Molecular Brain Research*, **81,** 129-39.

Moosmang, S., Biel, M., Hofmann, F. & Ludwig, A. (1999). Differential distribution of four hyperpolarization-activated cation channels in mouse brain. *Biological Chemistry*, **380,** 975-80.

Moratalla, R., Robertson, H.A. & Graybiel, A.M. (1992). Dynamic regulation of NGFI-A (zif268, egr1) gene expression in the striatum. *Journal of Neuroscience.*, **12,** 2609-2622.

Morelli, M., Pinna, A., Ruiu, S. & Del Zompo, M. (1999). Induction of Fos-like-immunoreactivity in the central extended amygdala by antidepressant drugs. *Synapse*, **31,** 1-4.

Morinobu, S., Strausbaugh, H., Terwilliger, R. & Duman, R.S. (1997). Regulation of c-Fos and NGF1-A by antidepressant treatments. *Synapse.*, **25,** 313-320.

Mumby, D.G., Glenn, M.J., Nesbitt, C. & Kyriazis, D.A. (2002). Dissociation in retrograde memory for object discriminations and object recognition in rats with perirhinal cortex damage. *Behavioural Brain Research*, **132,** 215-226.

Murphy, T.H., Worley, P.F. & Baraban, J.M. (1991). L-type voltage-sensitive calcium channels mediate synaptic activation of immediate early genes. *Neuron*, **7,** 625-635.

Murray, C.J.L. & Lopez, A.D. (2001). The Global Burden of Disease: *World Health Organisation.*

Nalepa, I., Kreiner, G., Kowalska, M., Sanak, M., Zelek-Molik, A. & Vetulani, J. (2002). Repeated imipramine and electroconvulsive shock increase [alpha]1A-adrenoceptor mRNA level in rat prefrontal cortex. *European Journal of Pharmacology*, **444,** 151-159.

Nasevicius, A. & Ekker, S.C. (2000). Effective targeted gene 'knockdown' in zebrafish. *Nature Genetics.*, **26,** 216-220.

NISHINA, H., SATO, H., SUZUKI, T., SATO, M. & IBA, H. (1990). Isolation and characterization of fra-2, an additional member of the fos gene family. *Proceedings of the National Academy of Sciences of the United States of America*, **87**, 3619-3623.

NUTT, D. (1997). Mirtazapine: pharmacology in relation to adverse effects. *Acta Psychiatrica Scandinavica, Supplementum*, **391**, 31-7.

NUTT, D.J., FORSHALL, S., BELL, C., RICH, A., SANDFORD, J., NASH, J. & ARGYROPOULOS, S. (1999). Mechanisms of action of selective serotonin reuptake inhibitors in the treatment of psychiatric disorders. *European Neuropsychopharmacology*, **9**, S81-6.

O'DONOVAN, K.J., TOURTELLOTTE, W.G., MILBRANDT, J. & BARABAN, J.M. (1999). The EGR family of transcription-regulatory factors: Progress at the interface of molecular and systems neuroscience. *Trends in Neurosciences.*, **22**, 167-173.

O'NEILL, M.F., HICKS, C.A., SHAW, G., PARAMESWARAN, T., CARDWELL, G.P. & O'NEILL, M.J. (1998). Effects of 5-hydroxytryptamine2 receptor antagonism on the behavioral activation and immediate early gene expression induced by dizocilpine. *Journal of Pharmacology & Experimental Therapeutics.*, **286**, 839-846.

ONGUR, D. & PRICE, J.L. (2000). The organization of networks within the orbital and medial prefrontal cortex of rats, monkeys and humans. *Cerebral Cortex.*, **10**, 206-219.

OSTOW, M. (2002). Pramipexole for depression. *American Journal of Psychiatry*, **159**, 320-1.

PAPE, H.C. (1992). Adenosine promotes burst activity in guinea-pig geniculocortical neurones through two different ionic mechanisms. *Journal of Physiology*, **447**, 729-53.

PAPE, H.C. (1996). Queer current and pacemaker: the hyperpolarization-activated cation current in neurons. *Annual Review of Physiology*, **58**, 299-327.

PAPP, M., KLIMEK, V. & WILLNER, P. (1994). Parallel changes in dopamine D_2 receptor binding in limbic forebrain associated with chronic mild stress-induced anhedonia and its reversal by imipramine. *Psychopharmacology*, **115**, 441-6.

PAXINOS, G. & WATSON, C. (1986). *The Rat Brain in Stereotaxic Coordinates - 2nd edition*: Academic Press.

PENNYPACKER, K. (1998). AP-1 transcription factors: short- and long-term modulators of gene expression in the brain. *International Review of Neurobiology*, **42**, 169-97.

PRICE, L.H., MALISON, R.T., MCDOUGLE, C.J., MCCANCE-KATZ, E.F., OWEN, K.R. & HENINGER, G.R. (1997). Neurobiology of tryptophan depletion in depression: effects of m-chlorophenylpiperazine (mCPP). *Neuropsychopharmacology*, **17**, 342-50.

PRICE, L.H., MALISON, R.T., MCDOUGLE, C.J., PELTON, G.H. & HENINGER, G.R. (1998). The neurobiology of tryptophan depletion in depression: effects of intravenous tryptophan infusion. *Biological Psychiatry*, **43**, 339-47.

PROENZA, C., TRAN, N., ANGOLI, D., ZAHYNACZ, K., BALCAR, P. & ACCILI, E.A. (2002). Different Roles for the Cyclic Nucleotide Binding Domain and Amino Terminus in Assembly and Expression of Hyperpolarization-activated, Cyclic Nucleotide-gated Channels. *J. Biol. Chem.*, **277**, 29634-29642.

QIUYAN, Z., TEMSAMANI, J., IADAROLA, P.L., ZHIWEI, J. & AGRAWAL, S. (1996). Effect of Different Chemically Modified Oligodeoxynucleotides on Immune Stimulation. *Biochemical Pharmacology*, **51**, 173-182.

RAIT, V., SERGUEEV, D., SUMMERS, J., HE, K., HUANG, F., KRZYZANOWSKA, B. & SHAW, B.R. (1999a). Boranophosphate nucleic acids - A versatile DNA backbone. *Nucleosides & Nucleotides.*, **18**, 1379-1380.

RAIT, V.K. & SHAW, B.R. (1999b). Boranophosphates support the RNase H cleavage of polyribonucleotides. *Antisense & Nucleic Acid Drug Development.*, **9**, 53-60.

REINSTEIN, D.K. & ISAACSON, R.L. (1977). Clonidine sensitivity in the developing rat. *Brain Research.*, **135,** 378-82.

RICKELS, K., AMSTERDAM, J., CLARY, C., HASSMAN, J., LONDON, J., PUZZUOLI, G. & SCHWEIZER, E. (1990). Buspirone in depressed outpatients: a controlled study. *Psychopharmacology Bulletin*, **26,** 163-7.

ROBINSON, E.S.J. (Personal communication). Oligonucleotide infusion increases daily water intake.

ROBINSON, E.S.J., NUTT, D.J., JACKSON, H.C. & HUDSON, A.L. (2000). Behavioural and physiological effects induced by an infusion of antisense to alpha$_{2D}$-adrenoceptors in the rat. *British Journal of Pharmacology*, **130,** 153-159.

RODEN, D.M. & TAMKUN, M.M. (1994). Toward a molecular view of cardiac arrhythmogenesis. *Trends in Cardiovascular Medicine*, **4,** 278-285.

RUDORFER, M.V., GOLDEN, R.N. & POTTER, W.Z. (1984). Second-generation antidepressants. *Psychiatric Clinics of North America*, **7,** 519-34.

RUIGT, G., BERENDSEN, H., BLACKBURN-MUNRO, R., CONNICK, J., DIJCKS, F., EASON, S., GARRITSEN, A., VIJN, P. & ANDREWS, J. (Personal communication). Pharmacological Basic Data Report on Org 34167. Organon Scientific Development Group Release Report No. NL0012601.

RUTTER, J.J., GUNDLAH, C. & AUERBACH, S.B. (1994). Increase in extracellular serotonin produced by uptake inhibitors is enhanced after chronic treatment with fluoxetine. *Neuroscience Letters*, **171,** 183-6.

SAGAR, S.M., SHARP, F.R. & CURRAN, T. (1988). Expression of c-fos protein in brain: Metabolic mapping at the cellular level. *Science.*, **240,** 1328-1331.

SALMINEN, O., LAHTINEN, S. & AHTEE, L. (1996). Expression of Fos protein in various rat brain areas following acute nicotine and diazepam. *Pharmacology, Biochemistry & Behavior*, **54,** 241-8.

SANDS, H., GOREY-FERET, L.J., COCUZZA, A.J., HOBBS, F.W., CHIDESTER, D. & TRAINOR, G.L. (1994). Biodistribution and metabolism of internally 3H-labeled oligonucleotides. I. Comparison of a phosphodiester and a phosphorothioate. *Molecular Pharmacology.*, **45,** 932-943.

SANDS, H., GOREY-FERET, L.J., SIEW PENG, H., BAO, Y., COCUZZA, A.J., CHIDESTER, D. & HOBBS, F.W. (1995). Biodistribution and metabolism of internally 3H-labeled oligonucleotides. II. 3',5'-Blocked oligonucleotides. *Molecular Pharmacology.*, **47,** 636-646.

SANTORO, B., CHEN, S., LUTHI, A., PAVLIDIS, P., SHUMYATSKY, G.P., TIBBS, G.R. & SIEGELBAUM, S.A. (2000). Molecular and functional heterogeneity of hyperpolarization-activated pacemaker channels in the mouse CNS. *Journal of Neuroscience*, **20,** 5264-75.

SANTORO, B., GRANT, S.G., BARTSCH, D. & KANDEL, E.R. (1997). Interactive cloning with the SH3 domain of N-src identifies a new brain specific ion channel protein, with homology to eag and cyclic nucleotide-gated channels. *Proceedings of the National Academy of Sciences of the United States of America*, **94,** 14815-20.

SANTORO, B., LIU, D.T., YAO, H., BARTSCH, D., KANDEL, E.R., SIEGELBAUM, S.A. & TIBBS, G.R. (1998). Identification of a gene encoding a hyperpolarization-activated pacemaker channel of brain. *Cell*, **93,** 717-29.

SANTORO, B. & TIBBS, G.R. (1999). The HCN gene family: molecular basis of the hyperpolarization-activated pacemaker channels. *Annals of the New York Academy of Sciences*, **868,** 741-64.

SARIN, P.S., AGRAWAL, S., CIVEIRA, M.P., GOODCHILD, J., IKEUCHI, T. & ZAMECNIK, P.C. (1988). Inhibition of acquired immunodeficiency syndrome virus by oligodeoxynucleoside methylphosphonates. *Proceedings of the National Academy of Sciences of the United States of America*, **85,** 7448-7451.

SATOH, T.O. & YAMADA, M. (2002). Multiple inhibitory effects of zatebradine (UL-FS 49) on the electrophysiological properties of retinal rod photoreceptors. *Pflugers Archiv European Journal of Physiology*, **443,** 532-40.

SCHILDKRAUT, J.J. (1965). The catecholamine hypothesis of affective disorders: a review of supporting evidence. *American Journal of Psychiatry*, **122,** 509-22.

SCHILDKRAUT, J.J., GORDON, E.K. & DURELL, J. (1965). Catecholamine metabolism in affective disorders. I. Normetanephrine and VMA excretion in depressed patients treated with imipramine. *Journal of Psychiatric Research*, **3,** 213-28.

SCHLINGENSIEPEN, K.H., LUNO, K. & BRYSCH, W. (1991). High basal expression of the zif/268 immediate early gene in cortical layers IV and VI, in CA1 and in the corpus striatum - An in situ hybridization study. *Neuroscience Letters.*, **122,** 67-70.

SCHOBITZ, B., PEZESHKI, G., PROBST, J.C., REUL, J.M.H.M., SKUTELLA, T., STOHR, T., HOLSBOER, F. & SPANAGEL, R. (1997). Centrally administered oligodeoxynucleotides in rats: occurrence of non-specific effects. *European Journal of Pharmacology*, **331,** 97-107.

SEBENS, J.B., KOCH, T. & KORF, J. (1996). Lack of cross-tolerance between haloperidol and clozapine towards Fos-protein induction in rat forebrain regions. *European Journal of Pharmacology*, **315,** 269-75.

SEIFERT, R., SCHOLTEN, A., GAUSS, R., MINCHEVA, A., LICHTER, P. & KAUPP, U.B. (1999). Molecular characterization of a slowly gating human hyperpolarization-activated channel predominantly expressed in thalamus, heart, and testis. *Proceedings of the National Academy of Sciences of the United States of America*, **96,** 9391-6.

SERRA, G., ARGIOLAS, A., KLIMEK, V., FADDA, F. & GESSA, G.L. (1979). Chronic treatment with antidepressants prevents the inhibitory effect of small doses of apomorphine on dopamine synthesis and motor activity. *Life Sciences*, **25,** 415-23.

SHARP, J.W. (1997). Phencyclidine (PCP) acts at sigma sites to induce c-fos gene expression. *Brain Research*, **758,** 51-8.

SHAW, D.R., RUSTAGI, P.K., KANDIMALLA, E.R., MANNING, A.N., ZHIWEI, J. & AGRAWAL, S. (1997). Effects of Synthetic Oligonucleotides on Human Complement and Coagulation. *Biochemical Pharmacology*, **53,** 1123-1132.

SHEN, L.X., KANDIMALLA, E.R. & AGRAWAL, S. (1998). Impact of mixed-backbone oligonucleotides on target binding affinity and target cleaving specificity and selectivity by Escherichia coli RNase H. *Bioorganic & Medicinal Chemistry*, **6,** 1695-1705.

SHENG, M., MCFADDEN, G. & GREENBERG, M.E. (1990). Membrane depolarization and calcium induce c-fos transcription via phosphorylation of transcription factor CREB. *Neuron.*, **4,** 571-582.

SHERMAN, A.D. & PETTY, F. (1980). Neurochemical basis of the action of antidepressants on learned helplessness. *Behavioral & Neural Biology.*, **30,** 119-134.

SHI, W., WYMORE, R., YU, H., WU, J., WYMORE, R.T., PAN, Z., ROBINSON, R.B., DIXON, J.E., MCKINNON, D. & COHEN, I.S. (1999). Distribution and prevalence of hyperpolarization-activated cation channel (HCN) mRNA expression in cardiac tissues. *Circulation Research*, **85,** e1-6.

SHIN, K.S., ROTHBERG, B.S. & YELLEN, G. (2001). Blocker state dependence and trapping in hyperpolarization-activated cation channels: evidence for an intracellular activation gate. *Journal of General Physiology*, **117,** 91-101.

SHOPSIN, B., FRIEDMAN, E. & GERSHON, S. (1976). Parachlorophenylalanine reversal of tranylcypromine effects in depressed patients. *Archives of General Psychiatry*, **33,** 811-9.

SHOPSIN, B., GERSHON, S., GOLDSTEIN, M., FRIEDMAN, E. & WILK, S. (1975). Use of synthesis inhibitors in defining a role for biogenic amines during imipramine treatment in depressed patients. *Psychopharmacology Communications*, **1,** 239-49.

SINGEWALD, N., SALCHNER, P. & SHARP, T. (2003). Induction of c-fos expression in specific areas of the fear circuitry in rat forebrain by anxiogenic drugs. *Biological Psychiatry*, **53,** 275-283.

SLEW PENG, H., BAO, Y., LESHER, T., MALHOTRA, R., MA, L.Y., FLUHARTY, S.J. & SAKAI, R.R. (1998). Mapping of RNA accessible sites for antisense experiments with oligonucleotide libraries. *Nature Biotechnology.*, **16,** 59-63.

SMITH, L., ANDERSEN, K.B., HOVGAARD, L. & JAROSZEWSKI, J.W. (2000). Rational selection of antisense oligonucleotide sequences. *European Journal of Pharmaceutical Sciences*, **11,** 191-198.

SOHAIL, M., HOCHEGGER, H., KLOTZBUCHER, A., LE GUELLEC, R., HUNT, T. & SOUTHERN, E.M. (2001). Antisense oligonucleotides selected by hybridisation to scanning arrays are effective reagents in vivo. *Nucleic Acids Research.*, **29,** 2041-2051.

SOHAIL, M. & SOUTHERN, E.M. (2000). Selecting optimal antisense reagents. *Advanced Drug Delivery Reviews*, **44,** 23-34.

SPENCER, C.M. & HOUPT, T.A. (2001). Dynamics of c-fos and ICER mRNA expression in rat forebrain following lithium chloride injection. *Molecular Brain Research*, **93,** 113-126.

SPYRAKI, C. & FIBIGER, H.C. (1980). Functional evidence for subsensitivity of noradrenergic alpha 2 receptors after chronic desipramine treatment. *Life Sciences*, **27,** 1863-7.

STAHL, S.M. (1998). Mechanism of action of serotonin selective reuptake inhibitors. Serotonin receptors and pathways mediate therapeutic effects and side effects. *Journal of Affective Disorders*, **51,** 215-35.

STAHL, S.M., KAISER, L., ROESCHEN, J., KEPPEL-HESSLINK, J.M. & ORAZEM, J. (1998). Effectiveness of ipsapirone, a 5-HT_{1A} partial agonist, in major depressive disorder: support for the role of 5-HT_{1A} receptors in the mechanism of action of serotonergic antidepressants. *International Journal of Neuropsychopharmacology*, **1,** 11-18.

STANLEY, M. & MANN, J.J. (1983). Increased serotonin-2 binding sites in frontal cortex of suicide victims. *Lancet*, **1,** 214-6.

STECIUK, M., KRAM, M., KRAMER, G.L. & PETTY, F. (1999). Decrease in stress-induced c-Fos-like immunoreactivity in the lateral septal nucleus of learned helpless rats. *Brain Research.*, **822,** 256-259.

STEIN, C.A. (1999). Two problems in antisense biotechnology: in vitro delivery and the design of antisense experiments. *Biochimica et Biophysica Acta (BBA) - Gene Structure and Expression*, **1489,** 45-52.

STEIN, C.A. & CHENG, Y.C. (1993). Antisense oligonucleotides as therapeutic agents - Is the bullet really magical? *Science.*, **261,** 1004-1012.

STRAFELLA, A.P., PAUS, T., BARRETT, J. & DAGHER, A. (2001). Repetitive transcranial magnetic stimulation of the human prefrontal cortex induces dopamine release in the caudate nucleus. *J Neurosci*, **21,** RC157.

STRECKER, R.E., MORAIRTY, S., THAKKAR, M.M., PORKKA-HEISKANEN, T., BASHEER, R., DAUPHIN, L.J., RAINNIE, D.G., PORTAS, C.M., GREENE, R.W. & MCCARLEY, R.W. (2000). Adenosinergic modulation of basal forebrain and preoptic/anterior hypothalamic neuronal activity in the control of behavioral state. *Behavioural Brain Research*, **115,** 183-204.

SULSER, F., BICKEL, M.H. & BRODIE, B.B. (1964). The action of desmethylimipramine in counteracting sedation and cholinergic effects of reserpine-like drugs. *Journal of Pharmacology & Experimental Therapeutics*, **144,** 321-330.

SULSER, F., VETULANI, J. & MOBLEY, P.L. (1978). Mode of action of antidepressant drugs. *Biochemical Pharmacology*, **27,** 257-61.

SUMMERTON, J. (1999). Morpholino antisense oligomers: The case for an RNase H-independent structural type. *Biochimica et Biophysica Acta - Gene Structure and Expression*, **1489,** 141-158.

SVOBODA, K.R. & LUPICA, C.R. (1998). Opioid inhibition of hippocampal interneurons via modulation of potassium and hyperpolarization-activated cation (Ih) currents. *Journal of Neuroscience*, **18,** 7084-98.

TABARA, H., SARKISSIAN, M., KELLY, W.G., FLEENOR, J., GRISHOK, A., TIMMONS, L., FIRE, A. & MELLO, C.C. (1999). The rde-1 gene, RNA interference, and transposon silencing in C. elegans. *Cell.*, **99,** 123-132.

TEKIN, S. & CUMMINGS, J.L. (2002). Frontal-subcortical neuronal circuits and clinical neuropsychiatry: An update. *Journal of Psychosomatic Research*, **53,** 647-654.

THASE, M.E. (1999). Antidepressant treatment of the depressed patient with insomnia. *Journal of Clinical Psychiatry.*, **60,** 28-31.

THIRIET, N., ZWILLER, J. & ALI, S.F. (2001). Induction of the immediate early genes egr-1 and c-fos by methamphetamine in mouse brain. *Brain Research*, **919,** 31-40.

TORRES, G., HOROWITZ, J.M., LAFLAMME, N. & RIVEST, S. (1998). Fluoxetine induces the transcription of genes encoding c-fos, corticotropin-releasing factor and its type 1 receptor in rat brain. *Neuroscience.*, **87,** 463-477.

TOULME, J.J. (1992). Artificial regulation of gene expression by complementary oligonucleotides - An overview. In *Antisense RNA and DNA*. ed Murray, J.A. pp. 175-194. New York: Wiley-Liss.

TRULLAS, R. & SKOLNICK, P. (1990). Functional antagonists at the NMDA receptor complex exhibit antidepressant actions. *European Journal of Pharmacology*, **185,** 1-10.

TURGEON, S.M. & CASE, L.C. (2001). The delayed effects of phencyclidine enhance amphetamine-induced behavior and striatal C-Fos expression in the rat. *Neuroscience*, **91,** 1265-75.

ULENS, C. & TYTGAT, J. (2001a). Functional heteromerization of HCN1 and HCN2 pacemaker channels. *Journal of Biological Chemistry*, **276,** 6069-72.

ULENS, C. & TYTGAT, J. (2001b). Gi- and Gs-coupled receptors up-regulate the cAMP cascade to modulate HCN2, but not HCN1 pacemaker channels. *Pflugers Archiv European Journal of Physiology*, **442,** 928-42.

VACCARI, T., MORONI, A., ROCCHI, M., GORZA, L., BIANCHI, M.E., BELTRAME, M. & DIFRANCESCO, D. (1999). The human gene coding for HCN2, a pacemaker channel of the heart. *Biochimica et Biophysica Acta*, **1446,** 419-25.

VANBERKEL, J.H. (Personal communication). Investigator's Brochure on Org 34167, Edition No. 2.

VANBERKEL, J.H. (2001). Investigator's Brochure on Org 34167, Edition No. 2.

VARGAS, G. & LUCERO, M.T. (2002). Modulation by PKA of the hyperpolarization-activated current (I<inf>h</inf>) in cultured rat olfactory receptor neurons. *Journal of Membrane Biology.*, **188,** 115-125.

VETULANI, J. & NALEPA, I. (2000). Antidepressants: past, present and future. *European Journal of Pharmacology*, **405,** 351-63.

VINADER-CAEROLS, C., COLLADO, P., SEGOVIA, S. & GUILLAMON, A. (2000). Estradiol masculinizes the posteromedial cortical nucleus of the amygdala in the rat. *Brain Research Bulletin*, **53,** 269-273.

WAHLESTEDT, C., GOLANOV, E., YAMAMOTO, S., YEE, F., ERICSON, H., YOO, H., INTURRISI, C.E. & REIS, D.J. (1993). Antisense oligodeoxynucleotides to NMDA-R1 receptor channel protect cortical neurons from excitotoxicity and reduce focal ischaemic infarctions. *Nature.*, **363,** 260-263.

WAINGER, B.J., DEGENNARO, M., SANTORO, B., SIEGELBAUM, S.A. & TIBBS, G.R. (2001). Molecular mechanism of cAMP modulation of HCN pacemaker channels. *Nature*, **411,** 805-10.

WANG, J., CHEN, S. & SIEGELBAUM, S.A. (2001). Regulation of hyperpolarization-activated HCN channel gating and cAMP modulation due to interactions of COOH terminus and core transmembrane regions. *Journal of General Physiology*, **118,** 237-50.

WARMKE, J.W. & GANETZKY, B. (1994). A family of potassium channel genes related to eag in Drosophila and mammals. *Proceedings of the National Academy of Sciences of the United States of America*, **91,** 3438-42.

WEDZONY, K. & CZYRAK, A. (1996). Competitive and non-competitive NMDA receptor antagonists induce c-Fos expression in the rat anterior cingulate cortex. *Journal of Physiology and Pharmacology*, **47,** 525-33.

WEISSMAN, M.M., BLAND, R.C., CANINO, G.J., FARAVELLI, C., GREENWALD, S., HWU, H.G., JOYCE, P.R., KARAM, E.G., LEE, C.K., LELLOUCH, J., LEPINE, J.P., NEWMAN, S.C., RUBIO-STIPEC, M., WELLS, J.E., WICKRAMARATNE, P.J., WITTCHEN, H.U. & YEH, E.K. (1996). Cross-national epidemiology of major depression and bipolar disorder. *Journal of American Medical Association*, **276,** 293-299.

WILLNER, P., LAPPAS, S., CHEETA, S. & MUSCAT, R. (1994). Reversal of stress-induced anhedonia by the dopamine receptor agonist, pramipexole. *Psychopharmacology*, **115,** 454-62.

WOLLMUTH, L.P. & HILLE, B. (1992). Ionic selectivity of Ih channels of rod photoreceptors in tiger salamanders. *Journal of General Physiology*, **100,** 749-65.

WOZNIAK, D.F., BROSNAN-WATTERS, G., NARDI, A., MCEWEN, M., CORSO, T.D., OLNEY, J.W. & FIX, A.S. (1996). MK-801 neurotoxicity in male mice: histologic effects and chronic impairment in spatial learning. *Brain Research*, **707,** 165-179.

WRZESINSKI, J., LEGIEWICZ, M. & CIESIOLKA, J. (2000). Mapping of accessible sites for oligonucleotide hybridization on hepatitis delta virus ribozymes. *Nucleic Acids Research.*, **28,** 1785-1793.

YEUNG, S.Y., MILLAR, J.A. & MATHIE, A. (1999). Inhibition of neuronal K(v) potassium currents by the antidepressant drug, fluoxetine. *British Journal of Pharmacology*, **128,** 1609-1615.

YOUNG, S.N., ERVIN, F.R., PIHL, R.O. & FINN, P. (1989). Biochemical aspects of tryptophan depletion in primates. *Psychopharmacology*, **98,** 508-11.

YOUNG, S.T., PORRINO, L.J. & IADAROLA, M.J. (1991). Cocaine induces striatal c-Fos-immunoreactive proteins via dopaminergic D1 receptors. *Proceedings of the National Academy of Sciences of the United States of America*, **88,** 1291-1295.

YU, D., ZHU, F.-G., BHAGAT, L., WANG, H., KANDIMALLA, E.R., ZHANG, R. & AGRAWAL, S. (2002). Potent CpG oligonucleotides containing phosphodiester linkages: in vitro and in vivo immunostimulatory properties. *Biochemical and Biophysical Research Communications*, **297,** 83-90.

YU, H., CHANG, F. & COHEN, I.S. (1993). Pacemaker current exists in ventricular myocytes. *Circulation Research*, **72,** 232-6.

ZAMARATSKI, E., PRADEEPKUMAR, P.I. & CHATTOPADHYAYA, J. (2001). A critical survey of the structure-function of the antisense oligo/RNA heteroduplex as substrate for RNase H. *Journal of Biochemical and Biophysical Methods*, **48,** 189-208.

ZAMECNIK, P.C. & STEPHENSON, M.L. (1978). Inhibition of Rous sarcoma virus replication and cell transformation by a specific oligodeoxynucleotide. *Proceedings of the National Academy of Sciences of the United States of America.*, **75,** 280-4.

ZANG, Z., FLORIN, W. & CREESE, I. (1994). Reduction in muscarinic receptors by antisense oligodeoxynucleotide. *Biochemical Pharmacology.*, **48,** 225-228.

ZANGENEHPOUR, S. & CHAUDHURI, A. (2002). Differential induction and decay curves of c-fos and zif268 revealed through dual activity maps. *Molecular Brain Research.*, **109,** 221-225.

ZERIAL, M., TOSCHI, L., RYSECK, R.P., SCHUERMANN, M., MULLER, R. & BRAVO, R. (1989). The product of a novel growth factor activated gene, fos B, interacts with JUN proteins enhancing their DNA binding activity. *EMBO Journal.*, **8,** 805-813.

ZHOU, L.W., ZHANG, S.P., QIN, Z.H. & WEISS, B. (1994). In vivo administration of an oligodeoxynucleotide antisense to the D2 dopamine receptor messenger RNA inhibits D2 dopamine receptor-mediated behavior and the expression of D2 dopamine receptors in mouse striatum. *Journal of Pharmacology & Experimental Therapeutics.*, **268,** 1015-1023.

ZIOLKOWSKA, B. & PRZEWLOCKI, R. (2002). Methods used in inducible transcription factor studies: focus on mRNA. In *Handbook of Chemical Neuroanatomy*. eds Kaczmarek, L.K. & Robertson, H.A. pp. 1-38: Elsevier.

ZONG, X., STIEBER, J., LUDWIG, A., HOFMANN, F. & BIEL, M. (2001). A single histidine residue determines the pH sensitivity of the pacemaker channel HCN2. *Journal of Biological Chemistry*, **276,** 6313-9.

Appendices

Appendix A – Buffers used

10 mM Phosphate Buffered Saline Solution pH 7.4

1. Dissolve 2.76 g di-sodium hydrogen orthophosphate in 100 ml dH_20 (Solution A).
2. In a separate container, dissolve 0.83 g sodium di-hydrogen orthophosphate in 30 ml dH_20 (Solution B).
3. Add 80.8 ml Solution A and 19.0 ml Solution B to 1900 ml dH_20 to make a final volume of 2 L.
4. Finally, add 18 g NaCl to the final solution.

4 % Paraformaldehyde

1. Add 24 g paraformaldehyde and 5.4 g NaCl in 600 ml DEPC-treated H_20.
2. Heat to approximately 80 °C to dissolve the paraformaldehyde.
3. When dissolved add 36 ml NaOH to clear solution.

Paraformaldehyde can be stored for 2 weeks at 4 °C

Gelatin subbing solution

1. Add 7.5 g gelatin and 0.9 g chromic potassium sulphate in 1.5 L dH_20.
2. Stir and heat solution (do not allow to boil) for 2 h to dissolve.

Acetic anhydride solution

1. Dissolve 11.15 g triethanolamine and 5.4 g NaCl in 600 ml DEPC-treated H_20.
2. Add 1.5 ml acetic anhydride and stir solution.
3. Adjust final pH to 8 with 10M NaOH (approximately 5 ml NaOH required for 600 ml)

Acid methanol

1. Add 20 ml concentrated hydrochloric acid (HCl) to 1 L methanol

20x standard sodium citrate solution

1. Dissolve 439.3 g NaCl in 2.5 L DEPC-treated H_20 to give a final concentration of 3 M.
2. Add 220.5 g trisodium citrate to create a final concentration of 0.3 M.
3. Adjust pH to 7 with NaOH.

'Maximalist' hybridisation solution

1. Into a sterile screw capped 50 ml tube add 25 ml formamide and 5 g dextran sulphate.
2. Shake well to speed up dissolving process.
3. Add 10 ml 20x SSC, 5 ml Denhardt's solution, 1 ml 10 mg / ml Salmon testes DNA, 0.5 ml 10 mg / ml Poly-A and 1 ml 1 M DTT.
4. To dissolve stir and heat (do not allow to boil).
5. Once dissolved make up to a final volume of 50 ml with DEPC-treated H_20.

Maximalist hybridisation buffer is stable for 6 months stored at 4°C.

0.2 and 0.4 % glacial acetic acid in ethanol

1. Add 1 ml glacial acetic acid to 400 ml 100 % ethanol (0.2 % glacial acetic acid in ethanol).
2. In a separate container add 1.6 ml glacial acetic acid to 400 ml 100 % ethanol (0.4 % glacial acetic acid).

0.25 % Cresyl Violet

1. Add 4.8 ml glacial acetic acid to 400 ml deionised H_20.
2. In a separate container dissolve 2.7 g sodium acetate in 100 ml deionised H_20.
3. Add the solutions together and stir to produce 200 mM acetate buffer.
4. Finally add 1 g cresyl violet to 400 ml 200 mM acetate buffer and stir continuously for 7 days.

3 M sodium acetate, pH 5.5

1. Dissolve 2.46 g sodium acetate in 10 ml DEPC-treated H_20.
2. 2. Adjust to a final pH of 5.5 with concentrated HCl.

0.1 M acetate buffer, pH 6.0

1. Dissolve 0.82 g sodium acetate in 100 ml dH_20 then adjust to pH 6.0 by adding glacial acetic acid.

Acetylcholinesterase incubating medium

1. Firstly, prepare 0.1 M acetate buffer, pH 6, 0.1 M sodium citrate and 0.03 M cupric sulphate solutions (all in dH_20)
2. To make 20 ml add 0.01 g acetylthiocholine iodide to 13 ml 0.1 M acetate buffer
3. Mix well then add 1 ml 0.1 M sodium citrate, 2 ml 0.03 M cupric sulphate, 4 ml dH_20 and 12 mg ethopropazine (inhibitor of butylcholinesterase).

Appendix B – Table of in situ hybridisation probes used during present study

Probe name	*Sequence*	*Complementary sequence*	*Accession number*	*Development time (days)*
5-HT_{1A}	5' – TTG CGC TCA TTT TTT CTC TCC AAG CAG GCG GGG GCA TAG GAG TTA – 3'	*Rattus norvegius* 5-HT_{1A} Bases 939 – 983	NM_012585	14 - 18
β-actin	5' - TGG ACC GGG ACG GAG GAG CTG CAA GGA GGT TGT ACT CGC GGG TGG – 3'	*Rattus norvegius* β-actin Bases 251 – 295	V01217	7
c-fos 1	5'- GGC TCC CAG TCT GCT GCA TAG AAG GAA CCA GAC AGG TCC ACA TCT GGC -3'	*Rattus norvegius c-fos* Bases 1001 - 1048	X06769	12
c-fos 2	5'- ACT GCA GCG GGA GGA TGA CGC CTC GTA GTC CGC GTT GAA ACC CGA GAA -3'	*Rattus norvegius c-fos* Bases 141 - 188	X06769	12
Egr-1	5' – TGG GAG CCC GAC TGA GTG GCG AAG GCT TTG ATA GTG GAT AGT GGA – 3'	*Rattus norvegius* NGFI-A Bases 2341 – 2585	M18416	7
HCN 1	5'- GCA GTT TTA ACC CTT TCC TGC TCC TTC TCC ACC GCC TTC T -3'	*Rattus norvegius* HCN 1 Bases 391 – 430	NM_053375	14 - 18
HCN 2	5'- CAC GCT GGC CAA GCT CTG CCT GCT GCA CCA TCT CAC GGT CAT ATT -3'	*Mus musculus* HCN 2 Bases 2041 – 2085	NM_008226	14 - 18
HCN 3	5' - AGG CGT CTC GCG TGC AGG GGT CGC CGC TTC G - 3'	*Mus musculus* HCN 3 Bases 134 - 164	NM_008227	70 - 77
HCN 4	5' - AGG CTG TAC AGC CGC TTG CGC ATG GAC GGC GGC AGC TTG TCC ATG -3'	*Homo sapiens* HCN 4 Bases 566 - 610	NM_005477	70 - 77

Appendix C – In situ probe validation

5-HT_{1A} probe validation

Figure C.1: *In situ* autoradiograms for 5-HT_{1A} probe validation.

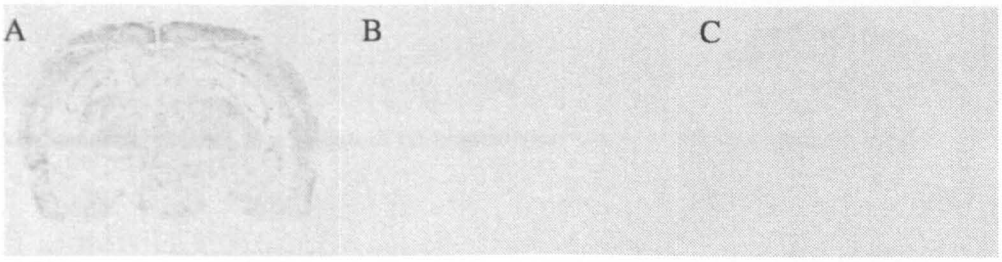

A = Standard protocol, B = RNase A pre-treated tissue and C = excess unlabelled probe

β-actin probe validation

Figure C.2: *In situ* autoradiograms for β-actin probe validation.

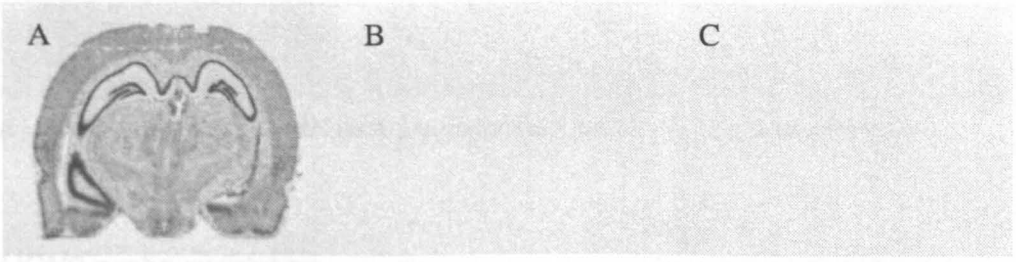

A = Standard protocol, B = RNase A pre-treated tissue and C = excess unlabelled probe

c-fos probe validation

Figure C.3: *In situ* autoradiograms for *c-fos* probe validation.

A = Standard protocol, B = RNase A pre-treated tissue and C = excess unlabelled probe

Egr-1 probe validation

Figure C.4: *In situ* autoradiograms for Egr-1 probe.

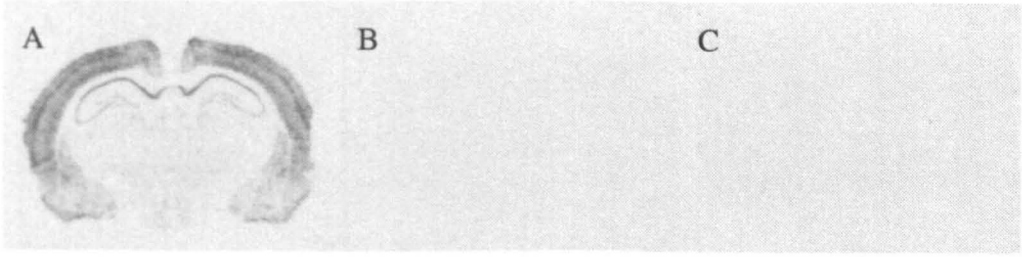

A = Standard protocol, B = RNase A pretreated tissue and C = excess unlabelled probe

HCN1 probe validation

Figure C.5: *In situ* autoradiograms for HCN1 probe validation.

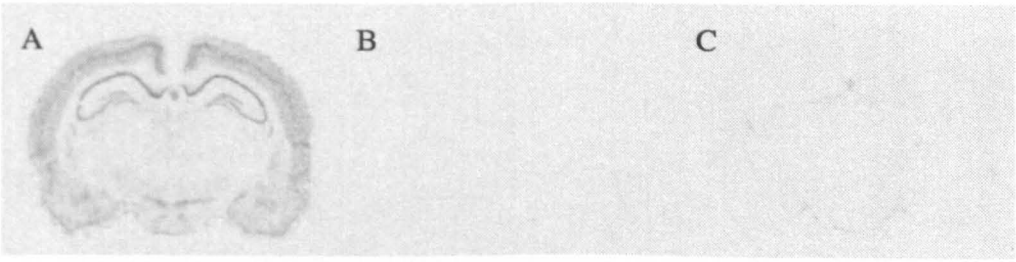

A = Standard protocol, B = RNase A pretreated tissue and C = excess unlabelled probe

HCN2 probe validation

Figure C.6: *In situ* autoradiograms for HCN2 probe validation.

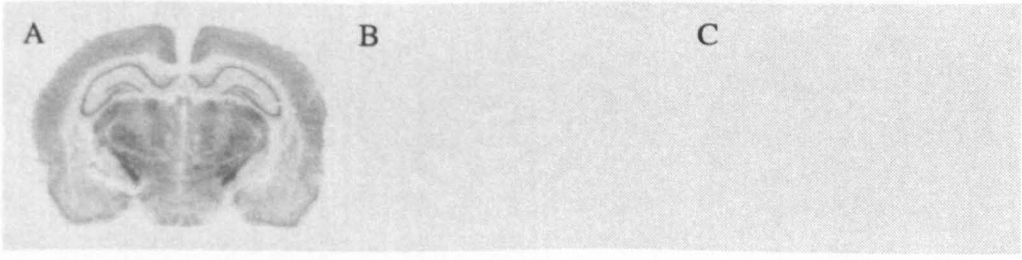

A = Standard protocolControl, B = RNase A pretreated tissue and C = excess unlabelled probe

HCN3 probe validation

Figure C.7: *In situ* autoradiograms for HCN3 probe validation.

A = Control, B = RNase A pretreated tissue and C = excess unlabelled probe

Appendix D – Raw data for figures and tables represented as % vehicle

Tables D.1 Raw data of chronic antidepressant studies A – C (4.7 to 4 mm relative to bregma)

5-HT1A mRNA expression	Vehicle Average	sem	Lithium Average	sem
M2 Ctx	57.13	12.33	57.73	3.95
Prelimbic ctx	62.98	11.38	61.17	4.61
VM orbital ctx	68.39	9.74	73.18	2.48
Ant. Olfact nuc	33.40	11.68	44.74	1.86

HCN1 mRNA expression	Vehicle Average	sem	Lithium Average	sem
M2 Ctx	16.61	0.65	16.87	1.33
Prelimbic ctx	20.99	1.21	21.15	1.77
VM orbital ctx	19.94	1.89	22.26	1.97
Ant. Olfact nuc	39.40	1.45	39.81	1.89

HCN2 mRNA expression	Vehicle Average	sem	Lithium Average	sem
M2 Ctx	127.33	2.94	122.16	2.40
Prelimbic ctx	140.10	5.79	132.79	4.63
VM orbital ctx	157.87	2.48	154.95	3.11
Ant. Olfact nuc	164.89	7.73	150.77	3.34

HCN3 mRNA expression	Vehicle Average	sem	Lithium Average	sem
M2 Ctx	63.46	8.35	62.11	12.25
Prelimbic ctx	103.45	11.07	101.78	23.19
VM orbital ctx	100.11	10.48	103.48	21.46
Ant. Olfact nuc	150.23	8.45	157.36	9.98

5-HT1A mRNA expression	Vehicle Average	sem	Fluoxetine Average	sem	Mirtazapine Average	sem
M2 Ctx	33.49	2.34	34.05	1.00	32.24	2.06
Prelimbic ctx	61.36	4.08	64.32	2.55	62.19	3.17
VM orbital ctx	55.30	4.16	64.94	3.49	57.12	2.25
Ant. Olfact nuc	58.62	5.78	73.08	5.80	73.18	3.94

HCN1 mRNA expression	Vehicle Average	sem	Fluoxetine Average	sem	Mirtazapine Average	sem
M2 Ctx	36.93	0.72	19.55	1.31	16.77	0.68
Prelimbic ctx	43.96	1.21	24.59	1.19	22.09	0.99
VM orbital ctx	48.48	0.84	27.27	1.71	23.89	0.60
Ant. Olfact nuc	41.33	2.52	22.56	1.51	19.86	0.60

HCN2 mRNA expression	Vehicle Average	sem	Fluoxetine Average	sem	Mirtazapine Average	sem
M2 Ctx	209.11	7.61	169.81	1.55	169.30	5.07
Prelimbic ctx	278.12	10.11	225.25	3.73	225.46	6.86
VM orbital ctx	232.94	10.15	187.33	4.12	187.18	7.68
Ant. Olfact nuc	204.28	2.11	179.08	7.21	179.34	4.78

HCN3 mRNA expression	Vehicle Average	sem	Fluoxetine Average	sem	Mirtazapine Average	sem
M2 Ctx	57.20	6.27	62.20	4.32	62.72	3.09
Prelimbic ctx	89.20	12.02	89.40	6.84	87.42	3.86
VM orbital ctx	83.46	10.71	87.86	6.50	85.81	3.53
Ant. Olfact nuc	100.82	7.57	121.14	4.86	125.21	2.93

5-HT1A mRNA expression	Vehicle Average	sem	Org 34167 Average	sem
M2 Ctx	56.43	2.17	64.46	2.63
Prelimbic ctx	81.90	4.85	82.79	1.95
VM orbital ctx	78.11	3.73	82.16	2.97
Ant. Olfact nuc	38.26	4.97	35.06	2.24

HCN1 mRNA expression	Vehicle Average	sem	Org 34167 Average	sem
M2 Ctx	24.34	2.87	24.68	1.08
Prelimbic ctx	32.47	3.33	33.18	2.67
VM orbital ctx	32.54	4.09	31.90	2.61
Ant. Olfact nuc	39.12	3.17	38.90	1.73

HCN2 mRNA expression	Vehicle Average	sem	Org 34167 Average	sem
M2 Ctx	154.91	4.05	152.53	6.87
Prelimbic ctx	165.00	5.88	162.01	2.52
VM orbital ctx	176.17	3.92	175.28	3.96
Ant. Olfact nuc	173.96	2.44	175.40	5.37

HCN3 mRNA expression	Vehicle Average	sem	Org 34167 Average	sem
M2 Ctx	52.43	7.11	38.65	4.61
Prelimbic ctx	81.27	7.69	75.42	10.40
VM orbital ctx	82.27	10.92	67.40	8.89
Ant. Olfact nuc	120.86	4.15	120.60	8.29

Tables D.2 Raw data of chronic antidepressant studies A – C (2.2 to 1.5 mm relative to bregma)

5-HT1A mRNA expression	Vehicle Average	sem	Org34167 Average	sem
Cing ctx	58.10	2.61	51.92	2.07
Ins ctx	34.07	1.20	33.13	1.78
Pir ctx	55.20	2.39	50.62	1.03
Septum	91.37	2.88	94.25	2.98
DM str	13.70	2.20	16.51	1.27
DL str	14.20	2.58	16.31	0.73
VL Str	10.55	1.94	15.18	1.48
VM str	11.56	1.82	15.21	1.23
AcbC	11.20	1.43	14.80	1.53
AcbSh	12.29	3.06	11.92	1.39

HCN1 mRNA expression	Vehicle Average	SD	n	sem	Org34167 Average	SD	n	sem
Cing ctx	30.76	4.11	6.00	1.68	29.88	6.24	6.00	2.55
Ins ctx	26.19	5.26	6.00	2.15	21.40	3.02	6.00	1.23
Pir ctx	45.32	9.33	6.00	3.81	37.90	6.14	6.00	2.51
Septum	41.24	8.94	6.00	3.65	38.15	9.19	6.00	3.75
DM str	6.05	0.90	6.00	0.37	6.70	1.48	6.00	0.60
DL str	5.76	1.08	6.00	0.44	6.96	1.25	6.00	0.51
VL Str	5.27	0.88	6.00	0.36	6.33	0.82	6.00	0.34
VM str	5.59	0.68	6.00	0.28	6.41	1.65	6.00	0.67
AcbC	6.37	0.39	6.00	0.16	7.09	1.46	6.00	0.60
AcbSh	7.27	2.21	6.00	0.90	6.37	1.18	6.00	0.48

HCN2 mRNA expression	Vehicle Average	sem	Org34167 Average	sem
Cing ctx	228.68	9.66	225.12	6.23
Ins ctx	155.93	6.46	121.86	3.46
Pir ctx	308.16	15.71	250.25	6.82
Septum	184.75	6.55	172.05	5.90
DM str	156.52	5.88	148.11	4.70
DL str	195.31	7.65	190.20	4.58
VL Str	162.56	8.86	150.45	4.58
VM str	125.89	6.00	110.74	4.78
AcbC	131.85	5.44	107.52	5.09
AcbSh	144.33	4.28	108.03	4.52

HCN3 mRNA expression	Vehicle Average	sem	Org34167 Average	sem
Cing ctx	27.62	1.07	28.20	2.13
Ins ctx	26.08	1.03	23.09	1.72
Pir ctx	24.56	1.51	31.97	4.08
Septum	16.85	1.47	28.61	6.15
DM str	12.46	0.67	10.29	1.14
DL str	10.88	0.73	10.21	0.60
VL Str	9.93	1.16	9.40	0.87
VM str	11.39	0.50	9.92	1.41
AcbC	12.49	0.52	9.55	0.69
AcbSh	14.07	1.51	11.08	1.61

5-HT1A mRNA expression	Vehicle Average	sem	Fluoxetine Average	sem	Mirtazapine Average	sem
Cing ctx	37.65	1.78	42.04	1.62	42.71	1.86
Ins ctx	58.65	2.20	63.10	4.67	65.81	3.46
DM str	52.50	2.63	48.72	0.79	49.82	1.79
DL str	98.76	5.52	98.33	3.08	105.24	5.17
VL Str	17.74	5.79	10.37	1.26	19.63	1.75
VM str	12.29	1.38	11.81	0.33	18.02	1.48
AcbC	8.73	1.30	11.30	1.36	16.95	1.13
AcbSh	9.25	1.64	8.78	1.25	13.37	1.43
Septum	11.00	3.03	7.58	1.14	13.85	1.31
Pir ctx	8.76	1.37	8.61	2.00	15.31	1.89

HCN1 mRNA expression	Vehicle Average	sem	Fluoxetine Average	sem	Mirtazapine Average	sem
Cing ctx	20.58	2.14	20.95	1.48	21.79	0.82
Ins ctx	16.84	1.64	18.06	1.56	18.78	0.76
DM str	3.54	0.20	3.34	0.25	3.55	0.12
DL str	3.22	0.23	3.39	0.33	3.66	0.15
VL Str	3.16	0.18	3.15	0.32	3.37	0.19
VM str	3.38	0.19	3.70	0.39	3.66	0.18
AcbC	3.41	0.28	3.68	0.41	3.55	0.24
AcbSh	4.65	1.10	4.00	0.46	4.12	0.15
Septum	19.20	1.72	20.12	1.34	20.93	0.74
Pir ctx	24.49	2.24	25.18	1.67	26.02	0.67

HCN2 mRNA expression	Vehicle Average	sem	Fluoxetine Average	sem	Mirtazapine Average	sem
Cing ctx	251.14	2.14	274.78	10.84	259.69	6.67
Ins ctx	174.87	15.85	163.54	9.65	157.88	6.58
Pir ctx	255.46	9.09	268.18	12.30	279.50	10.97
Septum	203.14	4.81	201.02	7.37	186.61	6.86
DM str	149.42	5.30	161.01	6.26	151.32	6.22
DL str	189.72	5.14	201.54	7.37	195.47	7.05
VL Str	174.54	6.57	176.90	9.79	168.39	8.17
VM str	126.58	4.43	133.98	4.79	125.97	5.50
AcbC	122.36	4.84	127.48	5.73	121.57	5.91
AcbSh	132.37	4.02	136.01	6.20	135.57	7.22

HCN3 mRNA expression	Vehicle Average	sem	Fluoxetine Average	sem	Mirtazapine Average	sem
Cing ctx	48.24	2.09	47.75	2.07	49.42	1.42
Ins ctx	35.19	3.96	31.96	1.54	30.85	1.69
Pir ctx	116.19	5.98	112.60	4.40	122.40	6.33
Septum	90.04	5.68	94.04	3.33	99.71	4.59
DM str	73.48	4.07	68.67	3.69	84.00	5.59
DL str	66.26	2.32	68.15	4.33	73.10	3.85
VL str	72.09	3.50	69.71	4.21	78.14	4.25
VM str	79.87	4.85	77.44	3.43	83.38	3.91
AcbC	76.25	5.18	78.16	4.81	82.23	2.87
AcbSh	74.50	3.02	79.09	2.89	82.48	4.49

Tables D.3 Raw data of chronic antidepressant studies A – C (-2.5 to -3.2 mm relative to bregma)

5-HT1A mRNA expression	Vehicle Average	sem	Lithium Average	sem
RSGb	4.17	1.02	3.74	0.78
S1 ctx	6.70	0.87	6.93	0.89
S2 ctx	5.26	0.61	5.49	0.55
Ins ctx	5.38	0.59	6.62	0.82
Pir ctx	9.95	1.09	9.75	0.57
CA1	18.60	1.14	18.37	0.99
CA2	18.36	2.09	18.88	1.08
CA3	27.10	1.42	30.87	1.39
Dg	53.26	3.28	55.87	2.58
Thal	2.71	0.25	3.12	0.36
CeA	2.09	0.34	2.49	0.37

HCN1 mRNA expression	Vehicle Average	sem	Lithium Average	sem
RSGb	58.98	6.10	67.14	3.92
S1	40.18	4.06	33.10	3.38
S2 ctx	46.38	4.86	37.48	3.39
Ins ctx	38.72	1.44	35.04	1.69
Pir ctx	45.40	7.49	40.21	3.88
MeA	79.53	2.34	65.12	4.36
CA1	71.82	5.46	70.87	3.24
CA2	53.95	2.96	56.78	2.33
CA3	41.48	6.04	46.98	3.41
Dg	23.12	8.77	18.43	1.65
Thalamus	48.20	4.55	48.74	3.60

HCN2 mRNA expression	Vehicle Average	sem	Lithium Average	sem
RSGb	67.37	4.89	58.24	2.67
S1	35.98	2.26	34.10	1.11
S2 ctx	41.61	3.01	37.09	1.47
Ins ctx	35.11	3.51	35.35	2.23
Pir ctx	26.63	1.21	28.90	1.89
MeA	36.88	2.06	37.19	2.07
CA1	38.28	2.38	38.73	2.74
CA2	57.85	3.81	52.54	2.57
CA3	39.73	2.56	41.49	2.66
Dg	71.24	6.01	64.41	3.77
Thalamus	28.90	3.14	32.34	1.80

HCN3 mRNA expression	Vehicle Average	sem	Lithium Average	sem
RSGb	29.73	3.13	28.20	3.04
S1 ctx	27.26	2.30	25.34	2.96
S2 ctx	28.23	2.36	23.84	2.89
Ins ctx	35.19	2.57	27.16	3.05
Pir ctx	33.30	3.06	27.20	2.54
CA1	26.28	1.97	23.13	1.71
CA2	35.45	2.94	31.44	3.36
CA3	39.33	3.65	34.37	4.33
Dg	37.12	2.30	33.64	3.48
Thalamus	30.34	2.14	25.74	1.79
CeA	nd	nd	nd	nd

5-HT1A mRNA expression	Vehicle Average	sem	Org 34167 Average	sem
RSGb	25.87	1.01	28.13	1.14
S1 ctx	37.49	1.18	39.63	0.76
S2 ctx	41.35	1.31	39.46	1.82
Ins ctx	39.57	0.94	41.87	1.51
Pir ctx	60.98	5.85	57.93	3.58
CA1	91.95	6.84	106.05	4.76
CA2	92.64	7.59	113.15	8.41
CA3	127.31	12.29	148.30	3.26
Dg	251.01	14.01	245.66	16.23
Thal	21.29	0.89	21.06	0.54
MeA	151.11	17.65	179.47	10.94

HCN1 mRNA expression	Vehicle Average	sem	Org 34167 Average	sem
RSGb	282.93	9.87	256.03	8.09
S1 ctx	162.81	9.06	142.71	3.40
S2 ctx	188.50	7.88	164.95	6.71
Ins ctx	176.16	10.47	157.00	3.60
Pir ctx	208.82	10.10	186.44	5.81
CeA	213.08	8.63	197.26	6.27
CA1	79.91	6.41	75.58	2.20
CA2	77.05	9.24	73.58	5.66
CA3	64.63	5.44	58.07	3.71
Dg	37.73	3.08	38.49	2.19
Thalamus	8.71	1.15	9.62	1.36

HCN2 mRNA expression	Vehicle Average	sem	Org 34167 Average	sem
RSGb	240.78	7.05	221.13	7.96
S1	144.22	4.97	127.86	3.50
S2 ctx	183.97	9.67	178.56	3.84
Ins ctx	136.25	6.70	128.58	4.01
Pir ctx	125.01	7.27	114.04	3.28
MeA	197.73	12.45	213.94	10.22
CA1	217.36	7.43	219.07	2.65
CA2	293.14	15.23	330.74	5.11
CA3	314.07	11.74	340.04	12.71
Dg	209.91	5.21	223.06	5.71
Thalamus	308.77	15.07	336.20	15.60

HCN3 mRNA expression	Vehicle Average	sem	Org 34167 Average	sem
RSGb	22.75	1.86	23.09	1.21
S1 ctx	19.52	0.79	17.90	1.02
S2 ctx	19.75	1.52	18.83	1.40
Ins ctx	21.73	1.21	21.34	2.13
Pir ctx	22.68	2.85	21.77	1.36
CA1	17.23	0.99	20.30	1.25
CA2	22.69	0.74	27.10	2.24
CA3	21.67	0.88	25.14	1.71
Den Gyrus	22.34	0.76	27.26	1.43
Thalamus	21.02	1.46	25.53	1.99
CeA	nd	nd	nd	nd

5-HT1A mRNA expression	Vehicle Average	sem	Fluoxetine Average	sem	Mirtazapine Average	sem
RSGb	25.26	1.77	26.29	2.19	25.38	1.86
S1 ctx	37.36	2.32	44.96	0.67	46.27	2.76
S2 ctx	42.08	1.94	47.46	2.22	50.95	2.92
Ins ctx	39.63	3.12	41.57	1.93	46.64	2.56
Pir ctx	72.19	3.87	67.09	1.57	73.51	2.83
CA1	101.67	7.76	105.83	8.85	108.92	3.71
CA2	63.42	7.24	74.10	6.99	69.14	4.69
CA3	142.95	9.68	131.15	4.30	146.98	7.07
Dg	233.74	14.84	223.95	6.29	248.23	5.01
Thal	18.71	0.65	22.15	0.77	24.33	2.31
MeA	141.07	4.19	119.93	5.53	118.66	9.31

HCN1 mRNA expression	Vehicle Average	sem	Fluoxetine Average	sem	Mirtazapine Average	sem
RSGb	40.97	4.40	36.64	1.29	43.57	3.60
S1 ctx	28.88	2.21	25.75	1.14	30.60	2.13
S2 ctx	29.83	2.31	26.37	0.80	31.38	1.78
Ins ctx	26.36	1.50	25.94	0.93	30.29	2.02
Pir ctx	29.93	2.66	28.17	1.38	31.21	2.43
CeA	31.28	3.19	29.79	0.81	35.99	3.04
CA1	67.11	6.81	63.17	2.81	70.19	5.37
CA2	59.74	5.12	63.46	4.62	66.63	5.08
CA3	50.70	3.15	48.17	1.57	50.38	2.72
Den Gyrus	41.22	3.61	38.44	2.68	43.13	3.95
Thalamus	7.35	1.00	8.60	0.68	10.36	0.54

HCN2 mRNA expression	Vehicle Average	sem	Fluoxetine Average	sem	Mirtazapine Average	sem
RSGb	328.95	9.40	308.39	12.11	327.54	12.91
S1 ctx	230.98	6.55	217.82	5.47	234.81	7.15
S2 ctx	222.52	8.37	225.96	10.82	220.27	6.37
Ins ctx	183.53	5.67	183.02	6.56	205.52	3.52
Pir ctx	158.26	7.06	157.64	7.02	165.44	8.54
MeA	254.68	21.44	256.93	21.20	229.86	6.97
CA1	310.80	15.70	283.83	15.40	303.45	23.71
CA2	356.25	11.39	384.82	13.13	375.50	14.29
CA3	356.24	8.08	371.50	13.93	378.57	14.54
Den Gyrus	217.79	4.04	227.28	5.11	231.73	8.77
Thalamus	353.81	7.04	366.70	11.86	371.58	7.60

HCN3 mRNA expression	Vehicle Average	sem	Fluoxetine Average	sem	Mirtazapine Average	sem
RSGb	71.24	4.25	78.99	9.22	94.24	9.03
S1 ctx	51.76	3.35	67.60	9.62	75.03	8.62
S2 ctx	70.66	8.53	75.99	9.66	95.47	11.33
Ins ctx	77.16	7.58	83.93	7.99	95.22	10.30
Pir ctx	70.22	4.53	85.32	12.10	87.63	7.22
CeAmygdala	#DIV/0!	#DIV/0!	#DIV/0!	#DIV/0!	#DIV/0!	#DIV/0!
CA1	63.46	3.26	68.73	7.90	68.36	6.15
CA2	77.48	3.94	82.42	7.54	85.09	3.54
CA3	78.35	3.22	83.93	7.11	79.43	5.66
Den Gyrus	85.22	3.38	92.92	7.18	94.96	5.89
Thalamus	72.35	5.04	77.46	5.10	81.77	5.58

Tables D.4 Raw data of chronic antidepressant studies A – C (-4.7 to -5.5 mm relative to bregma)

5-HT1A mRNA expression	Vehicle Average	sem	Org 34167 Average	sem
RSGb	3.01	0.17	3.83	0.17
V2 ctx	4.13	0.14	4.30	0.11
Au ctx	4.11	0.18	4.34	0.18
Prh ctx	4.23	0.17	4.43	0.17
PAG	4.41	0.37	4.18	0.17
Gen	2.46	0.14	2.42	0.18
VTA	3.66	0.43	4.25	0.53
PMCo	6.60	0.21	6.38	0.34
CA1	21.22	0.30	21.48	0.95
CA2	20.59	2.16	20.74	1.26
CA3	34.69	1.60	30.19	1.46
Dg	56.92	2.77	51.73	1.42

HCN1 mRNA expression	Vehicle Average	sem	Org 34167 Average	sem
RSGb	37.26	1.34	37.79	3.02
V2	26.09	1.14	26.77	2.50
Au ctx	28.43	2.28	29.13	2.70
Prh ctx	23.95	2.13	23.96	2.29
PAG	11.05	1.19	10.58	1.02
Gen	4.69	0.45	4.71	0.30
VTA	8.83	0.44	9.25	0.96
PMCo	24.79	2.74	24.93	2.78
CA1	399.57	17.25	370.15	13.56
CA2	354.37	15.22	324.48	10.53
CA3	227.12	11.09	220.90	6.28
Dg	198.26	7.13	193.62	2.86

HCN2 mRNA expression	Vehicle Average	sem	Org 34167 Average	sem
RSGb	308.91	5.85	322.59	8.90
V2 ctx	236.93	3.34	246.01	10.41
Au ctx	235.27	6.87	248.45	10.58
Prh ctx	150.53	2.65	157.14	6.05
PAG	244.49	7.06	240.42	18.81
Gen	359.97	11.86	415.66	27.87
VTA	209.35	3.97	208.81	7.74
PMCo	163.31	6.72	184.59	12.00
CA1	166.63	4.05	163.54	1.71
CA2	241.76	6.06	242.67	5.65
CA3	233.36	7.43	229.14	2.57
Dg	146.88	4.39	149.89	2.32

HCN3 mRNA expression	Vehicle Average	sem	Org 34167 Average	sem
RSGb	28.82	1.21	31.39	3.45
V2 ctx	25.67	1.02	26.15	2.60
Au ctx	25.82	1.54	28.33	2.97
Prh ctx	25.18	1.41	27.62	2.75
PAG	29.50	1.94	35.84	3.95
Gen	22.28	1.46	23.39	2.26
VTA	29.73	2.36	33.37	2.97
PMCo	22.27	1.18	25.17	2.43
CA1	20.08	0.97	22.32	2.57
CA2	30.21	1.87	37.01	4.27
CA3	34.76	2.44	42.19	4.90
Dg	29.21	1.74	33.03	3.45

5-HT1A mRNA expression	Vehicle Average	sem	Fluoxetine Average	sem	Mirtazapine Average	sem
RSGb	6.37	0.53	5.97	0.14	6.19	0.31
V2 ctx	7.82	0.54	8.22	0.16	8.05	0.27
Au ctx	8.58	0.42	7.83	0.28	7.89	0.27
Prh ctx	8.54	0.67	7.64	0.18	8.20	0.11
PAG	8.12	0.44	6.94	0.29	7.35	0.21
Gen	5.51	0.39	5.20	0.21	5.31	0.20
VTA	7.24	0.82	5.56	0.54	6.12	1.00
PMCo	9.55	0.40	9.95	0.44	9.76	0.47
CA1	29.10	0.59	29.91	0.82	28.86	0.61
CA2	30.43	1.30	34.75	3.72	35.52	2.53
CA3	44.47	0.70	47.42	1.46	44.64	1.31
Dg	64.27	1.95	69.01	0.49	67.65	0.78

HCN1 mRNA expression	Vehicle Average	sem	Fluoxetine Average	sem	Mirtazapine Average	sem
RSGb	174.98	7.88	184.36	4.69	160.60	6.56
V2 ctx	119.87	5.65	124.70	2.44	107.29	5.61
Au ctx	139.95	5.64	140.28	3.92	125.21	6.56
PrH ctx	118.76	4.68	124.46	3.89	103.06	7.32
PAG	40.89	2.16	42.04	3.71	34.65	3.76
Gen	19.76	2.57	14.88	1.90	12.91	2.41
VTA	38.95	1.17	34.27	3.66	32.37	3.29
PMCo	122.93	12.32	103.28	5.93	101.05	8.60
CA1	398.44	19.41	398.10	22.95	401.54	17.76
CA2	426.78	32.59	455.74	24.27	450.46	33.85
CA3	333.10	17.40	326.30	21.29	322.64	18.20
Dg	221.56	6.11	225.95	10.16	216.95	7.79

HCN2 mRNA expression	Vehicle Average	sem	Fluoxetine Average	sem	Mirtazapine Average	sem
RSGb	279.49	5.24	281.01	10.07	279.36	4.16
V2 ctx	219.31	7.01	222.60	7.52	220.12	1.45
Au ctx	237.73	3.95	250.25	10.20	238.74	4.59
PrH ctx	169.79	5.06	178.61	6.97	159.96	4.38
PAG	251.19	4.74	245.89	9.81	248.14	7.08
Gen	419.10	13.77	446.86	19.55	454.57	7.51
VTA	249.20	8.04	264.10	9.01	241.74	6.44
PMCo	138.28	4.65	138.97	4.37	145.11	3.66
CA1	240.51	4.81	240.12	7.32	230.55	4.09
CA2	328.76	15.20	313.93	6.90	283.69	8.01
CA3	354.47	7.96	345.19	9.07	327.10	5.44
Dg	215.13	2.64	222.96	6.11	210.49	1.95

HCN3 mRNA expression	Vehicle Average	sem	Fluoxetine Average	sem	Mirtazapine Average	sem
RSGb	27.20	2.06	27.52	1.75	30.41	0.93
V2 ctx	24.03	1.62	24.89	1.32	27.73	1.98
Au ctx	25.12	1.52	25.71	1.20	28.81	1.37
Prh ctx	25.65	1.43	27.19	1.08	29.75	1.56
PAG	34.12	2.15	32.32	1.52	35.95	1.62
Gen	23.02	1.06	24.26	1.06	27.22	1.34
VTA	31.56	1.70	34.00	1.63	38.36	1.15
PMCo	24.58	1.02	24.04	1.13	28.29	1.54
CA1	20.96	1.13	21.25	0.94	24.10	1.04
CA2	31.19	1.79	30.89	1.95	35.15	2.02
CA3	35.88	2.11	35.92	1.35	41.07	1.78
Dg	28.53	1.80	29.68	1.19	32.73	1.18

Appendix E – Published work

Papers:

SLATTERY, D.A., HUDSON, A.L. AND NUTT, D.J. (2003) Invited review: The evolution of antidepressant mechanisms *Fundamental and Clinical Pharmacology* (in press)

SUMNER, B.E.H., CRUISE, L., SLATTERY, D.A., HILL, D.R., SHAHID, M. AND HENRY, B. (2003) Testing the validity of *c-fos* expression profiling to aid the therapeutic classification of psychoactive drugs. *Psychopharmacology* (submitted).

SLATTERY, D.A., HENRY, B., HUDSON, A.L., MORROW, J.A, NUTT, D.J. (2003) Sites of increased neuronal activity following fluoxetine, mirtazapine, imipramine or lithium chloride administration throughout the rat brain (manuscript in preparation).

SLATTERY, D.A., HENRY, B., HUDSON, A.L., MORROW, J.A, NUTT, D.J. (2003) Chronic fluoxetine or mirtazapine administration, but not lithium chloride alters HCN1-3 mRNA expression in the rat brain (manuscript in preparation).

Abstracts:

SLATTERY, D.A., HUDSON, A.L., MORROW, J.A., HENRY, B., STEWART, C.A. AND NUTT, D.J. (2002) Chronic fluoxetine and mirtazapine but not lithium downregulate hyperpolarization-activated cyclic-nucleotide gated channel-1 mRNA levels in rat prefrontal cortex. *SFN abstract Program No 306.9*

SLATTERY, D.A., HUDSON, A.L., MORROW, J.A., HENRY, B. AND NUTT, D.J. (2001) *In vivo* phosphorothioate antisense oligonucleotide administration targeted to the hyperpolarization-activated cyclic-nucleotide gated channel *Journal of Psychopharmacology* **15** K5

SLATTERY, D.A., HUDSON, A.L. AND NUTT, D.J. (2000) Is there are functional link between potassium channel modulators and imidazoline I_2 sites *Journal of Psychopharmacology* **13** A45

SLATTERY, D.A., HUDSON, A.L. AND NUTT, D.J. (2000) Inhibition of imidazoline I_2 site binding by potassium channel modulators *British Journal of Pharmacology* **131** 39P

DEIGHAN, C., SLATTERY, D.A., MACKENZIE, J.F., COTECCHIA, S. AND MCGRATH, J.C. (1999) The characterisation of α1-adrenoceptors in murine liver using radioligand binding and transgenic mice *British Journal of Pharmacology* **128** 91P